

Density Functional Theory of Superconductivity in the  
Presence of a Magnetic Field

Dissertation

zur Erlangung des Doktorgrades der Naturwissenschaften  
(Dr. rer. nat.)

der

Naturwissenschaftlichen Fakultät II  
Chemie, Physik und Mathematik

der Martin-Luther-Universität  
Halle-Wittenberg

vorgelegt von

Herrn Andreas Linscheid  
geb. am 13.01.1985 in Herdecke



Datum der Verteidigung:  
26.03.2015

Gutachter:  
Prof. Dr. E. Gross (Betreuer), Prof. Dr. I. Mertig, Prof. Dr. L. Boeri



# Contents

|  |           |
|--|-----------|
| <b>A Note on Notation</b>  | <b>6</b>  |
| <b>Nomenclature</b>  | <b>7</b>  |
| Abbreviations . . . . .  | 7         |
| Symbols . . . . .  | 7         |
| <b>Introduction</b>  | <b>11</b> |
| <br>   |           |
| <b>I. Spin Density Functional Theory for Superconductors</b>                                     | <b>15</b> |
| <br>   |           |
| <b>1. Preparation: SC in a Magnetic Field</b>  | <b>16</b> |
| <br>   |           |
| <b>2. BCS and BdG in an Exchange-Splitting Field</b>   | <b>19</b> |
| <br>   |           |
| <b>3. SpinSCDFT: HK Theorem and KS Construction</b>  | <b>21</b> |
| 3.1. Hamiltonian of the Interacting System . . . . .   | 21        |
| 3.2. 1:1 Correspondence of External Potentials and Densities . . . . .                           | 24        |
| 3.2.1. Connection to the interacting system . . . . .  | 27        |
| 3.3. The Nuclear KS System . . . . .   | 29        |
| 3.4. Electronic Part: The Kohn-Sham-Bogoliubov-de-Gennes equations . . . . .                     | 31        |
| 3.4.1. The KS Hamiltonian in the Nambu-Anderson Notation . . . . .                               | 31        |
| 3.4.2. The Bogoliubov-Valatin Transformations . . . . .  | 32        |
| 3.4.3. Expansion in the Normal State KS System: Choosing the Closest Basis<br>Possible . . . . . | 33        |
| 3.4.4. The Electronic Densities . . . . .  | 35        |
| 3.5. Approximations to the KS System . . . . .   | 36        |
| 3.5.1. No Triplet Pairing, Collinear Nambu-Diagonal . . . . .                                    | 36        |
| 3.5.2. Spin Decoupling Approximation . . . . .   | 37        |
| 3.6. Symmetries of the SC KS System . . . . .  | 41        |
| 3.6.1. Translational Symmetry . . . . .  | 42        |
| 3.6.2. Gauge Invariance of the KS Hamiltonian . . . . .  | 42        |
| <br>   |           |
| <b>4. Interaction Matrix Elements</b>  | <b>44</b> |
| 4.1. Electron Phonon Matrix Elements . . . . .   | 44        |
| 4.2. Electronic Screening and Effective Interaction . . . . .                                    | 45        |
| 4.2.1. The Polarization Propagator . . . . .   | 45        |
| 4.2.2. The Effective Interaction in Fourier Space . . . . .                                      | 46        |
| 4.2.3. The Integral Representation of the Effective Coulomb Interaction . . . . .                | 46        |
| 4.2.4. The Coulomb Matrix Elements . . . . .   | 47        |

|  |           |
|--|-----------|
| <b>5. Many-Body Theory in the KS System</b>  | <b>48</b> |
| 5.1. Introduction to Green's Functions . . . . .   | 48        |
| 5.1.1. The Electronic GF . . . . .   | 48        |
| 5.1.2. The Spectral Representation of the Nambu GF . . . . .   | 51        |
| 5.1.3. KS GF . . . . .   | 52        |
| 5.1.4. The Phonon Propagator . . . . .   | 54        |
| 5.2. Perturbation Theory . . . . .   | 54        |
| 5.3. The SSE of SpinSCDFT . . . . .  | 58        |
| <b>6. Functionals and the Self-Consistency Cycle</b>   | <b>60</b> |
| 6.1. General Approach to a Self-Consistent Solution . . . . .  | 60        |
| 6.2. The $\mathcal{E}_{ij}$ Matrix as a Functional of $\mathbf{m}(\mathbf{r})$ and $n(\mathbf{r})$ . . . . .                         | 61        |
| 6.3. Construction of the $\Delta^s$ Matrix Functional . . . . .  | 62        |
| 6.3.1. Preparatory: General Procedure and Further Approximations. . . . .  | 62        |
| 6.3.2. Phononic Exchange SE . . . . .  | 65        |
| 6.3.3. Coulomb SE . . . . .  | 66        |
| 6.3.4. Symmetrized Components of the SE . . . . .  | 67        |
| 6.3.5. The Equation for $\Delta^s$ . . . . .   | 68        |
| 6.4. SDA: The Gap Equation. . . . .  | 69        |
| 6.4.1. The $(1, -1)$ Part of the SSE . . . . .   | 70        |
| 6.4.2. The Sham-Schlüter Operator . . . . .  | 71        |
| 6.4.3. Functional Contribution $M$ and $M'$ . . . . .  | 71        |
| 6.4.4. Functional Contribution $\mathcal{D}^s$ . . . . .   | 72        |
| 6.4.5. Functional Contribution $\mathcal{C}^s$ . . . . .   | 72        |
| 6.4.6. The Gap Equation . . . . .  | 73        |
| 6.5. The Linearized Gap Equation . . . . .   | 74        |
| 6.5.1. Implication Small $\chi_s(\mathbf{r}, \mathbf{r}')$ to Small $\Delta_{si}^s$ . . . . .  | 74        |
| 6.5.2. Small $\Delta_s^s$ Behavior of $ u_{k\sigma}^{k\alpha} ^2$ , $ v_{k-\sigma}^{-k\alpha} ^2$ and $E_{k\sigma}^\alpha$ . . . . . | 75        |
| 6.5.3. The Linear Sham-Schlüter Operator . . . . .   | 76        |
| 6.6. Isotropization of SpinSCDFT Equations. . . . .  | 77        |
| 6.6.1. The Isotropization Procedure . . . . .  | 77        |
| 6.6.2. Non-Linear, Isotropic Sham-Schlüter Operator . . . . .  | 79        |
| 6.6.3. Linearized, Isotropic Sham-Schlüter Operator . . . . .  | 81        |
| <b>7. Many-Body Excitation Spectrum and Eliashberg Equations</b>   | <b>83</b> |
| 7.1. The Isotropic Dyson Equation . . . . .  | 83        |
| 7.2. The Many-Body Green's Function with the KS Self-Energy . . . . .  | 84        |
| 7.2.1. Imaginary Axis Formulation . . . . .  | 85        |
| 7.2.2. Real Axis Formulation . . . . .   | 87        |
| 7.3. Eliashberg Equations of a Spin-Splitted System . . . . .  | 90        |
| <b>8. Application to an Exchange-Splitted Free Electron Gas Model</b>  | <b>95</b> |
| 8.1. Details of the Model . . . . .  | 95        |
| 8.1.1. The Double DOS Function $\varrho(\epsilon)$ of the Splitted Electron Gas . . . . .  | 96        |
| 8.1.2. The Model for the Phononic Coupling $\alpha^2 F$ . . . . .  | 96        |
| 8.1.3. The Model for the Coulomb Coupling $C^{\text{stat}}(\epsilon, \epsilon')$ . . . . .   | 97        |
| 8.2. Behavior of SpinSCDFT Kernels and $T_c(J)$ in the second order regime . . . . .   | 98        |
| 8.2.1. Critical Temperatures and the Shape of $\Delta_s^s$ . . . . .   | 98        |
| 8.2.2. Temperature Dependence of $\tilde{S}_\beta$ . . . . .   | 100       |
| 8.2.3. Splitting Dependence of $T_c$ . . . . .   | 102       |

|  |            |
|--|------------|
| 8.3. The Non-Linear Gap Equation . . . . .   | 104        |
| 8.4. The Effect of the Static Coulomb Interaction . . . . .  | 106        |
| 8.5. Solutions to the Eliashberg Equations . . . . .   | 108        |
| <b>II. Superconductivity of Surfaces: Lead Monolayer on Silicon</b>  | <b>111</b> |
| <b>Introduction</b>  | <b>112</b> |
| <b>9. Electronic and Phononic Properties of Pb on Si(111)</b>  | <b>113</b> |
| 9.1. Electronic Structure . . . . .  | 113        |
| 9.2. Phononic Structure . . . . .  | 114        |
| 9.3. Coulomb Coupling . . . . .  | 115        |
| 9.4. Interaction of Surface and Substrate . . . . .  | 116        |
| <b>10. The SC Si-Pb Surface without Magnetic Field</b>   | <b>117</b> |
| <b>11. The Si-Pb Surface in a Magnetic Field</b>   | <b>120</b> |
| 11.1. Isotropization of the Si – Pb Surface in a Magnetic Field . . . . .  | 120        |
| 11.2. Suppression of SC via a Magnetic Field . . . . .   | 121        |
| <b>Summary and Outlook</b>   | <b>122</b> |
| <b>Appendix</b>  | <b>123</b> |
| <b>A. Derivation of the Continuity Equation</b>  | <b>124</b> |
| <b>B. Relations for expansion coefficients in the Spin Decoupling Approximation</b>  | <b>127</b> |
| <b>C. The Coulomb Potential in Fourier Space and Integral Representations of <math>\chi^{pol}</math> and <math>\epsilon^{-1}</math>.</b> | <b>129</b> |
| C.1. The Coulomb Potential in Fourier Space . . . . .  | 129        |
| C.2. Integral Representation of $\chi^{pol}$ and $\epsilon^{-1}$ . . . . .   | 130        |
| <b>D. Analytic Matsubara Summations</b>  | <b>133</b> |
| <b>E. Inverse Spin-Decoupled KS Greensfunction</b>   | <b>136</b> |
| <b>F. Wick Theorem for Superconductors</b>   | <b>138</b> |
| <b>G. The KS Excitation Spectrum</b>   | <b>142</b> |
| <b>H. Limiting cases of the Eliashberg Equations</b>   | <b>145</b> |

# A Note on Notation

We try to use a notation as close as possible to that of the various individual fields of physics we use to obtain the SpinSCDFT equations (magnetism, Many-Body theory, superconductivity and DFT). Inevitably, this will cause naming convention conflicts. To increase readability, if a symbol follows one unique naming convention (for example  $\mathbf{A}(\mathbf{r})$ , the vector potential) we do not introduce it in the text but advise the reader to refer to the Nomenclature section. Due to the limited number of common symbols, some very different entities have a similar symbol. We hope the distinction is possible and in case of doubt advise the reader, again, to refer to the Nomenclature. The reader should make himself familiar with the following conventions that we will use throughout the thesis:

1. We define that all quantities are promoted to the space that the context requires. This means we take the direct product with the identity operator in all the spaces that are not explicitly referenced. Entities which are usually used in spin space, such as  $\sigma_{x,y,z}$ ,  $\mathbf{S}$ , ... become in the context of Nambu and Spin space  $\sigma_{x,y,z} \otimes \tau_0$ . If we want to *explicitly* point out that  $\tau_0$  is used, such as in a basis vector decomposition, we write  $\sigma_{x,y,z}\tau_0$ . From now on we reserve the symbol  $\otimes$  for the outer product of vectors, for clarity.
2. The indices  $\sigma$  and  $\mu$  always refer to the spin quantum number; the indices  $\alpha, \gamma = \{1, -1\}$  always label Nambu components. Indices  $i, j, k$  are a combined quantum number of band and Bloch vector for single electron states  $k \equiv (\mathbf{k}, n)$ . Here we have to pay attention to the type of single particle, the ones of the SC system and the (normal state) KS basis. In quantities that map the two types into each other ( $u, v$ ) we make the distinction by writing the basis vector as a superscript and the SC particle quantum number as a subscript:  $u_{[\text{SC particle}]}^{[\text{NS basis}]}$ . Otherwise the type of particle has to be deduced from the context.
3. We mostly use pure spinor operators (Nambu, as well as Spin spinors). We introduce the notation here for spin only but also use it for Nambu indices.  $\hat{\psi}_\sigma(\mathbf{r})$  is a spin vector with a spin quantum number and only one non-vanishing component, e.g.  $\hat{\psi}_\uparrow(\mathbf{r}) = \begin{pmatrix} \hat{\psi}(\mathbf{r} \uparrow) & 0 \end{pmatrix}^T$ . If we refer to the scalar component we promote the index to the argument  $\hat{\psi}(\mathbf{r}\sigma)$ . For spin spinors we use the arrow notation that in addition distinguishes the spinor from its scalar component. For Nambu and Spin vectors we use the symbol  $\Psi$ , so here *the distinction between the vector and its scalar components is only by the index being promoted to the argument*. Similarly we introduce Nambu and Spin matrices with a bar, e.g.  $\bar{G}(\mathbf{r}\tau, \mathbf{r}'\tau')$  and keep the symbol (with the bar) for the individual matrix elements. Thus,  $\bar{G}(\mathbf{r}\alpha\sigma\tau, \mathbf{r}'\alpha'\sigma'\tau')$  means the matrix element  $\alpha\sigma, \alpha'\sigma'$  in Nambu and Spin space.
4. The operator  $\cdot$  appears as a matrix product operation and as a generic vector contraction in various spaces. The meaning will be clear from the context.
5. In a list of arguments  $\mathbf{r}\alpha\sigma\tau \equiv \mathbf{r}, \alpha, \sigma, \tau$  we usually do not put commas to save space, except if we want to point out the distinction between one group and the other. We also put commas if the number of arguments may be ambiguous, such if there is a minus sign in front of a variable  $\mathbf{r}\alpha\sigma, -\tau \equiv \mathbf{r}, \alpha, \sigma, -\tau$  or we use the short hand notation with single integral numbers  $1, 2, 3 \dots$  where we want to easily distinguish  $1, 2$  from  $12$ .



# Nomenclature

## Abbreviations

|        |  |
|--------|--|
| SDA    | Spin Decoupling Approximation  |
| GW     | Approximation where the dressed vertex is replaced by the bare vertex in the SE on every occurrence. |
| RPA    | Random Phase Approximation   |
| KS     | Kohn-Sham  |
| (L)DOS | (Local) Density Of States  |
| SE     | Self-Energy  |
| DFT    | Density Functional Theory  |
| SC     | Superconductor, superconductivity and similar  |
| L(S)DA | Local (Spin) Density Approximation   |
| $xc$   | exchange-correlation   |
| FFLO   | Fulde-Ferrel-Larkin-Ovchinnikov  |
| BdG    | Bogoliubov-de Gennes   |
| NS     | Normals State  |
| BCS    | Bardeen Cooper and Schrieffer  |
| SSE    | Sham-Schlüter Equation   |
| GF     | Green's Function   |
| STM    | Scanning Tunneling Microscopy  |
| FS     | Fermi Surface  |

## Symbols

### Constants

|              |  |
|--------------|--|
| $c$          | The speed of light.                        |
| $m_e$        | The electron rest mass.                    |
| $e$          | The absolute value of the electron charge. |
| $g_s$        | The Landé factor $g_s \approx 2$ .         |
| $\mu_B$      | The Bohr magneton.                         |
| $\epsilon_0$ | The vacuum permittivity.                   |
| $k_B$        | The Boltzmann constant.                    |

### Basic variables

|                      |  |
|----------------------|--|
| $T$                  | The temperature in Kelvin.   |
| $\beta$              | The inverse temperature $\beta = 1/(k_B T)$ .  |
| $T_c$                | The SC transition temperature.   |
| $E_f$                | The Fermi energy.  |
| $\epsilon_{k\sigma}$ | The NS KS particle energy relative to $E_f$ .  |
| $E_k$                | The single particle energy eigenvalue with quantum number $k$ of an excitation on the SC ground state. |

|                                      |   |
|--------------------------------------|---|
| $\mathbf{A}(\mathbf{r})$             | The vector potential.   |
| $\phi(\mathbf{r})$                   | The scalar potential.   |
| $\mathbf{B}(\mathbf{r})$             | The magnetic field $\mathbf{B}(\mathbf{r}) = \nabla \times \mathbf{A}(\mathbf{r})$ .          |
| $\hat{\mathbf{p}}$                   | The momentum operator $\hat{\mathbf{p}} = -i\hbar\nabla$ .                                    |
| $\mathbf{r}, \mathbf{x}$             | The position in space. We use $r$ for the norm of a vector $\mathbf{r}$ .                     |
| $\bar{\mathbf{r}}, \bar{\mathbf{x}}$ | The position in the first unit cell.  |
| $\mathbf{q}, \mathbf{k}$             | The Bloch vector in the first Brillouin zone.   |
| $\bar{\mathbf{q}}, \bar{\mathbf{k}}$ | The Bloch vector in the full inverse space.   |
| $\mathbf{T}_i$                       | A translation of the direct lattice.  |
| $\mathbf{G}$                         | A translation of the inverse lattice.   |
| $\Omega_{\text{uc}}$                 | The volume of the unit cell.  |
| $N_q$                                | The number of unit cells in the lattice.  |
| $\theta(E)$                          | The Heavyside step function.  |
| $f_\beta(E)$                         | The Fermi function at inverse temperature $\beta$   |
| $n_\beta(E)$                         | The Bose-Einstein function at inverse temperature $\beta$                                     |
| $\hat{T}, \bar{T}$                   | The (imaginary) time ordering symbol.<br>In Nambu space it orders every individual component. |

### Densities and Potentials.

|   |   |
|---|---|
| $n(\mathbf{r})$                           | Density of all electrons.   |
| $\chi(\mathbf{r}, \mathbf{r}')$           | Density of condensed electron pairs.  |
| $\mathbf{m}(\mathbf{r})$                  | The magnetization density.  |
| $\Gamma(\mathbf{R}_1 \dots \mathbf{R}_N)$ | Density of nuclei.  |
| $\Delta^{\text{ext},s}$                   | The singlet/triplet vector of pair potentials $(\Delta_s^{\text{ext},s}, \Delta_{tx}^{\text{ext},s}, \Delta_{ty}^{\text{ext},s}, \Delta_{tz}^{\text{ext},s})^T$<br>for the interacting system (index ext) or the KS system (index s). |
| $\bar{v}_{xc}$                            | The $xc$ potential in Nambu and Spin space.   |

### Basic notation.

|                         |   |
|-------------------------|---|
| $\langle \dots \rangle$ | The thermal average $\text{Tr}\{\hat{\rho} \dots\}$ .   |
| $\hat{\rho}$            | The grand canonical statistical operator.   |
| $\cdot$                 | The vector contraction symbol, and generic matrix multiplication.   |
| $\otimes$               | The tensor (direct) product. Only used for the outer product of vectors.  |
| $[\dots, \dots]_\pm$    | The commutator for $+$ and the anticommutator for $-$ .   |
| $\Re$                   | The real part of a complex number or function.  |
| $\Im$                   | The imaginary part of a complex number or function.   |
| $\Re e$                 | The hermitian part of a matrix $\Re e A = \frac{1}{2}(A + A^\dagger)$ .<br>For symmetric matrices this is equivalent to the real part of every component.                                       |
| $\Im m$                 | The imaginary unit times the antihermitian part of a matrix<br>$\Im m A = \frac{1}{2i}(A - A^\dagger)$ .<br>For symmetric matrices this is equivalent to the imaginary part of every component. |
| $\hat{A}(\tau)$         | An operator in the imaginary Heisenberg picture $\hat{A}(\tau) = e^{\tau\hat{H}} \hat{A} e^{-\tau\hat{H}}$ .<br>Note that we include the Lagrange multiplier $\mu\hat{N}$ into $\hat{H}$ .      |
| $\hat{A}(t)$            | An operator in the Heisenberg picture $\hat{A}(t) \equiv e^{it\hat{H}} \hat{A} e^{-it\hat{H}}$ as above.  |

### Nambu and spin space symbols.

|                    |  |
|--------------------|--|
| $\sigma_{0,x,y,z}$ | The Pauli matrices in spin space<br>$\sigma_0 = \begin{pmatrix} 1 & 0 \\ 0 & 1 \end{pmatrix}, \sigma_x = \begin{pmatrix} 0 & 1 \\ 1 & 0 \end{pmatrix}, \sigma_y = \begin{pmatrix} 0 & -i \\ i & 0 \end{pmatrix}, \sigma_z = \begin{pmatrix} 1 & 0 \\ 0 & -1 \end{pmatrix}$ . |
| $\tau_{0,x,y,z}$   | The Pauli matrices in Nambu space.<br>We use the same convention as for the $\sigma_{0,x,y,z}$ .   |

|  |  |
|--|--|
| $\mathbf{S}$                                     | The vector of Pauli matrices $\mathbf{S} = \frac{1}{2}(\sigma_x, \sigma_y, \sigma_z)^T$ .  |
| $\Phi$   | The singlet/triplet vector $\Phi = (i\sigma_y, -\sigma_z, \sigma_0, \sigma_x)^T$ .   |
| $\vec{u}_k(\mathbf{r}), \vec{v}_k(\mathbf{r})$   | The spinor components of the $4 \times 2$ Bogoliubov-Valatin unitary transformation $\begin{pmatrix} \vec{u}_k(\mathbf{r}) & \vec{v}_k^*(\mathbf{r}) \\ \vec{v}_k(\mathbf{r}) & \vec{u}_k^*(\mathbf{r}) \end{pmatrix}$ .                                 |
| $\vec{u}_k^i, \vec{v}_k^i$                       | The expansion coefficients $\vec{u}_k^i = (u_k^{i\uparrow}, u_k^{i\downarrow})^T$ of $\vec{u}_k(\mathbf{r})$ in the NS KS orbitals $\vec{\varphi}_{i\sigma}$ .   |
| $u_{k\sigma}^{k\alpha}, v_{k-\sigma}^{-k\alpha}$ | Components of the eigenvector $g_{k\sigma}^\alpha = (u_{k\sigma}^{k\alpha}, v_{k-\sigma}^{-k\alpha})^T$ to the eigenvalue $E_{k\sigma}^\alpha$ of the KSBdG Eq. (3.152). These construct the Bogoliubov-Valatin transformation according to Eq. (3.167). |

### Hamilton operators.

|  |  |
|--|--|
| $\hat{H}$                                      | The interacting Hamiltonian of electrons and nuclei.   |
| $\hat{H}_{\text{KS}}$                          | The KS Hamiltonian yielding the same densities as $\hat{H}$  |
| $\hat{H}_s^e$                                  | The scalar electronic part of the KS Hamiltonian   |
| $\hat{H}_{\text{KS}}^e$                        | $\hat{H}_{\text{KS}} = \hat{H}_s^e + \hat{H}_s^n$ .  |
| $\hat{H}_c^{e0}$                               | The Hamiltonian yielding the normal state KS basis which is solvable on a computer.  |
| $\hat{H}_{\text{nc}}^{eT}$                     | The difference of $\hat{H}_c^{e0}$ from the full electronic KS Hamiltonian at finite temperature $\hat{H}_{\text{nc}}^{eT} = \hat{H}_s^e - \hat{H}_c^{e0}$ .   |
| $\hat{H}_s^n$                                  | The nuclear part of the KS Hamiltonian.  |
| $\hat{H}_0^n$                                  | The harmonic approximation to $\hat{H}_s^n$ .  |
| $\bar{H}_{\text{KS}}(\mathbf{r}, \mathbf{r}')$ | Defines the basis for the phonon operators $\hat{b}_{\lambda\mathbf{q}}$ .<br>The electronic SC KS Hamiltonian in first quantization as a Nambu-spin matrix $\hat{H}_s^e = \int d\mathbf{r} \int d\mathbf{r}' \Psi^\dagger(\mathbf{r}) \cdot \bar{H}_{\text{KS}}(\mathbf{r}, \mathbf{r}') \cdot \Psi(\mathbf{r}')$ . |

### Particle operators.

|  |  |
|--|--|
| $\hat{\gamma}_k^\dagger$               | The operator that creates the excitations on the SC ground state.  |
| $\hat{\Phi}_k$                         | The excitation on the SC ground state in the Nambu notation. We use $\hat{\Phi}_k(\alpha)$ to refer to individual scalar components of the 2 component vector. |
| $\hat{\psi}^\dagger(\mathbf{r}\sigma)$ | Creator of the electronic field at position $\mathbf{r}$ with spin $\sigma$ in a collinear basis system.   |
| $\hat{\psi}^\dagger(\mathbf{r})$       | The spinor field operator that creates both spin channels at the same time.  |
| $\hat{\Psi}(\mathbf{r})$               | The Nambu spinor with 4 components. $\hat{\Psi}(\mathbf{r}\alpha\mu)$ refers to individual scalar components.  |
| $\hat{\zeta}^\dagger(\mathbf{R})$      | The nuclear field creation operator.   |

### Perturbation theory.

|  |  |
|--|--|
| $\bar{G}$                                  | The interacting temperature Nambu GF.  |
| $\bar{G}^{\text{R}}$                       | The retarded Nambu GF.   |
| $\bar{G}^{\text{KS}}$                      | The SC KS systems electronic Nambu GF.   |
| $\bar{A}(\mathbf{r}, \mathbf{r}', \omega)$ | The spectral function of the Nambu GF.   |
| $\rho_{\mu,\alpha}(\mathbf{r}, \omega)$    | The LDOS relative to $E_f$ . Corresponds to the diagonal limit of $\bar{A}(\mathbf{r}, \mathbf{r}', \omega)$ . |
| $\bar{\Sigma}$                             | The Nambu Hartree SE.  |
| $\bar{\Sigma}^s$                           | $\bar{\Sigma}^s$ minus the Nambu $xc$ potential.   |
| $\bar{\Sigma}^{\text{KS}}$                 | $\bar{\Sigma}[\bar{G}]$ with $\bar{G}$ replaced by $\bar{G}^{\text{KS}}$ .                                     |
| $\chi^{\text{pol}}$                        | The polarization propagator.   |
| $D_{\text{ph}}, D_{\text{ph}}^0$           | The dressed and the bare (superscript 0) phonon propagator.  |

### Coupling matrix elements.

|  |   |
|--|---|
| $M_{ijkl\sigma\sigma'}^{\text{dyn}}(\omega)$ | The purely dynamical matrix elements of the effective Coulomb interaction in the NS KS basis. |
|--|---|

|                                       |  |
|---------------------------------------|--|
| $W_{ijkl\sigma\sigma'}^{\text{stat}}$ | The static matrix elements of the effective Coulomb interaction in the NS KS basis.  |
| $g_{kk'\sigma}^{\mathbf{q}\lambda}$   | The electron-phonon coupling matrix elements in a non-SC basis.  |
| $\alpha^2 F$                          | The isotropic electron-phonon coupling on the Nambu off diagonal.  |
| $\alpha^2 F_{\sigma}^{\text{D}}$      | The isotropic electron-phonon coupling on the Nambu diagonal.  |
| $C^{\text{stat}}$                     | The isotropic static Coulomb coupling on the Nambu off diagonal.   |
| $C^{\text{dyn}}$                      | The isotropic dynamic Coulomb on the Nambu off diagonal.   |
| <b>SDA Sham-Schlüter equation.</b>    |  |
| $S_{\beta}$                           | The SSE in the SDA written as $S_{\beta}[\Delta_s^s] \cdot \Delta_s^s = 0$ . We distinguish $S_{\beta} = S_{\beta}^{\text{M}} + S_{\beta}^{\text{D}} + S_{\beta}^{\text{c}}$ . |
| $S_{\beta}^{\text{M}}$                | The part due to $\bar{G}^{\text{KS}} \cdot \bar{v}_{xc} \cdot \bar{G}^{\text{KS}}$ in the SSE.   |
| $S_{\beta}^{\text{D}}$                | The part due to the Nambu diagonal of the SE in the SSE.   |
| $S_{\beta}^{\text{D,PHS}}$            | $S_{\beta}^{\text{D}}$ where SE contributions $\sim \tau_z$ are neglected.   |
| $S_{\beta}^{\text{c}}$                | The part due to the Nambu off-diagonal of the SE in the SSE.   |
| $S_{\beta}^{\text{sc}}$               | $S_{\beta}^{\text{c}}$ where SE contributions $\sim \sigma_x$ are neglected.   |
| $A$                                   | The small $\Delta_s^s$ limit of $A$ .  |
| <b>Isotropization.</b>                |  |
| $\varepsilon$                         | The center of energy $\frac{1}{2}(\varepsilon_{k\uparrow} + \varepsilon_{-k\downarrow})$ .   |
| $J$                                   | The splitting $\frac{1}{2}(\varepsilon_{k\uparrow} - \varepsilon_{-k\downarrow})$ .  |
| $\mathbf{e}$                          | The combination $(\varepsilon, J)$ .   |
| $F$                                   | The non-spin part of the isotropic Bogoliubov eigenvalue $\sqrt{\varepsilon^2 +  \Delta_s^s ^2}$ .   |
| $E_{\sigma}^{\alpha}$                 | The isotropic Bogoliubov eigenvalue $\text{sign}(\sigma)J + \text{sign}(\alpha)F$ .  |
| $\hat{I}_{k\sigma}(\mathbf{e})$       | The operator that averages a function $A_{k\sigma}$ on equal center of energy $\varepsilon$ and splitting $J$ surfaces.  |
| $\varrho(\mathbf{e})$                 | The double DOS, i.e. number of NS KS states on the intersection of the surfaces $\varepsilon$ and $J$ .  |
| $\varrho_{\sigma}(\mathbf{e})$        | The local double DOS similar to $\varrho(\mathbf{e})$ .  |

# Introduction

Superconductivity (SC) is one of the most fascinating effects ever observed in solid state physics.

Discovered by a vanishing of the DC resistance in 1911 by Kammerling Onnes [1], it was later found that a superconductor expels a static magnetic field (independent on the state before SC sets in) which is nowadays known as the Meissner-Ochsenfeld effect [2]. The superconducting phase is technologically important not only due to the obvious application in the transport of electric energy and the creation of ultra high magnetic fields, but also in precise measurement of magnetic fields owed to the flux quantization. Its microscopic explanation by Bardeen Cooper and Schrieffer (BCS) [3], more than 50 years after its initial discovery, turned out to be most influential even beyond the field of solid state physics. For example it has influenced the concepts of spontaneous symmetry breaking that was later employed in particle physics to explain a non-zero mass of fields that are otherwise required to show a zero mass by symmetry [4, 5]. This is commonly known as the Higgs mechanism.

While the fundamentals of SC are believed to be understood there are still open questions. These concern the explanation of the high-temperature (non-phononic) SC, the SC of surfaces or in general of systems in a very constrained geometry, but also the coexistence of magnetic ordering and SC. As an experimental fact all high- $T_c$  SC appears in the proximity to a magnetic phase. While in the high temperature SC spin-fluctuations are by many believed to substitute the phonons as coupling bosons, also different mechanisms are under debate [6, 7]. The most important open problems with the connection of magnetism and SC are mostly on a microscopic level. With many proposed models, we might argue that the inconclusive situation is due to the lack of first principle calculations that may clarify whether a given interaction is capable of explaining the observed experimental effects and thus proves to be predictive.

While one would expect the Meissner effect to render static magnetic fields in SC impossible there is experimental literature on the coexistence of magnetic ordering and SC (see Ref. [7, 8] for a review on the situation for the iron based SC or Ref. [9] in an interface). Theoretical studies on the coexistence are mainly based on models, due to the fact that the situation arises mostly in materials where the pairing mechanism is non-phononic and thus first principle calculations of SC are difficult. Powell *et al.* [10] discuss the inclusion of a homogenous magnetic field into a Hubbard model. Fulde and Ferrel [11] and independently Larkin and Ovchinnikov [12] (FFLO) derived a new, spatially inhomogeneous state in SC subject to a strong exchange-splitting. They start from a BCS model where pairing enters as a parameter and is not necessarily due to phononic coupling. Intensive research has tried to find this state in nature and has recently been successful in heavy fermion [13, 14] and organic SC [15]. Moreover in the proximity to a magnetic impurity there will be competition between the microscopic magnetic field and the superconducting host that can be visualized experimentally [16]. Even the onset of a Kondo effect is discussed when a magnetic atom or molecule is absorbed on the surface of a superconductor [17]. Again, to single out the effect of individual contributions such as direct Coulomb, magnetic or phononic couplings it would be desirable to simulate the competition of SC and magnetism on a microscopic scale from first principles.

It is the goal of this work to develop such an ab-initio theory, both the analytic derivation and the numerical implementation, to be able to compute physical observables that can be compared with experiment. Apart from  $T_c$  we are most interested in the (local) excitation spectrum, i.e. the (local) DOS because numerical predictions can be compared directly with experimental

STM maps.

So far there is very scarce literature on first principle magnetic calculations in SC. Schossmann and Schachinger have derived Eliashberg equations including the vector potential [18]. However, they set out from a self-energy that is taken to be local in real space with an empirical electron phonon coupling. It is not straight forward to generalize their approach to the case of ab-initio calculations, where the pairing interactions are usually taken to be local in the space of normal state quasi particles. Vonsovsky *et al.* [19] have derived Eliashberg equations, treating the magnetic field perturbatively except for a “on site” splitting parameter. They require the self-energy to be diagonal with respect to normal-state electronic orbitals which is similar to the main results obtained in this work. In general the assumption of a diagonal pairing interaction might pose an oversimplification when SC causes regions in the unit cell to lose their magnetic order. Starting from the magnetic normal state this can only be achieved if we allow the electronic states to hybridize due to SC. While in principle the perturbative expansion that leads to the Eliashberg equations can be easily generalized to a non-diagonal normal-state basis, the solution to the Dyson equation becomes computationally too demanding. If we wish to describe effects such as the FFLO phase or localized bound states in non-superconducting regions, we have to choose a theory that is numerically simple enough to cope with the much increased numerical complexity when hybridization is considered. Such a theory is the Density Functional Theory for SC [20]. As the most important point however, all Eliashberg based methods share the difficulties that arise when one attempts the inclusion of an ab initio Coulomb interaction. Thus, we choose the Density Functional Theory for SC as our starting point and include a magnetic field into the theory.

While magnetic fields, in a similar shape as in experiment, may in general be well embedded into the usual unit cell framework of a crystal (possibly with a reasonably large unit cell) the inclusion of a vector potential can be problematic. For example a static homogenous magnetic field requires a linearly diverging vector potential, thereby removing the lattice periodicity. An ab initio calculation thus seems more feasible with just the Zeemann term, i.e. the  $\mathbf{B} = \nabla \times \mathbf{A}$  field. This is only possible if the currents in the ground state are negligible. In the regime where SC is suppressed by the magnetic field this on the other hand might be a severe restriction. Note also that the Meissner effect appears in the current-current response function.

In the usual Density Functional Theory for SC one considers the one body density of electrons  $n(\mathbf{r})$ , the density of condensed electron pairs  $\chi(\mathbf{r}, \mathbf{r}')$  and the density of nuclei [21, 22, 20]. In this work, in Part I, we include the magnetization  $\mathbf{m}(\mathbf{r})$  as an additional density, neglecting currents to have a scheme that is easier applied in practice. Without the inclusion of currents the theory cannot describe mesoscopic structures like Abrikosov vortices, whose size is beyond the regime of ab-initio calculations for the near future anyhow. Functionals are developed based on many-body perturbation theory via the Sham-Schlüter connection. In addition to the full equations we discuss the following approximations: 1) singlet pairing, 2) no hybridization of electronic orbitals due to SC and 3) linearization of resulting equations in the pair potential only in the last step. During this work a code was developed that solves the linear and non-linear equations within a generalization of the so called Decoupling Approximation [22, 21], that amounts to the approximation 2). Ideas to extend the framework to a real competition of SC with magnetism are discussed while not implemented due to time limitations. Instead we apply the theory to superconducting surfaces where the penetration depth is much larger than the thickness, thus allowing the presence of an external magnetic field in the superconductor.

The SC of surfaces is an interesting subject on its own, even without the presence of magnetism, and many effects present in these constrained geometries cannot be easily included in this ab initio framework. In 1D and 2D there can be no SC due to the onset of long range fluctuations in the order parameter [23]. While the surface in reality does have a thickness and finite (albeit

large) size in  $x - y$  the theorems proving the absence of long range order do not apply. Still the susceptibility to fluctuations in the superconducting order parameter is expected to be large, effectively reducing the equilibrium magnitude of  $\chi(\mathbf{r}, \mathbf{r}')$  dynamically and thereby reducing the critical temperature. A functional that captures this effect will most likely involve the order parameter  $\chi(\mathbf{r}, \mathbf{r}')$  response function. Both, functional and response function are not available at present and, though definitely interesting, are beyond the scope of this thesis.

In Part II as an example of such systems we simulate a lead monolayer on Si(111) with a critical temperature in experiment of  $T_c = 1.8\text{K}$  [24]. A critical analysis of all the conventional approximations usually done in the theory of SC reveals that several have to be revisited in the context of surfaces. As the most important one we meet with the Coulomb interaction that acts very differently in the context of metallic surfaces on an insulating substrate as compared to bulk systems. As an important side note we find that the Coulomb interaction extends the condensed phase far into the substrate which will clearly affect the proximity to the 2D limit.





Part I.

Spin Density Functional Theory for  
Superconductors

# 1. Preparation: SC in a Magnetic Field

In this Part I we develop the ab-initio methods to describe the effect of a magnetic field in a SC system. As a first fundamental assumption we consider a SC as a system where

$$\chi_{\sigma\sigma'}(\mathbf{r}, \mathbf{r}') = \langle \hat{\psi}(\mathbf{r}\sigma)\hat{\psi}(\mathbf{r}'\sigma') \rangle \neq 0 \Leftrightarrow \text{SC}, \quad (1.1)$$

so  $\chi_{\sigma\sigma'}(\mathbf{r}, \mathbf{r}')$  is the order parameter of SC. There is little literature on the origin of the order parameter of SC. Most books start from  $\chi$  as the order parameter and then discuss the implication on e.g. excitation spectra and electromagnetic properties. While it is thus found  $\chi \neq 0 \Rightarrow \text{SC}$  the implication  $\text{SC} \Rightarrow \chi \neq 0$  is not so easy. Certainly, if we describe it with an  $N$  particle Schrödinger equation a finite block of lead will not be SC in this sense, because if we respect the particle number in every microscopic state in the ensemble  $\langle \hat{\psi}\hat{\psi} \rangle \equiv \chi = 0$ . The important question, however, is if the block of lead shows  $\chi \neq 0$  below the experimental critical temperature if we allow for coherent states, i.e. states  $|E\rangle$  that allow  $\langle E|\hat{\psi}\hat{\psi}|E\rangle \neq 0$ . Typically one obtains excellent results with this assumption  $\chi \neq 0 \Leftrightarrow \text{SC}$  and there are no indications that it has to be questioned. In the Diploma thesis [25] a review is given on how to interpret  $\chi$  as the wavefunction of SC electron pairs.

If we consider non-relativistic electrons and nuclei under the influence of a static classical magnetic field, the best starting point is the Pauli equation governed by the Pauli Hamiltonian. For the purpose of this discussion it is sufficient to consider just one electron without nuclei

$$\hat{H}_p = \frac{1}{2m_e} \left( (\hat{\mathbf{p}} - \frac{e}{c}\mathbf{A}(\mathbf{r}))^2 + e\phi(\mathbf{r}) \right) \sigma_0 - g_s \mu_B \mathbf{S} \cdot \mathbf{B}(\mathbf{r}). \quad (1.2)$$

This equation can be viewed as a weakly relativistic limit to the Dirac equation which can be extended also to a SC [26]. Starting from the Dirac equation of a SC as the most general equation, we may generate the weakly relativistic limit, i.e. the Pauli Hamiltonian for a SC from this equation. If we allow the electrons to pair and form a condensate we should in principle also consider pairing terms of first order in the speed of light  $c$ . For simplicity we do not include these effects here, nor do we consider the vector potential  $\mathbf{A}(\mathbf{r})$  in the main part of the thesis and we are left with the Zeemann term only. In Appendix A we comment on the case if orbital contributions are not neglected. Still, while dropping orbital and relativistic contributions, because the Cooper pairs of a normal SC are spin singlet we expect interesting effects and, ultimately, the suppression of SC if the field is strong enough.

In this Part I we derive an ab-initio theory for SC in a magnetic field. An overview of the tasks of this Part I is given in Fig. 1.1.

In Chapter 2 we briefly discuss and reproduce earlier results for a BCS model in a homogeneous exchange field which is qualitatively equivalent to a simple, special case of our more involved equations. We will compare numerical solutions with this simple model.

In Chapter 3 we develop the basic formalism of Spin DFT for SCs, finalizing with the so-called KSBdG equations. These constitute a unitary transformation that diagonalizes the single particle KS Hamiltonian in the presence of a pair potential. The KS system includes all exchange and correlation ( $xc$ ) effects in principle exactly. The particle interactions are moved into the  $xc$  potentials that, as usual in the context of DFT, are unknown in their exact form.

We conclude this chapter with a discussion on approximations of the  $xc$  potential matrix elements. Due to the, in general, low energy scale of the pairing interactions, usually the  $xc$

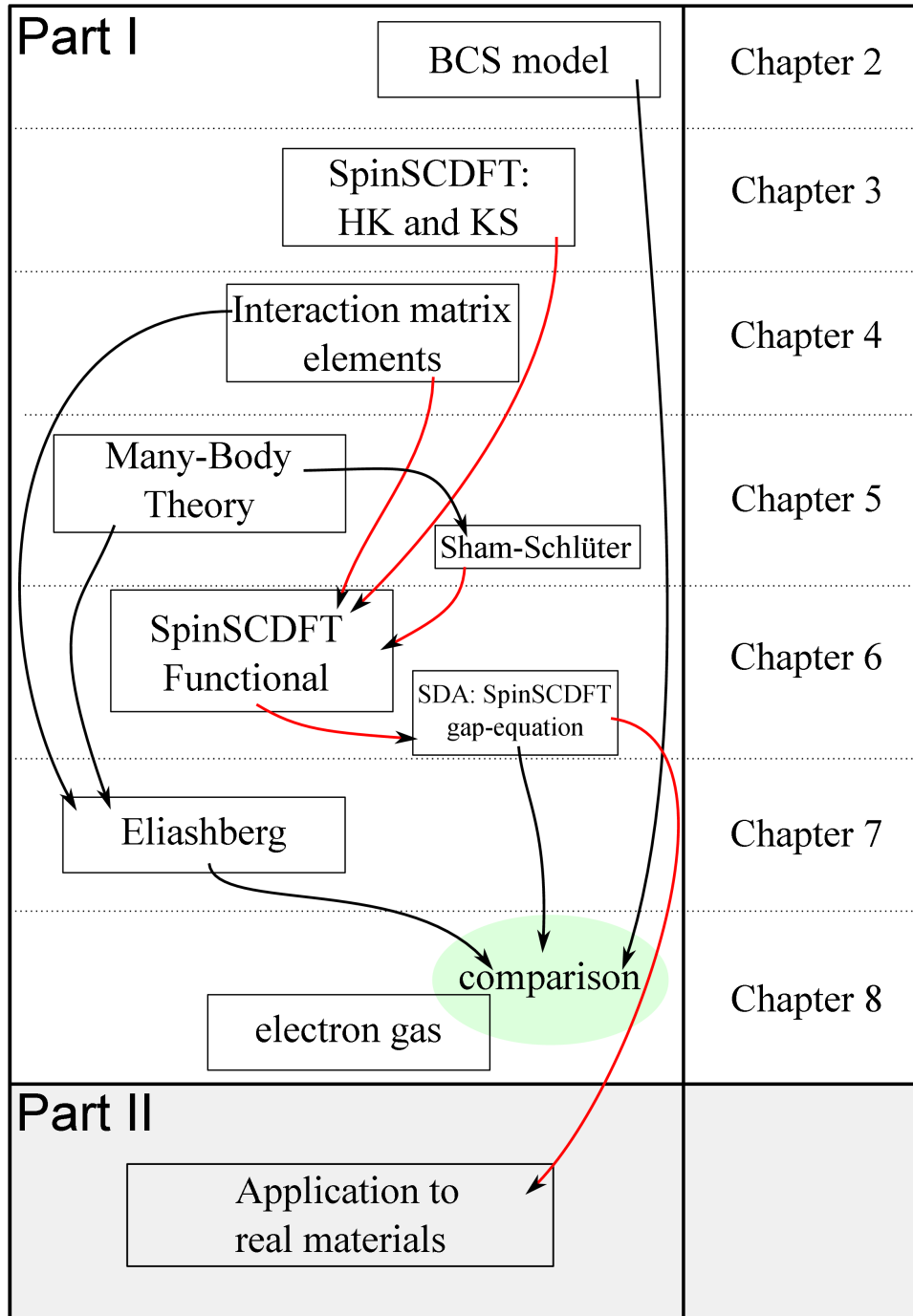


Figure 1.1.: Overview of the tasks in Part I.

pair potential does not induce hybridization among the normal state KS orbitals and the normal state densities are largely unaffected. The most important results are thus found neglecting these effects. In this case, solutions to the KSBdG equations are found analytically and take a particularly easy form. We point out that this form excludes the possibility to describe a FFLO state at this stage.

In Chapter 4, we discuss the most relevant interactions that are typically treated “on top” of the KS system. On top means here that these effects are usually not included into the  $xc$  potential but treated in perturbation theory starting from the KS system as a non-interacting system. While essential in the ab-initio theory of SC such effects are not easily included into a  $xc$  potential on the basis of the densities alone. We take the route via the Sham-Schlüter connection to derive a  $xc$  potential on the basis of perturbation theory. As a preparatory, in this chapter, equations for matrix elements in the KS system basis are computed.

We introduce perturbation theory for a spin polarized SC in Chapter 5. There we define and compute the single particle GF of the SC KS system and write down a Dyson equation that connects the KS system with the interacting GF. Considering the parts of the GF that correspond to the densities we arrive at the Sham-Schlüter connection.

This connection is essential to find approximations for the KS pair potential functional in the Chapter 6. In the most simple approximation, solving SpinSCDFT amounts to solving the SSE in the basis of normal state KS orbitals.

In Chapter 7, we extend the results of SpinSCDFT to observables that are easier to compute from the interacting GF namely the single particle excitation spectrum. First, we discuss the solution to the Dyson equation with the SE that we have used in the functional construction. From this solution we obtain improved excitation spectra. Second, we discuss the case when the SE is not approximated by replacing the interacting with the KS GF. This leads to the Eliashberg equations in the formalism introduced in the preceding Chapter. While they are numerically more demanding than SCDFT, especially if we attempt to include the electronic-state dependence of the interaction, due to Migdal’s theorem the solution is regarded as the reference in the purely phononic case.

We present numerical solutions of the resulting equations in Chapter 8 for the toy model of a spin splitted free electron gas with an attractive phonon coupling. Using this model we investigate the behavior of the functionals and compare with numerical solutions of Eliashberg theory and the results of Chapter 2. Because BCS theory considers a similar system, we expect results to be comparable, although our more sophisticated theory allows the calculation of  $T_c$ .

## 2. BCS and BdG in an Exchange-Splitting Field

The BCS theory of SC is built on the idea that single electrons form pairs due to an effectively attractive interaction. BCS proposed a wavefunction that has all the electrons condensed into one single two-electron wavefunction. The system shows a non-vanishing response to an externally applied vector potential, even in the static, homogeneous limit, which means it shows the Meissner effect [27]. It can be seen that the lack of (charged) particle conservation that was imposed by BCS translates into a continuity equation that is not fulfilled by the electrons alone [28]. Nambu showed that if, instead of bare coupling of electrons to the vector potential, one considers dressed, effective coupling, the resulting continuity equation contains a collective mode (later called Nambu-Goldstone mode) that adds to the current and charge. If a Coulomb interaction among the paired electrons is considered the excitations of the new Nambu-Goldstone field are pushed up to the plasma frequencies and no low lying excitations exist. We do not go into details of the derivation of the Meissner effect, but briefly discuss the BCS model of a system with a homogeneous magnetic field.

In a BCS model we replace the interactions among single electrons with an effective one, keeping only the matrix elements that couple the states  $k, \uparrow$  and  $-k, \downarrow$ . Then we perform a mean field approximation, replacing the pair creation  $\hat{c}_{-k\downarrow}^\dagger \hat{c}_{k\uparrow}^\dagger$  and annihilation operator  $\hat{c}_{k\uparrow} \hat{c}_{-k\downarrow}$  with their average in a (coherent) ground states that is determined self-consistently. The effective interaction is approximated with “a box” about the Fermi level (from  $-\Omega_d$  to  $\Omega_d$  which is the Debye phonon frequency cutoff and with height  $-V$ ) which leads to a fixed point equation for the mean field  $\Delta$ . In earlier works on the BCS model of a spin splitted system in the publications [29, 10] a peculiar behavior is found when one tries to linearize the BCS gap equation of the exchange splitted system

$$\frac{1}{\rho(0)V} = \int_0^{\Omega_d} d\varepsilon \frac{1}{\sqrt{\varepsilon^2 + \Delta^2}} (f_\beta(J - \sqrt{\varepsilon^2 + \Delta^2}) - f_\beta(J + \sqrt{\varepsilon^2 + \Delta^2})). \quad (2.1)$$

In the above equation  $\rho(0)$  is the DOS at the Fermi level and  $J$  is the splitting energy between up and down states.  $V$  is the effective attractive coupling parameter. With modern computers we easily solve Eq. (2.1) as a function of  $J$  and  $T$ <sup>1</sup> and recover the results of Ref. [29]. We normalize to  $\Delta_0$ , the solution for  $T \rightarrow 0$  and  $J = 0$ , and  $T_{c0}$  as the critical temperature for  $J = 0$  to remove the dependence on the parameters  $\rho(0)V$  and  $\Omega_d$ . In Fig. 2.1 a) we show results for this simple model. First, as the most important result, we see that below  $T/T_{c0} \approx 0.6$  the linearized  $T_c(J)$  curve (green) and the non-linear solutions deviate. We have to conclude that a solution with arbitrarily low  $\Delta$  does not exist below this temperature.

Although a solution to the non-linear equation (2.1) can be found even for large splittings  $J > \Delta_0/\sqrt{2}$ , comparing the free energy of this state

$$F_s = \rho(0) \sum_\sigma \int d\varepsilon \frac{2\varepsilon^2 + \text{sign}(\sigma)J + \Delta^2}{\varepsilon^2 + \Delta^2} f_\beta(\text{sign}(\sigma)J + \sqrt{\varepsilon^2 + \Delta^2}) + \frac{\Delta^2}{V}, \quad (2.2)$$

---

<sup>1</sup>We use  $\Omega_d = 0.2$  and  $\rho(0)V = 1.0$  in the numerical calculation.

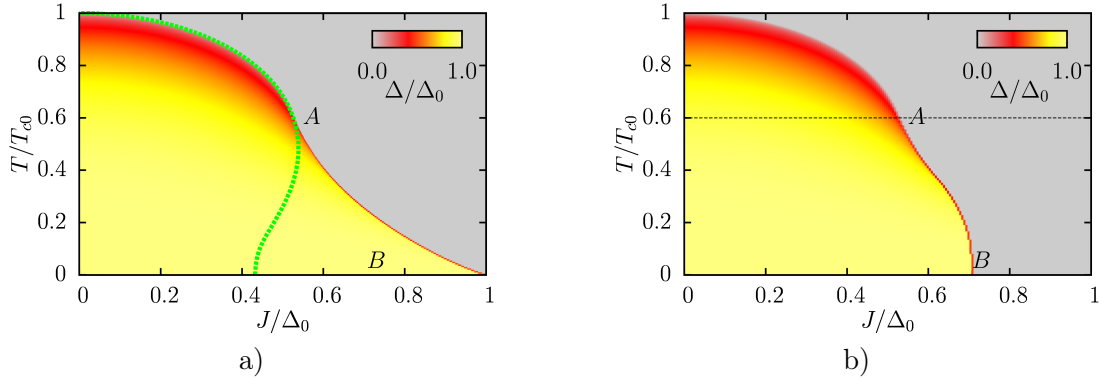


Figure 2.1.: BCS solutions for a spin splitted band structure [29]. In the panel a) we plot the solution  $\Delta$  whenever we can find one, while in b)  $\Delta$  is set to zero if the free energy favors the magnetic state. The green curve in a) shows the  $T_c(J)$  behavior from the linearized equation which has a curious shape that bends inwards. Below the thin dashed line in b) at the label  $A$  at  $T/T_{c0} \approx 0.6$  no solution with small  $\Delta$  exists and the transition is of first order. Label  $B$  at  $1/\sqrt{2}$  represents the Chandrasekhar-Clogston[30, 31] limit.

with the purely ferromagnetic state  $F_m = \rho(0)J^2$ , one is led to the conclusion that the latter is the more favorable one. We perform this comparison in Fig. 2.1 b) and plot the gap  $\Delta(T, J)$  only, if the SC state is the minimum of the free energy. The transition to the ferromagnetic state at  $T = 0$  at  $J = \Delta_0/\sqrt{2}$  (label  $B$  in Fig. 2.1 b) ) is called the Chandrasekhar-Clogston limit [30, 31]. The cross over from the SC to the magnetic phase is at finite  $\Delta$  and the transition is of first order. As can be seen in Fig. 2.1 b) this comparison cuts off the concave tail of the finite  $\Delta$  solutions in Fig. 2.1 a). In the plot we have normalized  $T$  by  $T_{c0}$  but note that  $\Delta_0$  and  $T_{c0}$  are related. BCS have estimated  $\Delta_0/(k_B T_c) \approx 1.75$ [3] in the weak coupling limit. Here we numerically obtain the slightly larger  $\Delta_0/(k_B T_c) \approx 1.91$  since we do not take the weak coupling limit in the integrals at this point. This analysis is crucial for the discussion of the more complicated equations in the context of Spin DFT for SCs in the next chapters.

Another interesting approach to describe SC in the presence of a magnetic field is presented by Powell *et al.* [10] who use a Hubbard model in connection with a homogenous exchange splitting. They treat the pairing part of the interactions among electrons in the system in the Hartree-Fock approximation, similar to BCS as described above and consequently arrive at a similar gap equation as compared to Eq. (2.1). The matrix elements of the KS system of Spin SCDFT within the spin decoupling approximation will turn out to have an similar analytic structure. Also, they give a discussion of why the transition is of first order. They note that the gap equation (2.1), and consequently  $\Delta$ , is independent on  $J$  at  $T = 0$ . At  $J = \Delta_0$  on the other hand the Fermi functions at  $T = 0$  in Eq. (2.1) add to zero and only the trivial solution  $\Delta = 0$  can be found. We see explicitly that  $\Delta = \Delta_0 \theta(\Delta_0 - J)$  and the transition is discontinuous  $T = 0$ .

### 3. SpinSCDFT: HK Theorem and KS Construction

The density functional approach to the many body problem consists of two fundamental steps. First, one realizes that the chosen set of densities contain all information of the interacting system under consideration. Second, one tries to reproduce the chosen set of densities of the exact system in an auxiliary solvable (read: non-interacting) KS system. This approach assumes that there is such a KS system (the KS potentials exist) for the interacting system under consideration. While the existence has been proven for normal state systems [32] under certain constraints, we shall always assume this so called  $v$ -representability in the context of this thesis. Choosing a non-interacting KS system involves single particle  $xc$  potentials which are functionals of these densities and need to be approximated in a practical calculation. In Section 3.1 of this Chapter we define the exact system. Then we choose a convenient set of densities  $n(\mathbf{r})$ ,  $\chi(\mathbf{r}, \mathbf{r}')$ ,  $\mathbf{m}(\mathbf{r})$  and  $\Gamma(\mathbf{R}_1 \dots \mathbf{R}_N)$  and prove the HK theorem in Section 3.2. Because the KS system is formally non-interacting, the nuclear and the electronic degrees of freedom separate and we discuss independently the nuclear part in Section 3.3 and the electronic part in Section 3.4. Taking the  $xc$  potentials as given, we find the unitary transformation that diagonalizes the electronic KS system for a SC in a magnetic field, resulting in the so called KSBdG equations. In Section 3.5 we discuss the special cases, first if we treat a singlet collinear SC and second if we further consider the case that SC pairs a quasi particle state with its time reversed only, which we refer to as the SDA. In Section 3.6 we discuss the consequence of symmetries in the KS system.

#### 3.1. Hamiltonian of the Interacting System

Consider the Hamiltonian in second quantization describing a solid state system<sup>1</sup>

$$\hat{H} = \hat{H}_e + \hat{H}_n + \hat{U}_{en} + \hat{H}_\Delta \quad (3.1)$$

with

$$\hat{H}_e = \hat{T}^e + \hat{V}^e + \hat{W}^{ee} - \mu\hat{N} + \hat{H}_B, \quad (3.2)$$

$$\hat{H}_n = \hat{T}^n + \hat{U}^{nn} + \hat{V}^n, \quad (3.3)$$

where

$$\hat{T}^e = \sum_{\sigma} \int d\mathbf{r} \hat{\psi}_{\sigma}^{\dagger}(\mathbf{r}) \frac{-\hbar^2}{2m_e} \nabla^2 \hat{\psi}_{\sigma}(\mathbf{r}) \quad (3.4)$$

Even though the Hamiltonian will in general not be diagonal in spin, i.e. we consider the non-collinear case, we work in the basis where  $\hat{\psi}_{\sigma}^{\dagger}(\mathbf{r})$  creates a particle at  $\mathbf{r}$  with spin  $\sigma$  which means we define the electronic field operator with respect to a collinear single particle basis. We work in pure basis sets in many parts of the thesis, also in different contexts. Doing so has the advantage that the coefficients carry a similar quantum number and this makes it easier to

---

<sup>1</sup>We define the general Hamiltonian  $\hat{H}$  such, that the term  $-\mu\hat{N}$  is included.

introduce approximations. We use the notation<sup>2</sup>

$$\hat{\psi}_{\uparrow}^{\dagger}(\mathbf{r}) \equiv \begin{pmatrix} \hat{\psi}^{\dagger}(\mathbf{r} \uparrow) \\ 0 \end{pmatrix} \quad \hat{\psi}_{\downarrow}^{\dagger}(\mathbf{r}) \equiv \begin{pmatrix} 0 \\ \hat{\psi}^{\dagger}(\mathbf{r} \downarrow) \end{pmatrix} \quad (3.5)$$

representing the fact that we use a pure spinor basis system. Because there will almost always be a sum over spin (as in Eq. (3.4)) we introduce

$$\hat{\psi}^{\dagger}(\mathbf{r}) \equiv \sum_{\sigma} \hat{\psi}_{\sigma}^{\dagger}(\mathbf{r}) \equiv \begin{pmatrix} \hat{\psi}^{\dagger}(\mathbf{r} \uparrow) \\ \hat{\psi}^{\dagger}(\mathbf{r} \downarrow) \end{pmatrix}. \quad (3.6)$$

This notation will reappear later in the Nambu notation and is chosen to clutter formulas with indices as little as possible. In this notation the density operator is  $\hat{n}(\mathbf{r}) = \hat{\psi}^{\dagger}(\mathbf{r}) \cdot \hat{\psi}(\mathbf{r})$  and the external potential operator reads

$$\hat{V}^e = \int d\mathbf{r} \hat{n}(\mathbf{r}) v_{\text{ext}}(\mathbf{r}), \quad (3.7)$$

the electronic interaction operator  $\hat{W}^{ee}$  with the potential field  $w_{\sigma\sigma'}(\mathbf{r}, \mathbf{r}')$  (typically the Coulomb interaction which is independent of spin)

$$\hat{W}^{ee} = \sum_{\sigma\sigma'} \int d\mathbf{r} \int d\mathbf{r}' \hat{\psi}^{\dagger}(\mathbf{r}\sigma) \hat{\psi}^{\dagger}(\mathbf{r}'\sigma') w_{\sigma\sigma'}(\mathbf{r}, \mathbf{r}') \hat{\psi}(\mathbf{r}'\sigma') \hat{\psi}(\mathbf{r}\sigma), \quad (3.8)$$

and the electron number operator is

$$\hat{N} = \int d\mathbf{r} \hat{n}(\mathbf{r}). \quad (3.9)$$

The particle number operator for the nuclei is

$$\hat{N}_n = \int d\mathbf{R} \hat{\zeta}^{\dagger}(\mathbf{R}) \hat{\zeta}(\mathbf{R}). \quad (3.10)$$

where the operator  $\hat{\zeta}(\mathbf{R})$  creates the nuclear field at location  $\mathbf{R}$ . For simplicity, we assume that all nuclei are identical so that the nuclear kinetic energy operator is

$$\hat{T}^n = \int d\mathbf{R} \hat{\zeta}^{\dagger}(\mathbf{R}) \frac{-\hbar^2}{2M} \nabla_{\mathbf{R}}^2 \hat{\zeta}(\mathbf{R}) \quad (3.11)$$

and the nuclear interacting (the Coulomb potential field) reads

$$\hat{U}^{nn} = \frac{e^2}{4\pi\epsilon_0} \frac{Z^2}{2} \int d\mathbf{R} \int d\mathbf{R}' \frac{\hat{\zeta}^{\dagger}(\mathbf{R}) \hat{\zeta}^{\dagger}(\mathbf{R}') \hat{\zeta}(\mathbf{R}') \hat{\zeta}(\mathbf{R})}{|\mathbf{R} - \mathbf{R}'|}. \quad (3.12)$$

Here  $Z$  is the nuclear charge. We assume an external potential acting on the nuclei of the form

$$\hat{V}^n = \int d\mathbf{R}_1 \dots \int d\mathbf{R}_{N_n} \hat{\zeta}^{\dagger}(\mathbf{R}_1) \dots \hat{\zeta}^{\dagger}(\mathbf{R}_{N_n}) W_{\text{ext}}(\mathbf{R}_1 \dots \mathbf{R}_{N_n}) \hat{\zeta}(\mathbf{R}_{N_n}) \dots \hat{\zeta}(\mathbf{R}_1). \quad (3.13)$$

The reason why we choose this unconventional  $N_n$ -body external nuclear potential is that a ordinary one-body potential would yield non-interacting nuclear-KS orbitals. So one chooses a many body potential that couples the nuclei and allows the existence of collective modes also

<sup>2</sup>We define  $-\sigma$  is always the opposite of  $\sigma$ .



in the KS system (KS phonons). The scheme is then more easily related to the standard Born-Oppenheimer approximation.

There also appears the Coulomb interacting between the electrons and the nuclei:

$$\hat{U}^{en} = \frac{Ze^2}{8\pi\epsilon_0} \int d\mathbf{R} \int d\mathbf{r} \frac{\hat{\zeta}^\dagger(\mathbf{R})\hat{n}(\mathbf{r})\hat{\zeta}(\mathbf{R})}{|\mathbf{R} - \mathbf{r}|}. \quad (3.14)$$

We assume that there is an external magnetic field acting through

$$\hat{H}_B = \int d\mathbf{r} \hat{\mathbf{m}}(\mathbf{r}) \cdot \mathbf{B}_{\text{ext}}(\mathbf{r}) \quad (3.15)$$

where<sup>3</sup>

$$\hat{\mathbf{m}}(\mathbf{r}) = -g_s\mu_B \hat{\psi}^\dagger(\mathbf{r}) \cdot \mathbf{S} \cdot \hat{\psi}(\mathbf{r}). \quad (3.16)$$

Typically the spontaneous magnetization is described by taking the limit  $\mathbf{B}_{\text{ext}}(\mathbf{r}) \rightarrow 0$  at the end of the derivation (after the thermodynamical limit is taken). Experimentally one always measures a finite time so the Ergodic hypothesis is not necessarily fulfilled. In the case of symmetry breaking as in ferromagnetism (the spin rotational symmetry is broken in a magnet), only the regions of phase space corresponding to a finite magnetization in one given direction are important on the time scales of the experiment. If  $\mathbf{B}_{\text{ext}}(\mathbf{r})$  was zero, identically, all microscopic states that are connected by a simple rotation in spin space had the same weight and would equally enter thermal averages and the magnetization has to average to zero. Here, in the mathematical description,  $\mathbf{B}_{\text{ext}}(\mathbf{r})$  breaks the spin rotational symmetry and allows the magnetization to build up as microscopic states favor a particular orientation in spin space. In a system that would undergo a phase transition to a magnetic state, this breaking - however small - leads to a finite magnetization. This is expressed by the self-consistent KS potential adopting a finite value, even if the external field is set to zero after an initial symmetry breaking.

Finally, the external pairing Hamiltonian is defined by

$$\hat{H}_\Delta = \frac{1}{2} \int d\mathbf{r} \int d\mathbf{r}' \sum_{\sigma\sigma'} \left( \Delta_{\sigma\sigma'}^{\text{ext}*}(\mathbf{r}, \mathbf{r}') \hat{\psi}(\mathbf{r}\sigma) \hat{\psi}(\mathbf{r}'\sigma') + \Delta_{\sigma\sigma'}^{\text{ext}}(\mathbf{r}, \mathbf{r}') \hat{\psi}^\dagger(\mathbf{r}'\sigma') \hat{\psi}^\dagger(\mathbf{r}\sigma) \right). \quad (3.17)$$

Due to the anticommutation relations, if  $\Delta_{\sigma\sigma'}^{\text{ext}}(\mathbf{r}, \mathbf{r}')$  has a totally symmetric part it cancels in the integral. As a consequence we need to consider only  $\Delta_{\sigma\sigma'}^{\text{ext}}(\mathbf{r}, \mathbf{r}')$  that are antisymmetric under particle exchange ( $\mathbf{r}\sigma \leftrightarrow \mathbf{r}'\sigma'$ ). We rewrite the potential using the Pauli matrices and the spinors which has the advantage of giving the potential a well defined symmetry in spin and real space. With the definitions

$$\Delta_s^{\text{ext}}(\mathbf{r}, \mathbf{r}') = \frac{1}{2} (\Delta_{\uparrow\downarrow}^{\text{ext}}(\mathbf{r}, \mathbf{r}') - \Delta_{\downarrow\uparrow}^{\text{ext}}(\mathbf{r}, \mathbf{r}')), \quad (3.18)$$

$$\Delta_{tx}^{\text{ext}}(\mathbf{r}, \mathbf{r}') = \frac{1}{2} (\Delta_{\downarrow\downarrow}^{\text{ext}}(\mathbf{r}, \mathbf{r}') - \Delta_{\uparrow\uparrow}^{\text{ext}}(\mathbf{r}, \mathbf{r}')), \quad (3.19)$$

$$\Delta_{ty}^{\text{ext}}(\mathbf{r}, \mathbf{r}') = \frac{1}{2} (\Delta_{\downarrow\downarrow}^{\text{ext}}(\mathbf{r}, \mathbf{r}') + \Delta_{\uparrow\uparrow}^{\text{ext}}(\mathbf{r}, \mathbf{r}')), \quad (3.20)$$

$$\Delta_{tz}^{\text{ext}}(\mathbf{r}, \mathbf{r}') = \frac{1}{2} (\Delta_{\uparrow\downarrow}^{\text{ext}}(\mathbf{r}, \mathbf{r}') + \Delta_{\downarrow\uparrow}^{\text{ext}}(\mathbf{r}, \mathbf{r}')) \quad (3.21)$$

and

$$\hat{\chi}(\mathbf{r}, \mathbf{r}') = \hat{\psi}(\mathbf{r}) \cdot \hat{\Phi}^* \cdot \hat{\psi}(\mathbf{r}'), \quad \Delta_{\text{ext}}(\mathbf{r}, \mathbf{r}') = (\Delta_s^{\text{ext}}, \Delta_{tx}^{\text{ext}}, \Delta_{ty}^{\text{ext}}, \Delta_{tz}^{\text{ext}})^T \quad (3.22)$$

<sup>3</sup>In principle, the internal energy is reduced if the magnetization and the magnetic field are parallel. We use a “negative” magnetization because this way DFT functionals for the magnetization are consistent in the sign convention among all densities. Note that this convention also affects the sign convention of response kernels and higher order derivatives.

where

$$\Phi = (i\sigma_y, -\sigma_z, \sigma_0, \sigma_x)^T, \quad (3.23)$$

the pair term becomes<sup>4</sup>

$$\hat{H}_\Delta = \frac{1}{2} \int d\mathbf{r} \int d\mathbf{r}' \left( \Delta^{\text{ext}*}(\mathbf{r}, \mathbf{r}') \cdot \hat{\chi}(\mathbf{r}, \mathbf{r}') + (\Delta^{\text{ext}*}(\mathbf{r}, \mathbf{r}') \cdot \hat{\chi}(\mathbf{r}, \mathbf{r}'))^\dagger \right). \quad (3.24)$$

Also here one takes the limit of  $\Delta^{\text{ext}}(\mathbf{r}, \mathbf{r}') \rightarrow 0$  at the end of the derivation. It is important to note that the starting point of our DFT is the system with already broken symmetries.

### 3.2. 1:1 Correspondence of External Potentials and Densities

In this Section, we show the first step in the scheme, commonly referred to as the Hohenberg-Kohn theorem. We shall see that there is only one set of external potentials leading to one set of densities

$$n(\mathbf{r}) = \langle \hat{n}(\mathbf{r}) \rangle \quad (3.25)$$

$$\chi(\mathbf{r}, \mathbf{r}') = \langle \hat{\chi}(\mathbf{r}, \mathbf{r}') \rangle \quad (3.26)$$

$$\mathbf{m}(\mathbf{r}) = \langle \hat{\mathbf{m}}(\mathbf{r}) \rangle \quad (3.27)$$

and the nuclear density

$$\Gamma(\mathbf{R}_1 \dots \mathbf{R}_N) = \langle \hat{\zeta}^\dagger(\mathbf{R}_1) \dots \hat{\zeta}^\dagger(\mathbf{R}_{N_n}) \hat{\zeta}(\mathbf{R}_{N_n}) \dots \hat{\zeta}(\mathbf{R}_1) \rangle. \quad (3.28)$$

Thus, the densities implicitly contain all information because the statistical operator is a functional of the external potentials and thereby a functional of the densities. The proof itself is analogue to the proof of the Hohenberg-Kohn theorem for finite temperature by Mermin [33]. We define the grand canonical potential functional

$$\Omega[\hat{\rho}] = \text{Tr} \left\{ \hat{\rho} \left( \hat{H} + \frac{1}{\beta} \ln \hat{\rho} \right) \right\}, \quad (3.29)$$

with  $\hat{\rho}$  being a positive definite matrix with trace one. If we insert the equilibrium grand-canonical-statistical operator

$$\hat{\rho}_0 = \frac{e^{-\beta \hat{H}}}{\text{Tr} \{ e^{-\beta \hat{H}} \}}, \quad (3.30)$$

this functional becomes the equilibrium grand canonical potential

$$\Omega_0 \equiv \Omega[\hat{\rho}_0] = -\frac{1}{\beta} \ln(\text{Tr} \{ e^{-\beta \hat{H}} \}). \quad (3.31)$$

It is shown in Ref. [33] that  $\Omega_0$  is the minimum of  $\Omega[\hat{\rho}]$ .

$$\Omega[\hat{\rho}] > \Omega[\hat{\rho}_0], \quad \hat{\rho} \neq \hat{\rho}_0 \quad (3.32)$$

As for the normal state HK theorem, we assume that the map from densities to external potentials is not invertible, which means there is a set of densities that can be associated with two different sets of external potentials and show that this results in a contradiction. Let the system of

---

<sup>4</sup>Here,  $\cdot$  is used in two ways. First as the usual spin summation and second as the scalar product in  $4d$  singlet/triplet space, mapping to spin matrices. As the distinction is clear from the context we decide not to clutter the notation with an additional symbol.

unprimed external potentials be described by  $\hat{\rho}_0, \hat{H}$  and  $\Omega[\hat{\rho}]$  and the primed system by  $\hat{\rho}'_0, \hat{H}'$  and  $\Omega'[\hat{\rho}']$ . The primed Hamiltonian reads

$$\hat{H}' = \hat{T}^e + \hat{W}^{ee} + \hat{T}^n + \hat{U}^{nn} + \hat{U}_{en} + \hat{V}^{nn'} + \hat{V}^{ee'} - \mu' \cdot \hat{N} + \hat{H}'_{\Delta} + \hat{H}'_B. \quad (3.33)$$

So we can express the primed in terms of the unprimed Hamiltonian

$$\hat{H}' = \hat{H} + \hat{\Delta}H, \quad (3.34)$$

where difference term is

$$\hat{\Delta}H = (\hat{V}^{nn'} - \hat{V}^{nn}) + (\hat{H}'_B - \hat{H}_B) + (\hat{V}^{ee'} - \hat{V}^{ee}) - (\mu' + \mu) \cdot \hat{N} + (\hat{H}'_{\Delta} - \hat{H}_{\Delta}). \quad (3.35)$$

We can evaluate  $\Omega[\hat{\rho}_0]$  at the primed statistical operator and make use of the minimum principle of Eq. (3.32). Then we use the above relation to express the result in terms of the primed grand canonical potential.

$$\Omega[\hat{\rho}_0] < \Omega[\hat{\rho}'_0] = \text{Tr}\left\{\hat{\rho}'_0\left(\hat{H} + \frac{1}{\beta} \ln \hat{\rho}'_0\right)\right\} = \Omega'[\hat{\rho}'_0] + \text{Tr}\{\hat{\rho}'_0 \hat{\Delta}H\}. \quad (3.36)$$

On the other hand, the minimum principle is also valid for the primed system. An analogous procedure yields

$$\Omega'[\hat{\rho}'_0] < \Omega'[\hat{\rho}_0] = \text{Tr}\left\{\hat{\rho}_0\left(\hat{H}' + \frac{1}{\beta} \ln \hat{\rho}_0\right)\right\} = \Omega[\hat{\rho}_0] - \text{Tr}\{\hat{\rho}_0 \hat{\Delta}H\}. \quad (3.37)$$

The assumption is that the densities are equal in both primed and unprimed systems, i. e.

$$n(\mathbf{r}) = \text{Tr}\left\{\hat{\rho}_0 \hat{n}(\mathbf{r})\right\} = \text{Tr}\left\{\hat{\rho}'_0 \hat{n}(\mathbf{r})\right\} \quad (3.38)$$

$$\chi(\mathbf{r}, \mathbf{r}') = \text{Tr}\left\{\hat{\rho}_0 \chi(\mathbf{r}, \mathbf{r}')\right\} = \text{Tr}\left\{\hat{\rho}'_0 \chi(\mathbf{r}, \mathbf{r}')\right\} \quad (3.39)$$

$$\mathbf{m}(\mathbf{r}) = \text{Tr}\left\{\hat{\rho}_0 \hat{\mathbf{m}}(\mathbf{r})\right\} = \text{Tr}\left\{\hat{\rho}'_0 \hat{\mathbf{m}}(\mathbf{r})\right\} \quad (3.40)$$

$$\begin{aligned} \Gamma(\mathbf{R}_1 \dots \mathbf{R}_N) &= \text{Tr}\left\{\hat{\rho}_0 (\hat{\zeta}^\dagger(\mathbf{R}_1) \dots \hat{\zeta}^\dagger(\mathbf{R}_N) \hat{\zeta}(\mathbf{R}_N) \dots \hat{\zeta}(\mathbf{R}_1))\right\} \\ &= \text{Tr}\left\{\hat{\rho}'_0 (\hat{\zeta}^\dagger(\mathbf{R}_1) \dots \hat{\zeta}^\dagger(\mathbf{R}_N) \hat{\zeta}(\mathbf{R}_N) \dots \hat{\zeta}(\mathbf{R}_1))\right\} \end{aligned} \quad (3.41)$$

and thus

$$\text{Tr}\{\hat{\rho}'_0 \hat{\Delta}H\} \equiv \text{Tr}\{\hat{\rho}_0 \hat{\Delta}H\}. \quad (3.42)$$

We obtain a contradiction by adding both equations (3.36) and (3.37)

$$\Omega[\hat{\rho}_0] + \Omega'[\hat{\rho}'_0] < \Omega[\hat{\rho}_0] + \Omega'[\hat{\rho}'_0]. \quad (3.43)$$

We conclude that one set of densities is uniquely connected with one set of external potentials so that the map is invertible.

Since the set of densities  $(n(\mathbf{r}), \chi(\mathbf{r}, \mathbf{r}'), \mathbf{m}(\mathbf{r}), \Gamma(\mathbf{R}_1 \dots \mathbf{R}_N))$  uniquely determine the potentials  $(v_{\text{ext}}(\mathbf{r}), \Delta^{\text{ext}}(\mathbf{r}, \mathbf{r}'), \mathbf{B}_{\text{ext}}(\mathbf{r}), W_{\text{ext}}(\mathbf{R}_1 \dots \mathbf{R}_N))$  which in turn determines the statistical operator, all observables, including the grand canonical potential functional of Eq. (3.29) can be written as functionals of the four densities. Let us regard the external potentials, i. e. the system, as fixed from now on. The now fixed grand canonical functional reads

$$\Omega_{(v_{\text{ext}} - \mu, \Delta^{\text{ext}}, \mathbf{A}_{\text{ext}}, W_{\text{ext}})}[n, \chi, \mathbf{m}, \Gamma] = \langle \hat{H} \rangle - \frac{1}{\beta} S[n, \chi, \mathbf{m}, \Gamma] \quad (3.44)$$

where the entropy is given by

$$S[n, \boldsymbol{\chi}, \mathbf{m}, \Gamma] = -\text{Tr}\{\hat{\rho}_0[n, \boldsymbol{\chi}, \mathbf{m}, \Gamma] \ln(\hat{\rho}_0[n, \boldsymbol{\chi}, \mathbf{m}, \Gamma])\}. \quad (3.45)$$

Using the thermal average of the Hamiltonian we obtain

$$\begin{aligned} \Omega_{(v_{\text{ext}}-\mu, \Delta_{\text{ext}}, \mathbf{B}_{\text{ext}}, W_{\text{ext}})}[n, \boldsymbol{\chi}, \mathbf{m}, \Gamma] = \\ F[n, \boldsymbol{\chi}, \mathbf{m}, \Gamma] + \int \mathbf{m}(\mathbf{r}) \cdot \mathbf{B}_{\text{ext}}(\mathbf{r}) d\mathbf{r} \\ \int d\mathbf{r} (v_{\text{ext}}(\mathbf{r}) - \mu) \cdot n(\mathbf{r}) - \int d\mathbf{r} \int d\mathbf{r}' (\boldsymbol{\Delta}^{\text{ext}*}(\mathbf{r}, \mathbf{r}') \cdot \boldsymbol{\chi}(\mathbf{r}, \mathbf{r}') + \text{c.c.}) \end{aligned} \quad (3.46)$$

$$+ \int \dots \int d\mathbf{R}_1 \dots d\mathbf{R}_{N_n} \Gamma(\mathbf{R}_1, \dots, \mathbf{R}_{N_n}) W_{\text{ext}}(\mathbf{R}_1, \dots, \mathbf{R}_{N_n}), \quad (3.47)$$

where we have defined

$$F[n, \boldsymbol{\chi}, \mathbf{m}, \Gamma] \equiv \langle \hat{T}^e \rangle + \langle \hat{W}^{ee} \rangle - \langle \hat{T}^n \rangle + \langle \hat{U}^{nn} \rangle + \langle \hat{U}^{en} \rangle - \frac{1}{\beta} S[n, \boldsymbol{\chi}, \mathbf{m}, \Gamma]. \quad (3.48)$$

Note that  $F[n, \boldsymbol{\chi}, \mathbf{m}, \Gamma]$  is universal in the sense that it does not depend on any external potential, i. e. on any specific system. The minimum principle of Eq. (3.32) guarantees

$$\left. \frac{\delta \Omega_{(v_{\text{ext}}-\mu, \Delta_{\text{ext}}, \mathbf{B}_{\text{ext}}, W_{\text{ext}})}[n, \boldsymbol{\chi}_0, \mathbf{m}_0, \Gamma_0]}{\delta n(\mathbf{r})} \right|_{n=n_0} = 0 \quad (3.49)$$

$$\left. \frac{\delta \Omega_{(v_{\text{ext}}-\mu, \Delta_{\text{ext}}, \mathbf{B}_{\text{ext}}, W_{\text{ext}})}[n_0, \boldsymbol{\chi}, \mathbf{m}_0, \Gamma_0]}{\delta \boldsymbol{\chi}(\mathbf{r}, \mathbf{r}')} \right|_{\boldsymbol{\chi}=\boldsymbol{\chi}_0} = 0 \quad (3.50)$$

$$\left. \frac{\delta \Omega_{(v_{\text{ext}}-\mu, \Delta_{\text{ext}}, \mathbf{B}_{\text{ext}}, W_{\text{ext}})}[n_0, \boldsymbol{\chi}_0, \mathbf{m}, \Gamma_0]}{\delta \mathbf{m}(\mathbf{r})} \right|_{\mathbf{m}=\mathbf{m}_0} = 0 \quad (3.51)$$

$$\left. \frac{\delta \Omega_{(v_{\text{ext}}-\mu, \Delta_{\text{ext}}, \mathbf{B}_{\text{ext}}, W_{\text{ext}})}[n_0, \boldsymbol{\chi}_0, \mathbf{m}_0, \Gamma]}{\delta \Gamma(\mathbf{R}_1, \dots, \mathbf{R}_N)} \right|_{\Gamma=\Gamma_0} = 0 \quad (3.52)$$

where  $n_0, \boldsymbol{\chi}_0, \mathbf{m}_0$  and  $\Gamma_0$  are the equilibrium densities of the system with the fixed external potentials.  $\delta \mathbf{m}(\mathbf{r})$  ( $\delta \boldsymbol{\chi}(\mathbf{r}, \mathbf{r}')$ ) is shorthand for the variation with respect to the 3 (4) individual components. This is the variational principle of Spin SCDFT.

The second step in the formulation of a DFT is the assumption that the exact densities can be calculated in an auxiliary non-interacting system. For this assumption to hold one needs for every given set of densities a set of single particle potentials that reproduce these densities in a non-interacting system. Now the non interacting system is chosen so that the electrons do not interact with each other and the nuclei while the KS nuclei do interact via an effective  $N_n$ -body potential. The Hamiltonian reads

$$\hat{H}_{\text{KS}} = \hat{H}_s^e + \hat{H}_s^n, \quad (3.53)$$

where we have separated the Hamiltonian into an electronic  $\hat{H}_s^e$

$$\begin{aligned} \hat{H}_s^e \equiv \int d\mathbf{r} \hat{\psi}^\dagger(\mathbf{r}) \cdot \sigma_0 \left( \frac{1}{2m_e} (-i\hbar \nabla)^2 + v_s(\mathbf{r}) - \mu \right) \cdot \hat{\psi}(\mathbf{r}) \\ + \int d\mathbf{r} \hat{\mathbf{m}}(\mathbf{r}) \cdot \mathbf{B}_s(\mathbf{r}) - \frac{1}{2} \int d\mathbf{r} \int d\mathbf{r}' (\hat{\boldsymbol{\chi}}(\mathbf{r}, \mathbf{r}') \cdot \boldsymbol{\Delta}_s^*(\mathbf{r}, \mathbf{r}') + \text{h.c.}) \end{aligned} \quad (3.54)$$

and nuclear part  $\hat{H}_s^n$

$$\begin{aligned} \hat{H}_s^n &\equiv \int d\mathbf{R} \hat{\Phi}^\dagger(\mathbf{R}) \left( \frac{1}{2M} (-i\hbar \nabla_{\mathbf{R}})^2 \right) \hat{\Phi}(\mathbf{R}) + \\ &+ \int \dots \int d\mathbf{R}_1 \dots d\mathbf{R}_{N_n} \hat{\Phi}^\dagger(\mathbf{R}_1) \dots \hat{\Phi}^\dagger(\mathbf{R}_{N_n}) W_s(\mathbf{R}_1, \dots, \mathbf{R}_{N_n}) \hat{\Phi}(\mathbf{R}_1) \dots \hat{\Phi}(\mathbf{R}_{N_n}). \end{aligned} \quad (3.55)$$

In analogy to Eq. (3.47), the grand canonical potential for this non interacting system with densities  $(n_s(\mathbf{r}), \chi_s(\mathbf{r}, \mathbf{r}'), \mathbf{m}_s(\mathbf{r}), \Gamma_s(\mathbf{R}_1 \dots \mathbf{R}_{N_n}))$  reads

$$\begin{aligned} \Omega_{(v_s - \mu, \Delta_s, \mathbf{B}_s, W_s)}^s [n_s, \mathbf{m}_s, \chi_s, \Gamma_s] &= F_s[n_s, \mathbf{m}_s, \chi_s, \Gamma_s] + \int d\mathbf{r} (v_s(\mathbf{r}) - \mu) n_s(\mathbf{r}) \\ &+ \int d\mathbf{r} \mathbf{m}(\mathbf{r}) \cdot \mathbf{B}_s(\mathbf{r}) - \int d\mathbf{r} \int d\mathbf{r}' \left( \Delta_s^*(\mathbf{r}, \mathbf{r}') \cdot \chi_s(\mathbf{r}, \mathbf{r}') + \text{h.c.} \right) \\ &+ \int d\mathbf{R}_1 \dots \int d\mathbf{R}_{N_n} \Gamma_s(\mathbf{R}_1 \dots \mathbf{R}_{N_n}) W_s(\mathbf{R}_1 \dots \mathbf{R}_{N_n}) \end{aligned} \quad (3.56)$$

and with the universal functional

$$F_s[n_s, \mathbf{m}_s, \chi_s, \Gamma_s] = \langle \hat{T}^e \rangle [n_s, \mathbf{m}_s, \chi_s, \Gamma_s] + \langle T_s^n \rangle [n_s, \mathbf{m}_s, \chi_s, \Gamma_s] - \frac{1}{\beta} \cdot S_s[n_s, \mathbf{m}_s, \chi_s, \Gamma_s] \quad (3.57)$$

where  $S_s[n_s, \mathbf{m}_s, \chi_s, \Gamma_s]$  is the entropy of the non interacting system and  $T_s^n[n_s, \mathbf{m}_s, \chi_s, \Gamma_s]$  is the non interacting nuclear kinetic energy functional. Note that we have chosen the same temperature in the KS system that prevails in the interacting one. Since there is no coupling between the electrons and nuclei, the electronic and the nuclear Hamiltonian commute

$$[\hat{H}_s^n, \hat{H}_s^e] = 0 \quad (3.58)$$

and the equilibrium grand canonical potential takes the form

$$\begin{aligned} \Omega_{(v_s - \mu, \Delta_s, \mathbf{B}_s, W_s)} [n_{s,0}, \mathbf{m}_{s,0}, \chi_{s,0}, \Gamma_{s,0}] &= -\frac{1}{\beta} \ln(\text{Tr}\{e^{-\beta \cdot (\hat{H}_s^e + \hat{H}_s^n)}\}) \\ &= \Omega_{(v_s - \mu, \Delta_s, \mathbf{B}_s, W_s)}^e [n_{s,0}, \mathbf{m}_{s,0}, \chi_{s,0}, \Gamma_{s,0}] + \Omega_{(v_s - \mu, \Delta_s, \mathbf{B}_s, W_s)}^n [n_{s,0}, \mathbf{m}_{s,0}, \chi_{s,0}, \Gamma_{s,0}]. \end{aligned} \quad (3.59)$$

This means that the Fock space basis we use to evaluate the trace will be a product of electronic and nuclear wavefunctions. It is therefore possible to solve the electronic and nuclear Schrödinger equation separately as in a Born-Oppenheimer approximation [34].

### 3.2.1. Connection to the interacting system

To construct the KS system we need an expression for the KS potentials that yield the same densities as the given interacting system. We rewrite the grand potential and make use of the fact that we had assumed that we can represent every set of equilibrium densities in a KS system, i. e. we can insert the interacting densities into density functionals of the KS system

$$\begin{aligned} \Omega_{(v_{\text{ext}} - \mu, \Delta^{\text{ext}}, \mathbf{B}_{\text{ext}}, W_{\text{ext}})} [n, \chi, \mathbf{m}, \Gamma] &= F_s[n, \chi, \mathbf{m}, \Gamma] + F_{\text{xc}}[n, \chi, \mathbf{m}, \Gamma] + E_H^{ee}[n] + E_H^{en}[n, \Gamma] + \int d\mathbf{r} n(\mathbf{r}) (v_{\text{ext}}(\mathbf{r}) - \mu) \\ &- \iint d\mathbf{r} d\mathbf{r}' \left( \hat{\chi}(\mathbf{r}, \mathbf{r}') \cdot \Delta^{\text{ext}*}(\mathbf{r}, \mathbf{r}') + \text{h.c.} \right) + \int d\mathbf{r} \hat{\mathbf{m}}(\mathbf{r}) \cdot \mathbf{B}_{\text{ext}}(\mathbf{r}) \\ &+ \int d\mathbf{R}_1 \dots \int d\mathbf{R}_{N_n} \Gamma(\mathbf{R}_1 \dots \mathbf{R}_{N_n}) W_{\text{ext}}(\mathbf{R}_1 \dots \mathbf{R}_{N_n}) \end{aligned} \quad (3.61)$$

where we have explicitly included the Hartree potential

$$E_H^{ee}[n] = \frac{e^2}{4\pi\epsilon_0} \int d\mathbf{r} \int d\mathbf{r}' \frac{n(\mathbf{r})n(\mathbf{r}')}{2|\mathbf{r} - \mathbf{r}'|}, \quad (3.62)$$

as is can be treated exactly. The electron-nuclei interaction  $E_H^{en}[n, \Gamma]$  reads

$$E_H^{en}[n, \Gamma] = -Ze^2 \sum_{\alpha} \int d\mathbf{r} \int d\mathbf{R}_1 \dots \int d\mathbf{R}_{N_n} \frac{n(\mathbf{r})\Gamma(\mathbf{R}_1 \dots \mathbf{R}_{N_n})}{|\mathbf{r} - \mathbf{R}_{\alpha}|}. \quad (3.63)$$

To keep the relation exact the  $xc$  functional is introduced

$$F_{xc}[n, \boldsymbol{\chi}, \mathbf{m}, \Gamma] \equiv F[n, \boldsymbol{\chi}, \mathbf{m}, \Gamma] - F_s[n, \boldsymbol{\chi}, \mathbf{m}, \Gamma] - E_H^{ee}[n, \boldsymbol{\chi}] - E_H^{en}[n, \Gamma]. \quad (3.64)$$

We can apply the variational principle for the electronic density of Eq. (3.49) to our rewritten grand canonical potential of Eq. (3.61). This yields

$$0 = \frac{\delta}{\delta n(\mathbf{r})} \left( F_{xc}[n, \mathbf{m}_0, \boldsymbol{\chi}_0, \Gamma_0] + F_s[n, \mathbf{m}_0, \boldsymbol{\chi}_0, \Gamma_0] + E_H^{ee}[n] + E_H^{en}[n, \Gamma_0] + \int d\mathbf{r} (v_{\text{ext}}(\mathbf{r}) - \mu)n(\mathbf{r}) \right) \Big|_{n=n_0}. \quad (3.65)$$

We define, as in normal state DFT, the  $xc$  potential by

$$v_{xc}[n, \mathbf{m}, \boldsymbol{\chi}, \Gamma](\mathbf{r}) \equiv \frac{\delta F_{xc}}{\delta n(\mathbf{r})}[n, \mathbf{m}, \boldsymbol{\chi}, \Gamma] \quad (3.66)$$

and apply the functional derivative to defining equation of the non-interacting grand potential (Eq. 3.56) resulting in

$$\frac{\delta F_s[n_s, \mathbf{m}_s, \boldsymbol{\chi}_s, \Gamma_s]}{\delta n_s(\mathbf{r})} \Big|_{n_s=n_{s,0}} = \frac{\delta}{\delta n_s(\mathbf{r})} \left( \Omega_{(v_s-\mu, \Delta_s, \mathbf{m}_s, W_s)}[n_s, \mathbf{m}_s, \boldsymbol{\chi}_s, \Gamma_s] + \int d\mathbf{r}' n_s(\mathbf{r}') (v_s[n_s, \mathbf{m}_s, \boldsymbol{\chi}_s, \Gamma_s](\mathbf{r}) - \mu) \right) \Big|_{n_s=n_{s,0}}. \quad (3.67)$$

If we now fix the external potentials of  $\Omega_{(v_s-\mu, \Delta_s, \mathbf{m}_s, W_s)}$  to the ones that reproduce the interacting densities, the HK minimum principle Eq. (3.49) makes the functional derivative of the grand potential vanish in the equilibrium. The equilibrium densities are the same in both systems so we conclude that

$$\frac{\delta F_s}{\delta n_s(\mathbf{r})}[n_s, \mathbf{m}_0, \boldsymbol{\chi}_0, \Gamma_0] \Big|_{n_s=n_0} = -v_s[n_0, \mathbf{m}_0, \boldsymbol{\chi}_0, \Gamma_0](\mathbf{r}) + \mu. \quad (3.68)$$

Inserting this result in Eq. (3.65), we obtain

$$v_s[n_0, \mathbf{m}_0, \boldsymbol{\chi}_0, \Gamma_0](\mathbf{r}) = v_{\text{ext}}(\mathbf{r}) + v_{xc}[n_0, \mathbf{m}_0, \boldsymbol{\chi}_0, \Gamma_0](\mathbf{r}) + \int d\mathbf{r}' \frac{n_0(\mathbf{r}')}{|\mathbf{r} - \mathbf{r}'|} - Z \sum_{\alpha} \int d\mathbf{R}_1 \dots \int d\mathbf{R}_{N_n} \frac{\Gamma_0(\mathbf{R}_1, \dots, \mathbf{R}_{N_n})}{|\mathbf{r} - \mathbf{R}_{\alpha}|} \quad (3.69)$$

Deducing the form of  $\Delta_s(\mathbf{r}, \mathbf{r}')$  is very similar to  $v_s(\mathbf{r})$ . We use the variational principle for the anomalous density of the interacting system Eq. (3.50), insert the rewritten grand potential and define the  $xc$  anomalous potential

$$\frac{\delta F_{xc}[n, \mathbf{m}, \boldsymbol{\chi}, \Gamma]}{\delta \boldsymbol{\chi}^*(\mathbf{r}, \mathbf{r}')} \equiv -\Delta^{xc}[n, \mathbf{m}, \boldsymbol{\chi}, \Gamma](\mathbf{r}, \mathbf{r}'). \quad (3.70)$$

The minimum principle of the non interacting system yields

$$\left. \frac{\delta F_s[n_0, \mathbf{m}_0, \boldsymbol{\chi}_s, \Gamma_0]}{\delta \boldsymbol{\chi}_s^*(\mathbf{r}, \mathbf{r}')} \right|_{\boldsymbol{\chi}_s = \boldsymbol{\chi}_0} = \boldsymbol{\Delta}^s[n_0, \mathbf{m}_0, \boldsymbol{\chi}_0, \Gamma_0](\mathbf{r}, \mathbf{r}') \quad (3.71)$$

so that we obtain

$$\boldsymbol{\Delta}^s[n_0, \mathbf{m}_0, \boldsymbol{\chi}_0, \Gamma_0](\mathbf{r}, \mathbf{r}') = \boldsymbol{\Delta}^{\text{xc}}[n_0, \mathbf{m}_0, \boldsymbol{\chi}_0, \Gamma_0](\mathbf{r}, \mathbf{r}') + \boldsymbol{\Delta}^{\text{ext}}(\mathbf{r}, \mathbf{r}') . \quad (3.72)$$

The same procedure for the nuclear Kohn-Sham potential  $W_s(\mathbf{R}_1, \dots, \mathbf{R}_{N_n})$  yields with the definition of the nuclear  $xc$  potential

$$\frac{\delta F_{\text{xc}}[n, \mathbf{m}, \boldsymbol{\chi}, \Gamma]}{\delta \Gamma(\mathbf{R}_1, \dots, \mathbf{R}_{N_n})} \equiv W_{\text{xc}}[n, \mathbf{m}, \boldsymbol{\chi}, \Gamma](\mathbf{R}_1, \dots, \mathbf{R}_{N_n}) \quad (3.73)$$

the expression for the potential of the nuclear KS equation

$$W_s[n_0, \mathbf{m}_0, \boldsymbol{\chi}_0, \Gamma_0](\mathbf{R}_1, \dots, \mathbf{R}_{N_n}) = W_{\text{xc}}[n_0, \mathbf{m}_0, \boldsymbol{\chi}_0, \Gamma_0](\mathbf{R}_1, \dots, \mathbf{R}_{N_n}) + \sum_i \int d\mathbf{r} \frac{Ze^2 n_0(\mathbf{r})}{4\pi\epsilon_0 |\mathbf{r} - \mathbf{R}_i|} + W_{\text{ext}}(\mathbf{R}_1, \dots, \mathbf{R}_{N_n}) . \quad (3.74)$$

The last equation will connect the KS magnetic field with the external one. Define

$$\frac{\delta F_{\text{xc}}[n, \mathbf{m}, \boldsymbol{\chi}, \Gamma]}{\delta \mathbf{m}(\mathbf{r})} = \mathbf{B}_{\text{xc}}[n, \mathbf{m}, \boldsymbol{\chi}, \Gamma](\mathbf{r}) \quad (3.75)$$

then with the variational principle in the KS system

$$0 = \left. \frac{\delta F_s}{\delta \mathbf{m}_s(\mathbf{r})} [n_0, \mathbf{m}_s, \boldsymbol{\chi}_0, \Gamma_0] \right|_{\mathbf{m}_s = \mathbf{m}_0} + \mathbf{B}_s[n_0, \mathbf{m}_0, \boldsymbol{\chi}_0, \Gamma_0](\mathbf{r}) , \quad (3.76)$$

and the variational principle of the exact system

$$0 = \mathbf{B}_{\text{ext}}(\mathbf{r}) + \left. \frac{\delta F_s[n_0, \mathbf{m}_s, \boldsymbol{\chi}_0, \Gamma_0]}{\delta \mathbf{m}_s(\mathbf{r})} \right|_{\mathbf{m}_s = \mathbf{m}_0} + \left. \frac{\delta F_{\text{xc}}[n_0, \mathbf{m}, \boldsymbol{\chi}_0, \Gamma_0]}{\delta \mathbf{m}(\mathbf{r})} \right|_{\mathbf{m} = \mathbf{m}_0} \quad (3.77)$$

$$0 = \mathbf{B}_{\text{ext}}(\mathbf{r}) - \mathbf{B}_s[n_0, \mathbf{m}_0, \boldsymbol{\chi}_0, \Gamma_0](\mathbf{r}) + \mathbf{B}_{\text{xc}}[n_0, \mathbf{m}_0, \boldsymbol{\chi}_0, \Gamma_0](\mathbf{r}) \quad (3.78)$$

we thus obtain

$$\mathbf{B}_s[n_0, \mathbf{m}_0, \boldsymbol{\chi}_0, \Gamma_0](\mathbf{r}) = \mathbf{B}_{\text{ext}}(\mathbf{r}) + \mathbf{B}_{\text{xc}}[n_0, \mathbf{m}_0, \boldsymbol{\chi}_0, \Gamma_0](\mathbf{r}) . \quad (3.79)$$

The essential advantage of the KS system, if chosen in this way, is that we can find the so called Bogoliubov-Valatin transformations in Section 3.4 to diagonalize the Hamiltonian.

### 3.3. The Nuclear KS System

In this Section we want to represent the nuclear KS system, described by the Hamiltonian in Eq. (3.55), in phononic operators. In order to obtain a non-interacting reference system with respect to which we define the single phonon operators we expand the nuclear KS potential

$W_s(\mathbf{R}_1, \dots, \mathbf{R}_{N_n})$  of Eq. (3.74) in a Taylor series in displacements  $\{\mathbf{u}\}$  about the set of fixed nuclear equilibrium coordinates  $\{\mathbf{R}_0\}$

$$\hat{H}_0^n = \sum_i \frac{-\hbar^2 \nabla_{\mathbf{u}_i}^2}{2M} + \sum_{a,b=x,y,z} \sum_{ij} A_{ij}^{ab} u_i^a u_j^b, \quad (3.80)$$

$$A_{ij}^{ab} = \left. \frac{W_s(\mathbf{R}_{01} + \mathbf{u}_i, \dots, \mathbf{R}_{0N_n} + \mathbf{u}_j)}{\partial u_i^a \partial u_j^b} \right|_{\{\mathbf{u}\}=\{\mathbf{0}\}}. \quad (3.81)$$

In this configuration  $W_s(\mathbf{R}_{01}, \dots, \mathbf{R}_{0N_n})$  is a functional of the densities  $n$ ,  $\mathbf{m}$ ,  $\chi$  and  $\Gamma$ . In practice it can be well approximated with the Born-Oppenheimer energy surface. Following Ref. [34, Page 108] we further note that from the translational invariance of the full problem follows first  $A_{ij}^{ab} = A_{0,j-i}^{ab}$  and second for the Fourier coefficient

$$A_{\mathbf{q}}^{ab} = \sum_i e^{i\mathbf{q} \cdot (\mathbf{R}_{0j} - \mathbf{R}_{0i})} A_{0,j-i}^{ab} \quad (3.82)$$

which can be shown to be symmetric  $A_{\mathbf{q}}^{ab} = A_{\mathbf{q}}^{ba}$  for each  $\mathbf{q}$ . The dynamical matrix  $D_{\mathbf{q}}^{ab}$  is introduced that diagonalizes the harmonic potential

$$\sum_{a'b'} D_{\mathbf{q}}^{aa'\dagger} A_{\mathbf{q}}^{a'b'} D_{\mathbf{q}}^{b'b} = A_{\mathbf{q}}^{\lambda} \delta_{a,b} \quad (3.83)$$

The diagonal form of the Hamiltonian describes a harmonic potential for collective normal modes that may be quantized with the usual phonon operators [34]

$$\hat{b}_{\mathbf{q}\lambda} = \frac{1}{\sqrt{2\hbar M \Omega_{\mathbf{q}\lambda}}} (M \Omega_{\mathbf{q}\lambda} \hat{Q}_{\mathbf{q}}^{\lambda} + i \hat{P}_{\mathbf{q}}^{\lambda\dagger}) \quad \hat{b}_{\mathbf{q}\lambda}^{\dagger} = \frac{1}{\sqrt{2\hbar M \Omega_{\mathbf{q}\lambda}}} (M \Omega_{\mathbf{q}\lambda} \hat{Q}_{\mathbf{q}}^{\lambda\dagger} - i \hat{P}_{\mathbf{q}}^{\lambda}) \quad (3.84)$$

where the normal coordinates  $\hat{Q}_{\mathbf{q}}^{\lambda}$  and  $\hat{P}_{\mathbf{q}}^{\lambda}$  are

$$\hat{Q}_{\mathbf{q}}^{\lambda} = \frac{1}{\sqrt{V}} \sum_i u_i^{\lambda} e^{i\mathbf{q} \cdot \mathbf{R}_{0i}} \quad \hat{P}_{\mathbf{q}}^{\lambda} = -i\hbar \frac{\partial}{\partial \hat{Q}_{\mathbf{q}}^{\lambda}} \quad (3.85)$$

and phonon frequency is given by

$$\Omega_{\mathbf{q}\lambda} = \sqrt{A_{\mathbf{q}}^{\lambda}/M}. \quad (3.86)$$

Very importantly we note that  $\Omega_{\mathbf{q}\lambda} = \Omega_{-\mathbf{q}\lambda}$  because of the symmetry  $\partial_{u_i^a} \partial_{u_j^b} \equiv \partial_{(-u_i^a)} \partial_{(-u_j^b)}$  in  $A_{ij}^{ab}$  and the consequence for its Fourier coefficient  $A_{\mathbf{q}}^{ab}$ . Now, similar to the electronic operators, we realize that this  $\hat{b}_{\mathbf{q}\lambda}$  create the many-body states of a hermitian operator

$$\hat{H}_0^n = \sum_{\mathbf{q}\lambda} \hbar \Omega_{\mathbf{q}\lambda} (\hat{b}_{\mathbf{q}\lambda}^{\dagger} \hat{b}_{\mathbf{q}\lambda} + \frac{1}{2}) \quad (3.87)$$

which form a complete basis. We may represent the true nuclear KS Hamiltonian  $\hat{H}_s^n$  of Eq. (3.55) using this operators, which results in  $n$  particle interactions for each of the coefficients of the Taylor series of  $W_s$ . All these complicated additional interactions may be viewed as dressing of the bare phonons. In practice phonon frequencies are computed e.g. with density functional perturbation theory [35] and the results compare well with experiment.



### 3.4. Electronic Part: The Kohn-Sham-Bogoliubov-de-Gennes equations

The electronic KS Hamiltonian  $\hat{H}_s^e$  is not diagonal in the electronic field since it involves terms proportional to  $\sim \psi\psi$ . Diagonalizing the SC KS system will bring it to the form

$$\hat{H}_s^e = E_0 + \sum_k E_k \hat{\gamma}_k^\dagger \hat{\gamma}_k \quad E_k \geq 0. \quad (3.88)$$

where  $\hat{\gamma}_k^\dagger$  creates a two component vector in spin space (the Hamiltonian is not diagonal in spin so the spin degrees of freedom are in the set  $\{k\}$ ),  $E_0$  is the ground state energy and the  $E_k$  are all positive.<sup>5</sup> In order to diagonalize the Hamiltonian in Eq. (3.54) we have to allow the combination of particles and holes to new operators that are partly both. Formally, if we view a particle and hole as spinor components

$$\begin{pmatrix} \hat{\psi}_\sigma(\mathbf{r}) \\ 0 \end{pmatrix}, \quad \begin{pmatrix} 0 \\ \hat{\psi}_\sigma^\dagger(\mathbf{r}) \end{pmatrix}, \quad (3.89)$$

the solution of Eq. (3.54) will not be a pure spinor. The translation into this so called Nambu space [28] will be the next section. Usually the derivation of the Bogoliubov-de-Gennes equations is done comparing commutators with the respective Hamiltonians [36]. The derivation we give in the next Subsections 3.4.1 and 3.4.2 takes a different route which is more transparent in explaining the appearing particle hole symmetry of the solutions but leads to the same results.

#### 3.4.1. The KS Hamiltonian in the Nambu-Anderson Notation

To deal with the problem of a non-pure spinor in particle-hole space we define a notation that is based on the one of Nambu [28] and Anderson [37]. In this Subsection our goal is to cast the KS Hamiltonian  $\hat{H}_s^e$  Eq. (3.54) into the new notation. We take, similar to spin space  $\hat{\Psi}_{\alpha\mu}(\mathbf{r})$ , with the notation that  $\alpha = 1$ , means ‘‘particle’’ or ‘‘up’’ and  $\alpha = -1$  means ‘‘hole’’ or ‘‘down’’ in Nambu space

$$\hat{\Psi}_{1,\uparrow}(\mathbf{r}) = \begin{pmatrix} \hat{\psi}(\mathbf{r} \uparrow) \\ 0 \\ 0 \\ 0 \end{pmatrix} \quad \hat{\Psi}_{1,\downarrow}(\mathbf{r}) = \begin{pmatrix} 0 \\ \hat{\psi}(\mathbf{r} \downarrow) \\ 0 \\ 0 \end{pmatrix} \quad \hat{\Psi}_{-1,\uparrow}(\mathbf{r}) = \begin{pmatrix} 0 \\ 0 \\ \hat{\psi}^\dagger(\mathbf{r} \uparrow) \\ 0 \end{pmatrix} \quad \hat{\Psi}_{-1,\downarrow}(\mathbf{r}) = \begin{pmatrix} 0 \\ 0 \\ 0 \\ \hat{\psi}^\dagger(\mathbf{r} \downarrow) \end{pmatrix}. \quad (3.90)$$

That means we define this operator as a pure spinor, also in Nambu space (with respect to a non-SC, collinear single particle system). The direct product results in a  $4 \times 4$  matrix in Nambu-Spin space (that has only one non-vanishing component)

$$\hat{\Psi}_{\alpha\mu}(\mathbf{r}) \otimes \hat{\Psi}_{\alpha'\mu'}^\dagger(\mathbf{r}') \equiv \begin{pmatrix} \delta_{\alpha,1} \delta_{\alpha',1} \hat{\psi}_\mu(\mathbf{r}) \otimes \hat{\psi}_{\mu'}^\dagger(\mathbf{r}') & \delta_{\alpha,1} \delta_{\alpha',-1} \hat{\psi}_\mu(\mathbf{r}) \otimes \hat{\psi}_{\mu'}^\dagger(\mathbf{r}') \\ \delta_{-\alpha,1} \delta_{\alpha',1} \hat{\psi}_\mu^\dagger(\mathbf{r}) \otimes \hat{\psi}_{\mu'}^\dagger(\mathbf{r}') & \delta_{-\alpha,1} \delta_{\alpha',-1} \hat{\psi}_\mu^\dagger(\mathbf{r}) \otimes \hat{\psi}_{\mu'}^\dagger(\mathbf{r}') \end{pmatrix} \quad (3.91)$$

We shall often write for brevity  $\hat{\Psi}(\mathbf{r})$  where the quantum numbers  $\mu, \alpha$  are omitted and all components are filled, formally as

$$\hat{\Psi}(\mathbf{r}) \equiv \sum_{\alpha\mu} \hat{\Psi}_{\alpha\mu}(\mathbf{r}) \equiv ( \hat{\psi}(\mathbf{r} \uparrow) \quad \hat{\psi}(\mathbf{r} \downarrow) \quad \hat{\psi}^\dagger(\mathbf{r} \uparrow) \quad \hat{\psi}^\dagger(\mathbf{r} \downarrow) )^{T_{\text{sn}}}. \quad (3.92)$$

<sup>5</sup>This form can be achieved by commuting the operators  $H = E_i \hat{a}_i^\dagger \hat{a}_i = \sum_{i|E_i < 0} + \sum_{i|E_i \geq 0} E_i \hat{a}_i^\dagger \hat{a}_i + \sum_{i|E_i < 0} |E_i| \hat{a}_i \hat{a}_i^\dagger$  and then redefining the negative energy operators as holes  $\hat{a}_i = \hat{b}_i^\dagger$ .

Note that if we commute two such operators, not only does the order of the components change, but the result is also transposed in spin and Nambu space. Therefore it is useful to define the special commutator<sup>6</sup>

$$[\hat{\Psi}(\mathbf{r}), \otimes \hat{\Psi}^\dagger(\mathbf{r}') ]_{\pm} \equiv \hat{\Psi}(\mathbf{r}) \otimes \hat{\Psi}^\dagger(\mathbf{r}') \pm (\hat{\Psi}(\mathbf{r}') \otimes \hat{\Psi}^\dagger(\mathbf{r}))^{T_{\text{sn}}} \quad (3.93)$$

that is equivalent to using the commutator in every individual component of the  $4 \times 4$  matrix. Then

$$[\hat{\Psi}_{\alpha\mu}(\mathbf{r}), \otimes \hat{\Psi}_{\alpha'\mu'}^\dagger(\mathbf{r}')]_{+} = \tau_0 \sigma_0 \delta(\mathbf{r} - \mathbf{r}') \delta_{\alpha\alpha'} \delta_{\mu\mu'} \quad (3.94)$$

$$[\hat{\Psi}(\mathbf{r}), \otimes \hat{\Psi}^\dagger(\mathbf{r}')]_{+} = \tau_0 \sigma_0 \delta(\mathbf{r} - \mathbf{r}') \quad (3.95)$$

$$[\hat{\Psi}(\mathbf{r}), \otimes \hat{\Psi}(\mathbf{r}')]_{+} = [\hat{\Psi}^\dagger(\mathbf{r}), \otimes \hat{\Psi}^\dagger(\mathbf{r}')]_{+} = 0. \quad (3.96)$$

If we address individual, scalar components of the vector  $\hat{\Psi}(\mathbf{r})$  we promote the quantum number to the bracket

$$\hat{\Psi}(\mathbf{r}\sigma\alpha) \equiv \delta_{\alpha,1} \hat{\psi}(\mathbf{r}\sigma) + \delta_{\alpha,-1} \hat{\psi}_\sigma^\dagger(\mathbf{r}\sigma). \quad (3.97)$$

We can now cast the Hamiltonian Eq. (3.54) into the new notation. For the kinetic energy we may introduce  $\lim_{\mathbf{r}' \rightarrow \mathbf{r}}$  and put  $\hat{\psi}_\sigma^\dagger(\mathbf{r}') \hat{\psi}_{\sigma'}(\mathbf{r})$  as  $\frac{1}{2} (\hat{\psi}_\sigma^\dagger(\mathbf{r}') \hat{\psi}_{\sigma'}(\mathbf{r}) + \hat{\psi}_\sigma^\dagger(\mathbf{r}') \hat{\psi}_{\sigma'}(\mathbf{r}))$  where we commute the latter term. Dropping the trace term

$$\frac{1}{2} \sum_{\sigma} \int d\mathbf{r} \lim_{\mathbf{r}' \rightarrow \mathbf{r}} \delta(\mathbf{r}' - \mathbf{r}) \left( -\frac{1}{2} (\hbar \nabla)^2 + v_s(\mathbf{r}) - \mu \right) - g_s \mu_B (\mathbf{S})_{\sigma\sigma} \cdot \mathbf{B}_s(\mathbf{r}) \quad (3.98)$$

which is an infinite complex number, that is however not operator valued and thus cancels out in every thermal average we obtain

$$\begin{aligned} \hat{H}_s^e &= \int d\mathbf{r} \int d\mathbf{r}' \hat{\Psi}^\dagger(\mathbf{r}) \cdot \frac{1}{2} \left( \left( -\frac{\hbar \nabla^2}{2m_e} + v_s(\mathbf{r}) - \mu \right) \sigma_0 \tau_z - \frac{g_s}{2} \mu_B \mathbf{S} \cdot \mathbf{B}_s(\mathbf{r}) (\tau_0 + \tau_z) \right. \\ &\quad \left. - \frac{g_s}{2} \mu_B \mathbf{S}^* \cdot \mathbf{B}_s(\mathbf{r}) (\tau_0 - \tau_z) \right) \delta(\mathbf{r} - \mathbf{r}') + i\tau_x \Im \Phi \cdot \Delta^s(\mathbf{r}, \mathbf{r}') + i\tau_y \Re \Phi \cdot \Delta^s(\mathbf{r}, \mathbf{r}') \cdot \hat{\Psi}(\mathbf{r}') \end{aligned} \quad (3.99)$$

Note that the changed order of the electronic fields implies a transposition in spin space on the  $(-1, -1)$  component that is equivalent to using  $\mathbf{S}^*$ .

### 3.4.2. The Bogoliubov-Valatin Transformations

In a similar notation, the diagonal KS Hamiltonian Eq. (3.88) becomes

$$\hat{H}_s^e = \sum_k \hat{\Phi}_k^\dagger \cdot \frac{1}{2} \begin{pmatrix} E_k & 0 \\ 0 & -E_k \end{pmatrix} \cdot \hat{\Phi}_k \quad (3.100)$$

with

$$\hat{\Phi}_{k,1} = \begin{pmatrix} \hat{\gamma}_k(\mathbf{r}) \\ 0 \end{pmatrix} \quad \hat{\Phi}_{k,-1} = \begin{pmatrix} 0 \\ \hat{\gamma}_k^\dagger(\mathbf{r}) \end{pmatrix} \quad \hat{\Phi}_k = \begin{pmatrix} \hat{\gamma}_k(\mathbf{r}) \\ \hat{\gamma}_k^\dagger(\mathbf{r}) \end{pmatrix}. \quad (3.101)$$

Also here we have dropped the infinite  $\sum_k E_k + E_0$  resulting from the commutator. Note that  $\hat{\Phi}_k$  is a two, not four, component vector because the spin may not be a good quantum number in the SC KS system. We may rotate the form in Eq. (3.99) to the form Eq. (3.100) by introducing a unitary transformation that we parametrize generically with four complex spinor functions. This

<sup>6</sup> $T_{\text{sn}}$  is a transposition in spin and Nambu space.

connection between  $\hat{\Psi}(\mathbf{r})$  and  $\hat{\Phi}_k$  is known as the Bogoliubov-Valatin transformation[38, 39]. We write it in the form

$$\hat{\Psi}(\mathbf{r}) = \sum_k \begin{pmatrix} \vec{u}_k(\mathbf{r}) & \vec{v}_k^*(\mathbf{r}) \\ \vec{v}_k(\mathbf{r}) & \vec{u}_k^*(\mathbf{r}) \end{pmatrix} \cdot \hat{\Phi}_k \quad \hat{\Phi}_k = \int d\mathbf{r} \begin{pmatrix} \vec{u}_k^*(\mathbf{r}) & \vec{v}_k^*(\mathbf{r}) \\ \vec{v}_k(\mathbf{r}) & \vec{u}_k(\mathbf{r}) \end{pmatrix} \cdot \hat{\Psi}(\mathbf{r}) \quad (3.102)$$

Note that in the first case the matrix is  $4 \times 2$  dimensional, and in the second  $2 \times 4$  because of the spinor property of the  $\vec{u}_k(\mathbf{r}), \vec{v}_k(\mathbf{r})$ . The requirement to be unitary reads

$$\int d\mathbf{r} \begin{pmatrix} \vec{u}_k^*(\mathbf{r}) & \vec{v}_k^*(\mathbf{r}) \\ \vec{v}_k(\mathbf{r}) & \vec{u}_k(\mathbf{r}) \end{pmatrix} \begin{pmatrix} \vec{u}_{k'}(\mathbf{r}) & \vec{v}_{k'}^*(\mathbf{r}) \\ \vec{v}_{k'}(\mathbf{r}) & \vec{u}_{k'}^*(\mathbf{r}) \end{pmatrix} = \tau_0 \delta_{kk'}, \quad (3.103)$$

$$\sum_k \begin{pmatrix} \vec{u}_k(\mathbf{r}') & \vec{v}_k^*(\mathbf{r}') \\ \vec{v}_k(\mathbf{r}') & \vec{u}_k^*(\mathbf{r}') \end{pmatrix} \begin{pmatrix} \vec{u}_k^*(\mathbf{r}) & \vec{v}_k^*(\mathbf{r}) \\ \vec{v}_k(\mathbf{r}) & \vec{u}_k(\mathbf{r}) \end{pmatrix} = \tau_0 \sigma_0 \delta(\mathbf{r} - \mathbf{r}'). \quad (3.104)$$

In going from Eq. (3.99) to Eq. (3.100), we identify

$$\int d\mathbf{r} \int d\mathbf{r}' \begin{pmatrix} \vec{u}_k^*(\mathbf{r}) & \vec{v}_k^*(\mathbf{r}) \\ \vec{v}_k(\mathbf{r}) & \vec{u}_k(\mathbf{r}) \end{pmatrix} \cdot \bar{H}_{\text{KS}}(\mathbf{r}, \mathbf{r}') \cdot \begin{pmatrix} \vec{u}_{k'}(\mathbf{r}') & \vec{v}_{k'}^*(\mathbf{r}') \\ \vec{v}_{k'}(\mathbf{r}') & \vec{u}_{k'}^*(\mathbf{r}') \end{pmatrix} = \begin{pmatrix} E_k & 0 \\ 0 & -E_k \end{pmatrix} \delta_{kk'} \quad (3.105)$$

where

$$\begin{aligned} \bar{H}_{\text{KS}}(\mathbf{r}, \mathbf{r}') = \delta(\mathbf{r} - \mathbf{r}') & \begin{pmatrix} \left(-\frac{\hbar^2 \nabla^2}{2m_e} + v_s(\mathbf{r}) - \mu\right) \sigma_0 - g_s \mu_B \mathbf{S} \cdot \mathbf{B}_s(\mathbf{r}) & 0 \\ 0 & -\left(-\frac{\hbar^2 \nabla^2}{2m_e} + v_s(\mathbf{r}) - \mu\right) \sigma_0 - g_s \mu_B \mathbf{S}^* \cdot \mathbf{B}_s(\mathbf{r}) \end{pmatrix} \\ & + \begin{pmatrix} 0 & \boldsymbol{\Phi} \cdot \boldsymbol{\Delta}^s(\mathbf{r}, \mathbf{r}') \\ -(\boldsymbol{\Phi} \cdot \boldsymbol{\Delta}^s(\mathbf{r}, \mathbf{r}'))^* & 0 \end{pmatrix}. \end{aligned} \quad (3.106)$$

Applying the inverse Bogoliubov-Valatin transformation from the left we obtain

$$\int d\mathbf{r}' \bar{H}_{\text{KS}}(\mathbf{r}, \mathbf{r}') \cdot \begin{pmatrix} \vec{u}_k(\mathbf{r}') & \vec{v}_k^*(\mathbf{r}') \\ \vec{v}_k(\mathbf{r}') & \vec{u}_k^*(\mathbf{r}') \end{pmatrix} = \begin{pmatrix} \vec{u}_k(\mathbf{r}') & \vec{v}_k^*(\mathbf{r}') \\ \vec{v}_k(\mathbf{r}') & \vec{u}_k^*(\mathbf{r}') \end{pmatrix} \cdot \begin{pmatrix} E_k & 0 \\ 0 & -E_k \end{pmatrix}. \quad (3.107)$$

This can be viewed as two redundant vector equations of which we usually consider the first

$$\int d\mathbf{r}' \bar{H}_{\text{KS}}(\mathbf{r}, \mathbf{r}') \begin{pmatrix} \vec{u}_k(\mathbf{r}') \\ \vec{v}_k(\mathbf{r}') \end{pmatrix} = E_k \begin{pmatrix} \vec{u}_k(\mathbf{r}) \\ \vec{v}_k(\mathbf{r}) \end{pmatrix}. \quad (3.108)$$

These are the Kohn-Sham-Bogoliubov-de-Gennes (KSBDG) equations for a magnetic system which generalize those of Ref. [20].  $\left(\vec{u}_k(\mathbf{r}) \quad \vec{v}_k^*(\mathbf{r})\right)^T$  leads to the equivalent negative eigenvalue  $-E_k$  which reflects the additional degrees of freedom that we have created in going to the  $2 \times 2$  Nambu formalism in particle hole space.

### 3.4.3. Expansion in the Normal State KS System: Choosing the Closest Basis Possible

The KSBDG equations pose a challenging set of integro-differential equations. A convenient simplification can be obtained by expanding this system in a set of non-SC eigenfunctions to the Hamiltonian

$$\hat{H}_n^e = \int d\mathbf{r} \hat{\psi}^\dagger(\mathbf{r}) \cdot \left(-\frac{\hbar^2 \nabla^2}{2m_e} + v_s(\mathbf{r}) - \mu\right) \cdot \hat{\psi}(\mathbf{r}) + \int d\mathbf{r} \hat{\mathbf{m}}(\mathbf{r}) \cdot \mathbf{B}_s(\mathbf{r}). \quad (3.109)$$

This basis has the advantage that the upper left and bottom right component of  $\bar{H}_{\text{KS}}$  in Nambu space is a diagonal matrix. Formally we may choose any basis. In practice we will take the KS

orbitals available from one of the electronic structure codes using an  $xc$  potential in, say, the LSDA. To introduce approximations at a later stage, we split the Hamiltonian  $\hat{H}_n^e$  of Eq. (3.109) according to  $\hat{H}_n^e = \hat{H}_c^{e0} + \hat{H}_{nc}^{eT}$  where  $\hat{H}_c^{e0}$  is a collinear zero temperature KS system and the eigenfunctions  $\{\vec{\varphi}_{k\sigma}\}$  are pure spinors<sup>7</sup>

$$\hat{H}_c^{e0}|\vec{\varphi}_{k\sigma}\rangle = \varepsilon_{k\sigma}|\vec{\varphi}_{k\sigma}\rangle \quad \vec{\varphi}_{k\uparrow}(\mathbf{r}) = \langle \mathbf{r} | \vec{\varphi}_{k\uparrow} \rangle = \begin{pmatrix} \varphi_k(\mathbf{r} \uparrow) \\ 0 \end{pmatrix} \quad \vec{\varphi}_{k\downarrow}(\mathbf{r}) = \begin{pmatrix} 0 \\ \varphi_k(\mathbf{r} \downarrow) \end{pmatrix}. \quad (3.110)$$

In this complete set  $\{\vec{\varphi}_{i\sigma}(\mathbf{r})\}$ , we expand the spinor coefficients

$$\vec{u}_k(\mathbf{r}) \equiv \sum_{j\sigma} u_k^{j\sigma} \vec{\varphi}_{j\sigma}(\mathbf{r}). \quad (3.111)$$

$$\vec{v}_k(\mathbf{r}) \equiv \sum_{j\sigma} v_k^{j\sigma} \vec{\varphi}_{j\sigma}^*(\mathbf{r}) \quad (3.112)$$

This special choice of basis  $\{\vec{\varphi}_{i\sigma}(\mathbf{r})\}$  will simplify the  $xc$  potential approximation. The eigenvalue  $\varepsilon_{k\sigma}$  is measured with respect to the Fermi level. The remaining part of  $\hat{H}_n^e$  is formally

$$\hat{H}_{nc}^{eT} = v_s[T](\mathbf{r}) - v_s^{\text{LSDA}}[T=0](\mathbf{r}) + \mathbf{B}_s[T](\mathbf{r}) - \mathbf{B}_s^{\text{LSDA}}[T=0](\mathbf{r}). \quad (3.113)$$

Further we expand the pair potential in the new basis

$$\Phi \cdot \Delta^s(\mathbf{r}, \mathbf{r}') = \sum_{i\sigma, j\sigma'} \Delta_{ij}^{s\sigma\sigma'} \vec{\varphi}_{i\sigma}(\mathbf{r}) \otimes \vec{\varphi}_{j\sigma'}(\mathbf{r}') \quad (3.114)$$

$$\Delta_{ij}^{s\sigma\sigma'} = \int d\mathbf{r} \int d\mathbf{r}' \vec{\varphi}_{i\sigma}^*(\mathbf{r}) \cdot (\Phi \cdot \Delta^s(\mathbf{r}, \mathbf{r}')) \cdot \vec{\varphi}_{j\sigma'}(\mathbf{r}'). \quad (3.115)$$

Note that expansion coefficient matrix  $\Delta_{ij}^{s\sigma\sigma'}$  behaves in a defined way to index swapping, due to the symmetries of the underlying pair potential  $\Delta^s(\mathbf{r}', \mathbf{r})$ , namely

$$\Delta_{ij}^{s\sigma\sigma'} = -\Delta_{ji}^{s\sigma'\sigma} \quad (3.116)$$

Note also that  $-(\Phi \cdot \Delta^s(\mathbf{r}, \mathbf{r}'))^*$  results in the adjoint matrix  $\Delta_{ij}^{s\dagger\sigma\sigma'}$ . We further introduce the temperature - and non-collinear matrix elements  $\mathcal{R}_{ij}^{\sigma\sigma'}$

$$\mathcal{R}_{ij}^{\sigma\sigma'} = \langle \vec{\varphi}_{i\sigma} | \hat{H}_{nc}^{eT} | \vec{\varphi}_{j\sigma'} \rangle \quad (3.117)$$

The NS KS orbitals are orthonormal so we act with  $\int d\mathbf{r} \vec{\varphi}_{l\sigma}^*(\mathbf{r}) \cdot \dots$  in the first row and with  $\int d\mathbf{r} \vec{\varphi}_{l\sigma}(\mathbf{r}) \cdot \dots$  in the second row of Eq. (3.108). Together with the expansion of the  $\vec{u}_k(\mathbf{r})$  and  $\vec{v}_k(\mathbf{r})$  of Eqs. (3.111) and (3.112) we obtain the KSBdG equations in KS space<sup>8</sup>

$$E_k \begin{pmatrix} u_k^{i\sigma} \\ v_k^{j\sigma} \end{pmatrix} = \sum_{j\sigma'} \begin{pmatrix} (\varepsilon_{i\sigma} \delta_{ij} \delta_{\sigma\sigma'} + \mathcal{R}_{ij}^{\sigma\sigma'}) & \Delta_{ij}^{s\sigma\sigma'} \\ \Delta_{ij}^{s\dagger\sigma\sigma'} & -(\varepsilon_{i\sigma} \delta_{ij} \delta_{\sigma\sigma'} + \mathcal{R}_{ji}^{\sigma'\sigma}) \end{pmatrix} \begin{pmatrix} u_k^{j\sigma'} \\ v_k^{j\sigma'} \end{pmatrix}. \quad (3.118)$$

We distinguish, as in the real space analog  $\Delta^s(\mathbf{r}, \mathbf{r}')$  of the Eqs. (3.18) to (3.21), the singlet/triplet parts of the pair potential expansion coefficient matrix

$$\begin{aligned} \Delta_{sij}^s &= \frac{1}{2}(\Delta_{sij}^{\uparrow\downarrow} - \Delta_{sij}^{\downarrow\uparrow}) & \Delta_{tyij}^s &= \frac{1}{2}(\Delta_{sij}^{\downarrow\downarrow} + \Delta_{sij}^{\uparrow\uparrow}) \\ \Delta_{txij}^s &= \frac{1}{2}(\Delta_{sij}^{\downarrow\downarrow} - \Delta_{sij}^{\uparrow\uparrow}) & \Delta_{tzij}^s &= \frac{1}{2}(\Delta_{sij}^{\uparrow\downarrow} + \Delta_{sij}^{\downarrow\uparrow}) \end{aligned} \quad (3.119)$$

<sup>7</sup>The index  $k = (\mathbf{k}, n)$  summarizes all quantum numbers except spin, namely Bloch vector  $\mathbf{k}$  and band index  $n$ .

<sup>8</sup>We call an entity represented in KS space when we refer to the matrix elements in the basis  $\{\vec{\varphi}_{i\sigma}(\mathbf{r})\}$ .

that are also condensed into the 4 component vector  $\Delta^s$ . This has the distinct advantage that we may always use the defined behavior under transposition  $\Delta_{sij}^s = \Delta_{sji}^s$  and  $\Delta_{tx|y|z_{ij}}^s = -\Delta_{tx|y|z_{ji}}^s$ . Defining the vector<sup>9</sup>

$$g_k = ( u_k^{1\uparrow} \quad u_k^{1\downarrow} \quad u_k^{2\uparrow} \quad \dots \mid v_k^{1\uparrow} \quad v_k^{1\downarrow} \quad v_k^{2\uparrow} \quad \dots )^T \quad (3.120)$$

and the matrix

$$\mathcal{E}_{ij}^{\sigma\sigma'} = (\varepsilon_{i\sigma}\delta_{ij}\delta_{\sigma\sigma'} + \mathcal{R}_{ij}^{\sigma\sigma'}) \quad (3.121)$$

we obtain the compact equation

$$\begin{pmatrix} \mathcal{E} & \Phi \cdot \Delta^s \\ (\Phi \cdot \Delta^s)^\dagger & -\mathcal{E}^T \end{pmatrix} g_k = E_k g_k. \quad (3.122)$$

In practice the unitary transformation Eq. (3.102) is not known beforehand but has to be determined from the above equation (or its real space analog). Consider the case that there are  $N$  degrees of freedom in the original KS system. If we thus solve the above linear  $2N \times 2N$  matrix equation on a computer we have to construct the  $u_k^{i\sigma}, v_k^{i\sigma}$  from the  $2N$  solutions. Note that by definition  $g_k$  corresponds to the positive eigenvalue  $E_k$  solutions. The negative ones, again by definition, are  $g_k^c = ( v_k^{1\uparrow*} \quad v_k^{1\downarrow*} \quad v_k^{2\uparrow*} \quad \dots \mid u_k^{1\uparrow*} \quad u_k^{1\downarrow*} \quad u_k^{2\uparrow*} \quad \dots )^T$ . (That  $g_k^c$  indeed give the negative eigenvalues is clear from Eq. (3.107).) Thus, we extract the  $N$   $u$  and  $v$  always from the positive branch solution  $g_k$  (there are  $N$ ) and the procedure is unique.

#### 3.4.4. The Electronic Densities

In this Subsection we want to express the electronic densities  $n(\mathbf{r}), \mathbf{m}(\mathbf{r})$  and  $\chi(\mathbf{r}, \mathbf{r}')$  in terms of the solutions to the KSBdG equation (3.118)  $g_k$ . The definition of the densities Eqs. (3.25) to (3.27) reads in Nambu space

$$n(\mathbf{r}) = \frac{1}{2} \langle \hat{\Psi}^\dagger(\mathbf{r}) \cdot \sigma_0 (\tau_0 + \tau_z) \cdot \hat{\Psi}(\mathbf{r}) \rangle \quad (3.123)$$

$$\mathbf{m}(\mathbf{r}) = \frac{1}{2} \langle \hat{\Psi}^\dagger(\mathbf{r}) \cdot \mathbf{S} (\tau_0 + \tau_z) \cdot \hat{\Psi}(\mathbf{r}) \rangle \quad (3.124)$$

$$\chi(\mathbf{r}, \mathbf{r}') = \frac{1}{2} \langle \hat{\Psi}^\dagger(\mathbf{r}) \cdot \Phi^* (\tau_x - i\tau_y) \cdot \hat{\Psi}(\mathbf{r}') \rangle. \quad (3.125)$$

Insertion of the Bogoliubov-Valatin transformations of Eq. (3.102) and using  $\langle \hat{\gamma}_k^\dagger \hat{\gamma}_k \rangle = f_\beta(E_k)$  and  $\langle \hat{\gamma}_k \hat{\gamma}_k^\dagger \rangle = 1 - f_\beta(E_k) = f_\beta(-E_k)$  yields

$$n(\mathbf{r}) = \sum_k (\vec{u}_k(\mathbf{r}) \cdot \sigma_0 \cdot \vec{u}_k^*(\mathbf{r}) f_\beta(E_k) + \vec{v}_k(\mathbf{r}) \cdot \sigma_0 \cdot \vec{v}_k^*(\mathbf{r}) f_\beta(-E_k)) \quad (3.126)$$

$$\mathbf{m}(\mathbf{r}) = \sum_k (\vec{u}_k(\mathbf{r}) \cdot \mathbf{S} \cdot \vec{u}_k^*(\mathbf{r}) f_\beta(E_k) + \vec{v}_k(\mathbf{r}) \cdot \mathbf{S} \cdot \vec{v}_k^*(\mathbf{r}) f_\beta(-E_k)) \quad (3.127)$$

$$\chi(\mathbf{r}, \mathbf{r}') = \sum_k (\vec{v}_k^*(\mathbf{r}) \cdot \Phi \cdot \vec{u}_k(\mathbf{r}') f(E_k) + \vec{u}_k(\mathbf{r}) \cdot \Phi^* \cdot \vec{v}_k^*(\mathbf{r}') f(-E_k)). \quad (3.128)$$

The expansion coefficients of the densities in the basis of the pure spinor NS KS orbitals  $\{\vec{\varphi}_{i\sigma}(\mathbf{r})\}$  are spin matrices:

$$n(\mathbf{r}) = \sum_{i\mu j\mu'} \vec{\varphi}_{i\mu}^*(\mathbf{r}) \cdot n_{ij}^{\mu\mu'} \cdot \vec{\varphi}_{j\mu'}(\mathbf{r}), \quad (3.129)$$

<sup>9</sup>The superscript 1, 2, ... means we have ordered the Bloch vectors and bands in some way.

where  $n_{ij}^{\mu\mu'}$  is a spin matrix for every combination  $(\mu\mu')$ . This is an artifact of the pure spinor notation, but note that component wise this is equivalent to

$$(n_{ij})_{\mu\mu'} = \delta_{\mu\mu'} \sum_k (u_k^{i\mu*} u_k^{j\mu'} f_\beta(E_k) + v_k^{i\mu} v_k^{j\mu'*} f_\beta(-E_k)) \quad (3.130)$$

$$(\mathbf{m}_{ij})_{\mu\mu'} = \mathbf{S}_{\mu\mu'} \sum_k (u_k^{i\mu*} u_k^{j\mu'} f_\beta(E_k) + v_k^{i\mu} v_k^{j\mu'*} f_\beta(-E_k)) \quad (3.131)$$

$$(\chi_{ij})_{\mu\mu'} = \Phi_{\mu\mu'}^* \sum_k (u_k^{j\mu'} v_k^{i\mu*} f_\beta(E_k) + u_k^{i\mu} v_k^{j\mu'*} f_\beta(-E_k)) \quad (3.132)$$

in terms of the scalar components  $\varphi_j(\mathbf{r}\mu)$ . Note also that  $\chi(\mathbf{r}, \mathbf{r}') = \sum_{ij} \vec{\varphi}_{i\mu}(\mathbf{r}) \cdot \chi_{ij}^{\mu\mu'} \cdot \vec{\varphi}_{j\mu'}(\mathbf{r}')$  without the conjugation of one basis vector.

SpinSCDFT allows to compute the exact number of condensed electrons. Because  $\chi(\mathbf{r}, \mathbf{r}')$  is the wavefunction of electron pairs that are condensed in the SC state [40, 25] the related density and number of condensed electrons read

$$n_{\text{SC}}(\mathbf{r}) = \int d\mathbf{r}' |\chi(\mathbf{r}, \mathbf{r}')|^2 \quad (3.133)$$

$$N_{\text{SC}} = \int d\mathbf{r} n_{\text{SC}}(\mathbf{r}). \quad (3.134)$$

We want to stress here that we have performed a basis expansion. No approximations have been introduced so far and the solutions  $g_k$  reproduce the exact densities of the interacting system.

### 3.5. Approximations to the KS System

In this Section we discuss implications if the KS potentials matrix elements in the NS KS basis only couple certain states. First, in Subsection 3.5.1, we drop triplet symmetric parts of the pair potential and find that spin becomes a good quantum number in the SC KS system. Second, in Subsection 3.5.2, we consider only diagonal parts ( $\propto \delta_{kk'}$ ) on the Nambu-diagonal ( $\propto \delta_{\alpha\alpha'}$ ) and only anti-diagonal parts ( $\propto \delta_{k,-k'}$ ) of the pair potential on the Nambu off diagonal ( $\propto \delta_{\alpha,-\alpha'}$ ). This assumption makes the solution of the SC KS system (in terms of the normal state KS system) trivial and we obtain a potential functional theory. This amounts to neglecting hybridization due to SC except for particle states  $k = (\mathbf{k}, n)$  with the corresponding hole state  $-k \equiv (-\mathbf{k}, n)$ . The latter type of approximation is in the context of SCDFT usually referred to as the Decoupling Approximation [21, 22].

#### 3.5.1. No Triplet Pairing, Collinear Nambu-Diagonal

There are very few examples where triplet SC appears in nature, all sharing a very low critical temperature [41, 42]. Thus, in most situations we can rely on a simplified theory that assumes the triplet pair potentials to be zero

$$\Delta^s = \begin{pmatrix} \Delta_s^s & 0 & 0 & 0 \end{pmatrix}, \quad (3.135)$$

which implies  $\Delta_{sij}^s = \Delta_{ij}^{s\uparrow\downarrow} = -\Delta_{ij}^{s\downarrow\uparrow}$  and  $\Delta_{ij}^{s\downarrow\downarrow} = \Delta_{ij}^{s\uparrow\uparrow} = 0$ . The assumption of collinearity means  $\mathcal{E}_{ij}^{\sigma\sigma'} \approx \varepsilon_{i\sigma} \delta_{ij} \delta_{\sigma\sigma'} + \mathcal{R}_{ij}^{\sigma\sigma'} \delta_{\sigma\sigma'}$  and we find the KSBdG Eq. (3.122) in the form

$$E_k \begin{pmatrix} u_k^{1\uparrow} \\ u_k^{1\downarrow} \\ u_k \\ \vdots \\ v_k^{1\uparrow} \\ v_k^{1\downarrow} \\ v_k \\ \vdots \end{pmatrix} = \sum_j \begin{pmatrix} \mathcal{E}_{1j}^{\uparrow} u_k^{j\uparrow} + \Delta_{s1j}^s v_k^{j\downarrow} \\ \mathcal{E}_{1j}^{\downarrow} u_k^{j\downarrow} - \Delta_{s1j}^s v_k^{j\uparrow} \\ \vdots \\ -\mathcal{E}_{1j}^{T\uparrow} v_k^{j\uparrow} + \Delta_{s1j}^{\dagger} u_k^{j\downarrow} \\ -\mathcal{E}_{1j}^{T\downarrow} v_k^{j\downarrow} - \Delta_{s1j}^{\dagger} u_k^{j\uparrow} \\ \vdots \end{pmatrix} \quad (3.136)$$

where we see that  $u_k^{i\uparrow}$  couples with  $v_k^{i\downarrow}$  but not with  $u_k^{i\downarrow}$ . Utilizing this fact we permute the above equations to the form

$$\tilde{g}_k = ( u_k^{1\uparrow} \quad u_k^{2\uparrow} \quad \dots \quad v_k^{1\downarrow} \quad \dots \mid u_k^{1\downarrow} \quad u_k^{2\downarrow} \quad \dots \quad v_k^{1\uparrow} \quad \dots )^T \quad (3.137)$$

and obtain

$$E_k \tilde{g}_k = \begin{pmatrix} \mathcal{E}^\uparrow & \Delta_s^s & 0 & 0 \\ \Delta_s^{s\dagger} & -\mathcal{E}^{T\downarrow} & 0 & 0 \\ 0 & 0 & \mathcal{E}^\downarrow & -\Delta_s^s \\ 0 & 0 & -\Delta_s^{s\dagger} & -\mathcal{E}^{T\uparrow} \end{pmatrix} \tilde{g}_k. \quad (3.138)$$

The spectrum of this block diagonal structure will separate into two kind of eigenfunctions to each individual block

$$g_{k\uparrow} = ( u_k^{1\uparrow} \quad u_k^{2\uparrow} \quad \dots \mid v_k^{1\downarrow} \quad \dots \mid 0 \quad 0 \quad \dots \mid 0 \quad \dots )^T \quad (3.139)$$

$$g_{k\downarrow} = ( 0 \quad 0 \quad \dots \mid 0 \quad \dots \mid u_k^{1\downarrow} \quad u_k^{2\downarrow} \quad \dots \mid v_k^{1\uparrow} \quad \dots )^T. \quad (3.140)$$

We see that the quantum numbers of the SC KS system split into spin channels  $k, k' \rightarrow k, \sigma$  solving individual, reduced equations

$$E_{k\sigma} g_{k\sigma} = \begin{pmatrix} \mathcal{E}^\sigma & \text{sign}(\sigma) \Delta_s^s \\ \text{sign}(\sigma) \Delta_s^{s\dagger} & -\mathcal{E}^{T-\sigma} \end{pmatrix} g_{k\sigma} \quad (3.141)$$

From the separate solutions  $g_{k\sigma}$  of the Eqs. (3.139) and (3.140) we find that in the singlet/collinear case  $u_{k\sigma}^{i\mu} \propto \delta_{\mu\sigma}$  and  $v_{k\sigma}^{i\mu} \propto \delta_{\mu,-\sigma}$ . We introduce a single spin notation

$$v_{k-\sigma}^i \equiv v_{k\sigma}^{i-\sigma} \quad (3.142)$$

$$u_{k\sigma}^i \equiv u_{k\sigma}^{i\sigma}. \quad (3.143)$$

Keep in mind that the spin  $\sigma$  in the short hand notation of  $u$  and  $v$  refers to the NS KS wavefunction basis  $\{\vec{\varphi}_{i\sigma}(\mathbf{r})\}$ . In the case of  $v_{k\sigma}^i$  the index corresponds to the spin-opposite eigenvalue  $E_{k,-\sigma}$  and eigenvector  $g_{k,-\sigma}$ !

We want to find the corresponding hole state  $g_{k\sigma}^c$ , i.e. the state with the opposite energy  $-E_{k\sigma}$ <sup>10</sup>. We define

$$g_{k\sigma}^c = ( v_{k-\sigma}^{1*} \quad v_{k-\sigma}^{2*} \quad \dots \mid u_{k\sigma}^{1*} \quad \dots )^T \quad (3.144)$$

and it is easily shown similar to the hole state for Eq. (3.122) that  $g_{k-\sigma}^c$  solves

$$-E_{k-\sigma} g_{k-\sigma}^c = \begin{pmatrix} \mathcal{E}^\sigma & \text{sign}(\sigma) \Delta_s^s \\ \text{sign}(\sigma) \Delta_s^{s\dagger} & -\mathcal{E}^{T-\sigma} \end{pmatrix} g_{k-\sigma}^c \quad (3.145)$$

We observe the fact that particle and hole are of different spin channels which means that the negative solution to a positive  $E_{k\sigma}$  stems from the spin inverted KSBdG equation. This is somewhat intuitive because one expects a hole to be the time-reversed, negative energy particle and, being an angular momentum operator, the spin is inverted under time inversion.

### 3.5.2. Spin Decoupling Approximation

Anderson extended the BCS model of SC to the ‘‘dirty limit’’ [43] essentially coupling a given single particle state with its time reversed. Nearly all microscopic theories on SC are build on this idea: Apart from the spin degenerate SCDFT [21] also the Eliashberg theory on SC [44].

<sup>10</sup>Many sensible definitions of the ‘‘hole’’ state exist. For example instead of positive excitation states one may just as well use the (weakly perturbed) electronic bands from a normal state calculation as particles and define the reflection at the Fermi energy as holes. The individual definitions differ by a ground state energy which cancels in any thermal average.

We introduce a similar approximation in this context assuming the potential matrix elements Eq. (3.115) to be

$$\Delta_{sij}^s = \Delta_{si,-j}^s \delta_{i,-j} \quad (3.146)$$

and in addition that the basis functions remain essentially unchanged in the SC:

$$\mathcal{E}_{ij}^\sigma \approx (\varepsilon_{i\sigma} + \mathcal{R}_{ii}^{\sigma\sigma}) \delta_{ij} \delta_{\sigma\sigma'}. \quad (3.147)$$

We thus assume that the NS KS basis  $\{\vec{\varphi}_{i\sigma}(\mathbf{r})\}$  describes the true quasi particle spectrum of the material without SC and that it is enough to consider how these states are paired with their time reversed to describe the SC phase. These constrains will provide a huge simplification of the theory since we may solve the KSBdG equations analytically. Choosing  $\Delta_{si,-j}^s \delta_{i,-j}$  instead of a diagonal matrix means we keep the matrix elements that correspond to the states  $\vec{\varphi}_{i\sigma}^*(\mathbf{r})$  and  $\vec{\varphi}_{-j-\sigma}^*(\mathbf{r})$ . In the spin degenerate limit this matches earlier work [21, 22] and leads to a strict momentum conservation at vertices in the diagrammatic derivation of  $xc$  potentials. Most importantly we will see later in Sec. 3.6 that for a system that does not depend on the absolute position in a lattice, this approximation  $\Delta_{si,-j}^s \delta_{i,-j}$  is exact for the Bloch vectors. A problem is that, if up- and down spin potential differ significantly it might be difficult to identify the “correct” states to pair. In a ferro magnet for example  $\vec{\varphi}_{n\mathbf{k}\uparrow}(\mathbf{r})$  and  $\vec{\varphi}_{n',-\mathbf{k}\downarrow}(\mathbf{r})$  are not uniquely related by a time reversal operation, because the band quantum index remains undefined. In fact, acting with a time reversal operator on  $\vec{\varphi}_{n\mathbf{k}\uparrow}(\mathbf{r})$  in general many different  $n'$  of  $\vec{\varphi}_{n',-\mathbf{k}\downarrow}(\mathbf{r})$  will overlap with the result. Thus inherent to the SDA is the assumption that up- and down channels differ little.

In approximating  $\mathcal{E}_{ij}^\sigma$  we may also keep diagonal corrections  $\mathcal{R}_{ii}^{\sigma\sigma}$ . These are omitted from now on but can be easily reconstructed.

Let us split the set of  $k = (\mathbf{k}, n)$  in two, where the one half we refer to as “negative”. For definiteness let this be the second half of  $N$  orbitals with the ordering used for  $g_{k\sigma}$

$$g_{k\sigma} = \left( u_{k\sigma}^1 \quad \dots \quad u_{k\sigma}^{N/2} \quad u_{k\sigma}^{-1} \quad \dots \quad u_{k\sigma}^{-N/2} \quad | \quad v_{k-\sigma}^1 \quad \dots \quad v_{k-\sigma}^{N/2} \quad v_{k-\sigma}^{-1} \quad \dots \quad v_{k-\sigma}^{-N/2} \right)^T \quad (3.148)$$

In this notation within the SDA the matrix of Eq. (3.141) has the form

$$\begin{pmatrix} \varepsilon_{1\uparrow} & 0 & 0 & \dots & 0 & \dots & \Delta_{s1,-1}^s & 0 \\ 0 & \ddots & \vdots & \ddots & \vdots & \ddots & 0 & \ddots \\ 0 & \dots & \varepsilon_{-1\uparrow} & 0 & \Delta_{s-1,1}^s & 0 & 0 & \dots \\ \vdots & \ddots & 0 & \ddots & 0 & \ddots & \vdots & \ddots \\ 0 & \dots & \Delta_{s-1,1}^{s*} & 0 & -\varepsilon_{1\downarrow} & 0 & 0 & \dots \\ \vdots & \ddots & 0 & \ddots & 0 & \ddots & \vdots & \ddots \\ \Delta_{s1,-1}^{s*} & 0 & 0 & \dots & 0 & \dots & -\varepsilon_{-1\downarrow} & 0 \\ 0 & \ddots & \vdots & \ddots & \vdots & \ddots & 0 & \ddots \end{pmatrix} \quad (3.149)$$

Pivoting, we can reduce this to a Block diagonal form (Starting with the  $\frac{3}{2}N + 1$  row/column that we pivot to 2 and so on)

$$\begin{pmatrix} \varepsilon_{1\uparrow} & \Delta_{s1,-1}^s & 0 & & & & & \\ \Delta_{s1,-1}^{s*} & -\varepsilon_{-1\downarrow} & 0 & & & & & \\ 0 & 0 & \ddots & 0 & 0 & 0 & & \\ & & & 0 & \varepsilon_{-1\uparrow} & \Delta_{s-1,1}^s & 0 & \\ & & & 0 & \Delta_{s-1,1}^{s*} & -\varepsilon_{1\downarrow} & 0 & \\ & & & 0 & 0 & 0 & \ddots & \end{pmatrix} \quad (3.150)$$



Due to the block diagonal form the eigenvectors are

$$\{g_{k\sigma} = \left( \dots 0 \ u_{k\sigma}^k v_{k-\sigma}^{-k} \ 0 \ \dots \right)^T\} \quad (3.151)$$

where  $k$  labels again all, “positive” and “negative” indices. Each of the independent problems is given by the  $2 \times 2$  matrix equation

$$E_{k\sigma} \begin{pmatrix} u_{k\sigma}^k \\ v_{k-\sigma}^{-k} \end{pmatrix} = \begin{pmatrix} \varepsilon_{k\sigma} & \text{sign}(\sigma)\Delta_{sk-k}^s \\ \text{sign}(\sigma)\Delta_{sk-k}^{s*} & -\varepsilon_{-k-\sigma} \end{pmatrix} \begin{pmatrix} u_{k\sigma}^k \\ v_{k-\sigma}^{-k} \end{pmatrix} \quad (3.152)$$

where  $g_{k\sigma}^c = \left( \dots 0 \ v_{k-\sigma}^{-k*} \ u_{k\sigma}^{k*} \ 0 \ \dots \right)^T$  solves the above equation with  $-\sigma$  with the eigenvalue  $-E_{k\sigma}$ . Note here that in terms of  $u_{k\sigma}^i$  and  $v_{k\sigma}^i$  this approximation requires all expansion coefficients of normal state wavefunctions to be zero, except the one with the same band and Bloch vector quantum numbers

$$u_{k\sigma}^i = u_{k\sigma}^k \delta_{ik} \quad (3.153)$$

$$v_{k\sigma}^i = v_{k\sigma}^{-k} \delta_{i,-k}. \quad (3.154)$$

Recalling the discussion at the beginning of this Subsection, we see how the two conditions Eqs. (3.146) and (3.147) for the pair potential and KS eigenvalues, respectively only allow for hybridization of a particle with its time reversed hole wavefunction. Because of the simple form of the KSBdG equations we may compute the solutions analytically. Similar to a numerical solution the problem appears that we have to construct the  $u_{k\sigma}^k, v_{k-\sigma}^{-k}$  from the eigenvectors. By definition the positive energy eigenvectors contain  $u_{k\sigma}^k, v_{k-\sigma}^{-k}$  in the form  $g_{k\mu} \sim (u_{k\mu}^k, v_{k-\mu}^{-k})$ , while the negative energy eigenvectors in the form  $g_{k\mu}^c \sim (v_{k\mu}^{-k*}, u_{k-\mu}^{k*})$ . In the analytic solution it is not known which eigenvalue is positive or negative. From the high energy limit  $\varepsilon_{k\mu} + \varepsilon_{-k-\mu} \gg \varepsilon_{k\mu} - \varepsilon_{-k-\mu}$  we take the name  $\pm$  for the branches. The eigenvalues to Eq. (3.152) are

$$E_{k\mu}^- = \frac{\varepsilon_{k\mu} - \varepsilon_{-k-\mu}}{2} - \sqrt{\left(\frac{\varepsilon_{k\mu} + \varepsilon_{-k-\mu}}{2}\right)^2 + |\Delta_{sk,-k}^s|^2} \quad (3.155)$$

$$E_{k\mu}^+ = \frac{\varepsilon_{k\mu} - \varepsilon_{-k-\mu}}{2} + \sqrt{\left(\frac{\varepsilon_{k\mu} + \varepsilon_{-k-\mu}}{2}\right)^2 + |\Delta_{sk,-k}^s|^2} \quad (3.156)$$

and the non-normalized eigenvectors can be written as

$$\tilde{g}_{k\mu}^- = \begin{pmatrix} \frac{\varepsilon_{-k-\mu} + E_{k\mu}^-}{\text{sign}(\mu)\Delta_{sk,-k}^{s*}} \\ 1 \end{pmatrix} \quad \tilde{g}_{k\mu}^+ = \begin{pmatrix} \frac{\varepsilon_{-k-\mu} + E_{k\mu}^+}{\text{sign}(\mu)\Delta_{sk,-k}^{s*}} \\ 1 \end{pmatrix} \quad \text{short: } \tilde{g}_{k\mu}^\alpha = \begin{pmatrix} \frac{\varepsilon_{-k-\mu} + E_{k\mu}^\alpha}{\text{sign}(\mu)\Delta_{sk,-k}^{s*}} \\ 1 \end{pmatrix} \quad (3.157)$$

We have 4 solutions that are related to each other in energy <sup>11</sup>

$$E_{k\mu}^- = \varepsilon_{k\mu} - \varepsilon_{-k-\mu} - E_{k\mu}^+ \quad (3.158)$$

$$E_{-k-\mu}^- = -E_{k\mu}^+ \quad (3.159)$$

$$E_{k\mu}^+ = \varepsilon_{k\mu} - \varepsilon_{-k-\mu} - E_{k\mu}^- \quad (3.160)$$

$$E_{-k-\mu}^+ = -E_{k\mu}^- \quad (3.161)$$

The situation is sketched in Fig. 3.1 . In the spin degenerate limit  $E_{k\mu}^+ = E_{-k-\mu}^+ = -E_{k\mu}^- = -E_{-k-\mu}^- \geq 0$ , thus here it is clear that  $u_{k\sigma}^k v_{k-\sigma}^{-k}$  can be simply taken from the (+) solution. In the present situation the condition has to be explicitly enforced with a  $\theta(E_{k\mu}^\alpha)$ ,  $\alpha = \pm$ . This

<sup>11</sup>from now on we will use the short hand notation  $\Delta_{sk}^s \equiv \Delta_{sk,-k}^s$

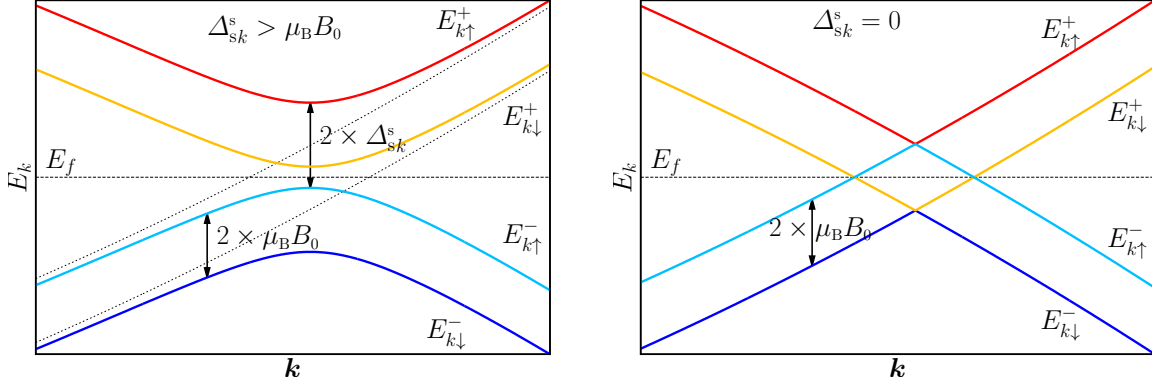


Figure 3.1.: Sketch of the Bogoliubov eigenvalues  $E_{k\mu}^{\pm}$  for a free electron gas with a splitting  $\epsilon_{k\sigma} = -(\hbar\mathbf{k})^2/(2m_e) + \text{sign}(\sigma)\mu_B B_0$ . We choose a constant  $\Delta_{sk}^s > \mu_B B_0$  in a) and  $\Delta_{sk}^s = 0$  in b). We plot the + Bogoliubov branch in red and orange for  $\uparrow$  and  $\downarrow$  and the - branch in light blue and dark blue for  $\uparrow$  and  $\downarrow$ , respectively. We indicate the  $\epsilon_{k\sigma}$  in a) as thin dashed lines. In a), the + branches are strictly larger than the Fermi Energy  $E_f$  and thus constitute the SC KS particle excitations. On the other hand for  $\Delta_{sk}^s < \mu_B B_0$  as in b), the + and - branch partly swap their order. When  $E_{k\uparrow}^- > E_f$  the SC KS particle excitations are from the - branch also.

means if a formula requires the coefficients  $u_{k\sigma}^k$  or  $v_{k-\sigma}^{-k}$  we have to consider both possibilities from the normalized  $g_{k\mu}^{\pm} = \tilde{g}_{k\mu}^{\pm}/|\tilde{g}_{k\mu}^{\pm}|$  that is

$$g_{k\mu}^{\alpha} = (u_{k\mu}^{k\alpha}, v_{k-\mu}^{-k\alpha})^T \quad (3.162)$$

and drop the negative part with  $\theta(E_{k\mu}^{\alpha})$ . We will soon see an example when we discuss the form of the Bogoliubov transformation in the SDA (Eq. (3.166)).

As noted, because the SDA allows to solve the KSBdG system analytically, we can express all KS wavefunction, i.e.  $g_k$  in terms of the potential  $\Delta_s^s$  matrix elements. Thus the theory becomes a potential functional theory. Several relation among the eigenvalues and single electron eigenvalues will prove useful in derivations. We give them in the Appendix B. Using those relation we find

$$|g_{k\mu}^{\alpha}| = \sqrt{\frac{|E_{k\mu}^{\alpha} + E_{-k-\mu}^{\alpha}|}{|E_{k\mu}^{\alpha} - \epsilon_{k\mu}|}} \quad (3.163)$$

and

$$v_{k-\mu}^{-k\alpha} = \sqrt{\frac{|E_{k\mu}^{\alpha} - \epsilon_{k\mu}|}{|E_{k\mu}^{\alpha} + E_{-k-\mu}^{\alpha}|}} \quad (3.164)$$

while passing we note that this equals  $v_{-k\mu}^{k-\alpha}$ . Further we see

$$u_{k\mu}^{k\alpha} = \text{sign}(\alpha)\text{sign}(\mu) \frac{\Delta_{sk}^s}{|\Delta_{sk}^s|} \sqrt{\frac{|\epsilon_{-k-\mu} + E_{k\mu}^{\alpha}|}{|E_{k\mu}^{\alpha} + E_{-k-\mu}^{\alpha}|}} \quad (3.165)$$

which is equal to  $u_{-k-\mu}^{k-\alpha}$ . We note a problem with the Bogoliubov-Valatin transformation Eq. (3.102) that read in the context of the SDA

$$\hat{\Psi}(\mathbf{r}) = \sum_{k\sigma,\alpha} \begin{pmatrix} u_{k\uparrow}^{k\alpha}\theta(E_{k\uparrow}^{\alpha})\varphi_k(\mathbf{r}\uparrow)\delta_{\sigma\uparrow} & u_{k\uparrow}^{k\alpha}\theta(-E_{k\uparrow}^{\alpha})\varphi_k(\mathbf{r}\uparrow)\delta_{\sigma\uparrow} \\ u_{k\downarrow}^{k\alpha}\theta(E_{k\downarrow}^{\alpha})\varphi_k(\mathbf{r}\downarrow)\delta_{\sigma\downarrow} & u_{k\downarrow}^{k\alpha}\theta(-E_{k\downarrow}^{\alpha})\varphi_k(\mathbf{r}\downarrow)\delta_{\sigma\downarrow} \\ v_{k\uparrow}^{-k\alpha}\theta(E_{k\downarrow}^{\alpha})\varphi_{-k}^*(\mathbf{r}\uparrow)\delta_{-\sigma,\uparrow} & v_{k\uparrow}^{-k\alpha}\theta(-E_{k\downarrow}^{\alpha})\varphi_{-k}^*(\mathbf{r}\uparrow)\delta_{-\sigma,\uparrow} \\ v_{k\downarrow}^{-k\alpha}\theta(E_{k\uparrow}^{\alpha})\varphi_{-k}^*(\mathbf{r}\downarrow)\delta_{-\sigma,\downarrow} & v_{k\downarrow}^{-k\alpha}\theta(-E_{k\uparrow}^{\alpha})\varphi_{-k}^*(\mathbf{r}\downarrow)\delta_{-\sigma,\downarrow} \end{pmatrix} \cdot \hat{\Phi}_{k\sigma}. \quad (3.166)$$

Because the spin is a good quantum number in the SC KS system it is more intuitive to promote  $\hat{\Phi}_k$  to a 4 component Nambu and spin vector similar to  $\hat{\Psi}$ . This leads to a  $4 \times 4$  Bogoliubov transformation in Nambu and spin space, that we write as<sup>12</sup>

$$\hat{\Psi}(\mathbf{r}) = \sum_{k\alpha} \begin{pmatrix} u_{k\uparrow}^{k\alpha} \theta(E_{k\uparrow}^\alpha) \varphi_k(\mathbf{r} \uparrow) & 0 & u_{k\uparrow}^{k\alpha} \theta(-E_{k\uparrow}^\alpha) \varphi_k(\mathbf{r} \uparrow) & 0 \\ 0 & u_{k\downarrow}^{k\alpha} \theta(E_{k\downarrow}^\alpha) \varphi_k(\mathbf{r} \downarrow) & 0 & u_{k\downarrow}^{k\alpha} \theta(-E_{k\downarrow}^\alpha) \varphi_k(\mathbf{r} \downarrow) \\ 0 & v_{k\uparrow}^{-k\alpha} \theta(E_{k\downarrow}^\alpha) \varphi_{-k}^*(\mathbf{r} \uparrow) & 0 & v_{k\uparrow}^{-k\alpha} \theta(-E_{k\downarrow}^\alpha) \varphi_{-k}^*(\mathbf{r} \uparrow) \\ v_{k\downarrow}^{-k\alpha} \theta(E_{k\uparrow}^\alpha) \varphi_{-k}^*(\mathbf{r} \downarrow) & 0 & v_{k\downarrow}^{-k\alpha} \theta(-E_{k\uparrow}^\alpha) \varphi_{-k}^*(\mathbf{r} \downarrow) & 0 \end{pmatrix} \cdot \hat{\Phi}_k. \quad (3.167)$$

Note that in the example of Fig. (3.1) (right) for  $|\Delta_{sk}^s| < \frac{\varepsilon_{k\mu} - \varepsilon_{-k-\mu}}{2}$  in a certain range in  $k$  (the red and light blue lines in the range of  $k$  in the middle of the plot) only states with  $E_{k\uparrow}^\pm$  are positive while all  $E_{k\downarrow}^\pm$  are negative. We observe that in this case the Bogoliubov transformations Eq. (3.102) are singular and thus not unitary because none of the  $\alpha$  branches to a given spin is positive. Thus,  $\hat{\Psi}(\mathbf{r})$  does not depend on, e.g.  $\hat{\Phi}_k(\uparrow)$ . Ultimately this is a consequence of our initial requirement that all  $E_{k,\sigma}$  of the SC KS system Eq. (3.88) are positive which cannot be met for a given spin channel and set of quantum numbers  $k, \sigma$  in this example. We may overcome this problem only by relaxing the condition  $E_{k,\sigma} \geq 0$  of the SC KS system Eq. (3.88). If we, for example, had chosen  $E_{k\sigma}^+$  as excitations of the SC KS system in Eq. (3.88) the *Bogoliubov transformation remains unitary*. On the other hand we loose the interpretation of the ground state having only positive energy excitations. This problem was realized before in the context of BCS theory, see for example the discussion in Ref. [29].

Formally, we arrive at the same equations if we always choose the  $E_{k\sigma}^+$  as excitations, independent on the sign of  $E_{k\sigma}^+$ . We have to accept that this region  $E_{k\sigma}^+ < 0$  is equivalent to excitations on the SC ground state that reduce the energy. At the price of redefining the ground state energy, with the rewriting  $-|E_k| \hat{\gamma}_k^\dagger \hat{\gamma}_k \equiv -|E_k| + |E_k| \hat{\gamma}_k^\dagger \hat{\gamma}_k$  with  $\hat{\gamma}_k = \hat{\gamma}_k^\dagger$  we can go to a hole picture where the problem does not appear. The ground state will correspond to the minimal energy solutions, thus all  $\hat{\gamma}_k$  states with negative energies will be occupied. Note that the  $\hat{\gamma}_k$  are the Bogoliubov transformed electron field so we interpret this negative  $E_k$  region as to be occupied by normal electrons with all pairs broken. As is clear from the independence on the ground state energy in thermal expectation values in statistical physics observables are independent on our interpretation what to use as the ground state.

We want to close this Section with a note about the FFLO phase. The key to obtain a FFLO solution is to allow finite momentum pairing but it is not correct to simply interpret the Bloch vector as the momentum of the electron state. In fact we will see in Sec. 3.6.1 that if the pair potential is independent on the absolute position in the lattice its matrix elements are diagonal in the Bloch vector. By analogy with the free electron gas in a periodic lattice we see that the finite momentum pairing will translate into off-diagonal band pairing. Thus excluding this possibility means already at this step that we exclude the FFLO state solution.

## 3.6. Symmetries of the SC KS System

In this Section we give a discussion of the implication of certain very general symmetries, namely an independence of the pair potential on the absolute position in the lattice in Subsection 3.6.1 and a type of gauge symmetry in Subsection 3.6.2.

<sup>12</sup>We choose the arbitrary ordering of the matrix coefficients to  $(\uparrow, \downarrow, \uparrow, \downarrow)$  for the spin of the NS KS basis as rows and  $(\uparrow, \downarrow, \uparrow, \downarrow)$  for the columns in the SC KS system.

### 3.6.1. Translational Symmetry

In this Subsection we want to clarify the effect of assumed translational invariance of the order parameter and the pair potential. We discuss only the pair potential because the discussion for  $\chi$  is the same. Now

$$\Delta^s(\mathbf{r} + \mathbf{T}_i, \mathbf{r}' + \mathbf{T}_i) = \Delta^s(\mathbf{r}, \mathbf{r}') \quad (3.168)$$

where  $\mathbf{T}_i$  is a lattice vector, so that the potential is independent on the absolute position in the lattice. As we intend to solve the problem in the basis of Bloch KS orbitals we need to deduce the consequences of this symmetry on matrix elements. These are, omitting the spin label in this subsection<sup>13</sup>

$$\begin{aligned} \Delta^s_{n\mathbf{k}n'\mathbf{k}'} &= \int d\mathbf{r} \int d\mathbf{r}' \vec{\varphi}_{n\mathbf{k}}(\mathbf{r}) \cdot (\Phi \cdot \Delta^s(\mathbf{r}, \mathbf{r}')) \cdot \vec{\varphi}_{n'\mathbf{k}'}(\mathbf{r}') \quad (3.169) \\ &= \sum_{ij} \int d\bar{\mathbf{r}} \int d\bar{\mathbf{r}}' \vec{\varphi}_{n\mathbf{k}}(\bar{\mathbf{r}} + \mathbf{T}_i) \cdot (\Phi \cdot \Delta^s(\bar{\mathbf{r}} + \mathbf{T}_i, \bar{\mathbf{r}}' + \mathbf{T}_j)) \cdot \vec{\varphi}_{n'\mathbf{k}'}(\bar{\mathbf{r}}' + \mathbf{T}_j). \quad (3.170) \end{aligned}$$

We reorder the sum in a way that lattice vectors  $\mathbf{T}_j$  are fixed and then all  $\mathbf{T}_i \rightarrow \mathbf{T}_i + \mathbf{T}_j$  are summed, we obtain together with (3.168)

$$\Delta^s_{n\mathbf{k}n'\mathbf{k}'} = \sum_i \int d\bar{\mathbf{r}} \int d\bar{\mathbf{r}}' \vec{\varphi}_{n\mathbf{k}}(\bar{\mathbf{r}}) \cdot (\Phi \cdot \Delta^s(\bar{\mathbf{r}} + \mathbf{T}_i, \bar{\mathbf{r}}')) \cdot \vec{\varphi}_{n'\mathbf{k}'}(\bar{\mathbf{r}}') e^{i\mathbf{k} \cdot \mathbf{T}_i} \delta_{\mathbf{k}', -\mathbf{k}}. \quad (3.171)$$

Here we have used that  $\sum_j e^{i\mathbf{T}_j \cdot (\mathbf{k}' + \mathbf{k})} = N_q \delta_{\mathbf{k}', -\mathbf{k}}$  and  $\vec{\varphi}_{n\mathbf{k}}$  as the periodic part of the KS Bloch function. This means that, in fact,  $\Delta^s_{ij}$  is for many cases anti diagonal in the Bloch vector part (it pairs  $\mathbf{k}$  with  $-\mathbf{k}$ ).

### 3.6.2. Gauge Invariance of the KS Hamiltonian

We inferred the KSBdG equations from the condition that the Hamiltonian is diagonal in the new fields  $\hat{\Phi}_k$  (resulting in Eq. (3.105)). In the basis of NS KS orbitals of Section 3.4.3 we can equivalently state the condition for the diagonality of the Nambu KS Hamiltonian  $\bar{H}_{\text{KS}}$  Eq. (3.105) as

$$E_k \tau_z \delta_{kk'} = \sum_{ij} \begin{pmatrix} g_k & g_k^c \end{pmatrix}_i^\dagger \begin{pmatrix} \mathcal{E} & \Phi \cdot \Delta^s \\ (\Phi \cdot \Delta^s)^\dagger & -\mathcal{E}^T \end{pmatrix}_{ij} \begin{pmatrix} g_{k'} & g_{k'}^c \end{pmatrix}_j. \quad (3.172)$$

The left hand side is  $\sim \tau_z \delta_{kk'}$  and this condition is, in fact, independent on a rotation about the  $\tau_z$  axis in Nambu space [28, 37]. Such a rotation with the angle  $\xi_k \in \mathbb{R}$  is generated by  $\tau_z$  in the following way: Because of  $\tau_z^{2n} = \tau_0$  and  $\tau_i \tau_j = \delta_{ij} + i \sum_k \varepsilon_{ijk} \tau_k$

$$e^{-i\tau_z \frac{\xi_k}{2}} = \tau_0 \cos(\xi_k/2) - i\tau_z \sin(\xi_k/2) \quad (3.173)$$

follows

$$e^{-i\tau_z \frac{\xi_k}{2}} \tau_z e^{i\tau_z \frac{\xi_k}{2}} = \tau_z \quad (3.174)$$

$$e^{-i\tau_z \frac{\xi_k}{2}} \tau_y e^{i\tau_z \frac{\xi_k}{2}} = \tau_y \cos(\xi_k) - \tau_x \sin(\xi_k) \quad (3.175)$$

$$e^{-i\tau_z \frac{\xi_k}{2}} \tau_x e^{i\tau_z \frac{\xi_k}{2}} = \tau_x \cos(\xi_k) + \tau_y \sin(\xi_k). \quad (3.176)$$

<sup>13</sup> $\bar{\mathbf{r}}$  and  $\bar{\mathbf{r}}'$  are defined to be within the first unit cell.

Now the rotated Eq. (3.172) takes the form

$$E_k(\tau_z)' \delta_{kk'} \equiv E_k \tau_z \delta_{kk'} = \sum_{ij} (g_k \ g_k^c)'_i \begin{pmatrix} \mathcal{E} & \Phi \cdot \Delta_s \\ (\Phi \cdot \Delta_s)^\dagger & -\mathcal{E}^T \end{pmatrix}'_{ij} (g_{k'} \ g_{k'}^c)'_j \quad (3.177)$$

where here the prime on  $\bar{O}'_{kk'}$  indicates that we have a rotated matrix according to  $\bar{O}'_{kk'} \equiv e^{-i\tau_z \frac{\xi_k}{2}} \bar{O}_{kk'} e^{i\tau_z \frac{\xi_{k'}}{2}}$ . We may now use the primed unitary transformation  $(g_{k'} \ g_{k'}^c)'_j$  to construct  $\hat{\Phi}'_k$  but as can be seen from the scalar form of the KS Hamiltonian Eq. (3.100)

$$\hat{H}_s^{e'} \equiv \hat{H}_s^e \quad (3.178)$$

and thermal averages of operators do not depend on the choice of  $\xi_k$ . Thus we say the rotation by  $\xi_k$  is a gauge transformation since measurable quantities do not depend on it. We may choose it in any way that is convenient. This becomes of practical relevance if we consider the situation in the SDA with the analog of Eq. (3.172) being

$$\begin{pmatrix} \varepsilon_{k\mu} & \text{sign}(\mu) \Delta_{sk}^s \\ \text{sign}(\mu) \Delta_{sk}^{s*} & -\varepsilon_{-k-\mu} \end{pmatrix} = \frac{\varepsilon_{k\mu} - \varepsilon_{-k-\mu}}{2} \tau_0 + \frac{\varepsilon_{k\mu} + \varepsilon_{-k-\mu}}{2} \tau_z - \text{sign}(\mu) \Im \Delta_{sk}^s \tau_y + \text{sign}(\mu) \Re \Delta_{sk}^s \tau_x. \quad (3.179)$$

Choosing

$$\xi_k = \arctan\left(\frac{\Im \Delta_{sk}^s}{\Re \Delta_{sk}^s}\right) \quad (3.180)$$

after a little algebra we arrive at

$$\begin{pmatrix} \varepsilon_{k\mu} & \text{sign}(\mu) \Delta_{sk}^s \\ \text{sign}(\mu) \Delta_{sk}^{s*} & -\varepsilon_{-k-\mu} \end{pmatrix}' = \begin{pmatrix} \varepsilon_{k\mu} & \text{sign}(\mu) \tilde{\Delta}_{sk}^s \\ \text{sign}(\mu) \tilde{\Delta}_{sk}^s & -\varepsilon_{-k-\mu} \end{pmatrix} \quad (3.181)$$

with  $\tilde{\Delta}_{sk}^s = \text{sign}(\Re \Delta_{sk}^s) |\Delta_{sk}^s| \in \mathbb{R}$ . Thus our general complex decoupled pair potential is gauge equivalent to a purely real one. It is important to understand when this cannot be done: If  $\Delta_s^s$  is non-diagonal the  $k$ -local rotation angle does not have enough freedom to make either the hermitian or antihermitian part of the matrix  $\Delta_s^s$  vanish.

## Summary

In this Chapter we have extended the HK Theorem of SCDFT [20] to include apart from the normal density  $n(\mathbf{r})$ , the SC order parameter  $\chi(\mathbf{r}, \mathbf{r}')$  and the nuclear  $N$ -body density  $\Gamma(\mathbf{R}_1 \dots \mathbf{R}_N)$  also the magnetic density  $\mathbf{m}(\mathbf{r})$ . We have introduced a KS system of non-interacting electrons that are decoupled from the nuclei but reproduces the interacting densities exactly. We have written the electronic KS Hamiltonian in a  $2 \times 2$  Nambu-Anderson notation where the first component annihilates the electronic field and the second component creates it. The condition that the electronic KS system is diagonal leads to the KSBdG equations that constitute unitary transformations which mix creation and annihilation operators. Then, we have expanded the system in normal state, zero temperature KS orbitals because we expect these to be reasonably close to the quasi particle spectrum. In the most important approximation, the SDA, we only allow the mixing of a given KS orbital with its time reversed. In this case the only non-vanishing pair potential matrix elements in that basis can be chosen real by gauge symmetry.

## 4. Interaction Matrix Elements

Usually in the context of a DFT the interactions are incorporated via an  $xc$  potential that depends on the densities. For example the correlation part of the LDA includes a parametrization for the local density at a point  $\mathbf{r}$ . Our plan is to include collective interactions such as the electron phonon interaction into the SpinSCDFT functional that are not easily written as a density functional in the spirit of an LDA.

We intend to use diagrammatic perturbation theory starting from the KS as a formally non-interacting system which results in an equation for the  $xc$  potential for SpinSCDFT in terms of SE contributions. See Fig. 1.1 for an overview of the steps necessary. In this Chapter we introduce the interactions as they will appear in the SE contributions. As we did earlier in Chapter 3 we represent all entities in the basis of NS KS orbitals  $\{\tilde{\varphi}_{i\sigma}(\mathbf{r})\}$ . We briefly discuss the electron phonon matrix elements in Sec. 4.1 and the effective Coulomb matrix elements in Sec 4.2.

### 4.1. Electron Phonon Matrix Elements

In Sec. 3.3 we have introduced the bare nuclear KS system as the system with only the second order variation of the  $xc$  potential with respect to atomic displacements (the first order is zero), resulting in a system of well defined *bare* KS phonons  $\hat{b}_{\mathbf{q}\lambda}$ . We come back to this point in Section 5.1 where we define the (bare) phononic propagator.

The standard way to calculate the electron-phonon coupling is to adopt a heuristic picture to consider the coupling as given by the variation in the potential  $\frac{\delta v_{scf}(\mathbf{r}\sigma)}{\delta u_{\mathbf{q}\lambda}}$  in the KS system that is caused by the displacements from equilibrium of a certain mode  $u_{\mathbf{q}\lambda}$ [35]. The modes are computed using density functional perturbation theory [35]. This “scattering potential” creates overlap among the KS states which we take in the following as the electron-phonon matrix elements

$$g_{kk'\sigma}^{\mathbf{q}\lambda} = \int d\mathbf{r} \frac{\delta v_{scf}(\mathbf{r}\sigma)}{\delta u_{\mathbf{q}\lambda}} \varphi_k^*(\mathbf{r}\sigma) \varphi_{k'}(\mathbf{r}\sigma). \quad (4.1)$$

$v_{scf}(\mathbf{r}\sigma)$  is the full single particle potential in the KS system, i.e. we do not distinguish the magnetic part explicitly. In the case of non-collinear magnetism  $v_{scf}(\mathbf{r})$  may even be a spin matrix. We exclude this possibility here, as it involves additional summations in the functional construction, but it is straight forward to include. Explicit calculation of the object  $g_{kk'\sigma}^{\mathbf{q}\lambda}$ , for example in Ref. [35] shows that it conserves Bloch momentum  $g_{kk'\sigma}^{\mathbf{q}\lambda} \equiv g_{n\mathbf{k},n'\mathbf{k}+\mathbf{q}\sigma}^{\lambda} \delta_{\mathbf{k}',\mathbf{k}+\mathbf{q}}$ . This is in line with the usual momentum conservation at a coupling vertex in diagrammatic perturbation theory of Sec. 5.2. The deeper reason for this conservation law is the underlying (lattice periodic) translational symmetry.

## 4.2. Electronic Screening and Effective Interaction

The electrons interact with each other through the instantaneous Coulomb potential:<sup>1</sup>

$$V^{\text{Coul}}(\mathbf{r}, \mathbf{r}') = \frac{1}{4\pi\epsilon_0} \frac{1}{|\mathbf{r} - \mathbf{r}'|}. \quad (4.2)$$

which on the other hand is heavily screened in a solid, especially in a metal. In fact, a direct calculation using the “bare” Coulomb potential is unlikely to converge because of the delicate long range  $\mathbf{q} \rightarrow \mathbf{0}$  limit. We consider an effective interaction potential of the form

$$w(\mathbf{r}, \mathbf{r}', \nu_n) = \frac{1}{4\pi\epsilon_0} \frac{1}{|\mathbf{r} - \mathbf{r}'|} + \frac{1}{\hbar} \left( \frac{1}{4\pi\epsilon_0} \right)^2 \int d\mathbf{r}_1 \int d\mathbf{r}'_1 \frac{\chi^{\text{pol}}(\mathbf{r}_1, \mathbf{r}'_1, \nu_n)}{|\mathbf{r} - \mathbf{r}_1| |\mathbf{r}'_1 - \mathbf{r}'|} \quad (4.3)$$

with the polarization propagator  $\chi^{\text{pol}}$  and the Matsubara frequency  $\nu_n$  to be introduced later in this Section. The above equation can be reasoned from the intuitive picture that two charged test particles repel each other via the bare Coulomb interaction. In the presence of a surrounding medium we have to add the effect that the test charges locally polarizes the medium which adds to the bare potential, thus creating an effective interaction. Formally the equation follows e.g. from diagrammatic perturbation theory (Sec. 5.2) where we consider the bare Coulomb potentials plus the sum of all connected diagrams that have exactly two external Coulomb lines. We will come back to this point in Section 5.2; here we take the equation as given. Note that through the screening we obtain a non-trivial frequency dependence, i.e. dynamic, retardation effects.

The goal of this Section is to compute the Fourier representation of the above screened interaction  $w(\mathbf{r}, \mathbf{r}', \nu_n)$  in a lattice and write it into an integral representation that allows for an analytic Matsubara summation in diagrams. The analytic Matsubara summation of the (dynamic) Coulomb part is necessary because it is important to treat the phonon and Coulomb part in the same manner since differences between numerically and analytically summed contributions are rather large.<sup>2</sup> We shall try to represent the diagrammatic effective interaction in terms of the (physical) linear response polarization which can be effectively computed numerically. On this route we discuss the integral representation of the polarization propagator and the related dielectric function in the Appendix C which will lead us to the desired dynamical electronic interaction among electrons which can be summed analytically in Matsubara space. The Fourier components of the bare Coulomb potential are discussed in the Appendix C as well. We generalize a draft of A. Sanna<sup>3</sup> to the non-decoupled, non-spin degenerate case.

### 4.2.1. The Polarization Propagator

The screening in the effective interaction is determined by the polarization propagator<sup>4</sup> [34, 45]

$$\chi^{\text{pol}}(\mathbf{r}, \mathbf{r}', \tau_1 - \tau_2) \equiv -\langle T \hat{\Delta}n(\mathbf{r}, \tau_1) \hat{\Delta}n(\mathbf{r}', \tau_2) \rangle \quad (4.4)$$

with

$$\hat{\Delta}n(\mathbf{r}) = \hat{n}(\mathbf{r}) - \langle \hat{n}(\mathbf{r}) \rangle \quad (4.5)$$

<sup>1</sup>The elementary charge  $e$  is viewed as coupling at the vertex, so excluded from the interaction at this point.

<sup>2</sup>A. Sanna private communication.

<sup>3</sup>Unpublished

<sup>4</sup>Both, the imaginary time and the Nambu basis is usually called  $\tau$  in the literature and we shall keep that notation. We hope the distinction can be made by the indices  $0, x, y, z$  that uniquely identifies the Pauli matrices. In this time independent theory we work in Fourier space most of the time where the imaginary time does not appear.

in the Heisenberg picture.  $\chi^{pol}(\mathbf{r}, \mathbf{r}', \tau_1 - \tau_2)$  is periodic in the imaginary time difference  $\tau_1 - \tau_2$  according to  $\chi^{pol}(\mathbf{r}, \mathbf{r}', \tau_1 - \tau_2) = \chi^{pol}(\mathbf{r}, \mathbf{r}', \tau_1 - \tau_2 + n\hbar\beta)$  ( $n \in \mathbb{Z}$ ). Thus

$$\chi^{pol}(\mathbf{r}, \mathbf{r}', \nu_n) = \int_0^{\hbar\beta} d\tau \chi^{pol}(\mathbf{r}, \mathbf{r}', \tau) e^{i\nu_n \tau} = \int_0^{\hbar\beta} d\tau \langle \hat{\Delta}n(\mathbf{r}, \tau) \hat{\Delta}n(\mathbf{r}', 0) \rangle e^{i\nu_n \tau} \quad (4.6)$$

with  $\nu_n = 2n \frac{\pi}{\hbar\beta}$ . We always assume independence of the absolute position in the lattice which leads to Fourier coefficients  $\chi^{pol}(\mathbf{q}, \mathbf{G}, \mathbf{G}', \nu_n)$  (see Appendix C). They are related to the original polarization propagator Fourier coefficients via  $\chi^{pol}(\mathbf{q} + \mathbf{G}, \mathbf{q}' + \mathbf{G}', \nu_n) = N_q \chi^{pol}(\mathbf{q}, \mathbf{G}, \mathbf{G}', \nu_n) \delta_{\mathbf{q}, \mathbf{q}'}$ .

#### 4.2.2. The Effective Interaction in Fourier Space

The Fourier coefficients of the effective interaction Eq. (4.3) can be straight forwardly computed. The independence of the bare Coulomb potential and  $\chi^{pol}(\mathbf{r}, \mathbf{r}', \nu_n)$  on the absolute position implies the same symmetry for the effective interaction. Then we insert the Fourier representation of the polarization propagator, use the orthonormality relations  $\sum_{\mathbf{T}_i} e^{i(\mathbf{q} - \mathbf{q}') \cdot \mathbf{T}_i} = N_q \delta_{\mathbf{q}', \mathbf{q}}$  and  $\int d\bar{\mathbf{r}} e^{i(\mathbf{G} - \mathbf{G}') \cdot \bar{\mathbf{r}}} = \Omega_{UC} \delta_{\mathbf{G}, \mathbf{G}'}$  and

$$w(\mathbf{q} + \mathbf{G}, \mathbf{q}' + \mathbf{G}', \nu_n) = -\frac{N_q \Omega_{UC}}{\epsilon_0 |\mathbf{q} + \mathbf{G}|^2} \delta_{\mathbf{G}', \mathbf{G}} \delta_{\mathbf{q}', \mathbf{q}} + \frac{N_q e^2}{\hbar \epsilon_0^2} \frac{\chi^{pol}(\mathbf{q}, \mathbf{G}, \mathbf{G}', \nu_n)}{|\mathbf{q} + \mathbf{G}'|^2 |\mathbf{q} + \mathbf{G}|^2} \delta_{\mathbf{q}, \mathbf{q}'}. \quad (4.7)$$

Usually, the interaction is described in terms of a dielectric function  $w(\mathbf{q}, \mathbf{G}, \mathbf{G}', \nu_n) = \sum_{\mathbf{G}_1} V^{Coul}(\mathbf{q}, \mathbf{G}, \mathbf{G}_1) \epsilon^{-1}(\mathbf{q}, \mathbf{G}_1, \mathbf{G}', \nu_n)$  where we introduce

$$\epsilon^{-1}(\mathbf{q}, \mathbf{G}, \mathbf{G}', \nu_n) = \delta_{\mathbf{G}, \mathbf{G}'} + \frac{e^2}{\hbar \epsilon_0} \frac{\chi^{pol}(\mathbf{q}, \mathbf{G}, \mathbf{G}', \nu_n)}{\Omega_{UC} |\mathbf{q} + \mathbf{G}'|^2}. \quad (4.8)$$

The integral representation (with the function  $\epsilon^{-1}$  on the real frequency axis) is given in Appendix C. We use it in the next Subsection to compute the integral representation of the effective Coulomb interaction.

#### 4.2.3. The Integral Representation of the Effective Coulomb Interaction

Using the integral representation of Eq. (C.34) we have

$$w(\mathbf{q}, \mathbf{G}, \mathbf{G}', \nu_n) = -\frac{e^2 \Omega_{UC}}{\epsilon_0 |\mathbf{q} + \mathbf{G}|^2} \left( \int_0^\infty \frac{d\omega}{\pi} \frac{2\omega \Im \mathbf{m} \epsilon^{-1}(\mathbf{q}, \mathbf{G}, \mathbf{G}', \omega)}{\omega^2 + \nu_n^2} + \delta_{\mathbf{G}, \mathbf{G}'} \right) \quad (4.9)$$

In the above expression appears the bare Coulomb interaction with a peculiar low  $\mathbf{q} + \mathbf{G}$  limit. To avoid an unscreend Coulomb interaction we separate

$$w(\mathbf{q}, \mathbf{G}, \mathbf{G}', \nu_n) = \underbrace{w(\mathbf{q}, \mathbf{G}, \mathbf{G}', 0)}_{w_{stat}(\mathbf{q}, \mathbf{G}, \mathbf{G}', \nu_n)} + \underbrace{w(\mathbf{q}, \mathbf{G}, \mathbf{G}', \nu_n) - w(\mathbf{q}, \mathbf{G}, \mathbf{G}', 0)}_{w_{dyn}(\mathbf{q}, \mathbf{G}, \mathbf{G}', \nu_n)} \quad (4.10)$$

Because  $w_{stat}(\mathbf{q}, \mathbf{G}, \mathbf{G}', \nu_n)$  is a constant in the Matsubara frequencies there is no need for an integral representation and we can directly take

$$w_{stat}(\mathbf{q}, \mathbf{G}, \mathbf{G}', \nu_n) = -\frac{\epsilon^{-1}(\mathbf{q}, \mathbf{G}, \mathbf{G}', 0)}{\epsilon_0 |\mathbf{q} + \mathbf{G}|^2}. \quad (4.11)$$

On the other hand, the dynamical interaction in this form does not contain the bare Coulomb term

$$w_{dyn}(\mathbf{q}, \mathbf{G}, \mathbf{G}', \nu_n) = -\frac{1}{\epsilon_0 |\mathbf{q} + \mathbf{G}|^2} \int_0^\infty \frac{2d\omega}{\pi} \left( \frac{\omega}{\omega^2 + \nu_n^2} - \frac{1}{\omega} \right) \Im \mathbf{m} \epsilon^{-1}(\mathbf{q}, \mathbf{G}, \mathbf{G}', \omega). \quad (4.12)$$

We conclude this Section with equations for the coupling matrix elements, i.e. the overlap between KS orbitals introduced by the above interaction, separated into dynamic and static parts.



#### 4.2.4. The Coulomb Matrix Elements

The matrix elements of the effective Coulomb interaction  $W_{k_1 k_2 k_3 k_4 \sigma \sigma'}(\nu_n)$  in the KS basis  $\{\vec{\varphi}_{k\sigma}\}$  are easily computed using the lattice periodic part  $\vec{\phi}_{k\sigma}(\vec{\mathbf{r}})$  of the Bloch function

$$\vec{\varphi}_{k\sigma}(\vec{\mathbf{r}}) = \vec{\phi}_{k\sigma}(\vec{\mathbf{r}}) \frac{1}{\sqrt{N_q}} e^{i\vec{\mathbf{r}} \cdot \mathbf{k}}. \quad (4.13)$$

The appearing orthonormality relation shows that the interaction conserves the Bloch momentum. However, there may be an Umklapp processes with  $\mathbf{G}_q$  that is uniquely defined by  $\mathbf{k}_4 - \mathbf{k}_3$  as the reciprocal grid vector so that  $\mathbf{G}_q - (\mathbf{k}_4 - \mathbf{k}_3 - \mathbf{q}) \in 1$ . Brillouin zone. With this vector we consider the static and dynamic parts of the interaction separately.

**Static** The static matrix elements are given by Eq. (4.11) as

$$\begin{aligned} W_{k_1 k_2 k_3 k_4 \sigma \sigma'}^{\text{stat}} &= \int_{\text{UC}} d\vec{\mathbf{r}} \int_{\text{UC}} d\vec{\mathbf{r}}' \vec{\phi}_{k_1 \sigma}^*(\vec{\mathbf{r}}) \cdot \vec{\phi}_{k_2 \sigma}(\vec{\mathbf{r}}) \sum_{\mathbf{G}, \mathbf{G}'} \frac{e^2 \epsilon^{-1}(\mathbf{G}_q + \mathbf{k}_4 - \mathbf{k}_3, \mathbf{G}, \mathbf{G}', 0)}{N_q \Omega_{\text{UC}}^2 \epsilon_0 |\mathbf{G}_q + \mathbf{k}_4 - \mathbf{k}_3 + \mathbf{G}|^2} e^{i(\mathbf{G} + \mathbf{G}_q) \cdot \vec{\mathbf{r}}} \\ &\times e^{-i(\mathbf{G}' + \mathbf{G}_q) \cdot \vec{\mathbf{r}}'} \vec{\phi}_{k_3 \sigma'}^*(\vec{\mathbf{r}}') \cdot \vec{\phi}_{k_4 \sigma'}(\vec{\mathbf{r}}') \delta_{\mathbf{k}_4 + \mathbf{k}_2, \mathbf{k}_3 + \mathbf{k}_1}. \end{aligned} \quad (4.14)$$

**Dynamic** Introducing the dynamical matrix elements

$$\begin{aligned} M_{k_1 k_2 k_3 k_4 \sigma \sigma'}^{\text{dyn}}(\omega) &= \int_{\text{UC}} d\vec{\mathbf{r}} \int_{\text{UC}} d\vec{\mathbf{r}}' \vec{\phi}_{k_1 \sigma}^*(\vec{\mathbf{r}}) \cdot \vec{\phi}_{k_2 \sigma}(\vec{\mathbf{r}}) \sum_{\mathbf{G}, \mathbf{G}'} \frac{\Im \mathbf{m} \epsilon^{-1}(\mathbf{k}_1 - \mathbf{k}_2 + \mathbf{G}_q, \mathbf{G}, \mathbf{G}', \omega)}{e^{-2} \Omega_{\text{UC}}^2 N_q \epsilon_0 |\mathbf{k}_1 - \mathbf{k}_2 + \mathbf{G}_q + \mathbf{G}|^2} \\ &\times e^{i(\mathbf{G} + \mathbf{G}_q) \cdot \vec{\mathbf{r}}} e^{-i(\mathbf{G}' + \mathbf{G}_q) \cdot \vec{\mathbf{r}}'} \vec{\phi}_{k_3 \sigma'}^*(\vec{\mathbf{r}}') \cdot \vec{\phi}_{k_4 \sigma'}(\vec{\mathbf{r}}') \delta_{\mathbf{k}_4 + \mathbf{k}_2, \mathbf{k}_3 + \mathbf{k}_1}, \end{aligned} \quad (4.15)$$

we can write the interaction with an analytic dependence on Matsubara frequencies (as a spin matrix)

$$W_{k_1 k_2 k_3 k_4 \sigma \sigma'}^{\text{dyn}}(\nu_n) = \int_0^\infty \frac{d\omega}{\pi} \left( \frac{1}{i\nu_n + \omega} - \frac{1}{i\nu_n - \omega} - \frac{2}{\omega} \right) M_{k_1 k_2 k_3 k_4 \sigma \sigma'}^{\text{dyn}}(\omega). \quad (4.16)$$

**Symmetry** For future reference we note a symmetry of the coupling matrix elements. We use that  $w(\mathbf{q}, \mathbf{G}, \mathbf{G}', \nu_n)$  is hermitian which follows from Eq. (C.32) and the fact that the bare Coulomb interaction is real and symmetric. From this property follows

$$W_{k_1 k_2 k_3 k_4 \sigma \sigma'}^*(\nu_n) = W_{k_4 k_3 k_2 k_1 \sigma' \sigma}(\nu_n). \quad (4.17)$$

This symmetry is preserved in the matrix elements, static as well as dynamic.

# 5. Many-Body Theory in the KS System

The functional construction in previous works on SCDFE used Many-Body Theory [21, 22] amongst other methods. As mentioned in the previous Chapter 4 we follow a similar approach. We construct  $xc$  potentials from the SSE for a SC. The SSE in turn uses the property of the KS GF to reproduce the exact density. We define the GF of a spin polarized SC, the SC KS system and the phononic system in Section 5.1. In Section 5.2 we introduce diagrammatic perturbation theory and the form of the SE that is used for the rest of the thesis. In Section 5.3, we derive the SSE which is the basis for the functional construction in Chapter 6. Again see Fig. 1.1 for an overview.

## 5.1. Introduction to Green's Functions

In this Section we derive the electronic and phononic GFs as the main ingredient for the Sham-Schlüter equation. We start defining the electronic GF, both the exact and the KS version in Subsection 5.1.1, introduce the spectral function in Subsection 5.1.2 and compute the SC KS GF in Subsection 5.1.3. Finally, we turn to the phonon propagator in Subsection 5.1.4.

### 5.1.1. The Electronic GF

We introduce the GF with the  $\tau$  ordering symbol  $\bar{T}$  and the field operators in the Heisenberg picture

$$\bar{G}(\mathbf{r}\tau, \mathbf{r}'\tau') = -\langle \bar{T} \hat{\Psi}(\mathbf{r}\tau) \otimes \hat{\Psi}^\dagger(\mathbf{r}'\tau') \rangle \quad (5.1)$$

where we are using the notation of Sec. 3.4.1. Individual components of the GF are

$$\bar{G}(\mathbf{r}\tau, \mathbf{r}'\tau') = \begin{pmatrix} G(\mathbf{r}\tau, \mathbf{r}'\tau') & F(\mathbf{r}\tau, \mathbf{r}'\tau') \\ F^\dagger(\mathbf{r}\tau, \mathbf{r}'\tau') & G^\dagger(\mathbf{r}\tau, \mathbf{r}'\tau') \end{pmatrix} \quad (5.2)$$

$$= \begin{pmatrix} -\langle T \hat{\psi}(\mathbf{r}\tau) \otimes \hat{\psi}^\dagger(\mathbf{r}'\tau') \rangle & -\langle T \hat{\psi}(\mathbf{r}\tau) \otimes \hat{\psi}(\mathbf{r}'\tau') \rangle \\ -\langle T \hat{\psi}^\dagger(\mathbf{r}\tau) \otimes \hat{\psi}^\dagger(\mathbf{r}'\tau') \rangle & -\langle T \hat{\psi}^\dagger(\mathbf{r}\tau) \otimes \hat{\psi}(\mathbf{r}'\tau') \rangle \end{pmatrix} \quad (5.3)$$

The imaginary time ordering symbol in Nambu space  $\bar{T}$  is defined to act on every of the  $(4 \times 4)$  components individually which can be achieved by transposing in Nambu-spin space with the symbol  $T_{\text{sn}}$

$$\bar{T} \hat{\Psi}(\mathbf{r}\tau) \otimes \hat{\Psi}^\dagger(\mathbf{r}'\tau') \equiv \theta(\tau - \tau') \hat{\Psi}(\mathbf{r}\tau) \otimes \hat{\Psi}^\dagger(\mathbf{r}'\tau') - \theta(\tau' - \tau) (\hat{\Psi}^\dagger(\mathbf{r}'\tau') \otimes \hat{\Psi}(\mathbf{r}\tau))^{T_{\text{sn}}} \quad (5.4)$$

We use the commutator according to the rule Eq. (3.93) which essentially means to consider the commutator in every component independently. The thermal average and Heisenberg picture uses the scalar Hamilton operator  $\hat{H}$  which involves contractions of the vectors  $\hat{\Psi}(\mathbf{r}\tau)$ . As usual we find the equation of motion in the static case ( $\tau - \tau' \rightarrow \tau$ ) by taking the derivative  $-\hbar\partial_\tau$  of Eq. (5.1) [45, 34]. With the definition in Eq. (5.4) and Eq. (3.93) this is easily evaluated to

$$-\hbar\partial_\tau \bar{G}(\mathbf{r}\tau, \mathbf{r}'0) = \hbar\delta(\tau)\delta(\mathbf{r} - \mathbf{r}')\tau_0\sigma_0 + \hbar\langle \bar{T} [\hat{H}, \hat{\Psi}(\mathbf{r})]_-(\tau) \otimes \hat{\Psi}^\dagger(\mathbf{r}'0) \rangle \quad (5.5)$$

Let us define the notation

$$\begin{aligned} 1 &\equiv (\mathbf{r}\alpha\mu) & \delta_{1,1'} &\equiv \delta_{\alpha\alpha'}\delta_{\mu\mu'}\delta(\mathbf{r}-\mathbf{r}') \\ (-1) &\equiv (\mathbf{r},-\alpha\mu) & \int d1 &\equiv \int d\mathbf{r} \sum_{\alpha} \sum_{\mu}. \end{aligned} \quad (5.6)$$

Then the above equation becomes component wise (we keep the symbol  $\bar{G}$  but note that when we write  $\bar{G}(1\tau, 1', 0)$  we mean its scalar components, see also the Note on Notation in the beginning of the thesis.)

$$-\hbar\partial_{\tau}\bar{G}(1\tau, 1', 0) = \hbar\delta(\tau)\delta_{11'} + \hbar\langle T[\hat{H}, \hat{\Psi}(1)]_{-}(\tau)\hat{\Psi}^{\dagger}(1', 0)\rangle. \quad (5.7)$$

In general  $\hat{H}$  will contain a single particle  $\hat{H}^{(1)}$  and a two particle  $\hat{H}^{(2)}$  as

$$\hat{H} = \underbrace{\int d\mathbf{r} \int d\mathbf{r}' \hat{\Psi}^{\dagger}(\mathbf{r}) \cdot \frac{1}{2} \hat{H}^{(1)}(\mathbf{r}, \mathbf{r}') \cdot \hat{\Psi}(\mathbf{r}')}_{\hat{H}^{(1)}} + \underbrace{\int \dots d(1, 2, 3, 4) \hat{\Psi}^{\dagger}(1) \hat{\Psi}^{\dagger}(2) \frac{1}{4} \hat{H}^{(2)}(1, 2, 3, 4) \hat{\Psi}(3) \hat{\Psi}(4)}_{\hat{H}^{(2)}} \quad (5.8)$$

We note that  $\langle \bar{T}[\hat{H}, \hat{\Psi}(1)]_{-}(\tau)\hat{\Psi}^{\dagger}(1', 0)\rangle$  is a subtle quantity because it involves the contraction of  $\hat{\Psi}(\mathbf{r})$ 's in the commutator. We compute for the components

$$[\hat{\Psi}^{\dagger}(1), \hat{\Psi}(1')]_{+} = [\hat{\Psi}(1), \hat{\Psi}^{\dagger}(1')]_{+} = \delta_{11'} \quad (5.9)$$

$$[\hat{\Psi}(1), \hat{\Psi}(1')]_{+} = [\hat{\Psi}^{\dagger}(1), \hat{\Psi}^{\dagger}(1')]_{+} = \delta_{1,-1'}. \quad (5.10)$$

With these commutators we obtain

$$[\hat{H}^{(1)}, \hat{\Psi}(1)]_{-} = \frac{1}{2} \int d2 \hat{H}^{(1)}(2, -1) \hat{\Psi}^{\dagger}(2) - \frac{1}{2} \int d2 \hat{H}^{(1)}(1, 2) \hat{\Psi}(1). \quad (5.11)$$

Using  $\hat{\Psi}(\mathbf{r}'\alpha\mu) = \hat{\Psi}^{\dagger}(\mathbf{r}', -\alpha, \mu)$  we obtain

$$[\hat{H}^{(1)}, \hat{\Psi}(1)]_{-} = \frac{1}{2} \int d2 (\hat{H}^{(1)}(-2, -1) - \hat{H}^{(1)}(1, 2)) \hat{\Psi}(2). \quad (5.12)$$

To simplify this, we have to assume that in general

$$\hat{H}^{(1)}(\mathbf{r}', -\gamma, \mu, \mathbf{r}, -\alpha, \mu') = -\hat{H}^{(1)}(\mathbf{r}\alpha\mu', \mathbf{r}'\gamma\mu) \quad (5.13)$$

which is in particular true for the SC KS Hamiltonian Eq. (3.106)<sup>1</sup>, we find

$$[\hat{H}^{(1)}, \hat{\Psi}(1)]_{-} = - \int d2 \hat{H}^{(1)}(1, 2) \hat{\Psi}(2) \quad (5.14)$$

and thus

$$\int d2 \left( -\hbar\delta_{1,2}\partial_{\tau} - \hat{H}^{(1)}(1, 2) \right) \bar{G}(2\tau, 1'0) = \hbar\delta(\tau)\delta_{1,1'} + \langle T[\hat{H}^{(2)}, \hat{\Psi}(1)]_{-}(\tau)\hat{\Psi}^{\dagger}(1', 0)\rangle. \quad (5.15)$$

Let us be more specific and take  $\hat{H}^{(1)}(1, 2)$  as the kinetic energy plus the external single particle potentials. The inhomogeneity on the right hand side of Eq. (5.15) usually prevents a direct solution. Introducing the special non-interacting Hartree GF

$$\int d2 \left( -\hbar\delta_{1,2}\partial_{\tau} - \hat{H}^{(h)}(1, 2) \right) \bar{G}^0(2\tau, 1'0) = \hbar\delta(\tau)\delta_{1,1'} \quad (5.16)$$

<sup>1</sup>The proof uses the total antisymmetry of the pair potential.

with  $\hat{H}^{(h)}(1, 2)$  written as a Nambu-Spin matrix

$$\begin{aligned} \hat{H}^{(h)}(\mathbf{r}, \mathbf{r}') = & \left( \left( -\frac{\hbar^2 \nabla^2}{2m_e} + v_{\text{ext}}(\mathbf{r}) - \mu \right) \sigma_0 \tau_z - \frac{g_s \mu_B}{2} \mathbf{S} \cdot \mathbf{B}_{\text{ext}}(\mathbf{r}) (\tau_0 + \tau_z) - \frac{g_s \mu_B}{2} \mathbf{S}^* \cdot \mathbf{B}_{\text{ext}}(\mathbf{r}) (\tau_0 - \tau_z) \right. \\ & \left. + \frac{e^2}{4\pi\epsilon_0} \int d\mathbf{r}'' \frac{n(\mathbf{r}'')}{|\mathbf{r} - \mathbf{r}''|} \tau_z \sigma_0 \right) \delta(\mathbf{r} - \mathbf{r}') + i\tau_x \Im \Phi \cdot \Delta_{\text{ext}}(\mathbf{r}, \mathbf{r}') + i\tau_y \Re \Phi \cdot \Delta_{\text{ext}}(\mathbf{r}, \mathbf{r}') \end{aligned} \quad (5.17)$$

we add and subtract the term  $\frac{e^2}{4\pi\epsilon_0} \int d\mathbf{r}'' \frac{n(\mathbf{r}'')}{|\mathbf{r} - \mathbf{r}''|} \tau_z \sigma_0 \cdot \bar{G}(\mathbf{r}\tau, \mathbf{r}'0)$  in the equation of motion Eq. (5.15) and find

$$\int d2 \left( -\hbar\delta_{1,2} \partial_\tau - \hat{H}^{(h)}(1, 2) \right) \bar{G}(2, \tau, 1', 0) = \hbar\delta(\tau) \delta_{1,1'} + \int d2 d\tau' \bar{\Sigma}(1, 2, \tau - \tau') \bar{G}(2, \tau', 1', 0) \quad (5.18)$$

with the SE  $\bar{\Sigma}$  defined by the equation

$$\int d2 d\tau' \bar{\Sigma}(1, 2, \tau - \tau') \bar{G}(2, \tau', 1', 0) = \langle T[\hat{H}^{(2)}, \hat{\Psi}(1)]_-(\tau) \hat{\Psi}^\dagger(1', 0) \rangle - \frac{e^2}{4\pi\epsilon_0} \int d\mathbf{x} \frac{n(\mathbf{x})(\tau_z)_{\alpha\alpha'}}{|\mathbf{r} - \mathbf{x}|} \bar{G}(1, \tau, 1', 0) \quad (5.19)$$

In Sec. 5.2 we find an expansion for  $\bar{\Sigma}$  in terms of  $\bar{G}$  and the interaction potential which allows for a systematic approximation scheme. We will work mostly in frequency space, well adapted to this static problem

$$\bar{G}(1, 1', \omega_n) = \int d\tau \bar{G}(1\tau, 1', 0) e^{i\omega_n \tau} \quad (5.20)$$

$$\bar{G}(1\tau, 1', 0) = \frac{1}{2\pi} \sum_n \bar{G}(1, 1', \omega_n) e^{-i\omega_n \tau}, \quad (5.21)$$

for which the equation of motion reads

$$\int d2 \left( i\hbar\omega_n \delta_{1,2} - \hat{H}^{(h)}(1, 2) \right) \bar{G}(2, 1', \omega_n) = \hbar\delta_{1,1'} + \int d2 \bar{\Sigma}(1, 2, \omega_n) \bar{G}(2, 1', \omega_n). \quad (5.22)$$

For time independent systems the convolution theorem ensures that no frequency-integration has to be done at this point [45]. Using  $\int d2 \bar{G}^0(1, 2, \omega_n) \bar{G}^{0^{-1}}(2, 1', \omega_n) = \delta_{1,1'}$  and the Fourier transform of Eq. (5.16) we arrive at the Dyson equation

$$\bar{G}(1, 1', \omega_n) = \bar{G}^0(1, 1', \omega_n) + \int d(2, 2') \bar{G}^0(1, 2, \omega_n) \bar{\Sigma}(2, 2', \omega_n) \bar{G}(2', 1', \omega_n). \quad (5.23)$$

For a practicable application of the above equation we need to describe how to obtain  $\bar{\Sigma}(2, 2', \omega_n)$ . This procedure will be sketched in the next Section 5.2. Because we can add single particle potentials similar to the Hartree potential freely we may use the SC KS system as our non-interacting starting system. Introducing the KS GF

$$\int d\mathbf{x} \left( i\hbar\omega_n \delta(\mathbf{r} - \mathbf{x}) \tau_0 \sigma_0 - \underbrace{\left( \hat{H}^{(h)}(\mathbf{r}, \mathbf{x}) + \bar{v}_{\text{xc}}(\mathbf{r}, \mathbf{x}) \right)}_{\bar{H}_{\text{KS}}(\mathbf{r}, \mathbf{x})} \right) \cdot \bar{G}^{\text{KS}}(\mathbf{x}, \mathbf{r}', \omega_n) = \hbar\delta(\mathbf{r} - \mathbf{r}') \tau_0 \sigma_0 \quad (5.24)$$

with

$$\begin{aligned} \bar{v}_{\text{xc}}(\mathbf{r}, \mathbf{r}') \equiv & \left( v_{\text{xc}}(\mathbf{r}) \sigma_0 \tau_z - \frac{g_s e}{2m_e} \mathbf{S} \cdot \mathbf{B}_{\text{xc}}(\mathbf{r}) (\tau_0 + \tau_z) - \frac{g_s e}{2m_e} \mathbf{S}^* \cdot \mathbf{B}_{\text{xc}}(\mathbf{r}) (\tau_0 - \tau_z) \right) \delta(\mathbf{r} - \mathbf{r}') \\ & + i\tau_x \Im \Phi \Delta_{\text{xc}}(\mathbf{r}, \mathbf{r}') + i\tau_y \Re \Phi \Delta_{\text{xc}}(\mathbf{r}, \mathbf{r}') \end{aligned} \quad (5.25)$$

leads then to a similar Dyson equation as the SC KS system as the formally non-interacting system

$$\bar{G}(1, 1', \omega_n) = \bar{G}^{\text{KS}}(1, 1', \omega_n) + \int d(2, 2') \bar{G}^{\text{KS}}(1, 2, \omega_n) \underbrace{(\bar{\Sigma}(2, 2', \omega_n) - \bar{v}_{\text{xc}}(2, 2'))}_{\bar{\Sigma}^{\text{s}}(2, 2', \omega_n)} \bar{G}(2', 1', \omega_n). \quad (5.26)$$

### 5.1.2. The Spectral Representation of the Nambu GF

We arrive at the spectral representation for the Nambu GF along the lines that lead to Eq. (C.21) for the spectral representation of the polarization propagator. We use the periodicity of  $\bar{G}(\mathbf{r}, \mathbf{r}', \tau - \tau')^2$  to compute the Fourier element and obtain

$$\bar{G}(\mathbf{r}, \mathbf{r}', \omega_n) = \int_{-\infty}^{\infty} \frac{d\omega}{2\pi} \frac{\bar{A}(\mathbf{r}, \mathbf{r}', \omega)}{i\omega_n - \omega} \quad (5.27)$$

with the spectral function

$$\bar{A}(\mathbf{r}, \mathbf{r}', \omega) = 2\pi \sum_{i,j} (1 + e^{\beta(E_i - E_j)}) \langle E_i | \hat{\Psi}(\mathbf{r}) | E_j \rangle \otimes \langle E_j | \hat{\Psi}^\dagger(\mathbf{r}') | E_i \rangle \frac{e^{-\beta E_i}}{Z} \delta(\omega - \frac{1}{\hbar}(E_j - E_i)). \quad (5.28)$$

The spectral function is also the antihermitian part of the retarded GF. For the retarded GF defined by

$$i\bar{\mathcal{G}}^R(\mathbf{r}, \mathbf{r}', t) = \theta(t) \langle \hat{\Psi}(\mathbf{r}t) \otimes \hat{\Psi}^\dagger(\mathbf{r}'0) \rangle + \theta(-t) \langle (\hat{\Psi}^\dagger(\mathbf{r}'0) \otimes \hat{\Psi}(\mathbf{r}t))^{T_{\text{sn}}} \rangle \quad (5.29)$$

in turn we have to use the integral representation of the step function Eq. (C.24) and shift in the integration over  $\omega \rightarrow \omega - \frac{1}{\hbar}(E_j - E_i)$  to obtain the Fourier transform

$$i\bar{\mathcal{G}}^R(\mathbf{r}, \mathbf{r}', \omega) = \int_{-\infty}^{\infty} \frac{d\tilde{\omega}}{2\pi} \frac{\bar{A}(\mathbf{r}, \mathbf{r}', \tilde{\omega})}{\omega + i\eta - \tilde{\omega}} \quad (5.30)$$

Now the antihermitian part  $\Im\mathbf{m}(\bar{\mathcal{G}}^R(\mathbf{r}, \mathbf{r}', \omega))$  is identified to match

$$\bar{A}(\mathbf{r}, \mathbf{r}', \omega) = -2\Im\mathbf{m}(\bar{\mathcal{G}}^R(\mathbf{r}, \mathbf{r}', \omega)) \quad (5.31)$$

using Eq. (C.28).

**The LDOS** The physical interpretation of the spectral function of Eq. (5.28) comes by observing that its poles are at the exact Many-Body excitation energies  $E_j - E_i$ . In addition, the diagonal of  $\bar{A}(1, 1', \omega)$  is proportional to the overlap a single particle spinor field  $\hat{\Psi}^\dagger(1)$  creates between the many body states  $|E_i\rangle$  and  $|E_j\rangle$ . The Many-Body states have to differ by one particle precisely. Thus, the diagonal of the spectral function is proportional to the sum of single excitations times their local probability amplitude  $\bar{A}(1, 1, \omega) \propto \sum |(\langle E_j | \hat{\Psi}^\dagger(1) | E_i \rangle)|^2 \delta(\omega - \frac{1}{\hbar}(E_j - E_i))$ . This quantity is identified as the Local Density Of States (LDOS)

$$\rho_{\mu,\alpha}(\mathbf{r}, \omega) = \bar{A}(1, 1, \omega). \quad (5.32)$$

In a SC, considering spin, we find that the wavefunction has 4 components. It is possible to resolve the different channels in spin space, i.e. excite e.g. only the up branch in an STM experiment. Note that because  $\hat{\Psi}^\dagger(\mathbf{r}\mu\alpha) = \hat{\Psi}(\mathbf{r}\mu, -\alpha)$  if  $\rho_{\mu,\alpha=1}(\mathbf{r}, \omega)$  measures the particle excitation spectrum,  $\rho_{\mu,\alpha=-1}(\mathbf{r}, \omega)$  measures the hole excitation spectrum. We give a derivation of the formula for the KS (L)DOS in Sec. G.

<sup>2</sup>Shown e.g. in Ref. [45, Page 263] for the normal part of the GF. The result is easily generalized.

### 5.1.3. KS GF

In this section we want to compute the KS GF that satisfies the equation of motion Eq. (5.24). We apply the Bogoliubov Valatin transformation to Eq. (5.24) and use that it diagonalizes the Nambu KS Hamiltonian (compare Eq. (3.105)). The transformed equation of motion for the KS GF Eq. (5.24) then simply reads

$$(i\omega_n\tau_0 - \frac{1}{\hbar}E_k\tau_z) \cdot \bar{\mathfrak{G}}_{kk'}(\omega_n) = \delta_{kk'}\tau_0 \quad (5.33)$$

where

$$\bar{\mathfrak{G}}_{kk'}(\omega_n) = \int d\mathbf{r} \int d\mathbf{r}' \begin{pmatrix} \bar{u}_k^*(\mathbf{r}) & \bar{v}_k^*(\mathbf{r}) \\ \bar{v}_k(\mathbf{r}) & \bar{u}_k(\mathbf{r}) \end{pmatrix} \cdot \bar{G}^{\text{KS}}(\mathbf{r}, \mathbf{r}', \omega_n) \cdot \begin{pmatrix} \bar{u}_{k'}(\mathbf{r}') & \bar{v}_{k'}(\mathbf{r}') \\ \bar{v}_{k'}^*(\mathbf{r}') & \bar{u}_{k'}^*(\mathbf{r}') \end{pmatrix} \quad (5.34)$$

and

$$\bar{\mathfrak{G}}_{kk'}(\omega_n) = \delta_{kk'}\tau_0 \cdot \left( i\omega_n\tau_0 - \frac{1}{\hbar}E_k\tau_z \right)^{-1} = \begin{pmatrix} \frac{\delta_{kk'}}{i\omega_n - \frac{1}{\hbar}E_k} & 0 \\ 0 & \frac{\delta_{kk'}}{i\omega_n + \frac{1}{\hbar}E_k} \end{pmatrix}. \quad (5.35)$$

We can directly use the transformed, diagonal, single particle KS GF. In most cases, however, we work in real space. Here, applying the back transformation, the KS GF that solves Eq. (5.24) takes the shape

$$\begin{aligned} \bar{G}^{\text{KS}}(\mathbf{r}, \mathbf{r}', \omega_n) &= \sum_k \frac{1}{i\omega_n - \frac{1}{\hbar}E_k} \begin{pmatrix} \bar{u}_k(\mathbf{r}) \otimes \bar{u}_k^*(\mathbf{r}') & \bar{u}_k(\mathbf{r}) \otimes \bar{v}_k^*(\mathbf{r}') \\ \bar{v}_k(\mathbf{r}) \otimes \bar{u}_k^*(\mathbf{r}') & \bar{v}_k(\mathbf{r}) \otimes \bar{v}_k^*(\mathbf{r}') \end{pmatrix} \\ &+ \sum_k \frac{1}{i\omega_n + \frac{1}{\hbar}E_k} \begin{pmatrix} \bar{v}_k^*(\mathbf{r}) \otimes \bar{v}_k(\mathbf{r}') & \bar{v}_k^*(\mathbf{r}) \otimes \bar{u}_k(\mathbf{r}') \\ \bar{u}_k^*(\mathbf{r}) \otimes \bar{v}_k(\mathbf{r}') & \bar{u}_k^*(\mathbf{r}) \otimes \bar{u}_k(\mathbf{r}') \end{pmatrix}. \end{aligned} \quad (5.36)$$

We complete the derivation of the KS-Nambu GF by representing it in the basis of the orthonormal spinors<sup>3</sup>

$$\langle \mathbf{r} | \Psi_{i\alpha\mu}^{\text{KS}} \rangle \equiv \Psi_{i\alpha\mu}^{\text{KS}}(\mathbf{r}) = \begin{pmatrix} \delta_{\alpha,1} \vec{\varphi}_{i\mu}(\mathbf{r}) \\ \delta_{\alpha,-1} \vec{\varphi}_{i\mu}^*(\mathbf{r}) \end{pmatrix}. \quad (5.37)$$

Again we insist on a pure spinor basis, also in Nambu space. This makes it significantly easier to introduce approximations or special cases where, e.g. triplet contributions are dropped. If we had taken a basis of non-pure spinors these triplet parts were hidden in the set of quantum numbers in a similar way as  $k$  of the SC KS system includes the spin degrees of freedom.

We compute the matrix elements

$$\bar{G}^{\text{KS}}(\mathbf{r}, \mathbf{r}', \omega_n) = \sum_{i\alpha\mu j\alpha'\mu'} G_{i\alpha\mu j\alpha'\mu'}^{\text{KS}}(\omega_n) \langle \mathbf{r} | \Psi_{i\alpha\mu}^{\text{KS}} \rangle \otimes \langle \Psi_{j\alpha'\mu'}^{\text{KS}} | \mathbf{r}' \rangle \quad (5.38)$$

$$G_{i\alpha\mu j\alpha'\mu'}^{\text{KS}}(\omega_n) = \int d\mathbf{r} \int d\mathbf{r}' \langle \Psi_{i\alpha\mu}^{\text{KS}} | \mathbf{r} \rangle \cdot \bar{G}^{\text{KS}}(\mathbf{r}, \mathbf{r}', \omega_n) \cdot \langle \mathbf{r}' | \Psi_{j\alpha'\mu'}^{\text{KS}} \rangle. \quad (5.39)$$

The fact that with the choice of pure spinors all quantum numbers translate one to one into the matrix elements allows us to use the same notation with the bar for matrices in Nambu-spin space. With the expansion in NS KS orbitals of  $u$  and  $v$  in the Eqs. (3.111) and (3.112) and

<sup>3</sup>These spinors are nothing else than the normal state KS basis, written in the Nambu notation. Note in particular that these are pure Nambu-spinors.

the orthonormality of the KS orbitals the matrix elements are straight forward to obtain and we group them into a Nambu and spin matrix notation<sup>4</sup>

$$\bar{G}_{ij}^{\text{KS}}(\omega_n) = \sum_k \left( \frac{1}{i\omega_n - \frac{1}{\hbar}E_k} \begin{pmatrix} \vec{u}_k^i \otimes \vec{u}_k^{j*} & \vec{u}_k^i \otimes \vec{v}_k^{j*} \\ \vec{v}_k^i \otimes \vec{u}_k^{j*} & \vec{v}_k^i \otimes \vec{v}_k^{j*} \end{pmatrix} + \frac{1}{i\omega_n + \frac{1}{\hbar}E_k} \begin{pmatrix} \vec{v}_k^{i*} \otimes \vec{v}_k^j & \vec{v}_k^{i*} \otimes \vec{u}_k^j \\ \vec{u}_k^{i*} \otimes \vec{v}_k^j & \vec{u}_k^{i*} \otimes \vec{u}_k^j \end{pmatrix} \right). \quad (5.40)$$

Similar to the real space definition Eq. (5.2) we also use the notation

$$\bar{G}_{ij}^{\text{KS}}(\omega_n) = \begin{pmatrix} G_{ij}^{\text{KS}}(\omega_n) & F_{ij}^{\text{KS}}(\omega_n) \\ F_{ij}^{\text{KS}\dagger}(\omega_n) & G_{ij}^{\text{KS}\dagger}(\omega_n) \end{pmatrix}. \quad (5.41)$$

**The KS GF of a Collinear Singlet System** Assuming collinearity and neglecting triplet contribution makes the spin a good quantum number in the SC KS system (compare Sec. 3.5.1). Note that the basis  $\Psi_{i\alpha\mu}^{\text{KS}}$  still defines the spin label of  $G_{i\alpha\mu j\alpha'\mu'}^{\text{KS}}$  and the spin index of  $v_{k\mu}^i$  refers to the KS wavefunction. The solution of the KSBdG equation, however, is of opposite spin  $-\mu$  and the spin label of  $E_{k\mu}$  refers to the SC KS system. Thus  $v_{k\mu}^{i*}$  appears with opposite  $E_{k,-\mu}$  in the following equation for  $\bar{G}_{ij}^{\text{KS}}$

$$\bar{G}_{ij}^{\text{KS}}(\omega_n) = \sum_k \begin{pmatrix} \frac{u_{k\uparrow}^i u_{k\uparrow}^{j*} + v_{k\uparrow}^{i*} v_{k\uparrow}^j}{i\omega_n - \frac{1}{\hbar}E_{k\uparrow}} + \frac{v_{k\uparrow}^{i*} v_{k\uparrow}^j}{i\omega_n + \frac{1}{\hbar}E_{k\downarrow}} & 0 & 0 & \frac{u_{k\uparrow}^i v_{k\downarrow}^{j*} + v_{k\uparrow}^{i*} u_{k\downarrow}^j}{i\omega_n - \frac{1}{\hbar}E_{k\uparrow}} + \frac{v_{k\uparrow}^{i*} u_{k\downarrow}^j}{i\omega_n + \frac{1}{\hbar}E_{k\downarrow}} \\ 0 & \frac{u_{k\downarrow}^i u_{k\downarrow}^{j*} + v_{k\downarrow}^{i*} v_{k\downarrow}^j}{i\omega_n - \frac{1}{\hbar}E_{k\downarrow}} + \frac{v_{k\downarrow}^{i*} v_{k\downarrow}^j}{i\omega_n + \frac{1}{\hbar}E_{k\uparrow}} & \frac{u_{k\downarrow}^i v_{k\uparrow}^{j*} + v_{k\downarrow}^{i*} u_{k\uparrow}^j}{i\omega_n - \frac{1}{\hbar}E_{k\downarrow}} + \frac{v_{k\downarrow}^{i*} u_{k\uparrow}^j}{i\omega_n + \frac{1}{\hbar}E_{k\uparrow}} & 0 \\ 0 & \frac{v_{k\uparrow}^i u_{k\downarrow}^{j*} + u_{k\uparrow}^{i*} v_{k\downarrow}^j}{i\omega_n - \frac{1}{\hbar}E_{k\downarrow}} + \frac{u_{k\uparrow}^{i*} v_{k\downarrow}^j}{i\omega_n + \frac{1}{\hbar}E_{k\uparrow}} & \frac{v_{k\uparrow}^i v_{k\uparrow}^{j*} + u_{k\uparrow}^{i*} u_{k\uparrow}^j}{i\omega_n - \frac{1}{\hbar}E_{k\downarrow}} + \frac{u_{k\uparrow}^{i*} u_{k\uparrow}^j}{i\omega_n + \frac{1}{\hbar}E_{k\uparrow}} & 0 \\ \frac{v_{k\downarrow}^i u_{k\uparrow}^{j*} + u_{k\downarrow}^{i*} v_{k\uparrow}^j}{i\omega_n - \frac{1}{\hbar}E_{k\uparrow}} + \frac{u_{k\downarrow}^{i*} v_{k\uparrow}^j}{i\omega_n + \frac{1}{\hbar}E_{k\downarrow}} & 0 & 0 & \frac{v_{k\downarrow}^i v_{k\downarrow}^{j*} + u_{k\downarrow}^{i*} u_{k\downarrow}^j}{i\omega_n - \frac{1}{\hbar}E_{k\uparrow}} + \frac{u_{k\downarrow}^{i*} u_{k\downarrow}^j}{i\omega_n + \frac{1}{\hbar}E_{k\downarrow}} \end{pmatrix} \quad (5.42)$$

**The KS GF of a Spin-Decoupled System** Further assuming the SDA (Subsection 3.5.2), due to reduced shape of the unitary Bogoliubov-Valatin transformations, we obtain a GF that is (anti)diagonal in KS orbitals. There we had pointed out that we have to sum both branches  $\alpha$  and exclude the negative  $E_{k\mu}^\alpha$  one with a step function because it is not known a priori if an eigenvalue is positive (see Subsection 3.5.2). This was however necessary in order to make the correct identification  $(u, v)$  with the eigenvector to an eigenvalue. Recall that the coefficients translate according to  $v_{k\uparrow}^{i*} \rightarrow v_{-k\uparrow}^{k*} \delta_{i,-k}$  and  $u_{k\sigma}^i \rightarrow u_{k\sigma}^k \delta_{ik}$ . Together with the important relations among the coefficients Eq. (B.18), Eq. (B.16) and  $E_{k\mu}^\alpha = -E_{-k-\mu}^{-\alpha}$  (compare Eqs. (3.158) to (3.161)) we obtain

$$\bar{G}_{ij}^{\text{KS}}(\omega_n) = \sum_\alpha \begin{pmatrix} \frac{|u_{i\uparrow}^{i\alpha}|^2 \delta_{ij}}{i\omega_n - \frac{1}{\hbar}E_{i\uparrow}^\alpha} & 0 & 0 & \frac{u_{i\uparrow}^{i\alpha} (v_{i\downarrow}^{-i\alpha})^* \delta_{i,-j}}{i\omega_n - \frac{1}{\hbar}E_{i\uparrow}^\alpha} \\ 0 & \frac{|u_{i\downarrow}^{i\alpha}|^2 \delta_{ij}}{i\omega_n - \frac{1}{\hbar}E_{i\downarrow}^\alpha} & \frac{u_{i\downarrow}^{i\alpha} (v_{i\uparrow}^{-i\alpha})^* \delta_{i,-j}}{i\omega_n - \frac{1}{\hbar}E_{i\downarrow}^\alpha} & 0 \\ 0 & \frac{(u_{i\uparrow}^{i\alpha})^* v_{i\downarrow}^{-i\alpha} \delta_{i,-j}}{i\omega_n + \frac{1}{\hbar}E_{i\uparrow}^\alpha} & \frac{|u_{i\uparrow}^{i\alpha}|^2 \delta_{ij}}{i\omega_n + \frac{1}{\hbar}E_{i\uparrow}^\alpha} & 0 \\ \frac{(u_{i\downarrow}^{i\alpha})^* v_{i\uparrow}^{-i\alpha} \delta_{i,-j}}{i\omega_n + \frac{1}{\hbar}E_{i\downarrow}^\alpha} & 0 & 0 & \frac{|u_{i\downarrow}^{i\alpha}|^2 \delta_{ij}}{i\omega_n + \frac{1}{\hbar}E_{i\downarrow}^\alpha} \end{pmatrix}. \quad (5.43)$$

We have used that  $|u_{i\uparrow}^{i\alpha}|^2 \theta(E_{i\uparrow}^\alpha) + |u_{i\uparrow}^{i\alpha}|^2 \theta(-E_{i\uparrow}^\alpha) \equiv |u_{i\uparrow}^{i\alpha}|^2$ .

<sup>4</sup>We use  $\vec{u}_k^i = (u_k^{i\uparrow} \quad u_k^{i\downarrow})^T$  with the expansion coefficients of  $\vec{u}_k(\mathbf{r})$  in  $\vec{\varphi}_{i\sigma}(\mathbf{r})$  Eq. (3.111). Similar for  $\vec{v}_k^i$ .

### 5.1.4. The Phonon Propagator

We define the phonon propagator as the term that appears in the bare electron-phonon interaction. The electron-phonon matrix elements couple to the operator  $\hat{\phi}_{\lambda\mathbf{q}}(\tau)$

$$\hat{\phi}_{\lambda\mathbf{q}}(\tau) = \hat{b}_{\lambda\mathbf{q}}(\tau) + \hat{b}_{\lambda,-\mathbf{q}}^\dagger(\tau) \equiv \hat{\phi}_{\lambda,-\mathbf{q}}^\dagger(\tau) \quad (5.44)$$

with operators  $\hat{b}_{\lambda\mathbf{q}}$  of Eq. (3.84) in the imaginary time Heisenberg picture<sup>5</sup>. Thus, we take the phonon propagator to be defined in general by

$$D_{\text{ph}}(\lambda\mathbf{q}, \lambda'\mathbf{q}', \tau, \tau') = \langle \hat{T} \hat{\phi}_{\lambda\mathbf{q}}(\tau) \hat{\phi}_{\lambda'\mathbf{q}'}(\tau') \rangle. \quad (5.45)$$

In this thesis we are mainly concerned with the harmonic approximation to lattice vibrations and we want to neglect multi-phonon scattering. Thus we are interested primarily in the bare propagator of the non-interacting system of phonons

$$D_{\text{ph}}^0(\lambda\mathbf{q}, \lambda'\mathbf{q}', \tau, \tau') = \langle \hat{T} \hat{\phi}_{\lambda\mathbf{q}}(\tau) \hat{\phi}_{\lambda'\mathbf{q}'}(\tau') \rangle_0. \quad (5.46)$$

The Hamiltonian to evaluate the trace  $\langle \dots \rangle_0$  in is given by Eq. (3.87). We insert the definition of  $\hat{\phi}_{\lambda\mathbf{q}}(\tau)$  and commute the time-evolution operator to the left side. In Fourier space ( $\tau - \tau' \rightarrow \tau$ )

$$D_{\text{ph}}^0(\lambda\mathbf{q}, \lambda'\mathbf{q}', \nu_n) = \frac{1}{2} \int_{-\hbar\beta}^{\hbar\beta} d\tau e^{i\nu_n\tau} D_{\text{ph}}^0(\lambda\mathbf{q}, \lambda'\mathbf{q}', \tau) \quad (5.47)$$

with, again, discrete  $\nu_n = \frac{2n\pi}{\hbar\beta}$ , because of the periodicity in the time argument. Then we obtain for this non-interacting system

$$D_{\text{ph}}^0(\lambda\mathbf{q}, \lambda'\mathbf{q}', \nu_n) = \delta_{\mathbf{q},-\mathbf{q}'} \delta_{\lambda\lambda'} \frac{2\Omega_{\mathbf{q}\lambda}}{(\nu_n)^2 + (\Omega_{\mathbf{q}\lambda})^2} \equiv \delta_{\mathbf{q},-\mathbf{q}'} \delta_{\lambda\lambda'} \left( \frac{1}{i\nu_n + \Omega_{\mathbf{q}\lambda}} - \frac{1}{i\nu_n - \Omega_{\mathbf{q}\lambda}} \right). \quad (5.48)$$

## 5.2. Perturbation Theory

We have introduced the SE in Eq. (5.19) that prevents a direct solution of the equation of motion for the GF. We have no method to compute the SE directly, but it is possible to represent it as a Taylor series in the difference of the potential in the (non-interacting) starting system and interacting system. The series can be cast into a self-consistent equation that sums an infinite set of diagrams when it is solved to self-consistency.

Following the books [19] and [45] we show that the diagrammatic perturbation series for the SE  $\bar{\Sigma}(1, 1', \omega_n)$  is essentially the same as for a non-SC system. The only difference is to replace the normal GFs  $G(\mathbf{r}, \mathbf{r}', \omega_n)$  and the vertices  $\Gamma$  with their Nambu analogs  $\bar{G}(1, 1', \omega_n)$  and  $\bar{\Gamma}$ .

We aim to evaluate  $\langle \hat{T} [\hat{H}^\dagger, \hat{\Psi}(1)]_-(\tau) \hat{\Psi}^\dagger(1', 0) \rangle$  where  $\hat{H}^\dagger \equiv \hat{H} - \hat{H}_0$ . We use  $\hat{H}_0$  to point out that the derivation is independent on the specific choice. In most cases we take it simply as the kinetic energy plus external one-particle potentials. Our task will involve the calculation of thermal averages in the interacting system, but we may introduce the following time evolution operator to circumvent this problem

$$\hat{U}(\tau, \tau') = e^{\tau\hat{H}_0} e^{-(\tau-\tau')\hat{H}} e^{-\tau'\hat{H}_0}. \quad (5.49)$$

We use the notation  $\langle \dots \rangle_0 \equiv \text{Tr} \{ e^{-\beta\hat{H}_0} \dots \} / \text{Tr} \{ e^{-\beta\hat{H}_0} \}$  and notice that

$$\langle T e^{-\tau\hat{H}} [\hat{H}^\dagger, \hat{\Psi}(1)] e^{-\tau\hat{H}} \hat{\Psi}^\dagger(1', 0) \rangle = \frac{\langle T \hat{U}(\beta, \tau) [\hat{H}^\dagger, \hat{\Psi}(1)]_-(\tau) \hat{\Psi}^\dagger(1', 0) \rangle_0}{\langle \hat{U}(\beta, 0) \rangle_0}. \quad (5.50)$$

<sup>5</sup>Formally the interacting Hamiltonian is the full KS Hamiltonian of Eq. (3.55) which includes arbitrarily high  $N$  phonon interactions.



The time evolution operator satisfies the differential equation

$$\partial_\tau \hat{U}(\tau, \tau') = -\hat{H}_I^1(\tau) \hat{U}(\tau, \tau') \quad (5.51)$$

with  $\hat{H}_I^1(\tau) = e^{\tau \hat{H}_0} \hat{H}^1 e^{-\tau \hat{H}_0}$  and the usual formal solution

$$\hat{U}(\tau, \tau') = T(e^{\int_{\tau'}^{\tau} \hat{H}_I^1(\tau'') d\tau''}) = T(e^{-\int_{\tau'}^{\tau} \hat{H}_I^1(\tau'') d\tau''}). \quad (5.52)$$

In Ref. [45, Section 8] it is demonstrated that for two Heisenberg operators under the time ordering symbol one may replace the Heisenberg picture with the interaction picture so that

$$\langle T e^{-\tau \hat{H}} [\hat{H}^1, \hat{\Psi}(1)]_- e^{-\tau \hat{H}} \hat{\Psi}^\dagger(1') \rangle = \frac{\langle T \hat{U}(\beta, 0) [\hat{H}_I^1, \hat{\Psi}_I(1)]_-(\tau) \hat{\Psi}_I^\dagger(1', 0) \rangle_0}{\langle \hat{U}(\beta, 0) \rangle_0}. \quad (5.53)$$

Before we can evaluate this expression, we need to translate the interaction  $\hat{H}_I^1$  into the Nambu formalism. Let us consider a local two particle interaction  $w_{\mu\mu'}(\mathbf{r}, \mathbf{r}')$ . Due to the time ordering symbol we do not have to worry about commutators when we rearrange the field operators and obtain<sup>6</sup>

$$\langle T \dots \hat{H}_I^1(\tau) \dots \rangle_0 = \sum_{\mu\mu'} \iint w_{\mu\mu'}(\mathbf{r}, \mathbf{r}') \langle T \dots \hat{\psi}_{I\mu}^\dagger(\mathbf{r}\tau) \hat{\psi}_{I\mu'}^\dagger(\mathbf{r}'\tau) \hat{\psi}_{I\mu'}(\mathbf{r}'\tau) \hat{\psi}_{I\mu}(\mathbf{r}\tau) \dots \rangle_0 d\mathbf{r} d\mathbf{r}' \quad (5.54)$$

$$= \frac{1}{4} \sum_{\mu\mu'} \iint w_{\mu\mu'}(\mathbf{r}, \mathbf{r}') \langle T \dots \hat{\Psi}_{I\mu}^\dagger(\mathbf{r}\tau) \cdot \tau_z \sigma_0 \cdot \hat{\Psi}_{I\mu}(\mathbf{r}\tau) \hat{\Psi}_{I\mu'}^\dagger(\mathbf{r}'\tau) \cdot \tau_z \sigma_0 \cdot \hat{\Psi}_{I\mu'}(\mathbf{r}'\tau) \dots \rangle_0 d\mathbf{r} d\mathbf{r}'. \quad (5.55)$$

Here we use  $\hat{\Psi}_\mu \equiv \sum_\alpha \hat{\Psi}_{\alpha\mu}$ . In a more elegant way we can represent the interaction as a tensor

$$\langle T \dots \hat{H}_I^{1nl}(\tau) \dots \rangle_0 = \frac{1}{4} \int d(1..4) \langle T \dots \hat{\Psi}_I^\dagger(1\tau) (\hat{\Psi}_I(2\tau) w(1..4) \hat{\Psi}_I^\dagger(3\tau)) \hat{\Psi}_I(4\tau) \dots \rangle_0. \quad (5.56)$$

Tensor matrix elements of  $w(1..4)$  must have the symmetry

$$w_{\alpha\alpha'\beta\beta'}^{\sigma\sigma'\mu\mu'}(\mathbf{r}_1\mathbf{r}_2\mathbf{r}_3\mathbf{r}_4) = -w_{-\alpha',-\alpha\beta\beta'}^{\sigma'\sigma\mu\mu'}(\mathbf{r}_2\mathbf{r}_1\mathbf{r}_3\mathbf{r}_4) = w_{-\alpha',-\alpha,-\beta',-\beta}^{\sigma'\sigma\mu'\mu}(\mathbf{r}_2\mathbf{r}_1\mathbf{r}_4\mathbf{r}_3) \quad (5.57)$$

if the interaction corresponds to a potential that can be defined without Nambu-space. The symmetries then follow from the property of the commutator and their relation to the original interaction in its normal, non-Nambu form. Also hermitian, totally antisymmetric anomalous potentials satisfy this condition. In the following we are only concerned with interactions that satisfy this condition. Their form in Nambu space is always  $\propto \Psi^\dagger \cdot \tau_z \cdot \Psi \Psi^\dagger \cdot \tau_z \cdot \Psi$ . Now it is straight forward to compute the commutator  $[\hat{H}^1, \hat{\Psi}(1)]_-$ <sup>7</sup>

$$\begin{aligned} & \langle T \dots [\hat{H}_I^1(\tau), \hat{\Psi}_I(1')] \hat{\Psi}_I^\dagger(4) \rangle_0 \\ &= \frac{1}{2} \int d1d2d3 (w(1, 2, 1', 3) + w(1', 3, 1, 2)) \langle T \dots \hat{\Psi}_I^\dagger(1) \hat{\Psi}_I(2) \hat{\Psi}_I^\dagger(4) \hat{\Psi}_I(3) \rangle_0. \end{aligned} \quad (5.58)$$

Further if the interaction is symmetric

$$\begin{aligned} & \langle T \dots [\hat{H}_I^1(\tau), \hat{\Psi}_I(1')] \hat{\Psi}_I^\dagger(4) \rangle_0 \\ &= \int d1d2d3 w(1, 2, 1', 3) \langle T \dots \hat{\Psi}_I^\dagger(1) \hat{\Psi}_I(2) \hat{\Psi}_I^\dagger(4) \hat{\Psi}_I(3) \rangle_0. \end{aligned} \quad (5.59)$$

<sup>6</sup>The ... indicate further  $\hat{H}_I^1$  in the Heisenberg picture at different  $\tau_{1,2,\dots}$ .

<sup>7</sup>We include  $\tau$  into the abbreviation  $1 \equiv (\mathbf{r}\alpha\mu\tau)$

Making use of the above equation requires the evaluation of the thermal average of a set of field operators. Expanding the time evolution operator of Eq. (5.52) to  $n$ th order we may use a generalized Wick theorem

$$\int d2 \dots w(2, 3, 4, 5) \dots \langle T \{ \hat{\Psi}_I(1) \hat{\Psi}_I(2) \dots \hat{\Psi}_I^\dagger(1') \} \rangle_0 = \int d2 \dots w(2, 3, 4, 5) \dots \left\{ \text{Sum of all possible contractions} \right\} \quad (5.60)$$

where a contraction is defined to be  $\langle T \hat{\Psi}_I(1) \hat{\Psi}_I^\dagger(1') \rangle_0$ . We demonstrate this theorem in the Appendix F. The procedure and the result is very similar to normal diagrammatic perturbation theory with the exception that we have to give reasons why  $\langle T \hat{\Psi}_I(1) \hat{\Psi}_I^\dagger(1') \rangle_0$  appears but  $\langle T \hat{\Psi}_I(1) \hat{\Psi}_I(1') \rangle_0$  not. We discuss the details in Appendix F, but mention here that for potentials with the symmetry of Eq. (5.57) the diagrams considering anomalous Nambu field averages are equivalent to the ones with just the usual GF. Thus in the sum for an  $N$  particle interaction we obtain a multiplicity of  $2^N$  that, in fact, cancels the factor  $1/2^N$  we obtained in translating into the Nambu notation.

Note that we may separate the tensor matrix elements  $w(1, 2, 3, 4)$  into a vertex part and an interaction. To keep the simple Nambu-scalar form of the interaction we introduce the bare vertex as to contain the  $\tau_z$  we obtained from the anticommutator. For the screened Coulomb interaction (and any interaction that is local in spin space) we may keep a spin scalar form as it is independent of spin. Thus the bare vertex for the Coulomb interaction becomes

$$\Gamma^{\text{Coul}}(\mathbf{r}_1, \mathbf{r}_2, \mathbf{r}_3) = e\sigma_0\tau_z\delta(\mathbf{r}_1 - \mathbf{r}_2)\delta(\mathbf{r}_2 - \mathbf{r}_3). \quad (5.61)$$

and we have chosen the vertices to be Spin-Nambu matrices. Given an (effective) interaction that is non-local in spin space we may choose to symmetrize its tensor matrix elements  $w(1, 2, 3, 4)$  to be  $\propto \sigma_{0,x,y,z}\sigma_{0,x,y,z}$  and then perform the separation into vertices and scalar interactions. We are at the starting point of the discussion to include magnetic fluctuations into the theory. These however are the content of a different thesis [46] and will not be considered here.

Now that we recover the diagrammatic expansion of the normal system, all results that are based on the topology of diagrams can be directly transferred. This means one can show that the denominator will cancel all disconnected diagrams from the sum of all contractions, just as for the normal metal. Rules for this expansion are discussed in every book on Many Body perturbation theory e.g. [45] and we only briefly repeat the results for  $n$ th order.

1. Draw all topologically distinct diagrams containing  $n$  GFs using the diagrammatic notation of Fig. 5.1.
2. Attach a factor of  $(-\hbar^{-1})^n$ .
3. Sum/integrate all degrees of freedom of an inner vertex.
4. Multiply a factor of  $-1$  for every fermionic loop.
5. Interpret equal times in a GF as

$$\bar{G}(\mathbf{r}\tau, \mathbf{r}'\tau) = \begin{pmatrix} G(\mathbf{r}\tau, \mathbf{r}'\tau^+) & F(\mathbf{r}\tau, \mathbf{r}'\tau^+) \\ F^\dagger(\mathbf{r}\tau, \mathbf{r}'\tau^+) & G^\dagger(\mathbf{r}\tau^+, \mathbf{r}'\tau) \end{pmatrix} \quad (5.62)$$

The last rule is different from the usual approach, but follows the same reasoning. Such terms arise from a contraction term within the interaction Hamiltonian and thus must have the same ordering [45]. This means in particular that we have to treat the hole GF different from the particle part in taking the first time argument infinitesimally before the second.

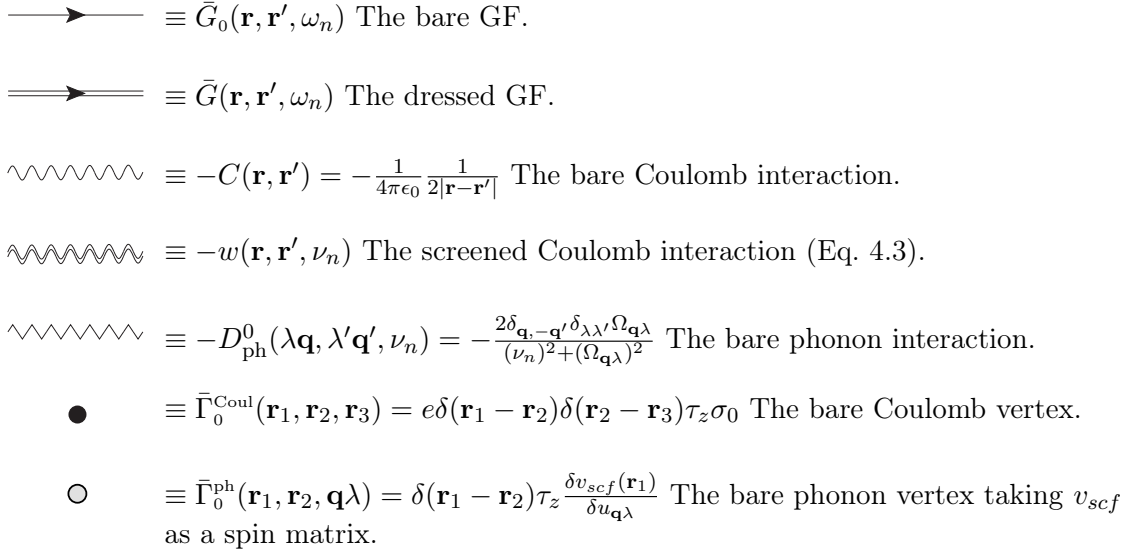


Figure 5.1.: Diagrammatic notation.

We conclude this section by pointing out the connection to a diagrammatic expansion of the SE we met with in Eq. (5.19). From the relation Eq. (5.59) and Wicks theorem it is found that we may factor out

$$\frac{\langle T\hat{U}(\beta, 0)[\hat{H}_I^{\dagger}(\tau), \hat{\Psi}_I(1)] \otimes \hat{\Psi}_I^{\dagger}(1') \rangle_0}{\langle \hat{U}(\beta, 0) \rangle_0} \equiv \int d2\tilde{\Sigma}(1, 2)\bar{G}_0(2, 1') \quad (5.63)$$

where  $\tilde{\Sigma}(1, 2)$  is called the reducible SE. In a diagrammatic language it contains all diagrams with two external propagator connectors. Because we have seen that this defines the full GF diagrammatically, along the line of [47] we define the irreducible SE as the sum of all the diagrams that cannot be separated by cutting a single propagator line. We can separate every GF diagram into a part that cannot be split cutting a single propagator line (that is possibly zero) and the rest. We note that the rest is build of the same kind, so that we can write every GF diagram as a sequence of irreducible SE insertions that are connected with single propagator lines. The full GF is the sum of all SE insertions and the above set of diagrams is then equivalently written as

$$\int d2\tilde{\Sigma}(1, 2)\bar{G}^0(2, 1') \equiv \int d2\tilde{\Sigma}^{\text{irr}}(1, 2)\bar{G}(2, 1') \quad (5.64)$$

because both sides generate all diagrams. Here we separate the Hartree diagram

$$\begin{aligned} \text{Hartree diagram} &= \frac{-\hbar^{-1}e^2}{4\pi\epsilon_0} \int d\mathbf{r}' \sum_{\alpha\mu\alpha'\mu'} \frac{(\tau_z\sigma_0)_{\alpha\mu\alpha'\mu'}(-\bar{G}(\mathbf{r}'\tau, \mathbf{r}'\tau))_{\alpha\mu\alpha'\mu'}}{2|\mathbf{r}-\mathbf{r}'|} \tau_z\sigma_0 = \frac{e^2\hbar^{-1}}{4\pi\epsilon_0} \int d\mathbf{r}' \frac{n(\mathbf{r}')\tau_z\sigma_0}{|\mathbf{r}-\mathbf{r}'|} \end{aligned} \quad (5.65)$$

from  $\tilde{\Sigma}^{\text{irr}}(\mathbf{r}, \mathbf{r}', \tau - \tau')$  to arrive at the usual definition of the SE  $\bar{\Sigma}(\mathbf{r}, \mathbf{r}', \tau - \tau')$  of Eq. (5.19). Note that the SE, as introduced before, is a functional of the bare GF and the perturbation  $\hat{H}_I^{\dagger}$  that leads via Eq. (5.63) from bare to the interaction system. In fact, the SE  $\bar{\Sigma}$  can be introduced via the Hedin equations, where it is a functional of the interacting GF. This is important as it shows that the Dyson equation is linear in the addition and subtraction of single particle potentials such as  $\bar{v}_{xc}$ . The idea to separate blocks of diagrams into individual objects can be pursued further. We define the polarization propagator

$$\chi^{\text{pol}}(\mathbf{r}\tau, \mathbf{r}'\tau') = \{\text{sum of all connected diagrams with two external interaction line connectors}\} \quad (5.66)$$

that matches the object introduced in Eq. (4.3) and thus defines the effective interaction. Further we introduce the dressed vertex

$$\Gamma^{\text{Coul}}(\mathbf{r}_1, \mathbf{r}_2, \mathbf{r}_3) = \left\{ \begin{array}{l} \text{sum of all connected diagrams with two GF- and one} \\ \text{interaction line connector where it is not possible to separate} \\ \text{parts cutting a single GF or interaction line} \end{array} \right\}. \quad (5.67)$$

Since these sets are always chosen such that they mutually exclude each other we see that we may write the SE as

$$\bar{\Sigma}(\mathbf{r}\tau, \mathbf{r}'\tau') = \text{diagram: a wavy line from left to right, a semi-circular arc above it, and a shaded triangle on the right side of the wavy line.} \quad (5.68)$$

where diagrammatically we have introduced

$$\Gamma^{\text{Coul}}(\mathbf{r}_1, \mathbf{r}_2, \mathbf{r}_3) = \text{diagram: a shaded triangle pointing to the right.} \quad (5.69)$$

The discussion is readily extended to additional interactions e.g. the phonon interaction. We will use the starting approximation for the SE

$$\bar{\Sigma}(\mathbf{r}, \mathbf{r}', \omega_n) \approx \text{diagram: wavy line with two arcs above it} + \text{diagram: wavy line with one arc above it} + \text{diagram: wavy line with a loop above it}. \quad (5.70)$$

This means we immediately drop vertex corrections in the electronic part. While it can be shown that these vertex corrections are small for the phonon interaction (Migdal's theorem [48]) this approximation is of practical nature for the Coulomb potential as these are simply too demanding to be computed. Also we do not consider a dressing of the phonon interaction, but take the KS phonons as a reasonably good approximation [35]. Moreover, in principle, we have to update the screened Coulomb interaction every iteration which is not considered due to numerical complexity. Further will the phononic Hartree diagram not be considered in the functional construction. We will come back to this point later in the thesis in Section 6.3. The subsets of diagrams satisfy five connected self-consistent equations themselves, commonly known as the Hedin equations. This very elegant set of equations can be derived using a functional derivative approach that does not rely on the topology of subsets of diagrams and naturally relates the vertex to the functional derivative of the SE with respect to the GF. The presentation of the Hedin equations for a SC [49] however is beyond the scope of this thesis.

### 5.3. The SSE of SpinSCDFT

The SSE [50, 51] allows the construction of an  $xc$  potential from Many-Body perturbation theory via the condition that the densities of the KS system must be equal to those of the (approximated) Many-Body system. With this requirement, every approximate SE directly yields an approximation for the  $xc$  potentials.

The densities  $n(\mathbf{r})$ ,  $\mathbf{m}(\mathbf{r})$  and  $\chi(\mathbf{r}, \mathbf{r}')$  are obtained, as a first step by taking the limit  $\tau \rightarrow \tau'$ , which is equivalent to a Matsubara summation over frequencies

$$\lim_{\tau \rightarrow \tau'} \bar{G}(\mathbf{r}, \mathbf{r}', \tau - \tau') = \lim_{\tau \rightarrow \tau'} \frac{1}{\beta} \sum_{\omega_n} \bar{G}(\mathbf{r}, \mathbf{r}'\omega_n) e^{i\omega_n(\tau - \tau')} = \frac{1}{\beta} \sum_{\omega_n} \bar{G}(\mathbf{r}, \mathbf{r}'\omega_n). \quad (5.71)$$

Then, by symmetrizing in spin space, we obtain the individual densities<sup>8</sup>

$$\frac{1}{\beta} \sum_{\omega_n} F(\mathbf{r}, \mathbf{r}' \omega_n) = \boldsymbol{\chi}(\mathbf{r}, \mathbf{r}') \cdot \boldsymbol{\Phi}^* \quad (5.72)$$

$$\frac{1}{\beta} \sum_{\omega_n} G(\mathbf{r}, \mathbf{r} \omega_n) = n(\mathbf{r})\sigma_0 + \mathbf{m}(\mathbf{r}) \cdot \mathbf{S}^* \quad (5.73)$$

$$\frac{1}{\beta} \sum_{\omega_n} F^\dagger(\mathbf{r}, \mathbf{r}' \omega_n) = \boldsymbol{\chi}^*(\mathbf{r}, \mathbf{r}') \cdot \boldsymbol{\Phi} \quad (5.74)$$

$$\frac{1}{\beta} \sum_{\omega_n} G^\dagger(\mathbf{r}, \mathbf{r} \omega_n) = -n(\mathbf{r})\sigma_0 - \mathbf{m}(\mathbf{r}) \cdot \mathbf{S}. \quad (5.75)$$

The minus sign in Eq. (5.75) is because of the special definition of the equal time limit Eq. (5.62) that does not swap the field operators. By construction these densities are also obtained from the KS GF. Thus we have with Eq. (5.26)

$$\begin{aligned} 0 &= \frac{1}{\beta} \sum_{\omega_n} \int d(\mathbf{x}, \mathbf{x}') [\bar{G}^{\text{KS}}(\mathbf{r}, \mathbf{x}, \omega_n) \cdot \bar{\Sigma}^{\text{s}}(\mathbf{x}, \mathbf{x}', \omega_n) \cdot \bar{G}(\mathbf{x}', \mathbf{r}, \omega_n)]_{\alpha, \alpha} \\ 0 &= \frac{1}{\beta} \sum_{\omega_n} \int d(\mathbf{x}, \mathbf{x}') [\bar{G}^{\text{KS}}(\mathbf{r}, \mathbf{x}, \omega_n) \cdot \bar{\Sigma}^{\text{s}}(\mathbf{x}, \mathbf{x}', \omega_n) \cdot \bar{G}(\mathbf{x}', \mathbf{r}', \omega_n)]_{\alpha, -\alpha} \end{aligned} \quad (5.76)$$

The point is to arrive at a condition for the  $xc$  potential. Moving the  $xc$  potential from the KS SE to the left hand side of the equation we obtain

$$\begin{aligned} &\frac{1}{\beta} \sum_{\omega_n} \int d(\mathbf{x}, \mathbf{x}') [\bar{G}^{\text{KS}}(\mathbf{r}, \mathbf{x}, \omega_n) \cdot \bar{v}_{xc}(\mathbf{r}, \mathbf{x}) \cdot \bar{G}(\mathbf{x}', \mathbf{r}, \omega_n)]_{\alpha, \alpha} \\ &= \frac{1}{\beta} \sum_{\omega_n} \int d(\mathbf{x}, \mathbf{x}') [\bar{G}^{\text{KS}}(\mathbf{r}, \mathbf{x}, \omega_n) \cdot \bar{\Sigma}(\mathbf{x}, \mathbf{x}', \omega_n) \cdot \bar{G}(\mathbf{x}', \mathbf{r}, \omega_n)]_{\alpha, \alpha} \\ &\frac{1}{\beta} \sum_{\omega_n} \int d(\mathbf{x}, \mathbf{x}') [\bar{G}^{\text{KS}}(\mathbf{r}, \mathbf{x}, \omega_n) \cdot \bar{v}_{xc}(\mathbf{r}, \mathbf{x}) \cdot \bar{G}(\mathbf{x}', \mathbf{r}', \omega_n)]_{\alpha, -\alpha} \\ &= \frac{1}{\beta} \sum_{\omega_n} \int d(\mathbf{x}, \mathbf{x}') [\bar{G}^{\text{KS}}(\mathbf{r}, \mathbf{x}, \omega_n) \cdot \bar{\Sigma}(\mathbf{x}, \mathbf{x}', \omega_n) \cdot \bar{G}(\mathbf{x}', \mathbf{r}', \omega_n)]_{\alpha, -\alpha} \end{aligned} \quad (5.77)$$

This equation is the basis of the functional construction in the next chapter. We have decomposed the density into spin symmetric parts, i.e.  $(\sigma_0, \mathbf{S})^T$  on the Nambu diagonal and  $\boldsymbol{\Phi}$  on the Nambu-offdiagonal. Thus we obtain independent SSE for each of these 16 scalar orthonormal components. Note that we may take the equation also for every Nambu-spin component individually which, of course, also makes 16 independent equations.

## Summary

We have introduced the electronic spin and Nambu GF  $\bar{G}$  as the central object in Many-Body theory. It satisfies a matrix valued, self-consistent Dyson equation and we can start from any single particle Hamiltonian we wish. As the most important example we have discussed the SC KS Hamiltonian with the GF  $\bar{G}^{\text{KS}}$  as the unperturbed (formally) non-interacting system. Two particle interactions create an inhomogeneity in the Dyson equation that we have rewritten into the SE  $\bar{\Sigma}$ . We have introduced a diagrammatic perturbative expansion for  $\bar{\Sigma}$  that is essentially equivalent to the usual perturbation expansion except that we replace vertices  $\Gamma$  and the usual electronic GF  $G$  with  $4 \times 4$  spin and Nambu analogs  $\bar{\Gamma}$  and  $\bar{G}$ . In a final step we have used that  $\bar{G}$  must equal  $\bar{G}^{\text{KS}}$  by construction in the limits in which the GF reproduces the densities. This led us to the SSE which connects the  $\bar{v}_{xc}$  potential with an approximation to the SE.

<sup>8</sup>The special equal time limit for  $G^\dagger$  discussed in Sec. (5.2) ensures that  $\mathbf{m}(\mathbf{r}) \cdot \mathbf{S}$  is not transposed.

## 6. Functionals and the Self-Consistency Cycle

In this Chapter we use the Sham-Schlüter connection of Eq. (5.77) to obtain a density functional for the anomalous pair potential  $\Delta^s$ . The presence of a SC condensate may change also the normal state densities. In a non-magnetic SC the condensate changes the electronic density  $n(\mathbf{r})$  only in an extremely narrow region about the Fermi level. To a good approximation this density change can be neglected. However, magnetism and SC tend to compete and we do not expect the magnetic density to be unaffected by the SC condensation. Thus we start the chapter in Section 6.1 with a discussion on how to treat those changes in a self consistency cycle.

In Section 6.2 we show how we include the density changes into an updated  $xc$  potential for the Nambu diagonal. We point out that the approach is feasible in practice.

In Section 6.3 we are concerned with the derivation of an  $xc$  potential for the Nambu off-diagonal where we use the SSE of Sec. 5.3 and an approximation to the SE using diagrammatic perturbation theory introduced in Sec. 5.2.

The nature of the KS system changes drastically when we apply the SDA of Subsection 3.5.2. In this case the solutions to the KSBdG equations (3.152)  $u$  and  $v$  are analytically known in terms of the KS potential and single particle energies. Thus, the diagrams of the SE which depend on  $u$  and  $v$  are known, explicit functionals of the pair potential  $\Delta_s^s$ . Thus, the potential term  $\bar{G}^{KS} \cdot \bar{v}_{xc} \cdot \bar{G}$  in the Sham-Schlüter connection of Eq. (5.77) loses its special status as the only term that depends on the potential. We choose to interpret the SSE as a (non-linear) operator that maps the potential to zero  $S_\beta[\Delta_s^s] \cdot \Delta_s^s = 0$  and construct a gap equation in Section 6.4.

As a final step we assume the interactions only to dependent on the energy and spin separation of the states. At the end of this chapter we have functionals available so that we could directly attempt to solve them on a computer. This, however, we postpone to Chapter 8 after we have extended our results in the direction of Many-Body Perturbation Theory in Chapter 7. This will yield for example improved excitation spectra on the basis of the interacting GF.

### 6.1. General Approach to a Self-Consistent Solution

In the context of any DFT the accuracy of results is tied to the quality of available density functionals. The essential ingredient to the KSBdG equations Eq. (3.122) are the matrix elements  $\mathcal{E}$  (the “normal” part of the Hamiltonian on the Nambu diagonal) and  $\Delta^s$  (the matrix elements of the pair potential on the Nambu off-diagonal). These matrix elements as functionals of the densities are the subject of this Chapter with the focus on  $\mathcal{E}$  in the Section 6.2 and on  $\Delta^s$  in the Section 6.3. In this Section we propose a general procedure on how to iterate the KS system until its densities and potentials (as functionals of the densities) are consistent.

To obtain the basis functions  $\varphi_k(\mathbf{r}\sigma)$  we will take one of the known functionals as e.g. the LSDA and compute them with one of the electronic structure codes available [52, 53]. Assuming we had solved Eq. (3.122) for some starting  $\Delta^s$  we may compute the new set of densities  $n(\mathbf{r})$ ,  $\mathbf{m}(\mathbf{r})$  and  $\chi(\mathbf{r}, \mathbf{r}')$  as given in Subsection 3.2.1. We refer to the starting densities with a small subscript 0. Obviously, evaluating the functionals  $v_{xc}$  and  $\mathbf{B}_{xc}$  at different densities  $n(\mathbf{r})$ ,  $\mathbf{m}(\mathbf{r})$  will result in corrections to  $\mathcal{E}$  of Eq. (3.121). Not considering the temperature corrections, (SC is a low

temperature phenomenon where  $v_{xc}(T = 0)$  is expected to be a good approximation) we may view these changed matrix elements in essentially two ways. First, let us view  $v_{xc}$  as a spin matrix for a moment (i.e. we include  $\mathbf{B}_{xc}$  into  $v_{xc}$ ) then with

$$V_{ij\sigma\sigma'}^C = \langle \vec{\varphi}_{i\sigma} | v_{xc}[n, \mathbf{m}, \boldsymbol{\chi}] - v_{xc}[n_0, \mathbf{m}_0, \boldsymbol{\chi}_0] | \vec{\varphi}_{j\sigma'} \rangle \quad (6.1)$$

we have the old matrix  $\mathcal{E}_{ij}^0$  Eq. (3.121) plus the corrections  $V_{ij}^C$ . Because SC is expected to change the density and thus the eigenfunctions only very close to the Fermi level,  $V_{ij}^C$  will be non-zero only for these states.

We note however that if we include non-diagonal corrections  $V_{ij}^C$  to the electronic spectrum  $\varepsilon_k$  we lose the SDA. If we want density corrections and the SDA at the same time we can use the following, second, approach:

1. Compute  $\mathcal{E}_{ij}^0$  and  $V_{ij}^C$  for given densities.
2. Diagonalize  $\mathcal{E}_{ij} = \mathcal{E}_{ij}^0 + V_{ij}^C$  and keep the unitary matrix  $U$  that connects the old and the new matrix.
3. Perform the Spin-Decoupling Approximation with respect to these solutions.
4. Update the densities and start at (1.) up until self consistency is reached.

If we want to describe the FFLO phase [11, 12] our theory has to allow finite momentum pairing. As mentioned before in the discussion at the end of Subsection 3.5.2, we have to go beyond the SDA to treat FFLO states.

Note that the proposed second scheme changes the meaning of the SDA in every iteration because the basis states it refers to change. In practice the dependence of  $v_{xc}$  on  $\boldsymbol{\chi}$  is expected to be weak due to the low energy scale of SC. We guess its influence will be mostly indirect via a change in single KS state occupations. Thus when we discuss how to extract correction matrix elements  $V_{ij}^C$  in the next section we omit the functional dependence on  $\boldsymbol{\chi}$  as well as temperature effects beyond the SC pair potential.

## 6.2. The $\mathcal{E}_{ij}$ Matrix as a Functional of $\mathbf{m}(\mathbf{r})$ and $n(\mathbf{r})$ .

With both, either scheme one or two of the last Section 6.1, we need to update the matrix  $\mathcal{E}_{ij}$  for updated densities  $\mathbf{m}(\mathbf{r})$  and  $n(\mathbf{r})$ . The Hamiltonian defining the basis  $\{\vec{\varphi}_{i\sigma}\}$  is fixed at this point, thus we obtain a correction  $V_{ij}^C$  to the original matrix elements  $\mathcal{E}_{ij}^0$  of the form of Eq. (6.1). A technical problem is that  $v_{xc}[n, \mathbf{m}]$  in one of the common approximations such as the LSDA is non-linear in the densities and can practically only be evaluated in real space where we work in the space of KS orbitals.

Because of the limited energy region of SC about the Fermi level, these corrections  $V_{ij}^C$  are expected to be of importance also only in this range of  $\mathcal{O}(0.1\text{eV})$ . We use a simple separation of the density from orbitals far away from the Fermi level

$$n_{\text{fix}}(\mathbf{r}) = \sum_{(ij) \in S} \sum_{\sigma\sigma'} \varphi_{i\sigma}^*(\mathbf{r}) (n_{ij})_{\sigma\sigma'} \varphi_{j\sigma'}(\mathbf{r}) \quad S = \{i | |\varepsilon_i| > \varepsilon_b\} \quad (6.2)$$

where  $\varepsilon_b$  will have to be chosen large enough in order that all relevant  $V_{ij}^C$  appearing in a self consistent cycle can be captured. The rest of the density contributions we consider dependent on the condensation<sup>1</sup>

$$n_{\text{var}}(\mathbf{r}) = \sum_{(ij) \notin S} \sum_{\sigma\sigma'} \varphi_{i\sigma}^*(\mathbf{r}) \varphi_{j\sigma'}(\mathbf{r}) (n_{ij})_{\sigma\sigma'} , \quad (6.3)$$

<sup>1</sup>We need to insert the unitary transformation  $U$  to keep the  $\varphi_{i\sigma}(\mathbf{r})$  fix every iteration if we choose option two.

and  $n(\mathbf{r}) = n_{\text{fix}}(\mathbf{r}) + n_{\text{var}}(\mathbf{r})$ . Similar for the magnetic density  $\mathbf{m}(\mathbf{r}) = \mathbf{m}_{\text{fix}}(\mathbf{r}) + \mathbf{m}_{\text{var}}(\mathbf{r})$  with  $(\mathbf{m}_{ij})_{\sigma\sigma'}$  of Eq. (3.131). We define the matrix

$$M_{ij}^{\sigma\sigma'}(\mathbf{r}) = \varphi_i^*(\mathbf{r}\sigma)\varphi_j(\mathbf{r}\sigma') \quad (6.4)$$

and see that in terms of this object

$$V_{ij\sigma\sigma'}^{\text{C}} = \int d\mathbf{r} M_{ij}^{\sigma\sigma'}(\mathbf{r}) (v_{\text{xc}}[n, \mathbf{m}](\mathbf{r}) - v_{\text{xc}}[n_0, \mathbf{m}_0](\mathbf{r})) \quad (6.5)$$

$$n_{\text{var}}(\mathbf{r}) = \sum_{(ij) \notin S} \sum_{\sigma} M_{ij}^{\sigma\sigma}(\mathbf{r}) \sum_k (u_k^{i\sigma*} u_k^{j\sigma} f_{\beta}(E_k) + v_k^{i\sigma} v_k^{j\sigma*} f_{\beta}(-E_k)). \quad (6.6)$$

Keeping  $n_{\text{fix}}(\mathbf{r})$  and  $\mathbf{m}_{\text{fix}}(\mathbf{r})$  fix,  $M_{ij}^{\sigma\sigma'}(\mathbf{r})$  for  $(ij) \notin S$  is enough to update the normal state densities. The standard task to evaluate the exchange correlation potential in several approximations is implemented in many numerical packages<sup>2</sup>. To show the feasibility of the approach we perform an order of size estimate for  $M_{ij}^{\sigma\sigma'}(\mathbf{r})$ . A reasonable matrix carrying quantum numbers  $(i \times j) = (n, n', \mathbf{k})$  with states close to the Fermi energy could have the following values: A real space grid of dimension  $\{\mathbf{r}\} = \mathcal{O}(10^6)$ , a set of electronic bands  $(n \times n') = \mathcal{O}(10^2)$  - and a set of Bloch vectors close to the Fermi surface  $\{\mathbf{k}\} = \mathcal{O}(10^1)$ . This means a size of order

$$M_{ij}^{\sigma\sigma'}(\mathbf{r}) = \mathcal{O}(10^0) \text{GByte} \quad (6.7)$$

which is feasible on modern computer systems. Thus we have a realistic scheme to include competition between the magnetic density and SC in an ab-initio framework.

### 6.3. Construction of the $\Delta^{\text{s}}$ Matrix Functional

The functionals yielding the best results in a unsplitted SCDFE are constructed via many-body perturbation theory using the SSE Eq. (5.77) [54, 55].

We introduce further approximations in Subsection 6.3.1 and present the final form of the SE as it will be used in the functional. This will lead to a matrix equation for the pair potential matrix elements.

In Subsection 6.3.2 we compute the SE contributions that arise from the first order phonon-exchange diagram and in Subsection 6.3.3 we give the equations for the equivalent Coulomb diagram.

While these SE contributions suffice to calculate the functional expression, we decide to investigate the SE in a different basis in Subsection 6.3.4. The choice of basis is due to individual contributions to the inverse GF and the densities. We note that in a very important approximation to the phononic coupling, we have to drop the contributions from basis vectors containing  $\tau_z$ . Moreover this form makes the solution of the Dyson equation (7.9) in Chapter 7 much easier.

Finally, in Subsection 6.3.5, we derive the equation for the  $\Delta^{\text{s}}$  matrix.

#### 6.3.1. Preparatory: General Procedure and Further Approximations.

As the Many-Body GF is not available without a full, numerically expensive solution of the Dyson equation, we replace  $\bar{G}(\mathbf{r}, \mathbf{r}', \omega_n)$  with the SC KS GF  $\bar{G}^{\text{KS}}(\mathbf{r}, \mathbf{r}', \omega_n)$  on all occurrences

$$\bar{G} \rightarrow \bar{G}^{\text{KS}}, \quad \bar{\Sigma}[\bar{G}] \rightarrow \bar{\Sigma}[\bar{G}^{\text{KS}}] \equiv \bar{\Sigma}^{\text{KS}}. \quad (6.8)$$

<sup>2</sup>See for example libxc: <http://www.tddft.org/programs/octopus/wiki/index.php/Libxc>



This is a severe approximation and its effect is not easily understood. While A. Sanna could show that  $\bar{G} \rightarrow \bar{G}^{\text{KS}}$  outside the SE has only a small effect in the non-splitted case, it is known that this approximation for the SE violates Migdal's theorem and leads to a systematic underestimation of the critical temperature [54]. Nevertheless it is of great importance to understand the physics of the functional resulting from the replacement Eq. (6.8). In analogy to the non-magnetic case we expect that the results obtained in this way are qualitatively correct in many aspects and represent the basis of future improvements of the functional. In this work as a first approach to the generalized spin-splitted case, we rely on the simple replacement throughout the entire thesis. We are going to discuss approaches to improve the functional in the last part of this Subsection.

**Additional Approximations** It has been observed that computing the GW quasi particle band structure in a metal yields essentially the KS bands (compare Ref. [56, Fig. 2]) and moreover the densities of the two systems are approximately equal. Thus, at least in the spin degenerate case, the GW corrections on a KS band structure of a metal can usually be safely neglected. For practical reason we use a similar assumption for the spin part

$$\begin{aligned} & \int d(\mathbf{x}, \mathbf{x}') \frac{1}{\beta^2} \sum_{n, n'} w^{\text{RPA}}(\mathbf{x}, \mathbf{x}', \omega_n - \omega_{n'}) G^{\text{KS}}(\mathbf{r}, \mathbf{x}, \omega_n) \cdot \sigma_0 \cdot G^{\text{KS}}(\mathbf{x}, \mathbf{x}', \omega_{n'}) \cdot \sigma_0 \cdot G^{\text{KS}}(\mathbf{x}', \mathbf{r}', \omega_n) \\ \approx & \frac{1}{\beta} \int d\mathbf{x} \sum_n G^{\text{KS}}(\mathbf{r}, \mathbf{x}, \omega_n) \cdot (v_{xc}^{\text{LSDA}}(\mathbf{x}) \sigma_0 - g_s \mu_B \mathbf{S} \cdot \mathbf{B}_{xc}^{\text{LSDA}}(\mathbf{x})) \cdot G^{\text{KS}}(\mathbf{x}, \mathbf{r}', \omega_n). \end{aligned} \quad (6.9)$$

This way we drop the construction of the diagonal KS potential from the SSE.

Moreover the phononic Hartree diagram is neglected. Similar to the electronic Hartree diagram in Eq. (5.65), it is proportional to  $\tau_z$ . Terms like this are zero if particle hole symmetry is present, i.e. the single particle states are symmetric with their time reversed state about the Fermi energy. We compute the inverse SC KS GF in the Appendix E with the result

$$\begin{aligned} (\bar{G}^{\text{KS}})_{ij}^{-1}(\omega_n) &= \delta_{ij} \left( i\hbar\omega_n \tau_0 \sigma_0 - \left( \frac{\varepsilon_{i\uparrow} + \varepsilon_{-i\downarrow}}{2} \right) \tau_z \sigma_0 - \left( \frac{\varepsilon_{i\uparrow} - \varepsilon_{-i\downarrow}}{2} \right) \tau_z \sigma_z \right) \\ &+ \delta_{i,-j} \left( (i\tau_y)(i\sigma_y) \Re \Delta_{s_i}^s + \tau_x (i\sigma_y) i \Im \Delta_{s_i}^s \right). \end{aligned} \quad (6.10)$$

Terms in the SE  $\propto \tau_z$  add to the single particle energies. In other words: The Hartree diagram changes the Fermi energy (the  $\sigma_0 \tau_z$  symmetric part) and the single particle spin separation (the  $\sigma_z \tau_z$  symmetric part). In general we do not consider such corrections important. In fact, we will remove all energy asymmetric terms in the equations implemented during this work. The reason is that for numerical simplicity we want to replace the phononic coupling with an only phonon-frequency dependent object, the well known Eliashberg function  $\alpha^2 F(\omega)$ . If this is done one encounters integrals of the form  $\sum_k \frac{1}{\varepsilon_k} \rightarrow \int d\varepsilon \frac{1}{\varepsilon}$  [54] in all asymmetric terms  $\propto \tau_z$  which are logarithmically divergent. The physical reason is that computing the change in the Fermi energy is a global property of the band structure. This means one has to consider how the interaction changes the dispersion and occupation of states well below (or above) the Fermi level because the full dispersion has to be integrated to obtain  $N$  particles. If one replaces the state depended coupling with the value at the Fermi level, which is the heart of the  $\alpha^2 F(\omega)$  approximation, we do not obtain reasonable results for Fermi energy shifts. If we wish to include this effects, i.e. integrate the full coupling, in principle also the phononic Hartree diagram has to be considered but this is not done in this work.

With the expression for the  $xc$  potential Eq. (5.25), inserting these approximations the Sham-

Schlüter Eq. (5.77) becomes

$$\begin{aligned} & \frac{1}{\beta} \int d(\mathbf{x}\mathbf{x}') \sum_n \bar{G}^{\text{KS}}(\mathbf{r}, \mathbf{x}, \omega_n) \cdot \begin{pmatrix} 0 & \Phi \cdot \Delta^s(\mathbf{x}, \mathbf{x}') \\ -(\Phi \cdot \Delta^s(\mathbf{x}, \mathbf{x}'))^* & 0 \end{pmatrix} \cdot \bar{G}^{\text{KS}}(\mathbf{x}', \mathbf{r}', \omega_n) = \\ & = \frac{1}{\beta} \int d\mathbf{x} \int d\mathbf{x}' \sum_n \bar{G}^{\text{KS}}(\mathbf{r}, \mathbf{x}, \omega_n) \cdot (\bar{\Sigma}_{\text{ph}}^{\text{KS}}(\mathbf{x}, \mathbf{x}', \omega_n) + \bar{\Sigma}_{\text{Coul}}^{\text{KS}}(\mathbf{x}, \mathbf{x}', \omega_n)) \cdot \bar{G}^{\text{KS}}(\mathbf{x}', \mathbf{r}', \omega_n) \end{aligned} \quad (6.11)$$

with<sup>3 4</sup>

$$\begin{aligned} \bar{\Sigma}_{\text{ph}}^{\text{KS}}(\mathbf{x}, \mathbf{x}', \omega_n) &= -\frac{1}{\beta} \sum_{n'} \sum_{\mathbf{q}\lambda} D_{\text{ph}}^0(\lambda\mathbf{q}, \omega_n - \omega_{n'}) \tau_z \frac{\delta v_{\text{scf}}(\mathbf{x})}{\delta u_{\mathbf{q}\lambda}} \cdot \\ & \bar{G}^{\text{KS}}(\mathbf{x}, \mathbf{x}', \omega_{n'}) \cdot \tau_z \frac{\delta v_{\text{scf}}(\mathbf{x}')}{\delta u_{-\mathbf{q}\lambda}} \end{aligned} \quad (6.12)$$

$$\begin{aligned} \bar{\Sigma}_{\text{Coul}}^{\text{KS}}(\mathbf{x}, \mathbf{x}', \omega_n) &= -\frac{e^2}{\beta} \sum_{n'} w(\mathbf{x}, \mathbf{x}', \omega_n - \omega_{n'}) \tau_z \sigma_0 \cdot \\ & \begin{pmatrix} 0 & F^{\text{KS}}(\mathbf{x}, \mathbf{x}', \omega_{n'}) \\ F^{\text{KS}\dagger}(\mathbf{x}, \mathbf{x}', \omega_{n'}) & 0 \end{pmatrix} \cdot \tau_z \sigma_0 \end{aligned} \quad (6.13)$$

We have represented the SC KS system in the basis of normal state KS orbitals. Thus, we apply a similar representation of Eq. (6.11) in KS orbitals to extract  $\Delta^s$ . Formally, we use the spinor wavefunctions Eq. (5.37)  $\{\Psi_{i\sigma\alpha}^{\text{KS}}\}$  and use the same Nambu and Spin matrix notation for the expansion coefficients (compare Subsection 5.1.3). Using a symbolic notation the SSE Eq. (6.11) reads

$$\bar{G}^{\text{KS}} \cdot \bar{v}_{\text{xc}} \cdot \bar{G}^{\text{KS}} = \bar{G}^{\text{KS}} \cdot \bar{\Sigma}^{\text{KS}} \cdot \bar{G}^{\text{KS}}, \quad (6.14)$$

which we solve for the coefficient matrices  $\Delta^s$  contained in  $\bar{v}_{\text{xc}}$ .

**The Role of Eliashberg Theory for SCDFT** Due to Migdal's theorem [48] Eliashberg theory [44] is essentially correct up to order  $m_e/M$  for the electron-phonon interaction. We discuss the spin splitted extension to Eliashberg theory in Chapter 7. It provides us with what Monte Carlo calculations are for normal state DFT: An quasi-exact reference frame for the electron phonon coupling to parametrize parts of the functionals.

In practice the reliable way to understand the effect of the replacement  $\bar{G} \rightarrow \bar{G}^{\text{KS}}$  is to compute  $\bar{G}(\mathbf{r}, \mathbf{r}', \omega_n)$  via Many-Body perturbation theory and compare self consistent solutions of both approaches. While it seems that we loose the advantage of the numerical simplicity of DFT as compared to Many-Body perturbation theory, it has to be understood that this procedure can be used once for a reference material (e.g. the free electron gas) to obtain a functional. In fact A. Sanna et. al.<sup>5</sup> used a similar procedure in the SC electron gas to fit a replacement (KS-)GF and SE in Eq. (6.8) to the Many-Body GF and SE with a small set of parameters. Thus, SCDFT has assimilated the advantages of Eliashberg theory while keeping its own advantages, here in particular the easy and numerically cheap inclusion of the Coulomb interaction. This functional leads to results for real material that are in very good agreement with experiment.

<sup>3</sup>Note the minus sign is from the Feynman rules where the interaction carries a minus sign

<sup>4</sup>We are using  $D_{\text{ph}}^0(\lambda\mathbf{q}, \omega_n - \omega_{n'})$  as short hand for the  $\mathbf{q}$ -diagonal full object Eq. (5.48), but remember that  $\mathbf{q}'$  of Eq. (5.48) is  $\mathbf{q}' = -\mathbf{q}$ .

<sup>5</sup>To be published.

### 6.3.2. Phononic Exchange SE

The phononic SE matrix elements are computed as

$$\bar{\Sigma}_{\text{ph } i\sigma j\sigma'}^{\text{KS}\alpha\alpha'}(\omega_n) = \int d\mathbf{r} \int d\mathbf{r}' \langle \Psi_{i\sigma\alpha}^{\text{KS}} | \mathbf{r} \rangle \cdot \bar{\Sigma}_{\text{ph}}^s(\mathbf{r}, \mathbf{r}', \omega_n) \cdot \langle \mathbf{r}' | \Psi_{j\sigma'\alpha'}^{\text{KS}} \rangle \quad (6.15)$$

$$= \frac{1}{\beta} \sum_{n'\mathbf{q}\lambda} \sum_{kk'} D_{\text{ph}}^0(\lambda\mathbf{q}, \omega_n - \omega_{n'}) (g_{ik\sigma}^{\lambda\mathbf{q}} \delta_{\alpha,1} - g_{ki\sigma}^{\lambda\mathbf{q}} \delta_{\alpha,-1}) \times \\ \times G_{k\sigma\alpha k'\sigma'\alpha'}^{\text{KS}}(\omega_{n'}) (g_{k'j\sigma'}^{\lambda-\mathbf{q}} \delta_{\alpha',1} - g_{jk'\sigma'}^{\lambda-\mathbf{q}} \delta_{\alpha',-1}) \quad (6.16)$$

Where we have used the electron-phonon coupling defined in Eq. (4.1). With the equations for the GF Eq. (5.40) and the phonon propagator Eq. (5.48), we evaluate the individual Nambu components of Eq. (6.16) to

$$\bar{\Sigma}_{\text{ph } i\sigma j\sigma'}^{\text{KS}1,1}(\omega_n) = \sum_{\mathbf{q}\lambda kk'l} g_{ik\sigma}^{\lambda\mathbf{q}} g_{k'j\sigma'}^{\lambda-\mathbf{q}} (u_l^{k\sigma} (u_l^{k'\sigma'})^* I_s(\hbar\Omega_{\mathbf{q}\lambda}, E_l, \omega_n) + \\ + (v_l^{k\sigma})^* v_l^{k'\sigma'} I_s(\hbar\Omega_{\mathbf{q}\lambda}, -E_l, \omega_n)) \quad (6.17)$$

$$\bar{\Sigma}_{\text{ph } i\sigma j\sigma'}^{\text{KS}1,-1}(\omega_n) = - \sum_{\mathbf{q}\lambda kk'l} g_{ik\sigma}^{\lambda\mathbf{q}} g_{j k'\sigma'}^{\lambda-\mathbf{q}} (u_l^{k\sigma} (v_l^{k'\sigma'})^* I_s(\hbar\Omega_{\mathbf{q}\lambda}, E_l, \omega_n) + \\ + (v_l^{k\sigma})^* u_l^{k'\sigma'} I_s(\hbar\Omega_{\mathbf{q}\lambda}, -E_l, \omega_n)) \quad (6.18)$$

$$\bar{\Sigma}_{\text{ph } i\sigma j\sigma'}^{\text{KS}-1,1}(\omega_n) = - \sum_{\mathbf{q}\lambda kk'l} g_{ki\sigma}^{\lambda\mathbf{q}} g_{k'j\sigma'}^{\lambda-\mathbf{q}} (v_l^{k\sigma} (u_l^{k'\sigma'})^* I_s(\hbar\Omega_{\mathbf{q}\lambda}, E_l, \omega_n) + \\ + (u_l^{k\sigma})^* v_l^{k'\sigma'} I_s(\hbar\Omega_{\mathbf{q}\lambda}, -E_l, \omega_n)) \quad (6.19)$$

$$\bar{\Sigma}_{\text{ph } i\sigma j\sigma'}^{\text{KS}-1,-1}(\omega_n) = \sum_{\mathbf{q}\lambda kk'l} g_{ki\sigma}^{\lambda\mathbf{q}} g_{j k'\sigma'}^{\lambda-\mathbf{q}} (v_l^{k\sigma} (v_l^{k'\sigma'})^* I_s(\hbar\Omega_{\mathbf{q}\lambda}, E_l, \omega_n) + \\ + (u_l^{k\sigma})^* u_l^{k'\sigma'} I_s(\hbar\Omega_{\mathbf{q}\lambda}, -E_l, \omega_n)) . \quad (6.20)$$

The Matsubara summation in  $I_s(\hbar\Omega_{\mathbf{q}\lambda}, E_k, \omega_n)$  is evaluated using that  $e^{\beta i\hbar\omega_\nu} = -1$  with the result

$$Y_1(\hbar\Omega_{\mathbf{q}\lambda}, E_k, \omega_n) = \frac{\hbar^2}{\beta} \sum_{\omega_\nu} \frac{1}{i\hbar\omega_\nu - E_k} \frac{1}{i\hbar(\omega_n - \omega_\nu) + \hbar\Omega_{\mathbf{q}\lambda}} \quad (6.21)$$

$$= \hbar^2 \frac{n_\beta(\hbar\Omega_{\mathbf{q}\lambda}) + f_\beta(E_k)}{\hbar\Omega_{\mathbf{q}\lambda} - E_k + i\hbar\omega_n} \quad (6.22)$$

$$I_s(\hbar\Omega_{\mathbf{q}\lambda}, E_k, \omega_n) = Y_1(\hbar\Omega_{\mathbf{q}\lambda}, E_k, \omega_n) - Y_1(-\hbar\Omega_{\mathbf{q}\lambda}, E_k, \omega_n) \quad (6.23)$$

$$= \hbar^2 \frac{n_\beta(\hbar\Omega_{\mathbf{q}\lambda}) + f_\beta(E_k)}{\hbar\Omega_{\mathbf{q}\lambda} - E_k + i\hbar\omega_n} + \hbar^2 \frac{f_\beta(E_k) - 1 - n_\beta(\hbar\Omega_{\mathbf{q}\lambda})}{\hbar\Omega_{\mathbf{q}\lambda} + E_k - i\hbar\omega_n} \quad (6.24)$$

Note also that  $Y_1(-\hbar\Omega_{\mathbf{q}\lambda}, E_k, \omega_n) = (Y_1(\hbar\Omega_{\mathbf{q}\lambda}, -E_k, \omega_n))^*$  and thus

$$I_s(\hbar\Omega_{\mathbf{q}\lambda}, E_k, \omega_n) = Y_1(\hbar\Omega_{\mathbf{q}\lambda}, E_k, \omega_n) - (Y_1(\hbar\Omega_{\mathbf{q}\lambda}, -E_k, \omega_n))^* . \quad (6.25)$$

**Singlet SC in the KS System** If we disregard triplet SC and non-collinear magnetism as discussed in the Subsection 3.5.1, inserting the corresponding KS GF Eq. (5.42) modifies the Eqs. (6.17) - (6.20) to

$$\bar{\Sigma}_{\text{ph } i\sigma j\sigma'}^{\text{KS}1,1}(\omega_n) = \delta_{\sigma\sigma'} \sum_{\mathbf{q}\lambda k k'l} g_{ik\sigma}^{\lambda\mathbf{q}} g_{k'l\sigma}^{\lambda-\mathbf{q}} (u_{l\sigma}^k u_{l\sigma}^{k'*} I_s(\hbar\Omega_{\mathbf{q}\lambda}, E_{l\sigma}, \omega_n) + v_{l\sigma}^{k*} v_{l\sigma}^{k'} I_s(\hbar\Omega_{\mathbf{q}\lambda}, -E_{l,-\sigma}, \omega_n)) \quad (6.26)$$

$$\bar{\Sigma}_{\text{ph } i\sigma j\sigma'}^{\text{KS}1,-1}(\omega_n) = -\delta_{\sigma,-\sigma'} \sum_{\mathbf{q}\lambda k k'l} g_{ik\sigma}^{\lambda\mathbf{q}} g_{j'k',-\sigma}^{\lambda-\mathbf{q}} (u_{l\sigma}^k v_{l-\sigma}^{k'*} I_s(\hbar\Omega_{\mathbf{q}\lambda}, E_{l\sigma}, \omega_n) + v_{l\sigma}^{k*} u_{l-\sigma}^{k'} I_s(\hbar\Omega_{\mathbf{q}\lambda}, -E_{l-\sigma}, \omega_n)) \quad (6.27)$$

$$\bar{\Sigma}_{\text{ph } i\sigma j\sigma'}^{\text{KS}-1,1}(\omega_n) = -\delta_{\sigma,-\sigma'} \sum_{\mathbf{q}\lambda k k'l} g_{ki\sigma}^{\lambda\mathbf{q}} g_{j'k',-\sigma}^{\lambda-\mathbf{q}} (v_{l\sigma}^k u_{l-\sigma}^{k'*} I_s(\hbar\Omega_{\mathbf{q}\lambda}, E_{l-\sigma}, \omega_n) + u_{l\sigma}^{k*} v_{l-\sigma}^{k'} I_s(\hbar\Omega_{\mathbf{q}\lambda}, -E_{l\sigma}, \omega_n)) \quad (6.28)$$

$$\bar{\Sigma}_{\text{ph } i\sigma j\sigma'}^{\text{KS}-1,-1}(\omega_n) = \delta_{\sigma\sigma'} \sum_{\mathbf{q}\lambda k k'l} g_{ki\sigma}^{\lambda\mathbf{q}} g_{j'k',\sigma}^{\lambda-\mathbf{q}} (v_{l\sigma}^k v_{l\sigma}^{k'*} I_s(\hbar\Omega_{\mathbf{q}\lambda}, E_{l-\sigma}, \omega_n) + u_{l\sigma}^{k*} u_{l\sigma}^{k'} I_s(\hbar\Omega_{\mathbf{q}\lambda}, -E_{l\sigma}, \omega_n)) . \quad (6.29)$$

**SDA** Furthermore, assuming the SDA, Subsection 3.5.2, with the corresponding form of the KS GF given in Eq. (5.43), the Eqs. (6.17) - (6.20) reduce to

$$\bar{\Sigma}_{\text{ph } i\sigma j\sigma'}^{\text{KS}1,1}(\omega_n) = \delta_{\sigma\sigma'} \sum_{\mathbf{q}\lambda k\alpha} g_{ik\sigma}^{\lambda\mathbf{q}} g_{j\sigma}^{\lambda-\mathbf{q}} |u_{k\sigma}^{k\alpha}|^2 I_s(\hbar\Omega_{\mathbf{q}\lambda}, E_{k\sigma}^\alpha, \omega_n) \quad (6.30)$$

$$\bar{\Sigma}_{\text{ph } i\sigma j\sigma'}^{\text{KS}1,-1}(\omega_n) = -\delta_{\sigma,-\sigma'} \sum_{\mathbf{q}\lambda k\alpha} g_{ik\sigma}^{\lambda\mathbf{q}} g_{j,-k,-\sigma}^{\lambda-\mathbf{q}} u_{k\sigma}^{k\alpha} (v_{k-\sigma}^{-k\alpha})^* I_s(\hbar\Omega_{\mathbf{q}\lambda}, E_{k\sigma}^\alpha, \omega_n) \quad (6.31)$$

$$\bar{\Sigma}_{\text{ph } i\sigma j\sigma'}^{\text{KS}-1,1}(\omega_n) = -\delta_{\sigma,-\sigma'} \sum_{\mathbf{q}\lambda k\alpha} g_{ki\sigma}^{\lambda\mathbf{q}} g_{-k,j,-\sigma}^{\lambda-\mathbf{q}} (u_{k\sigma}^{k\alpha})^* v_{k-\sigma}^{-k\alpha} I_s(\hbar\Omega_{\mathbf{q}\lambda}, -E_{k\sigma}^\alpha, \omega_n) \quad (6.32)$$

$$\bar{\Sigma}_{\text{ph } i\sigma j\sigma'}^{\text{KS}-1,-1}(\omega_n) = \delta_{\sigma\sigma'} \sum_{\mathbf{q}\lambda k\alpha} g_{ki\sigma}^{\lambda\mathbf{q}} g_{j\sigma}^{\lambda-\mathbf{q}} |u_{k\sigma}^{k\alpha}|^2 I_s(\hbar\Omega_{\mathbf{q}\lambda}, -E_{k\sigma}^\alpha, \omega_n) . \quad (6.33)$$

### 6.3.3. Coulomb SE

With the splitting of the effective interaction into dynamic and static parts (compare Sec. 4.2) we find that the matrix elements of the combination vertex, interaction, vertex (see Section 5.2 and especially Fig. 5.1):



$$(6.34)$$

can be computed as

$$\begin{aligned} & \sum_{\alpha_1\alpha'_1} \sum_{\mu\mu'} \langle \Psi_{i\sigma\alpha}^{\text{KS}} | \Gamma^{\text{Coul}} | \Psi_{k\mu\alpha_1}^{\text{KS}} \rangle \langle \Psi_{k\mu\alpha_1}^{\text{KS}} | w(\omega_n - \omega_{n'}) | \Psi_{k'\mu'\alpha'_1}^{\text{KS}} \rangle \langle \Psi_{k'\mu'\alpha'_1}^{\text{KS}} | \Gamma^{\text{Coul}} | \Psi_{j\alpha'\sigma'}^{\text{KS}} \rangle \\ & \equiv \left[ \int_0^\infty \frac{d\omega}{\pi} \left( \frac{2\omega}{(\omega_n - \omega_{n'})^2 + \omega^2} - \frac{2}{\omega} \right) \begin{pmatrix} M_{ikk'j}^{\text{dyn}}(\omega) & -M_{ikjk'}^{\text{dyn}}(\omega) \\ -M_{kik'j}^{\text{dyn}}(\omega) & M_{kijk'}^{\text{dyn}}(\omega) \end{pmatrix} \right]_{\alpha\sigma\alpha'\sigma'} + \\ & + \left[ \begin{pmatrix} W_{ikk'j}^{\text{stat}} & -W_{ikjk'}^{\text{stat}} \\ -W_{kik'j}^{\text{stat}} & W_{kijk'}^{\text{stat}} \end{pmatrix} \right]_{\alpha\sigma\alpha'\sigma'} . \end{aligned} \quad (6.35)$$

For the definition of  $M^{\text{dyn}}$  and  $W^{\text{stat}}$  see Eqs. (4.15) and (4.14), respectively. As discussed before in the Subsection 6.3.1 we do not consider the Nambu-diagonal components of

$\bar{\Sigma}_{\text{Coul } ij}^{\text{KS}}(\omega_n)$  and compute the two non-vanishing spin matrices

$$\begin{aligned} \bar{\Sigma}_{\text{Coul } i\sigma j\sigma'}^{\text{KS } 1,-1}(\omega_n) &= -\sum_{kk'l} \left( \int_0^\infty \frac{d\omega}{\pi} (u_l^{k\sigma} (v_l^{k'\sigma'})^* M_{ikjk'\sigma\sigma'}^{\text{dyn}}(\omega) Y_2(\hbar\omega, E_l, \omega_n) + \right. \\ &\quad \left. + (v_l^{k\sigma})^* u_l^{k'\sigma'} M_{ikjk'\sigma\sigma'}^{\text{dyn}}(\omega) Y_2(\hbar\omega, -E_l, \omega_n) \right) + \\ &\quad \left. + u_l^{k\sigma} (v_l^{k'\sigma'})^* W_{ikjk'\sigma\sigma'}^{\text{stat}} f_\beta(E_l) + (v_l^{k\sigma})^* u_l^{k'\sigma'} W_{ikjk'\sigma\sigma'}^{\text{stat}} f_\beta(-E_l) \right) \end{aligned} \quad (6.36)$$

$$\begin{aligned} \bar{\Sigma}_{\text{Coul } i\sigma j\sigma'}^{\text{KS } -1,1}(\omega_n) &= -\sum_{kk'l} \left( \int_0^\infty \frac{d\omega}{\pi} (v_l^{k\sigma} (u_l^{k'\sigma'})^* M_{kik'j\sigma\sigma'}^{\text{dyn}}(\omega) Y_2(\hbar\omega, E_l, \omega_n) + \right. \\ &\quad \left. + (u_l^{k\sigma})^* v_l^{k'\sigma'} M_{kik'j\sigma\sigma'}^{\text{dyn}}(\omega) Y_2(\hbar\omega, -E_l, \omega_n) \right) + \\ &\quad \left. + v_l^{k\sigma} (u_l^{k'\sigma'})^* W_{kik'j\sigma\sigma'}^{\text{stat}} f_\beta(E_l) + (u_l^{k\sigma})^* v_l^{k'\sigma'} W_{kik'j\sigma\sigma'}^{\text{stat}} f_\beta(-E_l) \right) \end{aligned} \quad (6.37)$$

where

$$Y_2(\hbar\omega, E, \omega_n) = I_s(\hbar\omega, E, \omega_n) - \frac{2\hbar}{\omega} f_\beta(E). \quad (6.38)$$

**Singlet SC in the KS system** Similar as for the phononic SE inserting the singlet KS GF Eq. (5.42) casts the Eqs. (6.36) and (6.37) into

$$\begin{aligned} \bar{\Sigma}_{\text{Coul } i\sigma j\sigma'}^{\text{KS } 1,-1}(\omega_n) &= -\delta_{\sigma,-\sigma'} \sum_{kk'l} \left( \int_0^\infty \frac{d\omega}{\pi} (u_{l\sigma}^k (v_{l-\sigma}^{k'})^* M_{ikjk'\sigma,-\sigma}^{\text{dyn}}(\omega) Y_2(\hbar\omega, E_{l\sigma}, \omega_n) \right. \\ &\quad \left. + (v_{l\sigma}^k)^* u_{l-\sigma}^{k'} M_{ikjk'\sigma,-\sigma}^{\text{dyn}}(\omega) Y_2(\hbar\omega, -E_{l-\sigma}, \omega_n) \right) + \\ &\quad \left. + u_{l\sigma}^k (v_{l-\sigma}^{k'})^* W_{ikjk'\sigma,-\sigma}^{\text{stat}} f_\beta(E_{l\sigma}) + (v_{l\sigma}^k)^* u_{l-\sigma}^{k'} W_{ikjk'\sigma,-\sigma}^{\text{stat}} f_\beta(-E_{l-\sigma}) \right) \end{aligned} \quad (6.39)$$

$$\begin{aligned} \bar{\Sigma}_{\text{Coul } i\sigma j\sigma'}^{\text{KS } -1,1}(\omega_n) &= -\delta_{\sigma,-\sigma'} \sum_{kk'l} \left( \int_0^\infty \frac{d\omega}{\pi} (v_{l\sigma}^k (u_{l-\sigma}^{k'})^* M_{kik'j\sigma,-\sigma}^{\text{dyn}}(\omega) Y_2(\hbar\omega, E_{l-\sigma}, \omega_n) \right. \\ &\quad \left. + (u_{l\sigma}^k)^* v_{l-\sigma}^{k'} M_{kik'j\sigma,-\sigma}^{\text{dyn}}(\omega) Y_2(\hbar\omega, -E_{l\sigma}, \omega_n) \right) + \\ &\quad \left. + v_{l\sigma}^k (u_{l-\sigma}^{k'})^* W_{kik'j\sigma,-\sigma}^{\text{stat}} f_\beta(E_{l-\sigma}) + (u_{l\sigma}^k)^* v_{l-\sigma}^{k'} W_{kik'j\sigma,-\sigma}^{\text{stat}} f_\beta(-E_{l\sigma}) \right) \end{aligned} \quad (6.40)$$

**SDA** Performing the SDA (Section 3.5.2) in the SC KS system results in a further simplified form

$$\begin{aligned} \bar{\Sigma}_{\text{Coul } i\sigma j\sigma'}^{\text{KS } 1,-1}(\omega_n) &= -\delta_{\sigma,-\sigma'} \sum_{k\alpha} u_{k\sigma}^{k\alpha} v_{k-\sigma}^{-k\alpha*} \left( W_{ikj,-k\sigma,-\sigma}^{\text{stat}} f_\beta(E_{k\sigma}^\alpha) + \right. \\ &\quad \left. + \int_0^\infty \frac{d\omega}{\pi} M_{ikj,-k\sigma,-\sigma}^{\text{dyn}}(\omega) Y_2(\hbar\omega, E_{k\sigma}^\alpha, \omega_n) \right) \end{aligned} \quad (6.41)$$

$$\begin{aligned} \bar{\Sigma}_{\text{Coul } i\sigma j\sigma'}^{\text{KS } -1,1}(\omega_n) &= -\delta_{\sigma,-\sigma'} \sum_{k\alpha} u_{k\sigma}^{k\alpha*} v_{k-\sigma}^{-k\alpha} \left( W_{ki,-k,j\sigma,-\sigma}^{\text{stat}} f_\beta(-E_{k\sigma}^\alpha) + \right. \\ &\quad \left. + \int_0^\infty \frac{d\omega}{\pi} M_{ki,-k,j\sigma,-\sigma}^{\text{dyn}}(\omega) Y_2(\hbar\omega, -E_{k\sigma}^\alpha, \omega_n) \right) \end{aligned} \quad (6.42)$$

### 6.3.4. Symmetrized Components of the SE

Note that the Dyson Eq. (5.26) may be written as  $\bar{G} = ((\bar{G}^{\text{KS}})^{-1} + \bar{\Sigma}^s)^{-1}$  so we have to compare the SE with the inverse KS GF and it is beneficial to represent both quantities in the same basis. Because the densities are chosen this way, the obvious basis in spin space are the vectors  $(\sigma_0, \mathbf{S})$

| $a$ | BV               | SE part           | $a$ | BV               | SE part                | $a$ | BV                   | SE part                    | $a$ | BV                      | SE part                    |
|-----|------------------|-------------------|-----|------------------|------------------------|-----|----------------------|----------------------------|-----|-------------------------|----------------------------|
| 1   | $\tau_0\sigma_0$ | $\Sigma_\omega^s$ | 5   | $\tau_z\sigma_0$ | $\Sigma_\varepsilon^s$ | 9   | $\tau_x(i\sigma_y)$  | $\Sigma_{\Im\Delta}^s$     | 13  | $(i\tau_y)(i\sigma_y)$  | $\Sigma_{\Re\Delta}^s$     |
| 2   | $\tau_0\sigma_x$ | $A_{\omega x}$    | 6   | $\tau_z\sigma_x$ | $\Sigma_{J_x}^s$       | 10  | $\tau_x(-\sigma_z)$  | $\Sigma_{\Im\Delta}^{T_x}$ | 14  | $(i\tau_y)(-\sigma_z)$  | $\Sigma_{\Re\Delta}^{T_x}$ |
| 3   | $\tau_0\sigma_y$ | $A_{\omega y}$    | 7   | $\tau_z\sigma_y$ | $\Sigma_{J_y}^s$       | 11  | $\tau_x(-i\sigma_0)$ | $\Sigma_{\Im\Delta}^{T_y}$ | 15  | $(i\tau_y)(-i\sigma_0)$ | $\Sigma_{\Re\Delta}^{T_y}$ |
| 4   | $\tau_0\sigma_z$ | $A_{\omega z}$    | 8   | $\tau_z\sigma_z$ | $\Sigma_J^s$           | 12  | $\tau_x(\sigma_x)$   | $\Sigma_{\Im\Delta}^{T_z}$ | 16  | $(i\tau_y)(\sigma_x)$   | $\Sigma_{\Re\Delta}^{T_z}$ |

Table 6.1.: Basis vector (BV) decomposition of the SE. We index the basis with the label  $a = (1, \dots, 16)$ . Symmetrized terms highlighted with a light red are supposed to vanish for a collinear singlet SC. From the remaining set, yellow highlighted parts break particle-hole symmetry.

and  $\Phi$  on the Nambu diagonal and off diagonal, respectively. For the choice of basis in the Nambu part, we note that from the equation of motion Eq. (5.24) we expect a frequency part  $\propto \tau_0$  and the Hamiltonian, energy part  $\propto \tau_z$ . Recall Subsection 3.4.1 on the Nambu KS Hamiltonian where we noted that the single particle energy is  $\propto \tau_z$  because of the Fermionic nature of the electrons. On the Nambu off-diagonal we choose  $\tau_x$  and  $(i\tau_y)$  because this splits the pair potential into imaginary and real part (compare the final form of the Nambu KS Hamiltonian Eq. (3.99)).

A full description in the non-collinear case requires 16 unit vectors, that we label with  $a = (1\dots 16)$ . They, as well as their corresponding scalar SE part, are given in Table 6.1. Note that the basis vectors as given in Table 6.1 are not normalized to 1. The properly normalized change of basis reads

$$(\text{SE part } a) = \frac{1}{4} \sum_{\alpha\alpha'\sigma\sigma'} (\text{Basis vector } a)_{\sigma\sigma'}^{\alpha\alpha'} (\bar{\Sigma}^{\text{KS}})_{\sigma\sigma'}^{\alpha\alpha'} \quad (6.43)$$

The name of the SE parts is due to their behavior as of parts of the inverse GF. As an example consider the basis vector  $\tau_0\sigma_0$ . The inverse SDA KS GF has a contribution along this direction of  $\delta_{ij}i\hbar\omega_n$  (see Appendix E, Eq. (E.15)) and  $\Sigma_\omega^s$  adds to this Matsubara frequency. The equations for each SE part of Table 6.1 are easily written down with the above Eq. (6.43) and the equations for the SE of the Subsections 6.3.2 and 6.3.3. We save space and do this only later in the thesis in some special cases where the number of terms is significantly reduced.

The SE parts  $A_{w(x,y,z)}$ , if they do not vanish, are certainly an interesting feature. We can interpret them in a way that they act as a spin dependent frequency renormalization which cannot be present in a non-interacting GF, or that they appear in the Hamiltonian as an imbalance of spin transposition. For the latter see the equation for  $\bar{v}_{xc}$  Eq. 5.25 which as a term  $\propto \tau_0(\Re\mathbf{S}) \cdot \mathbf{B}_{xc}$  that results from the spin transposition in the hole channel in going to the Nambu notation (see Subsection 3.4.1). Later, in Chapter 7, we come back to the term  $A_{wz}$  and we will see that it vanishes if the coupling is equal for both spin channels.

Note that the cell color red indicates that its contribution should not be present for a singlet, collinear SC. We find, however, that not all of those terms are indeed zero by construction even though the decoupled SC KS system is singlet and collinear. Whether or not it is correct to drop them is not immediately clear. In the numerical solutions in Chapter 8 we find that their effect is very small. Moreover yellow highlighted terms break particle-hole symmetry (these are all terms behaving as  $\tau_z$ ).

### 6.3.5. The Equation for $\Delta^s$

Using the representation of SE components Eq. (6.43) in the previous Subsection, we can now rewrite Eq. (6.14):

$$\bar{G}^{\text{KS}} \cdot \bar{v}_{xc} \cdot \bar{G}^{\text{KS}} \equiv \sum_a (\text{SE part } a) \bar{G}^{\text{KS}} \cdot (\text{Basis vector } a) \cdot \bar{G}^{\text{KS}}. \quad (6.44)$$

The matrix elements of the pair potential are contained in the term  $\bar{G}^{\text{KS}} \cdot \bar{v}_{\text{xc}} \cdot \bar{G}^{\text{KS}}$ . We want to rewrite this term in order that we have a tensor in singlet/triplet and Nambu space  $\mathfrak{P}$  that satisfies the following equation:

$$\bar{G}^{\text{KS}} \cdot \bar{v}_{\text{xc}} \cdot \bar{G}^{\text{KS}} \equiv \mathfrak{P} \cdot \begin{pmatrix} 0 & \Delta^{\text{s}} \\ \Delta^{\text{s}\dagger} & 0 \end{pmatrix}.$$

This allows to multiply the Sham-Schlüter Eq. (6.44) with the inverse of  $\mathfrak{P}$  (assuming that the inverse exists) from the left and have an explicit equation for the pair potential matrix elements. With the Eqs. (5.72) and (5.74) we identify

$$\begin{aligned} \mathfrak{P}_{kk'\alpha\alpha'}^{ij\alpha_1\alpha'_1} &= \frac{1}{\beta} \sum_n \sum_{\mu\mu'} \sum_{\sigma\sigma'} \bar{G}_{i\alpha\sigma k\mu\alpha_1}^{\text{KS}}(\omega_n) \left( \delta_{\alpha_1,1} \delta_{\alpha'_1,-1} \Phi_{\mu\mu'} + \delta_{\alpha_1,-1} \delta_{\alpha'_1,1} \Phi_{\mu\mu'}^* \right) \otimes \\ &\otimes \left( \delta_{\alpha,1} \delta_{\alpha',-1} \Phi_{\sigma\sigma'}^* + \delta_{\alpha,-1} \delta_{\alpha',1} \Phi_{\sigma\sigma'} \right) \bar{G}_{k'\alpha'_1\mu'j\sigma'\alpha'}^{\text{KS}}(\omega_n). \end{aligned} \quad (6.45)$$

Furthermore, we write the right hand side of Eq. (6.44) as  $\mathfrak{R}$  which is the sum of all 16 basis contributions  $\mathfrak{R}_a$ . Each contribution in turn is a Nambu matrix with singlet/triplet vectors on the off diagonal and  $(\sigma_0, \mathbf{S})$  symmetrized components on the diagonal

$$\begin{aligned} (\mathfrak{R}_a)_{kk'}^{\alpha\alpha'} &\equiv \frac{1}{\beta} \sum_n \sum_{ij} (\text{SE part } a)_{ij}(\omega_n) \sum_{\sigma\sigma'} \left( \delta_{\alpha,1} \delta_{\alpha',1} \begin{pmatrix} \sigma_0 \\ \mathbf{S} \end{pmatrix}_{\sigma\sigma'} + \right. \\ &+ \delta_{\alpha,1} \delta_{\alpha',-1} \Phi_{\sigma\sigma'}^* + \delta_{\alpha,-1} \delta_{\alpha',1} \Phi_{\sigma\sigma'} + \delta_{\alpha,-1} \delta_{\alpha',-1} \begin{pmatrix} \sigma_0 \\ \mathbf{S}^* \end{pmatrix}_{\sigma\sigma'} \left. \right) \times \\ &\times \left[ \bar{G}_{ki}^{\text{KS}}(\omega_n) \cdot (\text{Basis vector } a) \cdot \bar{G}_{jk'}^{\text{KS}}(\omega_n) \right]_{\alpha\sigma\alpha'\sigma'} \end{aligned} \quad (6.46)$$

The calculation of this objects is straight forward but tedious. We do not give the results in this thesis<sup>6</sup>. We summarize in a matrix equation for  $\Delta^{\text{s}}$  in singlet/triplet and KS space

$$\begin{pmatrix} 0 & \Delta^{\text{s}} \\ \Delta^{\text{s}\dagger} & 0 \end{pmatrix} = \mathfrak{P}^{-1} \cdot \sum_a \mathfrak{R}_a. \quad (6.47)$$

If the distinction between  $\Delta^{\text{s}}$  and  $\Delta^{\text{s}\dagger}$  is unimportant, as for example in the SDA ( $\Delta_s^{\text{s}}$  may be chosen real, compare Subsection 3.6.2), it is easier to extract  $\Delta^{\text{s}}$  from the  $(1, -1)$  component of Eq. (6.44) because we have to compute less individual terms. In the following we are mainly concerned with this special case. In earlier work on SCDFE [54, 57] the SSE equivalent to Eq. (6.44) was directly calculated with the GF in the Decoupling Approximation and  $\Delta_s^{\text{s}}$  was extracted from the  $(1, -1)$  component.

## 6.4. SDA: The Gap Equation.

As we have noted in the preceding Subsection 6.3.5 ( $\Delta_s^{\text{s}}$  can be chosen real, see Subsection 3.6.2) that we expect to being able to extract  $\Delta_s^{\text{s}}$  from the  $(1, -1)$  component of the Sham-Schlüter Eq. (6.44). As a preparatory for this Section, in Subsection 6.4.1 we thus further simplify the Sham-Schlüter connection to the  $(1, -1)$  part of Eq. (6.44), relevant for the SDA. Then, in Subsection 6.4.2, we interpret the SSE as an operator that maps  $\Delta_s^{\text{s}}$  to zero. We compute contributions to the operator in the Subsections 6.4.3, 6.4.4 and 6.4.5 before we finalize in the Subsection 6.4.6 with the gap equation of SpinSCDFE.

<sup>6</sup>As part of this work functional contributions beyond the SDA were derived but not implemented in the computer code. Since the expressions are huge and do not benefit clarity we made the decision not to present them here. Moreover the terms calculated are only the parts that add to the  $(1, -1)$  component of the Eq. (6.44).

### 6.4.1. The $(1, -1)$ Part of the SSE

Multiplying out the spin and Nambu matrix on the left hand side of Eq. (6.44),  $\frac{1}{\beta} \sum_n \sum_{kk'} \bar{G}_{ik}^{\text{KS}}(\omega_n) \cdot (\bar{v}_{xc})_{kk'} \cdot \bar{G}_{k'j}^{\text{KS}}(\omega_n)$  we find that the potential is hidden in the terms (using the symbolic notation)  $F^{\text{KS}} \Delta_s^\dagger F^{\text{KS}}$  and  $G^{\text{KS}} \Delta_s G^{\text{KS}\dagger}$ , that we write as

$$\begin{aligned} \sum_{\sigma\sigma'} \Phi_{1\sigma\sigma'}^* \langle \bar{\varphi}_{i\sigma}^* | G^{\text{KS}} \Delta_s G^{\text{KS}\dagger} | \bar{\varphi}_{-i\sigma'} \rangle &\equiv \left( \frac{1}{\beta} \sum_{n\mu\mu'\sigma\sigma'} G_{i\sigma i\mu}^{\text{KS}}(\omega_n) G_{-i\mu' -i\sigma'}^{\text{KS}\dagger}(\omega_n) \Phi_{1\sigma\sigma'}^* \Phi_{1\mu\mu'}^* \right) \Delta_{si}^s \quad (6.48) \\ &\equiv M_{i,-i}^{i,-i} \Delta_{si}^s \quad (6.49) \end{aligned}$$

$$\begin{aligned} \sum_{\sigma\sigma'} \Phi_{1\sigma\sigma'}^* \langle \bar{\varphi}_{i\sigma}^* | F^{\text{KS}} \Delta_s^\dagger F^{\text{KS}} | \bar{\varphi}_{-i\sigma'} \rangle &\equiv \left( \frac{1}{\beta} \sum_{n\mu\mu'\sigma\sigma'} F_{i\sigma -i\mu}^{\text{KS}}(\omega_n) F_{i\mu' -i\sigma'}^{\text{KS}}(\omega_n) \Phi_{1\sigma\sigma'}^* \Phi_{1\mu\mu'} \right) \Delta_{si}^{s*} \quad (6.50) \\ &\equiv M_{-i,i}^{i,-i} \Delta_{si}^{s*} \quad (6.51) \end{aligned}$$

On the right hand side of Eq. (6.44) with the SE diagrams, we distinguish terms involving the Nambu diagonal SE  $\mathfrak{D}_{i,-i}^s$ <sup>7</sup> and the Nambu off diagonal  $\mathfrak{C}_{i,-i}^s$ . According to Table (6.1) these are given by

$$\mathfrak{D}^s \equiv \sum_{a=1,\dots,8} \Phi_1^* \cdot (\text{SE part } a) [\bar{G}^{\text{KS}} \cdot (\text{Basis vector } a) \cdot \bar{G}^{\text{KS}}]_{\alpha=1,\alpha'=-1} \quad (6.52)$$

$$\mathfrak{C}^s \equiv \sum_{a=9,\dots,16} \Phi_1^* \cdot (\text{SE part } a) [\bar{G}^{\text{KS}} \cdot (\text{Basis vector } a) \cdot \bar{G}^{\text{KS}}]_{\alpha=1,\alpha'=-1} \quad (6.53)$$

We arrive at the  $(1, -1)$  part of Eq. (6.44) for  $\Delta^s$  in the SDA

$$M_{i,-i}^{i,-i} \Delta_{si}^s + M_{-i,i}^{i,-i} \Delta_{si}^{s*} = \mathfrak{D}_{i,-i}^s + \mathfrak{C}_{i,-i}^s. \quad (6.54)$$

Note that  $\mathfrak{D}^s$  and  $\mathfrak{C}^s$  have non-vanishing matrix elements  $i, j \neq i, -i$  because the SE is not intrinsically diagonal. Because they would invalidate the SDA, these matrix elements must be dropped. A similar situation is encountered in Chapter 7 where we discuss Many-Body approach. We see that dropping those matrix elements leads to very good results in general. In the next paragraph we give the terms  $\mathfrak{D}^s$  and  $\mathfrak{C}^s$  in more detail, pointing out that half of the contributions are zero.

**$\mathfrak{D}^s$  and  $\mathfrak{C}^s$  in detail** For  $\mathfrak{D}^s$ , we distinguish functional contributions that include only one SE part  $a = 1, \dots, 8$  from the first two columns in Table 6.1. Using  $m \in \{0, x, y, z\}$  these contributions are

$$\begin{aligned} \mathfrak{D}_s^{(\pm, m)} = &\sum_{nkk'} \sum_{\sigma\sigma'} \sum_{\mu\mu'} (\Phi_1^*)_{\sigma\sigma'} \frac{\sigma_{m\mu\mu'}}{4} (\bar{\Sigma}_{k\mu k'\mu'}^{\text{KS}1,1}(\omega_n) \pm \bar{\Sigma}_{k\mu k'\mu'}^{\text{KS}-1,-1}(\omega_n)) \times \\ &\times \left[ (G_{ik}^{\text{KS}}(\omega_n) \cdot \sigma_m \cdot F_{k'j}^{\text{KS}}(\omega_n) \pm F_{ik}^{\text{KS}}(\omega_n) \cdot \sigma_m \cdot G_{k'j}^{\text{KS}\dagger}(\omega_n)) \right]_{\sigma\sigma'} \quad (6.55) \end{aligned}$$

Here  $(\pm, m)$  corresponds to the basis vectors  $a = 1, \dots, 4$   $(+, 0, x, y, z)$  and  $a = 5, \dots, 8$   $(-, 0, x, y, z)$ . For example  $\mathfrak{D}_s^{(+,0)}$  corresponds to  $a = 1$  in Table 6.1, namely the basis vector  $\tau_0\sigma_0$  and SE  $\Sigma_\omega^s$ . Note that  $\mathfrak{D}_s^{(\pm, x, y)}$  are zero. This can be seen first noting that  $F_{kk'}^{\text{KS}}(\omega_n)$  is off diagonal in spin (see Eq. (5.41) and Eq. (5.43)) as well as  $(\Phi_1^*)_{\sigma\sigma'}$ . Then,  $\sigma_m$  must not be purely off diagonal or  $\mathfrak{D}_s^{(\pm, m)}$  is zero. Thus, the only non-vanishing contributions are

$$\mathfrak{D}_{i,-i}^s = \mathfrak{D}_{s i,-i}^{(+,0)} + \mathfrak{D}_{s i,-i}^{(-,0)} + \mathfrak{D}_{s i,-i}^{(+,z)} + \mathfrak{D}_{s i,-i}^{(-,z)} \quad (6.56)$$

<sup>7</sup>The name  $\mathfrak{D}$  refers to earlier work on SCDFT[54], where the Nambu-diagonal phonon contribution was called D Term.



Similarly for  $\mathfrak{C}^s$  ( $m = \{s, tx, ty, tz\}$ ,  $\pm, m$  corresponds to the basis vectors  $a = 9, \dots, 12$  for  $+, s \dots tz$  and  $a = 13, \dots, 16$  for  $-, s \dots tz$  of Table 6.1)

$$\begin{aligned} \mathfrak{C}_{i,-i}^{s(\pm,m)} &= \sum_{nk} \sum_{k'} \sum_{\mu\mu'} \sum_{\sigma\sigma'} (\Phi_1^*)_{\sigma\sigma'} \frac{\Phi_{m\mu\mu'}}{4} (\bar{\Sigma}_{k\mu k'\mu'}^{\text{KS}1,-1}(\omega_n) \pm \bar{\Sigma}_{k\mu k'\mu'}^{\text{KS}-1,1}(\omega_n)) \times \\ &\times \left[ (G_{ik}^{\text{KS}}(\omega_n) \cdot \Phi_m \cdot G_{k'j}^{\text{KS}\dagger}(\omega_n) \pm F_{ik}^{\text{KS}}(\omega_n) \cdot \Phi_m \cdot F_{k'j}^{\text{KS}}(\omega_n)) \right]_{\sigma\sigma'} \end{aligned} \quad (6.57)$$

where we note along the same lines that  $\mathfrak{C}_{i,-i}^{s(\pm,m)}$  is zero for  $m = ty, tz$  and

$$\mathfrak{C}_{i,-i}^s = \mathfrak{C}_{i,-i}^{s(+,s)} + \mathfrak{C}_{i,-i}^{s(-,s)} + \mathfrak{C}_{i,-i}^{s(+,tx)} + \mathfrak{C}_{i,-i}^{s(-,tx)}. \quad (6.58)$$

We evaluate the formulas for  $M, M', \mathfrak{D}_{i,-i}^s$  and  $\mathfrak{C}_{i,-i}^s$  in the Subsections 6.4.3, 6.4.4 and 6.4.5 after introducing the Sham-Schlüter operator in Subsection 6.4.2.

### 6.4.2. The Sham-Schlüter Operator

Within the SDA we use the  $u, v$  and  $E$  representation because it is more convenient. Note that we could also write the equations in terms of  $\Delta_{si}^s$  directly. This is fundamentally different from the case before introducing the SDA where  $u, v$  and  $E$  are numerical solutions of the KSBdG equations. The explicit dependence on the potential extends to the diagram contributions  $\mathfrak{D}_{i,-i}^s$  and  $\mathfrak{C}_{i,-i}^s$  so there is no uniquely defined way to solve the SSE for the potential  $\Delta_s^s$  because all appearing terms equally depend on  $\Delta_s^s$ . We define the Sham-Schlüter operator  $S_\beta^s$  that is the result of all contributions to the SSE (6.54) written to one side of the equation and pulling out  $\Delta_s^s$ . This operator is a non-linear functional of the potential  $\Delta_s^s$

$$S_\beta[\Delta_s^s] \cdot \Delta_s^s = 0 \quad (6.59)$$

As contributions to  $S_\beta$  we distinguish  $S_\beta^M$  that is due to  $M_{i,-i}^{i,-i} \Delta_{si}^s + M_{-i,i}^{i,-i} \Delta_{si}^{s*}$  and  $S_\beta^{\mathfrak{D}}$  that is due to  $\mathfrak{D}_{i,-i}^s$ , only including phonon contributions because the Coulomb diagrams have been removed from the Nambu diagonal (see the discussion at the beginning of Section 6.3). In turn  $S_\beta^{\mathfrak{C}} = S_{\text{ph}\beta}^{\mathfrak{C}} + S_{\text{Coul}\beta}^{\text{stat}\mathfrak{C}} + S_{\text{Coul}\beta}^{\text{dyn}\mathfrak{C}}$  is due to  $\mathfrak{C}_{i,-i}^s$  which has phononic and static and dynamic Coulomb contributions.

### 6.4.3. Functional Contribution $M$ and $M'$

Within the SDA the terms Eqs. (6.49) and (6.51) are straight forward to calculate using the components of the KS GF in the SDA Eq. (5.43) and the analytic Matsubara summation given in the Appendix D. The results are

$$M_{i,-i}^{i,-i} = \sum_{\sigma\alpha\alpha'} |u_{i\sigma}^{i\alpha}|^2 |v_{i-\sigma}^{-i\alpha'}|^2 P_s(E_{i\sigma}^\alpha, E_{i\sigma}^{\alpha'}) \quad (6.60)$$

$$M_{-i,i}^{i,-i} = \sum_{\sigma\alpha\alpha'} u_{i\sigma}^{i\alpha} (v_{i-\sigma}^{-i\alpha})^* u_{i\sigma}^{i\alpha'} (v_{i-\sigma}^{-i\alpha'})^* P_s(E_{i\sigma}^\alpha, E_{i\sigma}^{\alpha'}) \quad (6.61)$$

After a little algebra we find

$$M_{-i,i}^{i,-i} \Delta_{si}^{s*} = \Delta_{si}^s \sum_{\sigma\alpha\alpha'} \text{sign}(\alpha') \text{sign}(\alpha) |u_{i\sigma}^{i\alpha}|^2 |v_{i-\sigma}^{-i\alpha'}|^2 P_s(E_{i\sigma}^\alpha, E_{i\sigma}^{\alpha'}). \quad (6.62)$$

<sup>8</sup>The subscript  $\beta$  represents the temperature dependence of  $S_\beta$ .

The disappearance of  $\Delta_{s_i}^{s*}$  reflects the fact that  $\Delta_{s_i}^s$  can be chosen real and thus the  $(1, -1)$  component of the SSE contains all information. We introduce  $S_{\beta ij}^M = -(M_{i,-i}^{i,-i} + M_{-i,i}^{i,-i} \frac{\Delta_{s_i}^{s*}}{\Delta_{s_i}^s}) \delta_{ij}$  that multiplies  $\Delta_{s_i}^s$  on the left hand side of the SSE (6.54)

$$S_{\beta ij}^M = -\delta_{ij} \sum_{\sigma} \left( \frac{(\varepsilon_{i\sigma} + \varepsilon_{-i-\sigma})^2}{|E_{i\sigma}^+ - E_{i\sigma}^-|^2} P_s(E_{i\sigma}^+, E_{i\sigma}^-) + 2|u_{i\sigma}^{i+}|^2 |v_{i-\sigma}^{-i+}|^2 (P_s(E_{i\sigma}^+, E_{i\sigma}^+) + P_s(E_{i\sigma}^-, E_{i\sigma}^-)) \right). \quad (6.63)$$

#### 6.4.4. Functional Contribution $\mathfrak{D}^s$

Evaluating the equation (6.56) is straight forward: We use 1) the KS GF in the SDA Eq. (5.43) 2) the Nambu diagonal SE parts Eqs. (6.30) and (6.33) and 3) use the analytic Matsubara summations of the Appendix D. We obtain

$$\begin{aligned} \mathfrak{D}_{i,-i}^s &= \frac{1}{2} \sum_{\mathbf{q}\lambda} \sum_{k\mu\sigma} \sum_{\alpha_1\alpha_2\alpha_3} (1 + \text{sign}(\mu)\text{sign}(\sigma)) \frac{\text{sign}(\alpha_3)\Delta_{s_i}^s}{|E_{i\sigma}^+ - E_{i\sigma}^-|} (|u_{i\sigma}^{i\alpha_1}|^2 |u_{k\mu}^{k\alpha_2}|^2 g_{ik\mu}^{\lambda\mathbf{q}} g_{ki\mu}^{\lambda-\mathbf{q}} \\ &+ |v_{k-\mu}^{-k\alpha_2}|^2 |v_{i-\sigma}^{-i\alpha_1}|^2 g_{-k,-i,-\mu}^{\lambda\mathbf{q}} g_{-i,-k,-\mu}^{\lambda-\mathbf{q}}) L(\Omega_{\mathbf{q}\lambda}, E_{i\sigma}^{\alpha_1}, E_{k\mu}^{\alpha_2}, E_{i\sigma}^{\alpha_3}) \end{aligned} \quad (6.64)$$

The Matsubara integral  $L$ , together with symmetries and various limiting cases, is given in Appendix D. We see  $(1 + \text{sign}(\mu)\text{sign}(\sigma)) = 2\delta_{\sigma\mu}$  and introduce  $S_{\beta ij}^{\mathfrak{D}} = \delta_{ij} \mathfrak{D}_{i,-i}^s / \Delta_{s_i}^s$  with the result

$$\begin{aligned} S_{\beta ij}^{\mathfrak{D}} &= \delta_{ij} \sum_{\mathbf{q}\lambda} \sum_{k\sigma} \sum_{\alpha_1\alpha_2\alpha_3} \frac{\text{sign}(\alpha_3)}{|E_{i\sigma}^+ - E_{i\sigma}^-|} (|u_{i\sigma}^{i\alpha_1}|^2 |u_{k\sigma}^{k\alpha_2}|^2 g_{ik\sigma}^{\lambda\mathbf{q}} g_{ki\sigma}^{\lambda-\mathbf{q}} + \\ &+ |v_{k-\sigma}^{-k\alpha_2}|^2 |v_{i-\sigma}^{-i\alpha_1}|^2 g_{-k,-i,-\sigma}^{\lambda\mathbf{q}} g_{-i,-k,-\sigma}^{\lambda-\mathbf{q}}) L(\Omega_{\mathbf{q}\lambda}, E_{i\sigma}^{\alpha_1}, E_{k\sigma}^{\alpha_2}, E_{i\sigma}^{\alpha_3}) \end{aligned} \quad (6.65)$$

For later use we also mention the formula if we drop the contributions of the second column in Table 6.1, i.e. exclude SE contributions behaving as  $\tau_z^9$

$$\mathfrak{D}_{i,-i}^{\text{PHS}} = \mathfrak{D}_{s i,-i}^{(+,0)} + \mathfrak{D}_{s i,-i}^{(+,z)}, \quad (6.66)$$

which leads to

$$\begin{aligned} S_{\beta ij}^{\mathfrak{D}^{\text{PHS}}} &= \frac{1}{2} \delta_{ij} \sum_{\mathbf{q}\lambda} \sum_{k\sigma} \sum_{\alpha_1\alpha_2\alpha_3} \frac{\text{sign}(\alpha_3)}{|E_{i\sigma}^+ - E_{i\sigma}^-|} \left( (|u_{i\sigma}^{i\alpha_1}|^2 |u_{k\sigma}^{k\alpha_2}|^2 g_{ik\sigma}^{\lambda\mathbf{q}} g_{ki\sigma}^{\lambda-\mathbf{q}} + \right. \\ &+ |v_{k-\sigma}^{-k\alpha_2}|^2 |v_{i-\sigma}^{-i\alpha_1}|^2 g_{-k,-i,-\sigma}^{\lambda\mathbf{q}} g_{-i,-k,-\sigma}^{\lambda-\mathbf{q}}) L(\Omega_{\mathbf{q}\lambda}, E_{i\sigma}^{\alpha_1}, E_{k\sigma}^{\alpha_2}, E_{i\sigma}^{\alpha_3}) + \\ &+ (|u_{i\sigma}^{i\alpha_1}|^2 |u_{k\sigma}^{k\alpha_2}|^2 g_{ki\sigma}^{\lambda\mathbf{q}} g_{ik\sigma}^{\lambda-\mathbf{q}} + \\ &+ |v_{k-\sigma}^{-k\alpha_2}|^2 |v_{i-\sigma}^{-i\alpha_1}|^2 g_{-i,-k,-\sigma}^{\lambda\mathbf{q}} g_{-k,-i,-\sigma}^{\lambda-\mathbf{q}}) L(\Omega_{\mathbf{q}\lambda}, E_{i\sigma}^{\alpha_1}, -E_{k\sigma}^{\alpha_2}, E_{i\sigma}^{\alpha_3}) \left. \right). \end{aligned} \quad (6.67)$$

#### 6.4.5. Functional Contribution $\mathfrak{C}^s$

We evaluate the Eq. (6.58) separately for the Coulomb and phonon terms along the lines of Subsection (6.4.4). This means we use 1) the KS GF in the SDA Eq. (5.43) 2) the Nambu off diagonal SE parts (phonon) Eqs. (6.31) and (6.32) or (Coulomb) Eqs. (6.41) and (6.42) and 3) use the analytic Matsubara summations of the Appendix D. For brevity we directly give the results in terms of the Sham-Schlüter operator  $S_{\beta}^{\mathfrak{C}}$ .

<sup>9</sup>The name is chosen with a superscript PHS that indicates Particle-Hole Symmetric.

**Phonon Part** We arrive at

$$S_{\text{ph}\beta kk'}^{\mathfrak{e}} = -\sum_{\mathbf{q}\lambda\sigma\alpha_1\alpha_2\alpha_3} \frac{g_{kk'\sigma}^{\lambda\mathbf{q}} g_{-k,-k',-\sigma}^{\lambda-\mathbf{q}}}{\text{sign}(\alpha_2) |E_{k'\sigma}^+ - E_{k'\sigma}^-|} \left( |u_{k\sigma}^{k\alpha_1}|^2 |v_{k-\sigma}^{-k\alpha_3}|^2 + u_{k\sigma}^{k\alpha_1} v_{k-\sigma}^{-k\alpha_1*} u_{k\sigma}^{k\alpha_3} v_{k-\sigma}^{-k\alpha_3*} \frac{\Delta_{sk'}^{s*}}{\Delta_{sk'}} \right) L(\Omega_{\mathbf{q}\lambda}, E_{k\sigma}^{\alpha_1}, E_{k'\sigma}^{\alpha_2}, E_{k\sigma}^{\alpha_3}). \quad (6.68)$$

Here we have included intermediate triplet contributions  $\mathfrak{C}_{i,-i}^{s(+,tx)}$  and  $\mathfrak{C}_{i,-i}^{s(-,tx)}$  into to the functional. Whether this is sensible is not immediately clear, but we will see in Chapter 8 that the differences are tiny. For a further discussion we also mention the result if  $\mathfrak{C}_{\text{ph}\beta,-i}^{s(\pm,tx)}$  is dropped (note a sum over spin  $\mu$  that is not present in Eq. (6.68)), that reads

$$S_{\text{ph}\beta kk'}^{s\mathfrak{e}} = -\frac{1}{2} \sum_{\mathbf{q}\lambda\sigma\mu\alpha_1\alpha_2\alpha_3} \frac{g_{kk'\mu}^{\lambda\mathbf{q}} g_{-k,-k',-\mu}^{\lambda-\mathbf{q}}}{\text{sign}(\alpha_2) |E_{k'\mu}^+ - E_{k'\mu}^-|} \left( |u_{k\sigma}^{k\alpha_1}|^2 |v_{k-\sigma}^{-k\alpha_3}|^2 + u_{k\sigma}^{k\alpha_1} v_{k-\sigma}^{-k\alpha_1*} u_{k\sigma}^{k\alpha_3} v_{k-\sigma}^{-k\alpha_3*} \frac{\Delta_{sk'}^{s*}}{\Delta_{sk'}} \right) L(\Omega_{\mathbf{q}\lambda}, E_{k\sigma}^{\alpha_1}, E_{k'\mu}^{\alpha_2}, E_{k\sigma}^{\alpha_3}). \quad (6.69)$$

**Coulomb part** The approach for the Coulomb part is very similar. We note that with the symmetry of Eq. (4.17) we may write it as

$$S_{\text{Coul}\beta kk'}^{\text{stat}\mathfrak{e}} = -\sum_{\sigma} \sum_{\alpha_1\alpha_2\alpha_3} \frac{\text{sign}(\alpha_2)}{|E_{k'\sigma}^+ - E_{k'\sigma}^-|} \left( |u_{k\sigma}^{k\alpha_1}|^2 |v_{k-\sigma}^{-k\alpha_3}|^2 W_{kk',-k,-k'\sigma,-\sigma}^{\text{stat}} + u_{k\sigma}^{k\alpha_1} v_{k-\sigma}^{-k\alpha_1*} u_{k\sigma}^{k\alpha_3} v_{k-\sigma}^{-k\alpha_3*} \frac{\Delta_{sk'}^{s*}}{\Delta_{sk'}} W_{kk',-k,-k'\sigma,-\sigma}^{\text{stat}} \right) L_W(E_{k\sigma}^{\alpha_1}, E_{k'\sigma}^{\alpha_2}, E_{k\sigma}^{\alpha_3}) \quad (6.70)$$

$$S_{\text{Coul}\beta kk'}^{\text{dyn}\mathfrak{e}} = -\int_0^\infty \frac{d\omega}{\pi} \sum_{\sigma} \sum_{\alpha_1\alpha_2\alpha_3} \frac{\text{sign}(\alpha_2)}{|E_{k'\sigma}^+ - E_{k'\sigma}^-|} \left( |u_{k\sigma}^{k\alpha_1}|^2 |v_{k-\sigma}^{-k\alpha_3}|^2 M_{kk',-k,-k'\sigma,-\sigma}^{\text{dyn}}(\omega) + u_{k\sigma}^{k\alpha_1} v_{k-\sigma}^{-k\alpha_1*} u_{k\sigma}^{k\alpha_3} v_{k-\sigma}^{-k\alpha_3*} \frac{\Delta_{sk'}^{s*}}{\Delta_{sk'}} M_{kk',-k,-k'\sigma,-\sigma}^{\text{dyn}}(\omega) \right) L_M(\omega, E_{k\sigma}^{\alpha_1}, E_{k'\sigma}^{\alpha_2}, E_{k\sigma}^{\alpha_3}). \quad (6.71)$$

The functions  $L_M$  and  $L_W$  are also defined in the Appendix D. Dropping intermediate triplet parts we obtain  $S_{\text{Coul}\beta kk'}^{\text{stat}s\mathfrak{e}}$  and  $S_{\text{Coul}\beta kk'}^{\text{dyn}s\mathfrak{e}}$  which features a spin sum similar to Eq. (6.69).

### 6.4.6. The Gap Equation

Collecting the terms we write Eq. (6.59) as

$$S_\beta[\Delta_s^s] \cdot \Delta_s^s = \sum_{k'} (S_\beta^{\text{M}} + S_\beta^{\text{D}} + S_{\text{ph}\beta kk'}^{\mathfrak{e}} + S_{\text{Coul}\beta kk'}^{\text{stat}\mathfrak{e}} + S_{\text{Coul}\beta kk'}^{\text{dyn}\mathfrak{e}}) \Delta_{sk'}^s = 0. \quad (6.72)$$

One common method to solve a non-linear equation of this type is to use an invertible splitting matrix  $B_{kk'}$ . Doing so, we arrive at the non-linear gap equation of SpinSCDFT

$$0 = (S_\beta^{\text{M}} + S_\beta^{\text{D}} + S_{\text{ph}\beta}^{\mathfrak{e}} + S_{\text{Coul}\beta}^{\text{stat}\mathfrak{e}} + S_{\text{Coul}\beta}^{\text{dyn}\mathfrak{e}} + B - B) \cdot \Delta_s^s \quad (6.73)$$

$$\Delta_s^s = B^{-1} \cdot (S_\beta^{\text{M}} + S_\beta^{\text{D}} + S_{\text{ph}\beta}^{\mathfrak{e}} + S_{\text{Coul}\beta}^{\text{stat}\mathfrak{e}} + S_{\text{Coul}\beta}^{\text{dyn}\mathfrak{e}} + B) \cdot \Delta_s^s \quad (6.74)$$

Taking  $B = -S_\beta^{\text{M}}$  leads directly to the earlier SCDFT gap equation [21, 57, 54] in the spin degenerate limit. In fact, in all earlier work on SCDFT the problem was interpreted directly in this fix-point formulation with fixed  $B = -S_\beta^{\text{M}}$ . The best choice for  $B$  makes the spectrum of the

non-linear operator  $B^{-1} \cdot (S_\beta^{\text{M}} + S_\beta^{\text{D}} + S_{\text{ph}\beta}^{\text{e}} + S_{\text{Coul}\beta}^{\text{stat}\text{e}} + S_{\text{Coul}\beta}^{\text{dyn}\text{e}} + B)$  the most contracting [58], i.e. all its eigenvalues  $|\lambda_i[\Delta_s^{\text{s}}]| \ll 1$  which ensures a quick convergence to the fixed point that poses the solution to the SSE. Bad choices may prevent to find the solution even if it exists. Note that one may always solve the fixed point problem with the inverse operator  $\Delta_s^{\text{s}} = S_\beta \cdot \Delta_s^{\text{s}} \Leftrightarrow S_\beta^{-1} \cdot \Delta_s^{\text{s}} = \Delta_s^{\text{s}}$ . Thus,  $|\lambda_i[\Delta_s^{\text{s}}]| \gg 1$  is also a good choice in this sense.

## 6.5. The Linearized Gap Equation

From the BCS model Chapter 2 we know that for large magnetic fields the SC transition is of first order, so an arbitrarily small solution for the SC order parameter  $\chi$  does not exist. In this regime a linearization does not lead to meaningful results.

Given that we are in a regime where the SC transition is second order,  $\chi$  vanishes continuously when approaching the critical temperature. We have to investigate whether this continuous vanishing of  $\chi$  translates into a continuous vanishing of  $\Delta_s^{\text{s}}$ . We find this to be true, mathematically, in Subsection 6.5.1 although for a finite magnetic field the dependence of  $\chi_s$  on  $\Delta_s^{\text{s}}$  becomes weak at the Fermi level. Still we conclude that we can compute  $T_c$  from the small  $\Delta_s^{\text{s}}$  limit of  $S_\beta$  in a fairly large regime. It is important to study the linear equation because, numerically and analytically, it is much simpler. That is of tremendous value not only in the implementation where one has to compare to previous results that were almost all obtained from a linear equation.

We discuss in Subsection 6.5.2 how the main ingredient to the non-linear Sham-Schlüter operator  $S_\beta$  of Eq. (6.59) the  $|u_{k\sigma}^{k\alpha}|^2$ ,  $|v_{k-\sigma}^{-k\alpha}|^2$  and  $E_{k\sigma}^\alpha$  behave in the small  $\Delta_s^{\text{s}}$  limit.

Then, in Subsection 6.5.3 we report the small  $\Delta_s^{\text{s}}$  limits of the individual terms in Eq. (6.72) that contribute to  $S_\beta$ .

### 6.5.1. Implication Small $\chi_s(\mathbf{r}, \mathbf{r}')$ to Small $\Delta_{si}^{\text{s}}$

Consider the connection density to potential (easily derived in the SDA with the use of Eq. (3.132) and Eq. (3.128))

$$\chi_s(\mathbf{r}, \mathbf{r}') = \sum_{i\sigma} \Delta_{si}^{\text{s}} \frac{f_\beta(E_{i\sigma}^+) - f_\beta(E_{i\sigma}^-)}{|E_{i\sigma}^+ - E_{i\sigma}^-|} \varphi_i(\mathbf{r}\sigma) \varphi_{-i}(\mathbf{r}', -\sigma) \quad (6.75)$$

To conclude a continuous vanishing of  $\Delta_{si}^{\text{s}}$  we need to show  $\frac{f_\beta(E_{i\sigma}^+) - f_\beta(E_{i\sigma}^-)}{|E_{i\sigma}^+ - E_{i\sigma}^-|} \neq 0$  independent of  $\Delta_{si}^{\text{s}}$ . This is shown with  $A = \frac{\varepsilon_{i\sigma} - \varepsilon_{-i-\sigma}}{2}$  and  $B = \sqrt{\left(\frac{\varepsilon_{i\sigma} + \varepsilon_{-i-\sigma}}{2}\right)^2 + |\Delta_{si}^{\text{s}}|^2} \geq 0$ . Then  $\frac{f_\beta(E_{i\sigma}^+) - f_\beta(E_{i\sigma}^-)}{|E_{i\sigma}^+ - E_{i\sigma}^-|}$  reads

$$\frac{f_\beta(A+B) - f_\beta(A-B)}{2B} = -\frac{\tanh(\beta B)}{2B} \left( \frac{\cosh(\beta B)}{\cosh(\beta B) + \cosh(\beta A)} \right) < 0 \quad B \neq 0 \quad (6.76)$$

and, second, we find

$$\lim_{B \rightarrow 0} \frac{f_\beta(A+B) - f_\beta(A-B)}{2B} = -\frac{\beta}{2} \frac{1}{\cosh(\beta A)} < 0 \quad \text{q.e.d.} \quad (6.77)$$

We may simplify the search for  $T_c$  to the condition that the matrix  $S_\beta[\Delta_s^{\text{s}} = 0]$  of Eq. (6.59) be singular in the regime where the transition is of second order. We note a problem that for  $A > B$  and sufficiently low temperatures where  $\beta A \gg 1$  the translation  $\lim_{|\Delta| \rightarrow 0} \rightarrow \lim_{|\chi| \rightarrow 0}$  will become at least numerically problematic since  $\frac{f_\beta(E_{i\sigma}^+) - f_\beta(E_{i\sigma}^-)}{|E_{i\sigma}^+ - E_{i\sigma}^-|}$  is exponentially small in the regime

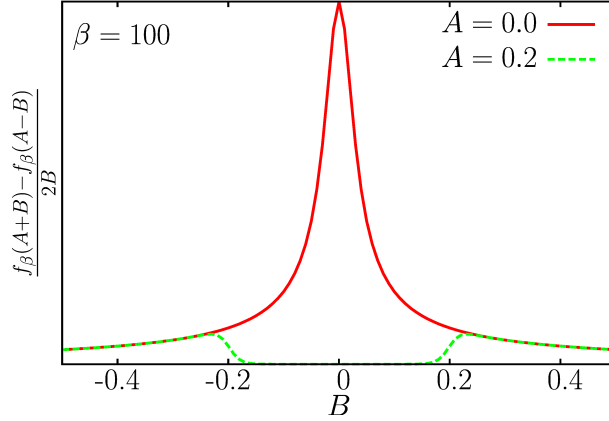


Figure 6.1.: Sketch of the function  $\frac{f_\beta(A+B) - f_\beta(A-B)}{2B}$  multiplying  $\Delta_{s_i}^s$  into the coefficients for  $\chi_s(\mathbf{r}, \mathbf{r}')$ .

$E_{i\sigma}^+ - E_{i\sigma}^- \approx 0$ , i.e. numerically zero. We sketch the function in Fig. 6.1. In the zero temperature limit the function approaches zero in the  $B \ll A$  region. This can cause fundamental problems because for a finite magnetic field the density depends only weakly on the value of  $\Delta_{s_i}^s$  at the Fermi level.

### 6.5.2. Small $\Delta_s^s$ Behavior of $|u_{k\sigma}^{k\alpha}|^2$ , $|v_{k-\sigma}^{-k\alpha}|^2$ and $E_{k\sigma}^\alpha$

Note that for a straight forward solution we should expand all quantities in the absolute value of that gap, because properties as  $E_{k\mu}^\alpha$  are not analytic in  $\Delta_s^s$  and thus not expandable in the complex sense. As an example we see that the Bogoliubov eigenvalue behaves as

$$E_{k\sigma}^\alpha = \frac{\varepsilon_{k\sigma} - \varepsilon_{-k-\sigma}}{2} + \text{sign}(\alpha) \left| \frac{\varepsilon_{k\sigma} + \varepsilon_{-k-\sigma}}{2} \right| + \frac{\text{sign}(\alpha) 2 |\Delta_{sk}^s|^2}{|\varepsilon_{k\sigma} + \varepsilon_{-k-\sigma}|} + \mathcal{O}\left(\frac{8 |\Delta_{sk}^s|^4}{|\varepsilon_{k\sigma} + \varepsilon_{-k-\sigma}|^3}\right) \quad (6.78)$$

This points out another problem with the series of  $E_{k\sigma}^\alpha$  in  $|\Delta_{sk}^s|$  when  $|\varepsilon_{k\sigma} + \varepsilon_{-k-\sigma}| \leq |\Delta_{sk}^s|$  which is the result of the convergence limitations of the Taylor series for the square root. Note however that the  $k$  space region where the series fails becomes arbitrary small at the critical temperature where by assumption  $|\Delta_{sk}^s| \rightarrow 0$ . We use the notation of Marques [54]: Linearized terms are given with a breve on top for example

$$\breve{E}_{k\sigma}^\alpha = \frac{\varepsilon_{k\sigma} - \varepsilon_{-k-\sigma}}{2} + \text{sign}(\alpha) \left| \frac{\varepsilon_{k\sigma} + \varepsilon_{-k-\sigma}}{2} \right|. \quad (6.79)$$

Then

$$\lim_{|\Delta_{sk}^s| \rightarrow 0} |u_{k\sigma}^{k\alpha}|^2 = \frac{\left| \frac{\varepsilon_{k\sigma} + \varepsilon_{-k-\sigma}}{2} + \text{sign}(\alpha) \left| \frac{\varepsilon_{k\sigma} + \varepsilon_{-k-\sigma}}{2} \right| \right|}{|\varepsilon_{k\sigma} + \varepsilon_{-k-\sigma}|} = \delta_{\alpha, \text{sign}(\varepsilon_{k\sigma} + \varepsilon_{-k-\sigma})} \quad (6.80)$$

$$\lim_{|\Delta_{sk}^s| \rightarrow 0} |v_{k-\sigma}^{-k\alpha}|^2 = \lim_{|\Delta_{sk}^s| \rightarrow 0} \frac{|E_{k\sigma}^\alpha - \varepsilon_{k\sigma}|}{|E_{k\sigma}^+ - E_{k\sigma}^-|} = \delta_{\alpha, -\text{sign}(\varepsilon_{k\sigma} + \varepsilon_{-k-\sigma})}. \quad (6.81)$$

If we evaluate  $\breve{E}_{k\sigma}^{\pm \text{sign}(\varepsilon_{k\sigma} + \varepsilon_{-k-\sigma})} = \frac{\varepsilon_{k\sigma} - \varepsilon_{-k-\sigma}}{2} \pm \frac{\varepsilon_{k\sigma} + \varepsilon_{-k-\sigma}}{2}$  we obtain either  $\varepsilon_{k\sigma}$  for + or  $-\varepsilon_{-k-\sigma}$  for -. Also we see that

$$\lim_{|\Delta_{sk}^s| \rightarrow 0} |u_{k\sigma}^{k\alpha}|^2 |v_{k-\sigma}^{-k\alpha}|^2 = \lim_{|\Delta_{sk}^s| \rightarrow 0} u_{k\sigma}^{k\alpha} v_{k-\sigma}^{-k\alpha*} = 0 \quad (6.82)$$

### 6.5.3. The Linear Sham-Schlüter Operator

Using the symmetry  $\Delta_{si}^s \equiv \Delta_{si,-i}^s = \Delta_{s-i,i}^s \equiv \Delta_{s-i}^s$  implied by the singlet symmetry (which means we may take  $i \rightarrow -i$  also in terms multiplying it without changing  $\Delta_{si}^s$ ) we find

$$\check{S}_{\beta ij}^M = -2\delta_{ij}P_s(\varepsilon_{i\uparrow}, -\varepsilon_{-i\downarrow}) \quad (6.83)$$

Using Eq. (6.65) and a bit of algebra we obtain

$$\begin{aligned} \check{S}_{\beta ij}^{\mathcal{D}} &= \frac{2\delta_{ij}}{\varepsilon_{i\uparrow} + \varepsilon_{-i\downarrow}} \sum_{\mathbf{q}\lambda k} \left( g_{ik\uparrow}^{\lambda\mathbf{q}} g_{ki\uparrow}^{\lambda-\mathbf{q}} (L(\Omega_{\mathbf{q}\lambda}, \varepsilon_{i\uparrow}, \varepsilon_{k\uparrow}, \varepsilon_{i\uparrow}) - L(\Omega_{\mathbf{q}\lambda}, \varepsilon_{i\uparrow}, \varepsilon_{k\uparrow}, -\varepsilon_{-i\downarrow})) \right. \\ &\quad \left. + g_{-k,-i\downarrow}^{\lambda\mathbf{q}} g_{-i,-k\downarrow}^{\lambda-\mathbf{q}} (L(\Omega_{\mathbf{q}\lambda}, \varepsilon_{-i\downarrow}, \varepsilon_{-k\downarrow}, \varepsilon_{-i\downarrow}) - L(\Omega_{\mathbf{q}\lambda}, \varepsilon_{-i\downarrow}, \varepsilon_{-k\downarrow}, -\varepsilon_{i\uparrow})) \right). \end{aligned} \quad (6.84)$$

Because  $L(\Omega_{\mathbf{q}\lambda}, \varepsilon_1, \varepsilon_2, \varepsilon_1) \sim \frac{1}{\varepsilon_2}$  only the state (or energy) dependence of the coupling matrix elements guaranties the convergence of the summation over  $k$ . To avoid the full, state dependent  $g_{kk'\sigma}^{\lambda\mathbf{q}}$ , we impose the particle-hole symmetrized term

$$\begin{aligned} \check{S}_{\beta kk'}^{\text{PHS}} &= \frac{\delta_{kk'}}{\varepsilon_{k\uparrow} + \varepsilon_{-k\downarrow}} \sum_{\mathbf{q}\lambda l} \left( g_{kl\uparrow}^{\lambda\mathbf{q}} g_{lk\uparrow}^{\lambda-\mathbf{q}} (L(\Omega_{\mathbf{q}\lambda}, \varepsilon_{k\uparrow}, \varepsilon_{l\uparrow}, \varepsilon_{k\uparrow}) + L(\Omega_{\mathbf{q}\lambda}, \varepsilon_{k\uparrow}, -\varepsilon_{l\uparrow}, \varepsilon_{k\uparrow}) \right. \\ &\quad \left. - L(\Omega_{\mathbf{q}\lambda}, \varepsilon_{k\uparrow}, \varepsilon_{l\uparrow}, -\varepsilon_{-k\downarrow}) - L(\Omega_{\mathbf{q}\lambda}, \varepsilon_{k\uparrow}, -\varepsilon_{l\uparrow}, -\varepsilon_{-k\downarrow}) \right) + \\ &\quad + g_{-k,-l\downarrow}^{\lambda\mathbf{q}} g_{-l,-k\downarrow}^{\lambda-\mathbf{q}} (L(\Omega_{\mathbf{q}\lambda}, \varepsilon_{-k\downarrow}, \varepsilon_{-l\downarrow}, \varepsilon_{-k\downarrow}) + L(\Omega_{\mathbf{q}\lambda}, \varepsilon_{-k\downarrow}, -\varepsilon_{-l\downarrow}, \varepsilon_{-k\downarrow}) \\ &\quad \left. - L(\Omega_{\mathbf{q}\lambda}, \varepsilon_{-k\downarrow}, \varepsilon_{-l\downarrow}, -\varepsilon_{k\uparrow}) - L(\Omega_{\mathbf{q}\lambda}, \varepsilon_{-k\downarrow}, -\varepsilon_{-l\downarrow}, -\varepsilon_{k\uparrow}) \right) \end{aligned} \quad (6.85)$$

This way, even when the state or energy dependence of the coupling matrix elements  $g_{kk'\sigma}^{\lambda\mathbf{q}}$  is not considered we always encounter  $L(\Omega_{\mathbf{q}\lambda}, \varepsilon_1, \varepsilon_2, \varepsilon_3) + L(\Omega_{\mathbf{q}\lambda}, \varepsilon_1, -\varepsilon_2, \varepsilon_3) \sim \frac{1}{A+\varepsilon_2} + \frac{1}{A-\varepsilon_2} \sim \frac{1}{\varepsilon_2}$  which means  $\check{S}_{\beta kk'}^{\text{PHS}}$  depends locally on the electronic structure about  $\varepsilon_2 \approx 0$ . While due to the special selection of SE contributions we have symmetrized the “inner” energy ( $l$ , that is summed) of the term we may try also to particle-hole symmetrizing the “outer” energy dependence  $k$ . We achieve this simply by averaging  $\check{S}_{\beta kk'}^{\text{PHS}}$  with itself where we substitute  $\varepsilon_{k\uparrow} \rightarrow -\varepsilon_{-k\downarrow}$  and  $\varepsilon_{-k\downarrow} \rightarrow -\varepsilon_{k\uparrow}$ . The result is<sup>10</sup>

$$\begin{aligned} \check{S}_{\beta kk'}^{\text{TPHS}} &= \frac{1}{2} \sum_{\mathbf{q}\lambda l} \frac{\delta_{kk'}}{\varepsilon_{k\uparrow} + \varepsilon_{-k\downarrow}} \left( g_{kl\uparrow}^{\lambda\mathbf{q}} g_{lk\uparrow}^{\lambda-\mathbf{q}} (L(\Omega_{\mathbf{q}\lambda}, \varepsilon_{k\uparrow}, \varepsilon_{l\uparrow}, \varepsilon_{k\uparrow}) + L(\Omega_{\mathbf{q}\lambda}, \varepsilon_{k\uparrow}, -\varepsilon_{l\uparrow}, \varepsilon_{k\uparrow}) \right. \\ &\quad \left. + L(\Omega_{\mathbf{q}\lambda}, \varepsilon_{-k\downarrow}, -\varepsilon_{l\uparrow}, \varepsilon_{-k\downarrow}) + L(\Omega_{\mathbf{q}\lambda}, \varepsilon_{-k\downarrow}, \varepsilon_{l\uparrow}, \varepsilon_{-k\downarrow}) \right) \\ &\quad + g_{-k,-l\downarrow}^{\lambda\mathbf{q}} g_{-l,-k\downarrow}^{\lambda-\mathbf{q}} (L(\Omega_{\mathbf{q}\lambda}, \varepsilon_{-k\downarrow}, \varepsilon_{-l\downarrow}, \varepsilon_{-k\downarrow}) + L(\Omega_{\mathbf{q}\lambda}, \varepsilon_{-k\downarrow}, -\varepsilon_{-l\downarrow}, \varepsilon_{-k\downarrow}) \\ &\quad \left. + L(\Omega_{\mathbf{q}\lambda}, \varepsilon_{k\uparrow}, -\varepsilon_{-l\downarrow}, \varepsilon_{k\uparrow}) + L(\Omega_{\mathbf{q}\lambda}, \varepsilon_{k\uparrow}, \varepsilon_{-l\downarrow}, \varepsilon_{k\uparrow}) \right) \end{aligned} \quad (6.86)$$

Now we turn our attention to the linearization of the  $S_{\beta}^e$  terms. With Eq. (6.68) and (6.69) we obtain

$$\check{S}_{\text{ph}\beta kk'}^e = -2 \sum_{\mathbf{q}\lambda} \frac{g_{kk'\uparrow}^{\lambda\mathbf{q}} g_{-k,-k'\downarrow}^{\lambda-\mathbf{q}}}{|\varepsilon_{k'\uparrow} + \varepsilon_{-k'\downarrow}|} (L(\Omega_{\mathbf{q}\lambda}, \varepsilon_{k\uparrow}, \check{E}_{k'\uparrow}^+ - \varepsilon_{-k\downarrow}) + L(\Omega_{\mathbf{q}\lambda}, \varepsilon_{-k\downarrow}, \check{E}_{-k'\downarrow}^+ - \varepsilon_{k\uparrow})) \quad (6.87)$$

and explicitly dropping intermediate triplet parts we find changing  $k' \rightarrow -k'$

$$\begin{aligned} \check{S}_{\text{ph}\beta kk'}^{se} &= - \sum_{\mathbf{q}\lambda} \left( \frac{g_{kk'\uparrow}^{\lambda\mathbf{q}} g_{-k,-k'\downarrow}^{\lambda-\mathbf{q}}}{|\varepsilon_{k'\uparrow} + \varepsilon_{-k'\downarrow}|} (L(\Omega_{\mathbf{q}\lambda}, \varepsilon_{k\uparrow}, \check{E}_{k'\uparrow}^+ - \varepsilon_{-k\downarrow}) - L(\Omega_{\mathbf{q}\lambda}, \varepsilon_{k\uparrow}, \check{E}_{k'\uparrow}^- - \varepsilon_{-k\downarrow})) \right. \\ &\quad \left. + \frac{g_{-k,k'\uparrow}^{\lambda\mathbf{q}} g_{k,-k'\downarrow}^{\lambda-\mathbf{q}}}{|\varepsilon_{k'\uparrow} + \varepsilon_{-k'\downarrow}|} (L(\Omega_{\mathbf{q}\lambda}, \varepsilon_{-k\downarrow}, \check{E}_{k'\uparrow}^+ - \varepsilon_{k\uparrow}) - L(\Omega_{\mathbf{q}\lambda}, \varepsilon_{-k\downarrow}, \check{E}_{k'\uparrow}^- - \varepsilon_{k\uparrow})) \right) \end{aligned} \quad (6.88)$$

<sup>10</sup>The “T” in “TPHS” stands for totally particle hole symmetrized.

To save space we limit the discussion to the unmodified Coulomb interaction, i.e. we allow for triplet SE parts. The static Coulomb interaction of Eq. (6.70) similarly becomes

$$\check{S}_{\text{Coul}\beta kk'}^{\text{stat}\mathcal{E}} = -2W_{kk',-k,-k'\uparrow,\downarrow}^{\text{stat}} P_s(\check{E}_{k'\uparrow}^+, -\check{E}_{-k'\downarrow}^+) P_s(\varepsilon_{k\uparrow}, -\varepsilon_{-k\downarrow}) \quad (6.89)$$

Due to the factorization of the Matsubara sum and the symmetry  $P_s(E_1, E_2) = P_s(-E_1, -E_2)$  this term remains unchanged by dropping triplet terms except that we average  $\frac{1}{2}(W_{kk',-k,-k'\uparrow,\downarrow}^{\text{stat}} + W_{-k,k',k,-k'\uparrow,\downarrow}^{\text{stat}})$ . By similarity to the phonon part we, obtain the dynamic Coulomb contribution

$$\check{S}_{\text{Coul}\beta kk'}^{\text{dyn}\mathcal{E}} = -2 \int_0^\infty d\omega \frac{M_{kk',-k,-k'\uparrow,\downarrow}^{\text{dyn}}(\omega)}{\pi |\varepsilon_{k'\uparrow} + \varepsilon_{-k'\downarrow}|} (L_M(\omega, \varepsilon_{k\uparrow}, \check{E}_{k'\uparrow}^+ - \varepsilon_{-k\downarrow}) + L_M(\omega, \varepsilon_{-k\downarrow}, \check{E}_{-k'\downarrow}^+ - \varepsilon_{k\uparrow})) \quad (6.90)$$

The linearized SSE (Eq. (6.72)) takes the shape

$$\check{S}_\beta \cdot \Delta_s^s = 0. \quad (6.91)$$

Which means  $\Delta_s^s$  is the right eigenfunction to a singular eigenvalue at the SC critical temperature. Thus,  $T_c$  may be computed from the condition  $\det \check{S}_\beta = 0$ .

## 6.6. Isotropization of SpinSCDFT Equations.

As compared to an equivalent Many-Body calculation, SCDFT is numerically not very demanding, in particular in the linear approximation. Still, in many cases it is found that the pair potential matrix elements  $\Delta_{sk}^s$  depend on the the Bloch vector  $\mathbf{k}$  mostly through the energy of the state  $\varepsilon_k$  they refer to. Assuming this feature from the beginning is the so called isotropic approximation. This further reduces the numerical effort and allows systematic studies of the behavior of the theory. Most of our numerical results are obtained in the isotropic approximation. In the Subsection (6.6.1) we define the isotropic approximation in detail together with an isotropization procedure and apply it to our non-linear and linear Sham-Schlüter operators Eqs. (6.72) and (6.91) in the Subsections 6.6.2 and 6.6.3, respectively.

### 6.6.1. The Isotropization Procedure

As mentioned in the introduction to this Section, often  $\Delta_{sk}^s$  depend on the the Bloch vector  $\mathbf{k}$  only through the energy of the state  $\varepsilon_k$  they refer to. We can make this formally an exact property by averaging the quantity, here namely  $\Delta_{sk}^s$  on the equal energy surface. This approximation is referred to as the isotropic approximation. Sometimes, however we need to split certain regions in  $k$  space, i.e. we group  $\Delta_{sk}^s$  belonging to a certain region in the unit cell and band and allow the gapfunction to depend on the specific region as well as the energy. If a we need to separate regions in  $k$  space to obtain a better critical temperature we call the system a **multiband** superconductor. A famous example is  $\text{MgB}_2$  [59].

The goal of an isotropization, i.e. averaging the gapfunction on a certain set, is that the Sham-Schlüter operators becomes numerically cheaper to compute. For this it is necessary to average the interaction matrix elements independently on a selected set of  $k$ . This way the rest of the kernel depends neither on  $k$  nor on  $k'$  any more. In order that the isotropization does not invalidate the result, we have to assume that the anisotropic gap does not vary much within the set selected for averaging. Clearly the latter will be an implicit assumption in many realistic cases as we try to avoid the more demanding anisotropic calculation. Taking a look at the SpinSCDFT formulas in the SDA (for example the Bogoliubov eigenvalues Eqs. (3.155)

to (3.156) or the inverse KS GF Eq. (E.15)), we find that quantities depend on  $\frac{\varepsilon_{k\uparrow} + \varepsilon_{-k\downarrow}}{2}$  and  $\frac{\varepsilon_{k\uparrow} - \varepsilon_{-k\downarrow}}{2}$ . Thus we define

$$\varrho(\varepsilon, J) = \sum_k \delta\left(\frac{\varepsilon_{k\uparrow} + \varepsilon_{-k\downarrow}}{2} - \varepsilon\right) \delta\left(\frac{\varepsilon_{k\uparrow} - \varepsilon_{-k\downarrow}}{2} - J\right) \quad (6.92)$$

$$\begin{aligned} \hat{I}_{k\sigma}(\varepsilon, J)A_{k,\sigma} &= \frac{1}{\varrho(\varepsilon, J)} \sum_k \delta\left(\frac{\varepsilon_{\text{sign}(\sigma)k\uparrow} + \varepsilon_{-\text{sign}(\sigma)k\downarrow}}{2} - \varepsilon\right) \times \\ &\times \delta\left(\frac{\varepsilon_{\text{sign}(\sigma)k\uparrow} - \varepsilon_{-\text{sign}(\sigma)k\downarrow}}{2} - J\right) A_{k,\sigma}, \end{aligned} \quad (6.93)$$

for arbitrary  $A_{k,\sigma}$ . We shall refer to the DOS like quantity  $\varrho(\varepsilon, J)$  as the **double DOS**, since it involves the product of two delta functions and represents the number of states with center of energy  $\varepsilon$  and energy splitting  $J$ . Correspondingly the operator  $\hat{I}_{k\sigma}(\varepsilon, J)$  averages quantities that depend on  $(k, \sigma)$  on shells of equal center-of-energy between two spin channels  $\frac{\varepsilon_{k\uparrow} + \varepsilon_{-k\downarrow}}{2}$  and their difference, the splitting  $\frac{\varepsilon_{k\uparrow} - \varepsilon_{-k\downarrow}}{2}$ . We call  $\hat{I}_{k\sigma}(\varepsilon, J)$  the **isotropization operator**. The result (image) of this operator does not depend on  $k$  and the index is merely a reminder on which variable the operator acts. Note that we have included  $\text{sign}(\sigma)$  into the sign of the  $k$  vectors. The advantage is best seen from the following example

$$A_\sigma(\varepsilon, J) \equiv \hat{I}_{k\sigma}(\varepsilon, J)A_{k,\sigma} = \frac{1}{\varrho(\varepsilon, J)} \left\{ \sum_k \delta\left(\frac{\varepsilon_{k\uparrow} + \varepsilon_{-k\downarrow}}{2} - \varepsilon\right) \delta\left(\frac{\varepsilon_{k\uparrow} - \varepsilon_{-k\downarrow}}{2} - J\right) A_{k,\uparrow} \quad \sigma = \uparrow \right. \\ \left. \sum_k \delta\left(\frac{\varepsilon_{-k\uparrow} + \varepsilon_{k\downarrow}}{2} - \varepsilon\right) \delta\left(\frac{\varepsilon_{-k\uparrow} - \varepsilon_{k\downarrow}}{2} - J\right) A_{k,\downarrow} \quad \sigma = \downarrow \right. \quad (6.94)$$

Note here

$$\begin{aligned} &\sum_k \delta\left(\frac{\varepsilon_{-k\uparrow} + \varepsilon_{k\downarrow}}{2} - \varepsilon\right) \delta\left(\frac{\varepsilon_{-k\uparrow} - \varepsilon_{k\downarrow}}{2} - J\right) A_{k,\downarrow} \\ &\equiv \sum_{-k} \delta\left(\frac{\varepsilon_{k\uparrow} + \varepsilon_{-k\downarrow}}{2} - \varepsilon\right) \delta\left(\frac{\varepsilon_{k\uparrow} - \varepsilon_{-k\downarrow}}{2} - J\right) A_{-k,\downarrow}. \end{aligned} \quad (6.95)$$

Thus  $A_\downarrow(\varepsilon, J)$  is the time-reversed of  $A_\uparrow(\varepsilon, J)$  and it was  $\text{sign}(\sigma)$  that preserved that symmetry in the most general case. If  $A_{k,\sigma}$  turns out to be time reversely symmetric, the choice becomes particularly handy because the resulting  $A(\varepsilon, J)$  is then independent of spin. Let us average the SSE (Eq. (6.72)) in the SDA which we write here as

$$0 = \int d\varepsilon' \int dJ' \sum_{k'} \delta\left(\frac{\varepsilon_{\text{sign}(\sigma')k'\uparrow} + \varepsilon_{-\text{sign}(\sigma')k'\downarrow}}{2} - \varepsilon'\right) \delta\left(\frac{\varepsilon_{\text{sign}(\sigma')k'\uparrow} - \varepsilon_{-\text{sign}(\sigma')k'\downarrow}}{2} - J'\right) S_{\beta_{kk'}} \Delta_{sk'}^s \quad (6.96)$$

Being a sum of different spin channels,  $S_{\beta_{kk'}}$  does not depend on spin. The isotropization procedure defined in Eq. (6.93) means to treat every spin summand of  $S_{\beta_{kk'}}$  according to its spin polarization. Applying the isotropization of  $k$  in addition to  $k'$  we obtain the isotropic SSE

$$0 = \int d\varepsilon' \int dJ' S_\beta(\varepsilon, J, \varepsilon', J') \Delta_s^s(\varepsilon', J') \quad (6.97)$$

with

$$S_\beta(\varepsilon, J, \varepsilon', J') = \hat{I}_{k\sigma}(\varepsilon, J) \varrho(\varepsilon', J') \hat{I}_{k'\sigma'}(\varepsilon', J') S_{\beta_{kk'}}. \quad (6.98)$$

We introduce the notation

$$\mathbf{e} \equiv (\varepsilon, J) \quad \int d\mathbf{e} \equiv \int d\varepsilon \int dJ \quad \delta(\mathbf{e} - \mathbf{e}') \equiv \delta(\varepsilon - \varepsilon') \delta(J - J'). \quad (6.99)$$

If we want to allow for multiband SC we simply extend  $\mathbf{e}$  with an additional isotropic-band index.



### 6.6.2. Non-Linear, Isotropic Sham-Schlüter Operator

In this Subsection we give the isotropic variant of the non-linear Sham-Schlüter operator Eq. (6.72). Its main ingredient are the expansion coefficient combinations  $|u_{i\sigma}^{i\alpha}|^2$ ,  $|v_{i-\sigma}^{-i\alpha}|^2$  and the Bogoliubov eigenvalues  $E_{i\sigma}^\alpha$  so we cast them into the isotropic formulation. For brevity we define

$$F(\mathbf{e}) = \sqrt{\varepsilon^2 + |\Delta_s^s(\mathbf{e})|^2}. \quad (6.100)$$

Now, consider the isotropization of

$$|u_{i\sigma}^{i\alpha}|^2 = \frac{\sqrt{(\frac{\varepsilon_{i\sigma} + \varepsilon_{-i-\sigma}}{2})^2 + |\Delta_{si}^s|^2} + \text{sign}(\alpha) \frac{\varepsilon_{i\sigma} + \varepsilon_{-i-\sigma}}{2}}{2\sqrt{(\frac{\varepsilon_{i\sigma} + \varepsilon_{-i-\sigma}}{2})^2 + |\Delta_{si}^s|^2}} \quad u^2(\mathbf{e}) = \frac{F(\mathbf{e}) + \varepsilon}{2F(\mathbf{e})} \quad (6.101)$$

$$|v_{i-\sigma}^{-i\alpha}|^2 = \frac{\sqrt{(\frac{\varepsilon_{i\sigma} + \varepsilon_{-i-\sigma}}{2})^2 + |\Delta_{si}^s|^2} - \text{sign}(\alpha) \frac{\varepsilon_{i\sigma} + \varepsilon_{-i-\sigma}}{2}}{2\sqrt{(\frac{\varepsilon_{i\sigma} + \varepsilon_{-i-\sigma}}{2})^2 + |\Delta_{si}^s|^2}} \quad v^2(\mathbf{e}) = \frac{F(\mathbf{e}) - \varepsilon}{2F(\mathbf{e})}. \quad (6.102)$$

First Eq. (B.18) in the Appendix provided us with the identity  $|u_{i\sigma}^{i\alpha}|^2 = |u_{-i-\sigma}^{-i\alpha}|^2 = |v_{i-\sigma}^{-i\alpha}|^2 = |v_{-i-\sigma}^{-i\alpha}|^2$  so with the Isotropization procedure Eq. (6.93) we obtain

$$\begin{aligned} \hat{I}_{i\sigma}(\mathbf{e})|u_{i\sigma}^{i+}|^2 &= u^2(\mathbf{e}) & \hat{I}_{i\sigma}(\mathbf{e})|v_{i-\sigma}^{-i+}|^2 &= v^2(\mathbf{e}) \\ \hat{I}_{i\sigma}(\mathbf{e})|u_{i\sigma}^{i-}|^2 &= v^2(\mathbf{e}) & \hat{I}_{i\sigma}(\mathbf{e})|v_{i-\sigma}^{-i-}|^2 &= u^2(\mathbf{e}). \end{aligned} \quad (6.103)$$

Moreover Eq. (B.16) results in

$$\hat{I}_{i\sigma}(\mathbf{e})u_{i\sigma}^{i\alpha*}v_{i-\sigma}^{-i\alpha} = \hat{I}_{i\sigma}(\mathbf{e})\frac{\text{sign}(\alpha)\Delta_{si}^{s*}}{\text{sign}(\sigma)|E_{i\sigma}^+ - E_{i\sigma}^-|} = \frac{\text{sign}(\sigma)\Delta_s^s(\mathbf{e})}{\text{sign}(\alpha)2F(\mathbf{e})}. \quad (6.104)$$

Also

$$\hat{I}_{i\sigma}(\mathbf{e})E_{i\sigma}^\alpha = E_\sigma^\alpha(\mathbf{e}) \quad E_\sigma^\alpha(\mathbf{e}) = \text{sign}(\sigma)J + \text{sign}(\alpha)F(\mathbf{e}), \quad (6.105)$$

and we drop the indication of the energy and splitting dependence in  $\Delta_s^s, E_\sigma^\alpha, F, u^2$  and  $v^2$ . We further see  $\frac{\Delta_s^s}{2F} = \sqrt{u^2v^2}$  and we can cast the full  $|\Delta_s^s|$  dependence back into  $u^2$  and  $v^2$ .

**Kernel Contribution  $S_\beta^M$**  In Eq. (6.63) we found an expression for the term  $S_\beta^M$  multiplying the KS potential. Isotropization according to Eq. (6.98) is done according to

$$\hat{I}_{k\sigma}(\mathbf{e})\varrho(\mathbf{e}')\hat{I}_{k'\sigma'}(\mathbf{e}')\delta_{kk'}\delta_{\sigma\sigma'}A_{k\sigma} = \delta(\mathbf{e}' - \mathbf{e})\hat{I}_{k\sigma}(\mathbf{e})A_{k\sigma} \quad (6.106)$$

$$\hat{I}_{k\sigma}(\mathbf{e})\varrho(\mathbf{e}')\hat{I}_{k'\sigma'}(\mathbf{e}')\delta_{k,-k'}\delta_{\sigma,-\sigma'}A_{k\sigma} = \delta(\mathbf{e}' - \mathbf{e})\hat{I}_{k\sigma}(\mathbf{e})A_{k\sigma} \quad (6.107)$$

which is clear from the definition Eq. (6.93). Thus with  $E_+^+ = -E_+^-$   $S_\beta^M$  of Eq. (6.63) is cast into

$$S_\beta^M(\mathbf{e}, \mathbf{e}') = -2\delta(\mathbf{e}' - \mathbf{e})\left(\frac{\varepsilon^2}{F^2}P_s(E_+^+, E_+^-) + 2u^2v^2(P_s(E_+^+, E_+^+) + P_s(E_+^-, E_+^-))\right). \quad (6.108)$$

**Kernel Contribution  $S_\beta^D$**  Here we have to average the phononic coupling. Without the simplifications that come with time-reversal symmetry, it turns out that the to-be-averaged matrix elements are different for the Nambu-diagonal and off-diagonal. We introduce the generalized Eliashberg function

$$\alpha^2 F_\sigma^D(\mathbf{e}, \mathbf{e}', \omega) = \hat{I}_{k\sigma}(\mathbf{e})\varrho(\mathbf{e}')\hat{I}_{k'\sigma'}(\mathbf{e}')\sum_{\lambda\mathbf{q}}g_{\text{sign}(\sigma)k, \text{sign}(\sigma)k'}^{\lambda\mathbf{q}}g_{\text{sign}(\sigma)k', \text{sign}(\sigma)k, \sigma}^{\lambda-\mathbf{q}}\delta(\Omega_{\mathbf{q}\lambda} - \omega). \quad (6.109)$$

The name  $\alpha^2 F_\sigma^D$  is a combined symbol and stems from the phonon coupling which is sometimes called  $\alpha$  and the density of states of the phonons named  $F$ . As it always appears in the above combination the standard notation of phononic coupling is  $\alpha^2 F(\omega)$  where one usually takes the coupling averaged on the Fermi surface only. Here we have introduced the spin-splitting generalization but in a similar manner we often consider only the frequency dependence. As discussed this requires the Matsubara sum to provide a cutoff for the appearing integrals which means we should take the particle-hole symmetric variant  $S_\beta^{\text{PHS}}$  in this approximation. Now starting from Eq. (6.65) it is straight forward to find its isotropic variant. We obtain with the notation  $u''^2 \equiv u^2(\mathbf{e}'')$

$$S_\beta^{\text{D}}(\mathbf{e}, \mathbf{e}') = \delta(\mathbf{e}' - \mathbf{e}) \int d\mathbf{e}'' \int d\omega \sum_{\sigma\alpha_1\alpha_2} \frac{\alpha^2 F_\sigma^D(\mathbf{e}, \mathbf{e}'', \omega)}{\text{sign}(\alpha_1)F} (u^2 \delta_{\alpha_1,1} + v^2 \delta_{\alpha_1,-1}) (u''^2 \delta_{\alpha_2,1} + v''^2 \delta_{\alpha_2,-1}) (L(\omega, E_\sigma^{\alpha_1}, E_\sigma^{\prime\alpha_2}, E_\sigma^{\alpha_1}) - L(\omega, E_\sigma^{\alpha_1}, E_\sigma^{\prime\alpha_2}, E_\sigma^{-\alpha_1})). \quad (6.110)$$

The particle-hole symmetrized version of Eq. (6.67) translates into a similar equation

$$S_\beta^{\text{PHS}}(\mathbf{e}, \mathbf{e}') = \delta(\mathbf{e}' - \mathbf{e}) \int d\mathbf{e}'' \int d\omega \sum_{\sigma\alpha_1\alpha_2\alpha_3} \frac{\alpha^2 F_\sigma^D(\mathbf{e}, \mathbf{e}'', \omega)}{2\text{sign}(\alpha_3)F} (u^2 \delta_{\alpha_1,1} + v^2 \delta_{\alpha_1,-1}) (u''^2 \delta_{\alpha_2,1} + v''^2 \delta_{\alpha_2,-1}) (L(\omega, E_\sigma^{\alpha_1}, E_\sigma^{\prime\alpha_2}, E_\sigma^{\alpha_3}) + L(\omega, E_\sigma^{\alpha_1}, -E_\sigma^{\prime\alpha_2}, E_\sigma^{\alpha_3})). \quad (6.111)$$

**Kernel Contribution  $S_\beta^{\text{C}}$**  For the phonon coupling on the Nambu off diagonal we meet with terms as

$$\alpha^2 F(\mathbf{e}, \mathbf{e}', \omega) = \hat{I}_{k\mu}(\mathbf{e}) \varrho(\mathbf{e}') \hat{I}_{k'\mu}(\mathbf{e}') \sum_{\lambda\mathbf{q}} g_{kk'\mu}^{\lambda\mathbf{q}} g_{-k,-k',-\mu}^{\lambda-\mathbf{q}} \delta(\Omega_{\mathbf{q}\lambda} - \omega) \quad (6.112)$$

That the result does not depend on  $\mu$  is due to the special definition of the isotropization procedure Eq. (6.93). We obtain directly from Eq. (6.68)

$$S_{\text{ph}\beta}^{\text{C}}(\mathbf{e}, \mathbf{e}') = - \int d\omega \sum_{\alpha_1\alpha_3} \frac{\alpha^2 F(\mathbf{e}, \mathbf{e}', \omega)}{2F'} \left( (u^2 \delta_{\alpha_1,1} + v^2 \delta_{\alpha_1,-1}) (u^2 \delta_{\alpha_3,-1} + v^2 \delta_{\alpha_3,1}) + \text{sign}(\alpha_1) \text{sign}(\alpha_3) u^2 v^2 \frac{\Delta_s^{s'*}}{\Delta_s^{s'}} \right) \sum_{\sigma\alpha_2} \text{sign}(\alpha_2) L(\omega, E_\sigma^{\alpha_1}, E_\sigma^{\alpha_2'}, E_\sigma^{\alpha_3}) \quad (6.113)$$

With a similar definition of the Coulomb coupling

$$C^{\text{stat}}(\mathbf{e}, \mathbf{e}') = \hat{I}_{k\sigma}(\mathbf{e}) \varrho(\mathbf{e}') \hat{I}_{k'\sigma'}(\mathbf{e}') (W_{kk',-k,-k',\sigma,-\sigma}^{\text{stat}})^* \quad (6.114)$$

$$C^{\text{dyn}}(\mathbf{e}, \mathbf{e}', \omega) = \hat{I}_{k\sigma}(\mathbf{e}) \varrho(\mathbf{e}') \hat{I}_{k'\sigma'}(\mathbf{e}') (M_{kk',-k,-k',\sigma,-\sigma}^{\text{dyn}}(\omega))^* \quad (6.115)$$

We obtain first for the static part

$$S_{\text{Coul}\beta}^{\text{stat}\text{C}}(\mathbf{e}, \mathbf{e}') = - \sum_{\alpha_1\alpha_2} C^{\text{stat}}(\mathbf{e}, \mathbf{e}') \left( (u^2 \delta_{\alpha_1,1} + v^2 \delta_{\alpha_1,-1}) (u^2 \delta_{\alpha_2,1} + v^2 \delta_{\alpha_2,-1}) + \text{sign}(\alpha_1) \text{sign}(\alpha_2) u^2 v^2 \frac{\Delta_s^{s'*}}{\Delta_s^{s'}} \right) \sum_{\sigma} P_s(E_\sigma^{\alpha_1}, E_\sigma^{\alpha_2}) P_s(E_\sigma^{\alpha_1'}, E_\sigma^{\alpha_2'}) \quad (6.116)$$

and for the dynamic part  $S_{\text{Coul}\beta}^{\text{dyn}\text{C}}$  we obtain the same equation as Eq. (6.113) except that  $\alpha^2 F$  is replaced by  $C^{\text{dyn}}$  and  $L$  with  $L_M$  of Eq. (D.21). We do not discuss the pure singlet term, we just mention that it involves a coupling term that behaves as  $g_{-kk'\mu}^{\lambda\mathbf{q}} g_{k,-k',-\mu}^{\lambda-\mathbf{q}}$  which leads to the same  $\alpha^2 F$  of Eq. (6.112).

### 6.6.3. Linearized, Isotropic Sham-Schlüter Operator

The linearized isotropic equations for the Sham-Schlüter operator contributions can be obtained in two equivalent ways. First, taking the small  $|\Delta_s^s|$  limit of Subsection 6.6.2 or, second, applying the isotropization procedure to the linearized anisotropic equations of subsection 6.5.3. For the latter it is important that

$$\varepsilon_{\text{sign}(\sigma)i\sigma} = \frac{\varepsilon_{i\uparrow} + \varepsilon_{-i\downarrow}}{2} + \text{sign}(\sigma) \frac{\varepsilon_{i\uparrow} - \varepsilon_{-i\downarrow}}{2} \quad (6.117)$$

and thus

$$\hat{I}_{i\sigma}(\mathbf{e})\varepsilon_{\text{sign}(\sigma)i\sigma} = \varepsilon + \text{sign}(\sigma)J \quad (6.118)$$

**Kernel Contribution  $S_\beta^M$**  The expression for the linear potential term in Eq. (6.83) together with  $P_s$  of Eq. (D.2) and the expression for  $\check{E}$  in Eq. (6.118) is readily found equal to

$$\check{S}_\beta^M(\mathbf{e}, \mathbf{e}') = -\delta(\mathbf{e} - \mathbf{e}')\hbar^2 \frac{f_\beta(J + \varepsilon) - f_\beta(J - \varepsilon)}{\varepsilon} \quad (6.119)$$

**Kernel Contribution  $S_\beta^S$**  Taking Eq. (6.84) for  $\check{S}_\beta^S$  and Eq. (6.118) we find

$$\begin{aligned} \check{S}_\beta^S(\mathbf{e}, \mathbf{e}') &= \frac{1}{\varepsilon} \delta(\mathbf{e}' - \mathbf{e}) \int d\mathbf{e}'' \int d\omega \left( \alpha^2 F_\uparrow^D(\mathbf{e}, \mathbf{e}'', \omega) (L(\Omega_{\mathbf{q}\lambda}, \varepsilon + J, \varepsilon'' + J'', \varepsilon + J) \right. \\ &\quad - L(\Omega_{\mathbf{q}\lambda}, \varepsilon + J, \varepsilon'' + J'', J - \varepsilon)) + \alpha^2 F_\downarrow^D(\mathbf{e}, \mathbf{e}'', \omega) (L(\Omega_{\mathbf{q}\lambda}, \varepsilon - J, \varepsilon'' - J'', \varepsilon - J) \\ &\quad \left. - L(\Omega_{\mathbf{q}\lambda}, \varepsilon - J, \varepsilon'' - J'', -J - \varepsilon)) \right) \end{aligned} \quad (6.120)$$

and similarly for the symmetrized version

$$\begin{aligned} \check{S}_\beta^{\text{HPS}}(\mathbf{e}, \mathbf{e}') &= \frac{1}{2\varepsilon} \delta(\mathbf{e}' - \mathbf{e}) \int d\mathbf{e}'' \int d\omega \left( \alpha^2 F_\uparrow^D(\mathbf{e}, \mathbf{e}'', \omega) \left( \right. \right. \\ &\quad L(\omega, \varepsilon + J, \varepsilon'' + J'', \varepsilon + J) + L(\omega, \varepsilon + J, -\varepsilon'' - J'', \varepsilon + J) \\ &\quad - L(\omega, \varepsilon + J, \varepsilon'' + J'', J - \varepsilon) - L(\Omega_{\mathbf{q}\lambda}, \omega, \varepsilon + J, -\varepsilon'' - J'', J - \varepsilon) \\ &\quad \left. + \alpha^2 F_\downarrow^D(\mathbf{e}, \mathbf{e}'', \omega) (L(\omega, \varepsilon - J, \varepsilon'' - J'', \varepsilon - J) + L(\omega, \varepsilon - J, J'' - \varepsilon'', \varepsilon - J) \right. \\ &\quad \left. - L(\Omega_{\mathbf{q}\lambda}, \varepsilon - J, \varepsilon'' - J'', -\varepsilon - J) - L(\Omega_{\mathbf{q}\lambda}, \omega, \varepsilon - J, J'' - \varepsilon'', -\varepsilon - J) \right). \end{aligned} \quad (6.121)$$

For treating the totally particle hole symmetric term note that we may integrate  $(-\varepsilon'')$  in the second term because the integration boundaries are symmetric

$$\begin{aligned} \check{S}_\beta^{\text{THPS}}(\mathbf{e}, \mathbf{e}') &= \frac{1}{4\varepsilon} \delta(\mathbf{e}' - \mathbf{e}) \int d\mathbf{e}'' \int d\omega \left( \right. \\ &\quad \left. (\alpha^2 F_\uparrow^D(\mathbf{e}, \mathbf{e}'', \omega) + \alpha^2 F_\downarrow^D(\varepsilon, J, -\varepsilon'', J'', \omega)) \times \right. \\ &\quad \left. (L(\omega, \varepsilon + J, \varepsilon'' + J'', \varepsilon + J) + L(\omega, \varepsilon + J, -\varepsilon'' - J'', \varepsilon + J) + \right. \\ &\quad \left. + L(\omega, \varepsilon - J, -\varepsilon'' - J'', \varepsilon - J) + L(\omega, \varepsilon - J, \varepsilon'' + J'', \varepsilon - J)) \right). \end{aligned} \quad (6.122)$$

Due to the locality in the state dependence  $\varepsilon''$  at the Fermi energy (fast decay in  $\varepsilon''$ ) of the Matzubara sums  $L$  of the particle hole symmetrized kernel it is often a good approximation to drop the energy dependence of the coupling  $\alpha^2 F^D$  in which case the effective coupling will be the average of both spin channels.

**Kernel Contribution**  $S_\beta^c$  We isotropize the term of Eq. (6.87) with the result

$$\check{S}_{\text{ph}\beta}^c(\mathbf{e}, \mathbf{e}') = -\int d\omega \frac{\alpha^2 F(\mathbf{e}, \mathbf{e}', \omega)}{|\varepsilon'|} (L(\omega, \varepsilon + J, |\varepsilon'| + J', J - \varepsilon) + L(\omega, \varepsilon - J, |\varepsilon'| - J', -\varepsilon - J)) \quad (6.123)$$

The purely singlet term, with what was noted in Subsection (6.6.2):  $g_{-k, k'\uparrow}^{\lambda\mathbf{q}} g_{k, -k'\downarrow}^{\lambda-\mathbf{q}} \equiv g_{k, k'\uparrow}^{\lambda\mathbf{q}} g_{-k, -k'\downarrow}^{\lambda-\mathbf{q}}$ , becomes

$$\begin{aligned} \check{S}_{\text{ph}\beta}^{\text{sc}}(\mathbf{e}, \mathbf{e}') &= -\int d\omega \frac{\alpha^2 F(\mathbf{e}, \mathbf{e}', \omega)}{2|\varepsilon'|} \left( L(\omega, \varepsilon + J, |\varepsilon'| + J', J - \varepsilon) - L(\omega, \varepsilon + J, J' - |\varepsilon'|, J - \varepsilon) \right. \\ &\quad \left. + L(\omega, \varepsilon - J, |\varepsilon'| + J', -J - \varepsilon) - L(\omega, \varepsilon - J, J' - |\varepsilon'|, -J - \varepsilon) \right) \end{aligned} \quad (6.124)$$

The Coulomb interaction takes the slightly simpler shape

$$\check{S}_{\text{Coul}\beta}^{\text{stat}\mathbf{e}}(\mathbf{e}, \mathbf{e}') = -\frac{\hbar^2}{2} C^{\text{stat}}(\mathbf{e}, \mathbf{e}') \frac{f_\beta(J' + |\varepsilon'|) - f_\beta(J' - |\varepsilon'|)}{|\varepsilon'|} \frac{f_\beta(J + \varepsilon) - f_\beta(J - \varepsilon)}{\varepsilon} \quad (6.125)$$

To obtain the dynamic Coulomb term just replace  $\alpha^2 F$  with  $C^{\text{dyn}}$  and  $L$  with  $L_M$  in Eq. (6.123).

Similar to Eq. (6.91), because the linearized  $\check{S}_\beta$  does not depend on  $\Delta_s^s$ , Eq. (6.97) requires that  $\Delta_s^s(\mathbf{e}') = 0$  if  $\check{S}_\beta$  is invertible. To find a non-trivial solution we have to search for the point where this is not the case, i.e.

$$\det(\check{S}_\beta) = 0 \quad (6.126)$$

## Summary

In this Chapter we have computed density functionals for the electronic KS System of Spin-SCDFT (Section 3.4) using Many-Body theory (Chapter 5), the interacting matrix elements (Chapter 4) in connection with the SSE (5.77). We have presented a strategy to either relax, or even to keep the SDA while including the possibility to change also the normal densities  $n(\mathbf{r})$  and  $\mathbf{m}(\mathbf{r})$ . Limiting the discussion of explicit results to the SDA, we have cast the SSE to a form where a solution  $\Delta_s^s$  is mapped to zero by the Sham-Schlüter operator  $S_\beta[\Delta_s^s] \cdot \Delta_s^s = 0$ , itself being a non-linear functional of  $\Delta_s^s$ . We argued that in small magnetic fields, we should be able to use the linearized equation  $\check{S}_\beta \cdot \Delta_s^s = 0$  to determine  $T_c$  although the SC order parameter is only weakly dependent on  $\Delta_s^s$  at the Fermi level. In a final step we have given the same equations in the isotropic approximation, i.e. assuming all individual quantities to depend on the electronic bands and Bloch vectors through the single particle energy  $\varepsilon_k$ , only. This will reduce the numerical effort even further.

# 7. Many-Body Excitation Spectrum and Eliashberg Equations

We start this Chapter with Section 7.1 where we cast the Dyson Eq. (5.26) to a form where the SE is diagonal (similar to the SDA) and isotropic. This equation (5.26) is the basis of the analysis in this Chapter.

The KS system is designed to reproduce the density of the interacting system. Still, in normal DFT its single particle excitation spectrum often closely resembles to the experimentally observed one. This fact can be viewed as a basis of modern solid state physics. We derive formulas for the KS excitation spectra in Appendix G but it will turn out in the numerical results in Sec. 8.3 that this is not always a good approximation in the context of SpinSCDFT. In the numerical solution of the equations of Chapter 6 in Chapter 8 we conclude that the KS DOS is not gaped while the system is a SC. Hence, in Section 7.2 we compute the equations for a correction to the KS spectra where the Dyson Eq. (7.2) is iterated once by inversion and the DOS is calculated from the resulting interacting GF. Because no self-consistency is implied all properties are fully determined by a converged previous SpinSCDFT calculation.

In Section 7.3 we go one step further and require self-consistence in the interacting GF and do not replace  $\bar{G}$  in the SE. Assuming all matrices to be diagonal in the KS basis and dropping the energy (i.e. state, not frequency) dependence of the couplings will allow us to cast the Dyson equation into a set of self-consistent equations for SE parts: The so called Eliashberg equations. These will serve as reference in the phonon-only approximation and can be the basis of a future improvement similar to the spin degenerate case.

Vonsovsky [19] discusses Eliashberg equations for system with an exchange splitting. While, the authors start from the non-SC Hartree system in Nambu notation, not the SC KS system, the approach is similar to ours in Section 7.3. In both cases the SE is constructed with first order phonon and Coulomb diagrams. Similar to our approach, only the diagonal matrix elements are considered. The splitting term  $J$  (compare Subsection 6.6.1) also appears in Ref. [19], but it does not come from an isotropization and is reasoned on the basis of a d-orbital exchange field. The rest of the spin interactions, i.e. dynamic spin excitation (namely magnons), are treated perturbatively in Ref. [19] while we do not consider them in the first place, see Section 5.2. While our approach focuses on the ab-initio calculation of a SC, lacking computer power the discussion in Ref. [19] is more phenomenological.

## 7.1. The Isotropic Dyson Equation

We start this Section casting the Dyson equation (Eq. (5.26)) into the Nambu-KS basis functions of Eq. (5.37). For the matrix elements our usual notation of  $4 \times 4$  matrices applies and we write the Dyson equation as

$$\bar{G}_{ij}(\omega_n) = \bar{G}_{ij}^{\text{KS}}(\omega_n) + \frac{1}{\hbar} \sum_{kl} \bar{G}_{ik}^{\text{KS}}(\omega_n) \cdot \bar{\Sigma}_{kl}^s(\omega_n) \cdot \bar{G}_{lj}(\omega_n). \quad (7.1)$$

Alternatively we may write the above equation as a matrix inversion

$$\bar{G}_{ij}(\omega_n) = \left( (\bar{G}^{\text{KS}})^{-1}_{ij}(\omega_n) - \frac{1}{\hbar} \bar{\Sigma}_{ij}^s(\omega_n) \right)^{-1}. \quad (7.2)$$

This form is most convenient if the SDA Subsection 3.5.2 is used (that we assume for the rest of this section) in the starting KS system because the inverse  $(\bar{G}^{\text{KS}})_{ij}^{-1}$  can be computed analytically. As demonstrated in the Appendix E

$$\begin{aligned} (\bar{G}^{\text{KS}})_{ij}^{-1}(\omega_n) &= \delta_{ij} (i\hbar\omega_n\tau_0\sigma_0 - (\frac{\varepsilon_{i\uparrow} + \varepsilon_{-i\downarrow}}{2})\tau_z\sigma_0 - (\frac{\varepsilon_{i\uparrow} - \varepsilon_{-i\downarrow}}{2})\tau_z\sigma_z) \\ &\quad + \delta_{i,-j} ((i\tau_y)(i\sigma_y)\Re\Delta_{si}^s + \tau_x(i\sigma_y)i\Im\Delta_{si}^s) \end{aligned} \quad (7.3)$$

Assuming that the full GF  $\bar{G}_{ij}(\omega_n)$  as well as the SC KS GF  $\bar{G}_{ij}^{\text{KS}}(\omega_n)$  of Eq. (7.3) depend only on the splitting  $J$  and center of energy  $\varepsilon$  we may introduce<sup>1</sup>

$$\bar{\Sigma}_n^s(\mathbf{e}, \mathbf{e}') = \hat{I}_{k\sigma}(\mathbf{e})\varrho(\mathbf{e}')\hat{I}_{l\sigma'}(\mathbf{e}')\bar{\Sigma}_{kl}^s(\omega_n) \quad (7.4)$$

$$\bar{G}_n(\mathbf{e}, \mathbf{e}') = \hat{I}_{i\sigma}(\mathbf{e})\varrho(\mathbf{e}')\hat{I}_{j\sigma'}(\mathbf{e}')\bar{G}_{ij}(\omega_n) \quad (7.5)$$

$$\bar{G}_n^{\text{KS}}(\mathbf{e}, \mathbf{e}') = \hat{I}_{i\sigma}(\mathbf{e})\varrho(\mathbf{e}')\hat{I}_{j\sigma'}(\mathbf{e}')\bar{G}_{ik}^{\text{KS}}(\omega_n). \quad (7.6)$$

The Dyson Eq. (7.2) reads with the above definitions

$$\bar{G}_n(\mathbf{e}, \mathbf{e}') = \left( \bar{G}_n^{\text{KS}-1}(\mathbf{e}, \mathbf{e}') + \bar{\Sigma}_n^s(\mathbf{e}, \mathbf{e}') \right)^{-1} \quad (7.7)$$

The isotropic KS GF Eq. (7.3) is diagonal in  $\mathbf{e}$  as well as in KS states and takes the shape

$$(\bar{G}_n^{\text{KS}}(\mathbf{e}))^{-1} \equiv i\hbar\omega_n\tau_0\sigma_0 - \varepsilon\tau_z\sigma_0 - J\tau_z\sigma_z + (i\tau_y)(i\tau_y)\Re\Delta_s^s + \tau_x(i\tau_y)i\Im\Delta_s^s. \quad (7.8)$$

We neglect all but the (off)diagonal matrix elements with respect to the KS basis and spin on the Nambu-(off)diagonal in the SE  $\bar{\Sigma}_{kl}^s(\omega_n)$ . This is similar to the approach to the SpinSCDFT functional where in the SDA (Subsection 3.5.2) we also drop those matrix elements in order not to invalidate the SDA (compare Section 6.4). Then, the Dyson equation becomes diagonal in energy and, for the diagonal part  $\bar{G}_n(\mathbf{e})$ , reads

$$\bar{G}_n(\mathbf{e}) = \left( (\bar{G}_n^{\text{KS}}(\mathbf{e}))^{-1} + \hbar^{-1}\bar{\Sigma}_n^s(\mathbf{e}) \right)^{-1}. \quad (7.9)$$

Following the convention of Eq. (5.41) we address non-vanishing components of  $\bar{G}_n(\mathbf{e})$  via

$$\bar{G}_n(\mathbf{e}) = \begin{pmatrix} G_{n\uparrow}(\mathbf{e}) & 0 & 0 & F_{n\uparrow}(\mathbf{e}) \\ 0 & G_{n\downarrow}(\mathbf{e}) & F_{n\downarrow}(\mathbf{e}) & 0 \\ 0 & F_{n\uparrow}^\dagger(\mathbf{e}) & G_{n\uparrow}^\dagger(\mathbf{e}) & 0 \\ F_{n\downarrow}^\dagger(\mathbf{e}) & 0 & 0 & G_{n\downarrow}^\dagger(\mathbf{e}) \end{pmatrix}. \quad (7.10)$$

## 7.2. The Many-Body Green's Function with the KS Self-Energy

As part of the numerical implementation and simulation of Chapter 8 we will find that the KS excitation spectrum is not what one would expect in a SC, namely it is not gaped in all situations still maintaining  $\chi \neq 0$ . As a next step we compute the interacting GF based on the SpinSCDFT results, i.e. taking the same SE  $\bar{\Sigma}^{\text{KS}}$  of Eq. (6.11) that we used for the functional construction in Section 6.3. Taking the (fixed) SE  $\bar{\Sigma}^{\text{KS}}$  means that the Dyson Eq. (7.9) can be solved once by inversion, without the need to iterate with an update of  $\bar{\Sigma}[\bar{G}]$ . Then we may extract excitation spectra from the resulting interacting GF as a next approximation to the full solution to the Dyson equation. This can be viewed equivalent to the common G0W0 (one cycle

<sup>1</sup>The index  $\sigma$  of the isotropization operators act according to the component of the matrix.

GW) approximation [60] that is well known to improve a KS band structure with respect to semiconductor gaps [61].

We invert the Dyson Eq. (7.9) in Subsection 7.2.1 and obtain a closed expression for the interacting (temperature) GF in terms of the  $\bar{\Sigma}^{\text{KS}}$  SE on the imaginary axis. In Subsection 7.2.2 we continue the temperature GF to the real axis. Because the only problematic objects in the continuation of the temperature GF are the SE parts, this is done essentially continuing those to the real axis.

### 7.2.1. Imaginary Axis Formulation

We use the results of the Subsections 6.3.2 and 6.3.3 where we apply the isotropization procedure. We introduce

$$\bar{\Sigma}_n^{\text{KS}}(\mathbf{e}) = \begin{pmatrix} \Sigma_{\uparrow n}^{\text{KS}1,1}(\mathbf{e}) & 0 & 0 & \Sigma_{\uparrow n}^{\text{KS}1,-1}(\mathbf{e}) \\ 0 & \Sigma_{\downarrow n}^{\text{KS}1,1}(\mathbf{e}) & \Sigma_{\downarrow n}^{\text{KS}1,-1}(\mathbf{e}) & 0 \\ 0 & \Sigma_{\uparrow n}^{\text{KS}-1,1}(\mathbf{e}) & \Sigma_{\uparrow n}^{\text{KS}-1,-1}(\mathbf{e}) & 0 \\ \Sigma_{\downarrow n}^{\text{KS}-1,1}(\mathbf{e}) & 0 & 0 & \Sigma_{\downarrow n}^{\text{KS}-1,-1}(\mathbf{e}) \end{pmatrix}, \quad (7.11)$$

where

$$\bar{\Sigma}_n^{\text{KS}}(\mathbf{e}) = \bar{\Sigma}_{\text{ph } n}^{\text{KS}}(\mathbf{e}) + \bar{\Sigma}_{\text{Coul } n}^{\text{KS}}(\mathbf{e}). \quad (7.12)$$

The phonon SE Eqs. (6.30) to (6.33) become

$$\Sigma_{\text{ph } \sigma n}^{\text{KS}1,1}(\mathbf{e}) = \int d\omega \int d\mathbf{e}' \alpha^2 F_{\sigma}^D(\mathbf{e}, \mathbf{e}', \omega) \sum_{\alpha} \frac{\text{sign}(\alpha)\varepsilon' + F'}{2F'} I_s(\omega, E_{\sigma}^{\alpha'}, \omega_n) \quad (7.13)$$

$$\Sigma_{\text{ph } \sigma n}^{\text{KS}-1,-1}(\mathbf{e}) = \int d\omega \int d\mathbf{e}' \alpha^2 F_{\sigma}^D(\mathbf{e}, \mathbf{e}', \omega) \sum_{\alpha} \frac{\text{sign}(\alpha)\varepsilon' + F'}{2F'} I_s(\omega, -E_{\sigma}^{\alpha'}, \omega_n) \quad (7.14)$$

$$\Sigma_{\text{ph } \sigma n}^{\text{KS}1,-1}(\mathbf{e}) = -\text{sign}(\sigma) \int d\omega \int d\mathbf{e}' \alpha^2 F(\mathbf{e}, \mathbf{e}', \omega) \sum_{\alpha} \frac{\text{sign}(\alpha)\Delta_s^{s'}}{2F'} I_s(\omega, E_{\sigma}^{\alpha'}, \omega_n) \quad (7.15)$$

$$\Sigma_{\text{ph } \sigma n}^{\text{KS}-1,1}(\mathbf{e}) = -\text{sign}(\sigma) \int d\omega \int d\mathbf{e}' \alpha^2 F(\mathbf{e}, \mathbf{e}', \omega) \sum_{\alpha} \frac{\text{sign}(\alpha)\Delta_s^{s'*}}{2F'} I_s(\omega, -E_{\sigma}^{\alpha'}, \omega_n) \quad (7.16)$$

Further, the Eqs. (6.41) and (6.42) become

$$\begin{aligned} \Sigma_{\text{Coul } \sigma n}^{\text{KS}1,-1}(\mathbf{e}) &= -\text{sign}(\sigma) \sum_{\alpha} \int d\mathbf{e}' \frac{\text{sign}(\alpha)\Delta_s^{s'}}{2F'} (C^{\text{stat}}(\mathbf{e}, \mathbf{e}') f_{\beta}(E_{\sigma}^{\alpha'})) \\ &\quad + \int_0^{\infty} \frac{d\omega}{\pi} C^{\text{dyn}}(\omega, \mathbf{e}, \mathbf{e}') Y_2(\omega, E_{\sigma}^{\alpha'}, \omega_n) \end{aligned} \quad (7.17)$$

$$\begin{aligned} \Sigma_{\text{Coul } \sigma n}^{\text{KS}-1,1}(\mathbf{e}) &= -\text{sign}(\sigma) \sum_{\alpha} \int d\mathbf{e}' \frac{\text{sign}(\alpha)\Delta_s^{s'*}}{2F'} (C^{\text{stat}}(\mathbf{e}, \mathbf{e}') f_{\beta}(-E_{\sigma}^{\alpha'})) \\ &\quad + \int_0^{\infty} \frac{d\omega}{\pi} C^{\text{dyn}}(\omega, \mathbf{e}, \mathbf{e}') Y_2(\omega, -E_{\sigma}^{\alpha'}, \omega_n). \end{aligned} \quad (7.18)$$

The correct SE  $\bar{\Sigma}^s$  for the Dyson equation starting from the KS system accounts for the  $xc$  potential. If we subtract  $((i\tau_y)(i\sigma_y)\Re\Delta_s^s(\mathbf{e}) + \tau_x(i\sigma_y)i\Im\Delta_s^s(\mathbf{e}))$  from the inverse KS GF in the Dyson equation the exchange correlation potential cancels as expected. Thus we have to solve

$$(\bar{G}_n(\mathbf{e}))^{-1} = \frac{1}{\hbar} \begin{pmatrix} i\hbar\omega_n - J - \varepsilon - \bar{\Sigma}_{\uparrow n}^{\text{KS}1,1} & 0 & 0 & -\bar{\Sigma}_{\uparrow n}^{\text{KS}1,-1} \\ 0 & i\hbar\omega_n + J - \varepsilon - \bar{\Sigma}_{\downarrow n}^{\text{KS}1,1} & -\bar{\Sigma}_{\downarrow n}^{\text{KS}1,-1} & 0 \\ 0 & -\bar{\Sigma}_{\uparrow n}^{\text{KS}-1,1} & i\hbar\omega_n + J + \varepsilon - \bar{\Sigma}_{\uparrow n}^{\text{KS}-1,-1} & 0 \\ -\bar{\Sigma}_{\downarrow n}^{\text{KS}-1,1} & 0 & 0 & i\hbar\omega_n - J + \varepsilon - \bar{\Sigma}_{\downarrow n}^{\text{KS}-1,-1} \end{pmatrix} \quad (7.19)$$

We perform a symmetrization according to Eq. (6.43) and with similar results as indicated in Table 6.1. Non-vanishing parts are, omitting  $\epsilon$  for a moment

$$\begin{aligned}
\Sigma_n^\omega &= \frac{1}{4} \sum_\sigma (\Sigma_{\sigma n}^{\text{KS1},1} + \Sigma_{\sigma n}^{\text{KS-1},-1}) & \Sigma_n^{t+} &= \frac{1}{4} \sum_\sigma (\Sigma_{\sigma n}^{\text{KS1},-1} + \Sigma_{\sigma n}^{\text{KS-1},1}) \\
A_n^{\omega z} &= \frac{1}{4} \sum_\sigma \text{sign}(\sigma) (\Sigma_{\sigma n}^{\text{KS1},1} + \Sigma_{\sigma n}^{\text{KS-1},-1}) & \Sigma_n^{t-} &= \frac{1}{4} \sum_\sigma (\Sigma_{\sigma n}^{\text{KS1},-1} - \Sigma_{\sigma n}^{\text{KS-1},1}) \\
\Sigma_n^\epsilon &= \frac{1}{4} \sum_\sigma (\Sigma_{\sigma n}^{\text{KS1},1} - \Sigma_{\sigma n}^{\text{KS-1},-1}) & \Sigma_n^{\Im\Delta} &= \frac{-i}{4} \sum_\sigma \text{sign}(\sigma) (\Sigma_{\sigma n}^{\text{KS1},-1} + \Sigma_{\sigma n}^{\text{KS-1},1}) \\
\Sigma_n^J &= \frac{1}{4} \sum_\sigma \text{sign}(\sigma) (\Sigma_{\sigma n}^{\text{KS1},1} - \Sigma_{\sigma n}^{\text{KS-1},-1}) & \Sigma_n^{\Re\Delta} &= \frac{1}{4} \sum_\sigma \text{sign}(\sigma) (\Sigma_{\sigma n}^{\text{KS1},-1} - \Sigma_{\sigma n}^{\text{KS-1},1}).
\end{aligned} \tag{7.20}$$

which means the full SE is

$$\begin{aligned}
\bar{\Sigma}_n &= \Sigma_n^\omega \tau_0 \sigma_0 + \Sigma_n^\epsilon \tau_z \sigma_0 + \Sigma_n^J \tau_z \sigma_z + A_n^{\omega z} \tau_0 \sigma_z \\
&\quad + \Sigma_n^{t+} \tau_x \sigma_x + \Sigma_n^{t-} (i\tau_y) \sigma_x + i\Sigma_n^{\Im\Delta} \tau_x (i\sigma_y) + \Sigma_n^{\Re\Delta} (i\tau_y) (i\sigma_y),
\end{aligned} \tag{7.21}$$

which we add to the inverse GF with the result

$$\begin{aligned}
\bar{G}_n^{-1} &= (i\hbar\omega_n - \Sigma_n^\omega) \tau_0 \sigma_0 - (J + \Sigma_n^J) \tau_z \sigma_z - (\epsilon + \Sigma_n^\epsilon) \tau_z \sigma_0 - A_n^{\omega z} \tau_0 \sigma_z + \\
&\quad - \Sigma_n^{\Re\Delta} (i\tau_y) (i\sigma_y) - i\Sigma_n^{\Im\Delta} \tau_x (i\sigma_y) - \Sigma_n^{t+} \tau_x \sigma_x - \Sigma_n^{t-} (i\tau_y) \sigma_x.
\end{aligned} \tag{7.22}$$

Now we may go through the steps of the Appendix E backwards to invert the inverse GF. There are, however, terms not present in the original KS GF, namely  $A_{\omega zn}$  and  $\Sigma_{t\pm n}$ . After some algebra we see the matrix inverse can be written as

$$G_{n\sigma}(\mathbf{e}) = \frac{1}{2\mathfrak{F}_{n\sigma}(\mathbf{e})} \sum_\gamma \frac{\mathfrak{F}_{n\sigma}(\mathbf{e}) + \text{sign}(\gamma) (\epsilon + \Sigma_n^\epsilon(\mathbf{e}) + \text{sign}(\sigma) A_n^{\omega z}(\mathbf{e}))}{i\hbar\omega_n - \Sigma_n^\omega(\mathbf{e}) - \text{sign}(\sigma) (J + \Sigma_n^J(\mathbf{e})) - \text{sign}(\gamma) \mathfrak{F}_{n\sigma}(\mathbf{e})} \tag{7.23}$$

$$G_{n\sigma}^\dagger(\mathbf{e}) = \frac{1}{2\mathfrak{F}_{n-\sigma}(\mathbf{e})} \sum_\gamma \frac{\mathfrak{F}_{n-\sigma}(\mathbf{e}) + \text{sign}(\gamma) (\epsilon + \Sigma_n^\epsilon(\mathbf{e}) - \text{sign}(\sigma) A_n^{\omega z}(\mathbf{e}))}{i\hbar\omega_n - \Sigma_n^\omega(\mathbf{e}) + \text{sign}(\sigma) (J + \Sigma_n^J(\mathbf{e})) + \text{sign}(\gamma) \mathfrak{F}_{n-\sigma}(\mathbf{e})} \tag{7.24}$$

$$F_{n\sigma}(\mathbf{e}) = \frac{\text{sign}(\sigma)}{2\mathfrak{F}_{n\sigma}(\mathbf{e})} \sum_\gamma \frac{\text{sign}(\gamma) (\Sigma_n^{\Re\Delta}(\mathbf{e}) + i\Sigma_n^{\Im\Delta}(\mathbf{e}) + \text{sign}(\sigma) (\Sigma_n^{t-}(\mathbf{e}) + \Sigma_n^{t+}(\mathbf{e})))}{i\hbar\omega_n - \Sigma_n^\omega(\mathbf{e}) - \text{sign}(\sigma) (J + \Sigma_n^J(\mathbf{e})) - \text{sign}(\gamma) \mathfrak{F}_{n\sigma}(\mathbf{e})} \tag{7.25}$$

$$F_{n\sigma}^\dagger(\mathbf{e}) = \frac{\text{sign}(\sigma)}{2\mathfrak{F}_{n-\sigma}(\mathbf{e})} \sum_\gamma \frac{\text{sign}(\gamma) (\Sigma_n^{\Re\Delta}(\mathbf{e}) - i\Sigma_n^{\Im\Delta}(\mathbf{e}) + \text{sign}(\sigma) (\Sigma_n^{t-}(\mathbf{e}) - \Sigma_n^{t+}(\mathbf{e})))}{i\hbar\omega_n - \Sigma_n^\omega(\mathbf{e}) + \text{sign}(\sigma) (J + \Sigma_n^J(\mathbf{e})) + \text{sign}(\gamma) \mathfrak{F}_{n-\sigma}(\mathbf{e})} \tag{7.26}$$

with

$$\begin{aligned}
\mathfrak{F}_{n\sigma}(\mathbf{e}) &= \left( (\epsilon + \Sigma_n^\epsilon(\mathbf{e}) + \text{sign}(\sigma) A_n^{\omega z}(\mathbf{e}))^2 + \left( \Sigma_n^{\Re\Delta} + i\Sigma_n^{\Im\Delta} + \text{sign}(\sigma) (\Sigma_n^{t+} + \Sigma_n^{t-}) \right) \times \right. \\
&\quad \left. \times \left( \Sigma_n^{\Re\Delta} - i\Sigma_n^{\Im\Delta} + \text{sign}(\sigma) (\Sigma_n^{t+} - \Sigma_n^{t-}) \right) \right)^{\frac{1}{2}}
\end{aligned} \tag{7.27}$$

$\mathfrak{F}_{n\sigma}$  is a generalization of the absolute value squared of energy plus  $\Delta_s^s$  that we have called  $F = \sqrt{\epsilon^2 + \Delta_s^s}$  earlier in Eq. (6.100). The appearance of triplet contributions in the GF are somewhat disturbing but are the result of the Nambu-offdiagonal SE terms Eqs. (7.15) and (7.16). With Eq. (7.20) the one cycle interacting GF Eqs. (7.23) to (7.26) may be computed numerically given the results of a converged SpinSCDFT calculation.



### 7.2.2. Real Axis Formulation

To obtain the (L)DOS, according to Eq. (5.31), we need the retarded GF. This can be computed from the temperature GF Eq. (7.9) via substitution of

$$i\omega_n \rightarrow \omega + i\eta \quad (7.28)$$

where  $\eta$  as always is a real positive infinitesimal [45]. To distinguish the real frequency  $\omega$  from the coupling frequency, e.g.  $\alpha^2 F(\omega)$ , will call the latter  $\Omega$  from now on. The expression Eqs. (7.23) to (7.26) remain essentially unchanged on the real axis, except that we have insert the SE parts Eq. (7.20) on the real axis and write  $i\hbar\eta + \hbar\omega$  instead of the Matsubara frequency. Here we have two options, first we may compute the SE parts Eq. (7.20) on the imaginary axis and use a numerical analytic continuation to the real axis, or we can compute analytic formulas for the real axis and use them. We choose the latter because then we can use the equations also far away from the Fermi level.

We will see that the SE parts, e.g.  $\Sigma_n^{\text{r}\Delta}(\epsilon)$ , on the real axis have to be computed via independent calculations of imaginary and real part. The dependence on the Matsubara index of the SE is only via the function  $I_s$  of Eq. (6.24) (or  $Y_2$  of Eq. (6.38) in the Coulomb case), i.e. the results of the first Matsubara summation in the SE. We first note that  $Y_1$  (Eq. (6.22)) as the main ingredient to  $I_s$  may be written as<sup>2</sup>

$$Y_{1\eta}(\Omega, E, \omega) = (n_\beta(\hbar\Omega) + f_\beta(E)) \left( \frac{(\Omega - \frac{1}{\hbar}E + \omega)^2}{(\Omega - \frac{1}{\hbar}E + \omega)^2 + \eta^2} \frac{\hbar}{\Omega - \frac{1}{\hbar}E + \omega} - i\pi\hbar \frac{1}{\pi} \frac{\eta}{(\Omega - \frac{1}{\hbar}E + \omega)^2 + \eta^2} \right). \quad (7.29)$$

We note that the first part cuts off the integral if  $\Omega - \frac{1}{\hbar}E + \omega \ll \eta$  and the second part is a nascent delta function. In the limit  $\eta \searrow 0$  we thus encounter the principle value operator and the delta distribution

$$\lim_{\eta \searrow 0} \frac{(\Omega - \frac{1}{\hbar}E + \omega)^2}{(\Omega - \frac{1}{\hbar}E + \omega)^2 + \eta^2} \frac{1}{\Omega - \frac{1}{\hbar}E + \omega} \equiv \hat{P} \frac{1}{\Omega - \frac{1}{\hbar}E + \omega}, \quad (7.30)$$

$$\lim_{\eta \searrow 0} \frac{1}{\pi} \frac{\eta}{(\Omega - \frac{1}{\hbar}E + \omega)^2 + \eta^2} \equiv \delta(\Omega - \frac{1}{\hbar}E + \omega), \quad (7.31)$$

so that

$$Y_{1\eta}(-\Omega, E, \omega) = \hbar \left( \hat{P} \frac{n_\beta(\hbar\Omega) + f_\beta(-E)}{\Omega + \frac{1}{\hbar}E - \omega} + i\pi\hbar\delta(\Omega - \frac{1}{\hbar}E + \omega) \right). \quad (7.32)$$

Thus

$$\begin{aligned} I_{s\eta}(\Omega, E, \omega) &= \hbar \hat{P} \frac{n_\beta(\hbar\Omega) + f_\beta(E)}{\Omega - \frac{1}{\hbar}E + \omega} - \hbar \hat{P} \frac{n_\beta(\hbar\Omega) + f_\beta(-E)}{\Omega + \frac{1}{\hbar}E - \omega} \\ &\quad - i\hbar\pi \left( (n_\beta(\hbar\Omega) + f_\beta(E)) \delta(\Omega - \frac{1}{\hbar}E + \omega) \right. \\ &\quad \left. + (n_\beta(\hbar\Omega) + f_\beta(-E)) \delta(\Omega + \frac{1}{\hbar}E - \omega) \right). \end{aligned} \quad (7.33)$$

<sup>2</sup>We attach an index  $\eta$  for the Matsubara sums we have analytically continued to the nearly real axis.

Using  $n_\beta(-E + \hbar\omega) + f_\beta(-E) = -(n_\beta(E - \hbar\omega) + f_\beta(E))$  we obtain

$$\begin{aligned}
& (I_{s\eta}(\hbar\Omega, E, \omega) \pm I_{s\eta}(\hbar\Omega, -E, \omega))\hbar^{-1} = \\
& = \hat{P} \frac{n_\beta(\hbar\Omega) + f_\beta(E)}{\Omega - \frac{1}{\hbar}E + \omega} \mp \hat{P} \frac{n_\beta(\hbar\Omega) + f_\beta(E)}{\Omega - \frac{1}{\hbar}E - \omega} - \hat{P} \frac{n_\beta(\hbar\Omega) + f_\beta(-E)}{\Omega + \frac{1}{\hbar}E - \omega} \pm \hat{P} \frac{n_\beta(\hbar\Omega) + f_\beta(-E)}{\Omega + \frac{1}{\hbar}E + \omega} \\
& - i\pi \left( (n_\beta(E - \hbar\omega) + f_\beta(E)) \left( \delta\left(\Omega - \frac{1}{\hbar}E + \omega\right) - \delta\left(\Omega + \frac{1}{\hbar}E - \omega\right) \right) \right. \\
& \left. \pm (n_\beta(E + \hbar\omega) + f_\beta(E)) \left( \delta\left(\Omega - \frac{1}{\hbar}E - \omega\right) - \delta\left(\Omega + \frac{1}{\hbar}E + \omega\right) \right) \right). \tag{7.34}
\end{aligned}$$

For the dynamic part of the Coulomb interaction the result is similar

$$Y_{2\eta}(\hbar\Omega, E, \omega) = I_{s\eta}(\hbar\Omega, E, \omega) - \frac{2\hbar}{\Omega} f_\beta(E). \tag{7.35}$$

Because of the very different nature of the imaginary and real part of the SE we compute both parts independently. Then with Eq. (7.34) for (+) we obtain

$$\begin{aligned}
\Im\Sigma^\omega(\mathbf{e}, \omega) &= -\hbar\pi \int d\mathbf{e}' \sum_{\mu\alpha} \frac{\text{sign}(\alpha)\varepsilon' + F'}{8F'} \left( (n_\beta(E_\mu^{\alpha'} - \hbar\omega) + f_\beta(E_\mu^{\alpha'})) \times \right. \\
& \times (\alpha^2 F_\mu^D(\mathbf{e}, \mathbf{e}', \hbar^{-1}E_\mu^{\alpha'} - \omega) - \alpha^2 F_\mu^D(\mathbf{e}, \mathbf{e}', \omega - \hbar^{-1}E_\mu^{\alpha'})) + \\
& + (n_\beta(E_\mu^{\alpha'} + \hbar\omega) + f_\beta(E_\mu^{\alpha'})) (\alpha^2 F_\mu^D(\mathbf{e}, \mathbf{e}', \hbar^{-1}E_\mu^{\alpha'} + \omega) \\
& \left. - \alpha^2 F_\mu^D(\mathbf{e}, \mathbf{e}', -\hbar^{-1}E_\mu^{\alpha'} - \omega)) \right) \tag{7.36}
\end{aligned}$$

$$\begin{aligned}
\Re\Sigma^\omega(\mathbf{e}, \omega) &= \hbar \int d\Omega \int d\mathbf{e}' \sum_{\mu\alpha} \frac{\text{sign}(\alpha)\varepsilon' + F'}{8F'} \alpha^2 F_\mu^D(\mathbf{e}, \mathbf{e}', \Omega) \left( \hat{P} \frac{n_\beta(\hbar\Omega) + f_\beta(E_\mu^{\alpha'})}{\Omega - \frac{1}{\hbar}E_\mu^{\alpha'} + \omega} \right. \\
& \left. - \hat{P} \frac{n_\beta(\hbar\Omega) + f_\beta(E_\mu^{\alpha'})}{\Omega - \frac{1}{\hbar}E_\mu^{\alpha'} - \omega} - \hat{P} \frac{n_\beta(\hbar\Omega) + f_\beta(-E_\mu^{\alpha'})}{\Omega + \frac{1}{\hbar}E_\mu^{\alpha'} - \omega} + \hat{P} \frac{n_\beta(\hbar\Omega) + f_\beta(-E_\mu^{\alpha'})}{\Omega + \frac{1}{\hbar}E_\mu^{\alpha'} + \omega} \right) \tag{7.37}
\end{aligned}$$

and very similar for  $\Im A^{\omega z}(\mathbf{e}, \omega)$  and  $\Re A^{\omega z}(\mathbf{e}, \omega)$  that only differ by putting a  $\text{sign}(\mu)$  into the spin sum. For the continuation of  $\Sigma_n^\varepsilon(\mathbf{e})$  to  $\Sigma^\varepsilon(\mathbf{e}, \omega)$  we obtain, taking the (-) in Eq. (7.34)

$$\begin{aligned}
\Im\Sigma^\varepsilon(\mathbf{e}, \omega) &= -\hbar\pi \int d\mathbf{e}' \sum_{\mu\alpha} \frac{\text{sign}(\alpha)\varepsilon' + F'}{8F'} \left( (n_\beta(E_\mu^{\alpha'} - \hbar\omega) + f_\beta(E_\mu^{\alpha'})) \times \right. \\
& \times (\alpha^2 F_\mu^D(\mathbf{e}, \mathbf{e}', \hbar^{-1}E_\mu^{\alpha'} - \omega) - \alpha^2 F_\mu^D(\mathbf{e}, \mathbf{e}', \omega - \hbar^{-1}E_\mu^{\alpha'})) \\
& - (n_\beta(E_\mu^{\alpha'} + \hbar\omega) + f_\beta(E_\mu^{\alpha'})) (\alpha^2 F_\mu^D(\mathbf{e}, \mathbf{e}', \hbar^{-1}E_\mu^{\alpha'} + \omega) \\
& \left. - \alpha^2 F_\mu^D(\mathbf{e}, \mathbf{e}', -\hbar^{-1}E_\mu^{\alpha'} - \omega)) \right) \tag{7.38}
\end{aligned}$$

$$\begin{aligned}
\Re\Sigma^\varepsilon(\mathbf{e}, \omega) &= \hbar \int d\Omega \int d\mathbf{e}' \sum_{\mu\alpha} \frac{\text{sign}(\alpha)\varepsilon' + F'}{8F'} \alpha^2 F_\mu^D(\mathbf{e}, \mathbf{e}', \Omega) \left( \hat{P} \frac{n_\beta(\hbar\Omega) + f_\beta(E_\mu^{\alpha'})}{\Omega - \frac{1}{\hbar}E_\mu^{\alpha'} + \omega} \right. \\
& \left. + \hat{P} \frac{n_\beta(\hbar\Omega) + f_\beta(E_\mu^{\alpha'})}{\Omega - \frac{1}{\hbar}E_\mu^{\alpha'} - \omega} - \hat{P} \frac{n_\beta(\hbar\Omega) + f_\beta(-E_\mu^{\alpha'})}{\Omega + \frac{1}{\hbar}E_\mu^{\alpha'} - \omega} - \hat{P} \frac{n_\beta(\hbar\Omega) + f_\beta(-E_\mu^{\alpha'})}{\Omega + \frac{1}{\hbar}E_\mu^{\alpha'} + \omega} \right) \tag{7.39}
\end{aligned}$$

and  $\Sigma^J(\mathbf{e}, \omega)$  has the same relation to  $\Sigma^\varepsilon(\mathbf{e}, \omega)$  as  $A^{\omega z}(\mathbf{e}, \omega)$  has to  $\Sigma^\omega(\mathbf{e}, \omega)$ , i.e. we put a  $\text{sign}(\mu)$  into the spin sum. The above equation again points out the problem in the  $\varepsilon'$  integral if the energy dependence of  $\alpha^2 F_\mu^D(\mathbf{e}, \mathbf{e}', \Omega)$  is neglected. Here  $E_\mu^{\alpha'} \rightarrow |\varepsilon'|$  for large  $\varepsilon'$  so there are parts in the integral that behave as  $\frac{1}{\varepsilon'}$  leading to logarithmic divergence. Thus we see explicitly that we cannot compute the energy renormalization without considering the influence of the interaction

on the full energy spectrum and quasi-particle occupations. To avoid double work we define yet another symbol

$$\mathcal{I}(\mathbf{e}, \mathbf{e}', \Omega) \equiv \alpha^2 F(\mathbf{e}, \mathbf{e}', \Omega) + \frac{\theta(\Omega)}{\pi} C^{\text{dyn}}(\Omega, \mathbf{e}, \mathbf{e}') \quad (7.40)$$

and the integrand

$$\begin{aligned} \Im \mathcal{B}_{\pm}(\mathbf{e}, \mathbf{e}', \omega) &= \hbar \pi \sum_{\mu\alpha} \text{sign}(\mu)^{\frac{1\pm 1}{2}} \frac{\text{sign}(\alpha)}{2F'} (n_{\beta}(E_{\mu}^{\alpha'} - \hbar\omega) + f_{\beta}(E_{\mu}^{\alpha'})) \times \\ &\quad \times (\mathcal{I}(\mathbf{e}, \mathbf{e}', \hbar^{-1}E_{\mu}^{\alpha'} - \omega) - \mathcal{I}(\mathbf{e}, \mathbf{e}', \omega - \hbar^{-1}E_{\mu}^{\alpha'})) \end{aligned} \quad (7.41)$$

$$\begin{aligned} \Re \mathcal{B}_{\pm}(\mathbf{e}, \mathbf{e}', \omega) &= -\hbar \sum_{\mu\alpha} \text{sign}(\mu)^{\frac{1\pm 1}{2}} \frac{\text{sign}(\alpha)}{4F'} \left( \int d\Omega \mathcal{I}(\mathbf{e}, \mathbf{e}', \Omega) \left( \hat{P} \frac{n_{\beta}(\hbar\Omega) + f_{\beta}(E_{\mu}^{\alpha'})}{\Omega - \frac{1}{\hbar}E_{\mu}^{\alpha'} + \omega} \right. \right. \\ &\quad \left. \left. - \hat{P} \frac{n_{\beta}(\hbar\Omega) + f_{\beta}(-E_{\mu}^{\alpha'})}{\Omega + \frac{1}{\hbar}E_{\mu}^{\alpha'} - \omega} \right) + f_{\beta}(E_{\mu}^{\alpha'}) (C^{\text{stat}}(\mathbf{e}, \mathbf{e}') - \int_0^{\infty} d\Omega \frac{2}{\pi\Omega} C^{\text{dyn}}(\Omega, \mathbf{e}, \mathbf{e}')) \right) \end{aligned} \quad (7.42)$$

which makes with

$$\begin{aligned} B_n^s(\mathbf{e}) &\equiv \Sigma_n^{\Re\Delta}(\mathbf{e}) + i\Sigma_n^{\Im\Delta}(\mathbf{e}) & B_n^t(\mathbf{e}) &\equiv \Sigma_n^{t+}(\mathbf{e}) + \Sigma_n^{t-}(\mathbf{e}) \\ B_n^{s*}(\mathbf{e}) &\equiv \Sigma_n^{\Re\Delta}(\mathbf{e}) - i\Sigma_n^{\Im\Delta}(\mathbf{e}) & B_n^{t*}(\mathbf{e}) &\equiv \Sigma_n^{t+}(\mathbf{e}) - \Sigma_n^{t-}(\mathbf{e}) \end{aligned} \quad (7.43)$$

the quantities read on the real axis

$$\begin{aligned} B^s(\mathbf{e}, \omega) &= \int d\mathbf{e}' \Delta_s^s \mathcal{B}_-(\mathbf{e}, \mathbf{e}', \omega) & B^t(\mathbf{e}, \omega) &= \int d\mathbf{e}' \Delta_s^s \mathcal{B}_+(\mathbf{e}, \mathbf{e}', \omega) \\ B^{s*}(\mathbf{e}, \omega) &= \int d\mathbf{e}' \Delta_s^{s*} \mathcal{B}_-(\mathbf{e}, \mathbf{e}', \omega) & B^{t*}(\mathbf{e}, \omega) &= \int d\mathbf{e}' \Delta_s^{s*} \mathcal{B}_+(\mathbf{e}, \mathbf{e}', \omega) \end{aligned} \quad (7.44)$$

and thus, Eq. (7.27) becomes on the real axis (omitting the arguments  $\mathbf{e}, \omega$ )

$$\mathfrak{F}_{\sigma} = \left( (\varepsilon + \Sigma^{\varepsilon} + \text{sign}(\sigma)A^{\omega z})^2 + (B^s + \text{sign}(\sigma)B^t)(B^{s*} + \text{sign}(\sigma)B^{t*}) \right)^{\frac{1}{2}}. \quad (7.45)$$

Note the symmetries

$$\begin{aligned} \Sigma^{\omega}(\mathbf{e}, \omega) &= -\Sigma^{\omega*}(\mathbf{e}, -\omega) & \Sigma^{\varepsilon}(\mathbf{e}, \omega) &= \Sigma^{\varepsilon*}(\mathbf{e}, -\omega) \\ A^{\omega z}(\mathbf{e}, \omega) &= -A^{\omega z*}(\mathbf{e}, -\omega) & \Sigma^J(\mathbf{e}, \omega) &= \Sigma^{J*}(\mathbf{e}, -\omega) \\ \mathcal{B}_-(\mathbf{e}, \mathbf{e}', \omega) &= \mathcal{B}_-^*(\mathbf{e}, \mathbf{e}', -\omega) \end{aligned} \quad (7.46)$$

while, without the Coulomb terms, we similarly find  $\mathcal{B}_+(\mathbf{e}, \mathbf{e}', \omega) = -\mathcal{B}_+^*(\mathbf{e}, \mathbf{e}', -\omega)$ . However, the frequency independent Coulomb part remains unchanged from the inversion  $\omega \rightarrow -\omega$ . We observe that the SE parts are weakly energy dependent; only through the state dependence of the coupling  $\alpha^2 F_{\mu}^D$ ,  $C^{\text{stat}}$  or  $C^{\text{dyn}}$ . Those couplings are typically rather broad on the very narrow energy scale of SC at the Fermi level. This also points out that the Many-Body term equivalent to our  $\Delta_s^s$  is in fact not strongly energy dependent but takes its significant shape in frequency space.

Now we can finally obtain the retarded GF with the equations from Eqs. (7.23) to (7.26) together with Eq. (7.27) for  $\mathfrak{F}_{n\sigma}(\mathbf{e})$  in terms of  $B$  and the corresponding SE parts constructed from real and imaginary part close to the real axis.

$$\bar{G}^{\text{R}}(\mathbf{e}, \omega) \equiv \lim_{\eta \rightarrow 0} \bar{G}(\mathbf{e}, -i\omega + \eta) \quad (7.47)$$

Then we can evaluate the DOS according to

$$\rho_{\sigma\alpha}(\omega) = -2 \int d\mathbf{e} \Im \bar{G}_{\sigma\alpha, \sigma\alpha}^{\text{R}}(\mathbf{e}, \omega) \varrho(\mathbf{e}) \quad (7.48)$$

We obtain the local DOS  $\rho_{\sigma\alpha}(\mathbf{r}, \omega)$  simply by replacing  $\varrho(\mathbf{e})$  with the local double DOS  $\varrho_{\sigma}(\mathbf{e}, \mathbf{r})$  of Eq. (G.16). The poles of  $\bar{\mathcal{G}}^{\text{R}}(\mathbf{e}, \omega)$  are shifted from  $\omega = 0$  due to the SC condensation. From the denominator of the equation for  $\bar{\mathcal{G}}^{\text{R}}(\mathbf{e}, \omega)$ , similar to Eq. (7.23) we obtain the condition

$$\hbar\omega_0 = \frac{\text{sign}(\sigma)(J + \Re\Sigma^J(\mathbf{e}, \omega_0)) + \text{sign}(\gamma)\Re\mathfrak{F}_{\sigma}(\mathbf{e}, \omega_0)}{1 - \Re\Sigma^{\omega}(\mathbf{e}, \omega_0)/(\hbar\omega_0)} \quad (7.49)$$

to find such a pole. At the same time we need to ensure that the imaginary part of the SE is small so that we have a well defined, stable quasi particle. To find the gap in the excitation spectrum of stable quasi-particles for given spin  $\sigma$ , we search the smallest (largest)  $\omega_{0\sigma}^{\gamma}(\mathbf{e})$  above (below) zero which leads to a pole very close to the real axis. The gap is half the distance from the largest pole below to the smallest pole above zero. Due to the symmetry relations Eqs. (7.46), Eq. 7.49 is approximately symmetric  $\omega_0$  (this symmetry  $\omega_0 \rightarrow -\omega_0$  is exact without Coulomb terms).

### 7.3. Eliashberg Equations of a Spin-Splitted System

Starting from Eq. (7.9) we may approach a different route which is not to replace  $\bar{G}$  with  $\bar{G}^{\text{KS}}$  in the self-energy. Due to Migdal's theorem and the quality of the phonon spectra and coupling matrix elements, the diagrammatic Hartree-Fock approximation to the self-energy is almost exact for the phonon interaction. As we have discussed before during the functional construction in Section 6.3, the numerical results of the final equations of this Section will serve as a reference we compare phonon parts of the SpinSCDFT functional to. Moreover we want to stress again that in a future work we can use the results of this Section to parametrize the SpinSCDFT functional.

The coupled equations for the symmetrized parts of self-energy are usually referred to as the Eliashberg equations [44]. For a system including splitted states, Eliashberg equations are derived in Ref. [19] although we do not follow the reference exactly. Thus, our final set of equations has a different shape. The numerical results will most likely be similar but we cannot be sure with certainty because non-linear calculations are not discussed in the Ref. [19].

We approximate the SE similar as before in Section 6.3 using the first order phonon and Coulomb exchange diagram

$$\bar{\Sigma}^s(\mathbf{r}, \mathbf{r}', \omega_n) \approx \bar{\Sigma}_{\text{ph}}(\mathbf{r}, \mathbf{r}', \omega_n) + \bar{\Sigma}_{\text{Coul}}(\mathbf{r}, \mathbf{r}', \omega_n) - \bar{v}_{\text{xc}}(\mathbf{r}, \mathbf{r}'), \quad (7.50)$$

but here we do not perform the replacement  $\bar{G} \rightarrow \bar{G}^{\text{KS}}$  so that

$$\bar{\Sigma}_{\text{ph}}(\mathbf{r}, \mathbf{r}', \omega_n) = \frac{1}{\beta} \sum_{n' \mathbf{q} \lambda} D_{\text{ph}}^0(\lambda \mathbf{q}, \omega_n - \omega_{n'}) \frac{\delta v_{\text{scf}}(\mathbf{r})}{\delta u_{\mathbf{q}\lambda}} \tau_z \cdot \bar{G}(\mathbf{r}, \mathbf{r}', \omega_{n'}) \cdot \frac{\delta v_{\text{scf}}(\mathbf{r}')}{\delta u_{-\mathbf{q}\lambda}} \tau_z \quad (7.51)$$

$$\bar{\Sigma}_{\text{Coul}}(\mathbf{r}, \mathbf{r}', \omega_n) = \frac{e^2}{\beta} \sum_{n'} w(\mathbf{r}, \mathbf{r}', \omega_n - \omega_{n'}) \tau_z \sigma_0 \cdot \bar{G}(\mathbf{r}, \mathbf{r}', \omega_{n'}) \cdot \tau_z \sigma_0 \quad (7.52)$$

Because we are primarily interested in the shape of the GF, we do not continue the self-energy to the real axis because there the integrals (principle values etc.) are rather slow and unstable to solve numerically. We aim to solve Eq. (7.9) which requires to compute  $\bar{\Sigma}_n^s(\mathbf{e})$ . Again, the  $xc$  potential cancels with the  $xc$  part of the inverse GF as it should.

We distinguish the GF and other properties of this Section from the (more heavily) approximated one of the previous Section 7.2 by putting a superscript E. The procedure is analog to Sec. 6.3 and Sec. 7.2. We discuss the equivalent of the symmetrized self-energy contributions Eq. (7.20). Here it is not possible to analytically sum the Matsubara frequencies so we simply

insert the form of the phonon propagator Eq. (5.48) or the dynamic Coulomb form Eq. (4.12). With the abbreviation<sup>3</sup>

$$\mathfrak{K}_{n,n'}^\mu(\mathbf{e}, \mathbf{e}') = \int d\omega \frac{2\omega\alpha^2 F_\mu^D(\mathbf{e}, \mathbf{e}', \omega)}{(\omega_n - \omega_{n'})^2 + \omega^2} \quad (7.53)$$

$$\begin{aligned} \mathfrak{L}_{n,n'}(\mathbf{e}, \mathbf{e}') &= C^{\text{stat}}(\mathbf{e}, \mathbf{e}') + \int d\omega \left( \frac{2\omega(\alpha^2 F(\mathbf{e}, \mathbf{e}', \omega) + \frac{2\theta(\omega)}{\pi} C^{\text{dyn}}(\omega, \mathbf{e}, \mathbf{e}'))}{(\omega_n - \omega_{n'})^2 + \omega^2} \right. \\ &\quad \left. - \frac{2\theta(\omega)}{\pi\omega} C^{\text{dyn}}(\omega, \mathbf{e}, \mathbf{e}') \right) \end{aligned} \quad (7.54)$$

we arrive at

$$\Sigma_n^{\text{E}\omega}(\mathbf{e}) = \frac{1}{4} \int d\mathbf{e}' \frac{1}{\beta} \sum_{n'\mu} \mathfrak{K}_{n,n'}^\mu(\mathbf{e}, \mathbf{e}') (G_{n'\mu}(\mathbf{e}') + G_{n'\mu}^\dagger(\mathbf{e}')) \quad (7.55)$$

$$A_n^{\text{E}\omega z}(\mathbf{e}) = \frac{1}{4} \int d\mathbf{e}' \frac{1}{\beta} \sum_{n'\mu} \text{sign}(\mu) \mathfrak{K}_{n,n'}^\mu(\mathbf{e}, \mathbf{e}') (G_{n'\mu}(\mathbf{e}') + G_{n'\mu}^\dagger(\mathbf{e}')) \quad (7.56)$$

$$\Sigma_n^{\text{E}\varepsilon}(\mathbf{e}) = \frac{1}{4} \int d\mathbf{e}' \frac{1}{\beta} \sum_{n'\mu} \mathfrak{K}_{n,n'}^\mu(\mathbf{e}, \mathbf{e}') (G_{n'\mu}(\mathbf{e}') - G_{n'\mu}^\dagger(\mathbf{e}')) \quad (7.57)$$

$$\Sigma_n^{\text{E}J}(\mathbf{e}) = \frac{1}{4} \int d\mathbf{e}' \frac{1}{\beta} \sum_{n'\mu} \text{sign}(\mu) \mathfrak{K}_{n,n'}^\mu(\mathbf{e}, \mathbf{e}') (G_{n'\mu}(\mathbf{e}') - G_{n'\mu}^\dagger(\mathbf{e}')). \quad (7.58)$$

and

$$\Sigma_n^{\text{E}\Im\Delta}(\mathbf{e}) = \frac{i}{4} \int d\mathbf{e}' \frac{1}{\beta} \sum_{n'\mu} \text{sign}(\mu) \mathfrak{L}_{n,n'}(\mathbf{e}, \mathbf{e}') (F_{n'\mu}(\mathbf{e}') + F_{n'\mu}^\dagger(\mathbf{e}')) \quad (7.59)$$

$$\Sigma_n^{\text{E}\Re\Delta}(\mathbf{e}) = -\frac{1}{4} \int d\mathbf{e}' \frac{1}{\beta} \sum_{n'\mu} \text{sign}(\mu) \mathfrak{L}_{n,n'}(\mathbf{e}, \mathbf{e}') (F_{n'\mu}(\mathbf{e}') - F_{n'\mu}^\dagger(\mathbf{e}')) \quad (7.60)$$

$$B_n^{\text{E}s}(\mathbf{e}) = \Sigma_n^{\text{E}\Re\Delta}(\mathbf{e}) + i\Sigma_n^{\text{E}\Im\Delta}(\mathbf{e}) = -\frac{1}{2} \int d\mathbf{e}' \frac{1}{\beta} \sum_{n'\mu} \text{sign}(\mu) \mathfrak{L}_{n,n'}(\mathbf{e}, \mathbf{e}') F_{n'\mu}(\mathbf{e}') \quad (7.61)$$

$$B_n^{\text{E}s^*}(\mathbf{e}) = \Sigma_n^{\text{E}\Re\Delta}(\mathbf{e}) - i\Sigma_n^{\text{E}\Im\Delta}(\mathbf{e}) = \frac{1}{2} \int d\mathbf{e}' \frac{1}{\beta} \sum_{n'\mu} \text{sign}(\mu) \mathfrak{L}_{n,n'}(\mathbf{e}, \mathbf{e}') F_{n'\mu}^\dagger(\mathbf{e}'). \quad (7.62)$$

Now the GF is inverted in the same way as in the Section 7.2. Note however that all triplet components  $B_n^t$  and  $B_n^{t^*}$  are assumed to be zero. As compared to Section 7.2 we will use a slight modification that is to introduce  $Z_n^{\text{E}}$  and rewrite

$$\begin{aligned} i\hbar\omega_n Z_n^{\text{E}}(\mathbf{e}) &= i\hbar\omega_n - \Sigma_n^{\text{E}\omega}(\mathbf{e}) & \tilde{\varepsilon}_n^{\text{E}}(\mathbf{e}) &= (\varepsilon + \Sigma_n^{\text{E}\varepsilon}(\mathbf{e})) / Z_n^{\text{E}}(\mathbf{e}) \\ \Delta_n^{\text{E}}(\mathbf{e}) &= B_n^{\text{E}s}(\mathbf{e}) / Z_n^{\text{E}}(\mathbf{e}) & \tilde{J}_n^{\text{E}}(\mathbf{e}) &= (J + \Sigma_n^{\text{E}J}(\mathbf{e})) / Z_n^{\text{E}}(\mathbf{e}) \\ \Delta_n^{\text{E}^*}(\mathbf{e}) &= B_n^{\text{E}s^*}(\mathbf{e}) / Z_n^{\text{E}}(\mathbf{e}) & \tilde{A}_n^{\text{E}\omega z}(\mathbf{e}) &= A_n^{\text{E}\omega z}(\mathbf{e}) / Z_n^{\text{E}}(\mathbf{e}). \end{aligned} \quad (7.63)$$

<sup>3</sup>Again, we drop the diagrammatic Coulomb corrections on the Nambu diagonal against the  $xc$  potential.

The result is

$$G_{n\sigma}^E(\mathbf{e}) = \frac{1}{2\mathfrak{F}_{n\sigma}^E(\mathbf{e})Z_n^E(\mathbf{e})} \sum_{\gamma} \frac{\mathfrak{F}_{n\sigma}^E(\mathbf{e}) + \text{sign}(\gamma)(\tilde{\varepsilon}_n^E(\mathbf{e}) + \text{sign}(\sigma)\tilde{A}_n^{E\omega z}(\mathbf{e}))}{i\hbar\omega_n - \text{sign}(\sigma)\tilde{J}_n^E(\mathbf{e}) - \text{sign}(\gamma)\mathfrak{F}_{n\sigma}^E(\mathbf{e})} \quad (7.64)$$

$$G_{n\sigma}^{E\dagger}(\mathbf{e}) = \frac{1}{2\mathfrak{F}_{n,-\sigma}^E(\mathbf{e})Z_n^E(\mathbf{e})} \sum_{\gamma} \frac{\mathfrak{F}_{n,-\sigma}^E(\mathbf{e}) + \text{sign}(\gamma)(\tilde{\varepsilon}_n^E(\mathbf{e}) - \text{sign}(\sigma)\tilde{A}_n^{E\omega z}(\mathbf{e}))}{i\hbar\omega_n + \text{sign}(\sigma)\tilde{J}_n^E(\mathbf{e}) + \text{sign}(\gamma)\mathfrak{F}_{n,-\sigma}^E(\mathbf{e})} \quad (7.65)$$

$$F_{n\sigma}^E(\mathbf{e}) = \frac{1}{2\mathfrak{F}_{n\sigma}^E(\mathbf{e})Z_n^E(\mathbf{e})} \sum_{\gamma} \frac{\text{sign}(\sigma)\text{sign}(\gamma)\Delta_n^E(\mathbf{e})}{i\hbar\omega_n - \text{sign}(\sigma)\tilde{J}_n^E(\mathbf{e}) - \text{sign}(\gamma)\mathfrak{F}_{n\sigma}^E(\mathbf{e})} \quad (7.66)$$

$$F_{n\sigma}^{E\dagger}(\mathbf{e}) = \frac{1}{2\mathfrak{F}_{n,-\sigma}^E(\mathbf{e})Z_n^E(\mathbf{e})} \sum_{\gamma} \frac{\text{sign}(\sigma)\text{sign}(\gamma)\Delta_n^{E*}(\mathbf{e})}{i\hbar\omega_n + \text{sign}(\sigma)\tilde{J}_n^E(\mathbf{e}) + \text{sign}(\gamma)\mathfrak{F}_{n,-\sigma}^E(\mathbf{e})} \quad (7.67)$$

and

$$\mathfrak{F}_{n\sigma}^E(\mathbf{e}) = \left( (\tilde{\varepsilon}_n^E(\mathbf{e}) + \text{sign}(\sigma)\tilde{A}_n^{E\omega z}(\mathbf{e}))^2 + \Delta_n^E(\mathbf{e})\Delta_n^{E*}(\mathbf{e}) \right)^{\frac{1}{2}}. \quad (7.68)$$

Here we see that the rewriting Eq. (7.63) means the poles of the Nambu-diagonal GFs are directly given at e.g.  $i\hbar\omega_n = \text{sign}(\sigma)\tilde{J}_n^E(\mathbf{e}) + \text{sign}(\gamma)\mathfrak{F}_{n,-\sigma}^E(\mathbf{e})$  which gives the right hand side of the equation an interpretation as a quasi particle energy. Without further simplifications this will be our final result for energy dependent couplings.

However, assuming the couplings to be energy independent and taking the value at the Fermi level

$$\mathfrak{K}_{n,n'}^{\mu}(\mathbf{e}, \mathbf{e}') \equiv \mathfrak{K}_{n,n'}^{\mu}(0, J, 0, J') \quad (7.69)$$

$$\mathfrak{L}_{n,n'}^{\mu}(\mathbf{e}, \mathbf{e}') \equiv \mathfrak{L}_{n,n'}^{\mu}(0, J, 0, J') \quad (7.70)$$

we may reduce the numerical effort to solve the set of equations. We expect that the discussion of Sec. 7.2 about the convergence of the energy integrals extends also to this case. Here  $\mathfrak{F}_{n\sigma}^E(\mathbf{e}) \rightarrow \varepsilon$  for large  $\varepsilon$  so  $G^E$  and  $G^{E\dagger}$  both behave as  $\frac{1}{\varepsilon}$ . Because also the function  $\tilde{\varepsilon}_n^E(\mathbf{e}) \rightarrow \varepsilon$  only the summand  $\gamma = +$  will be relevant in  $G^E$  and  $G^{E\dagger}$ . Thus, again, we arrive at a form  $G^E \pm G^{E\dagger} \rightarrow \frac{1}{A+\varepsilon} \pm \frac{1}{A-\varepsilon}$  behaving as  $\frac{1}{\varepsilon^2}$  only for (+). The  $F^E$ 's behave intrinsically as  $\frac{1}{\varepsilon^2}$  i.e. are local at the Fermi energy in the sense that the integral does not depend on the high, or low energy structure of the coupling (if it is bounded). Thus, together with the state dependence of the coupling, we have to drop energy and splitting renormalization

$$\Sigma_n^{E\varepsilon}(\mathbf{e}) = \Sigma_n^{EJ}(\mathbf{e}) = 0 \quad (7.71)$$

With this state-independence the following quantities do not depend on energy (but on splitting):  $Z_n^E, \Delta_n^E, \Delta_n^{E*}$  and  $\tilde{A}_n^{E\omega z}$ . Moreover  $\tilde{\varepsilon}_n^E(\mathbf{e}) \equiv \varepsilon/Z_n^E$  and  $\tilde{J}_n^E \equiv J/Z_n^E$ . For the following consideration we also drop the Coulomb interaction, static and dynamic because then we may analytically integrate  $F_{n'\mu}^E(\mathbf{e}')$  and  $F_{n'\mu}^{E\dagger}(\mathbf{e}')$  over energy in the Eqs. (7.61) and (7.62). In addition the approximation Eq. (7.69) is not well suited for the Coulomb interaction and, if used anyhow, leads to one single number that has to be taken as an adjustable parameter (referred to as  $\mu^*$  see e.g.[62]). Now with the abbreviation

$$m_{n,\sigma} = i\hbar\omega_n Z_n^E + \text{sign}(\sigma)\tilde{A}_n^{E\omega z} Z_n^E \quad (7.72)$$

$$a_n = -J^2 + (\tilde{A}_n^{E\omega z} Z_n^E)^2 + (Z_n^E)^2 \Delta_n^E \Delta_n^{E*} + (Z_n^E)^2 (\hbar\omega_n)^2 \quad (7.73)$$

$$b_n = 2\tilde{A}_n^{E\omega z} Z_n^E \quad (7.74)$$

$$c_n = 2i\hbar\omega_n Z_n^E J \quad (7.75)$$

and after some algebra we obtain the analytic energy dependence

$$G_{n\sigma}^E(\epsilon) + G_{n\sigma}^{E\dagger}(\epsilon) = \frac{-\text{sign}(\sigma)J - m_{n,\sigma} + \epsilon}{a_n + \epsilon^2 - \text{sign}(\sigma)(c_n + b_n\epsilon)} + \frac{\text{sign}(\sigma)J - m_{n,\sigma} - \epsilon}{a_n + \epsilon^2 + \text{sign}(\sigma)(c_n + b_n\epsilon)}. \quad (7.76)$$

Because this combination decays faster than  $\epsilon^{-1}$  for large  $\epsilon$ , we may compute the integral in the SE e.g. Eq. (7.55) as the sum of residues in the upper complex half plane. As it is not clear which of the four poles in the above function will be in the upper half we compute all residues. Adding those up, we obtain the energy integral in Eq. (7.55) and Eq. (7.56) with

$$\mathfrak{S}_{n,\sigma}^E = \sqrt{-((Z_n^E)^2 \Delta_n^E \Delta_n^{E*} - (i\hbar\omega_n Z_n^E - \text{sign}(\sigma)J)^2)} \quad (7.77)$$

as

$$\begin{aligned} \mathfrak{M}_{n\sigma} &= \int d\epsilon (G_{n\sigma}^E(\epsilon) + G_{n\sigma}^{E\dagger}(\epsilon)) \\ &= \pi i \left( \frac{i\hbar\omega_n Z_n^E - \text{sign}(\sigma)J}{\mathfrak{S}_{n,\sigma}^E} - 1 \right) \theta \left( \Im(-\text{sign}(\sigma)\tilde{A}_n^{E\omega z} Z_n^E - \mathfrak{S}_{n,\sigma}^E) \right) \\ &\quad + \pi i \left( -\frac{i\hbar\omega_n Z_n^E - \text{sign}(\sigma)J}{\mathfrak{S}_{n,\sigma}^E} - 1 \right) \theta \left( \Im(-\text{sign}(\sigma)\tilde{A}_n^{E\omega z} Z_n^E + \mathfrak{S}_{n,\sigma}^E) \right) \\ &\quad + \pi i \left( \frac{i\hbar\omega_n Z_n^E + \text{sign}(\sigma)J}{\mathfrak{S}_{n,-\sigma}^E} + 1 \right) \theta \left( \Im(\text{sign}(\sigma)\tilde{A}_n^{E\omega z} Z_n^E - \mathfrak{S}_{n,-\sigma}^E) \right) \\ &\quad + \pi i \left( -\frac{i\hbar\omega_n Z_n^E + \text{sign}(\sigma)J}{\mathfrak{S}_{n,-\sigma}^E} + 1 \right) \theta \left( \Im(\text{sign}(\sigma)\tilde{A}_n^{E\omega z} Z_n^E + \mathfrak{S}_{n,-\sigma}^E) \right). \end{aligned} \quad (7.79)$$

Further, for Eqs. (7.61) and (7.62) we integrate  $F_{n\sigma}^E(\epsilon)$  in energy (note that  $F_{n\sigma}^E(\epsilon) = \frac{\Delta_n^E(\epsilon)}{\Delta_n^{E*}(\epsilon)} F_{n,-\sigma}^{E\dagger}(\epsilon)$ ) where we define

$$\mathfrak{N}_n = \frac{1}{Z_n^E \Delta_n^E} \int d\epsilon (F_{n\uparrow}^E(\epsilon) - F_{n\downarrow}^E(\epsilon)) \quad (7.80)$$

$$\begin{aligned} &= \pi i \left( \frac{\theta(\Im(-\tilde{A}_n^{E\omega z} Z_n^E - \mathfrak{S}_{n,\uparrow}^E))}{\mathfrak{S}_{n,\uparrow}^E} - \frac{\theta(\Im(-\tilde{A}_n^{E\omega z} Z_n^E + \mathfrak{S}_{n,\uparrow}^E))}{\mathfrak{S}_{n,\uparrow}^E} \right. \\ &\quad \left. + \frac{\theta(\Im(\tilde{A}_n^{E\omega z} Z_n^E - \mathfrak{S}_{n,\downarrow}^E))}{\mathfrak{S}_{n,\downarrow}^E} - \frac{\theta(\Im(\tilde{A}_n^{E\omega z} Z_n^E + \mathfrak{S}_{n,\downarrow}^E))}{\mathfrak{S}_{n,\downarrow}^E} \right). \end{aligned} \quad (7.81)$$

We obtain the Eliashberg equations similar to their usual, spin-degenerate form [62], that only implicitly refer to the GF

$$Z_n^E(J) = 1 + \frac{i}{4\hbar\omega_n} \int dJ' \frac{1}{\beta} \sum_{n'\sigma} \mathfrak{K}_{n,n'}^\sigma(0, J, 0, J') \mathfrak{M}_{n'\sigma}(J') \quad (7.82)$$

$$\tilde{A}_n^{E\omega z}(J) = \frac{1}{4Z_n^E(J)} \int dJ' \frac{1}{\beta} \sum_{n'\sigma} \text{sign}(\sigma) \mathfrak{K}_{n,n'}^\sigma(0, J, 0, J') \mathfrak{M}_{n'\sigma}(J') \quad (7.83)$$

$$\Delta_n^E(J) = -\frac{1}{2Z_n^E(J)} \int dJ' \frac{1}{\beta} \sum_{n'} \mathfrak{L}_{n,n'}(0, J, 0, J') Z_{n'}^E(J') \Delta_{n'}^E(J') \mathfrak{N}_{n'}(J') \quad (7.84)$$

$$\Delta_n^{E*}(J) = -\frac{1}{2Z_n^E(J)} \int dJ' \frac{1}{\beta} \sum_{n'} \mathfrak{L}_{n,n'}(0, J, 0, J') Z_{n'}^E(J') \Delta_{n'}^{E*}(J') \mathfrak{N}_{n'}(J') \quad (7.85)$$

where

$$\mathfrak{R}_{n,n'}^\sigma(0, J, 0, J') = \int d\omega \frac{2\omega \alpha^2 F_\sigma^D(0, J, 0, J', \omega)}{(\omega_n - \omega_{n'})^2 + \omega^2} \quad (7.86)$$

$$\mathfrak{L}_{n,n'}(0, J, 0, J') = \int d\omega \frac{2\omega \alpha^2 F(0, J, 0, J', \omega)}{(\omega_n - \omega_{n'})^2 + \omega^2}. \quad (7.87)$$

Note that  $\mathfrak{R}_{n,n'}^\sigma$  and  $\mathfrak{L}_{n,n'}$  are symmetric in  $n$  and  $n'$ . Because  $\Delta_n^E$  and  $\Delta_n^{E*}$  satisfy the same equation and are not coupled, starting from the same initial values, they have to evolve equally. Thus we may simply take  $\Delta_n^E = \Delta_n^{E*}$  which is equivalent to assuming  $\Sigma_n^{E\Delta} = 0$ . Ultimately this is a consequence of the gauge transformation that rotates off diagonal Nambu components (compare Subsection 3.6.2).

If the coupling is spin independent  $\alpha^2 F_\sigma^D = \alpha^2 F_{-\sigma}^D$ , note  $\tilde{A}_n^{E\omega z} \propto \sum_{n'} (\mathfrak{M}_{n'\uparrow} - \mathfrak{M}_{n'\downarrow})$ . Then, if we start with  $\tilde{A}_n^{E\omega z} = 0$  it will remain zero in the self-consistency iteration. Starting with  $\tilde{A}_n^{E\omega z} \neq 0$  may shift the poles and invalidate this result. Studing the effect of a spin dependent coupling and thus a non-vanishing  $\tilde{A}_n^{E\omega z}$  is beyond the scope of this thesis.

High and low temperature limits are discussed in the Appendix H. In essence we prove that for high temperatures the system is not SC.

## Summary

No higher principle requires the KS DOS to be a reasonable approximation and in fact we find in the next Chapter 8 that it is not in some cases. We have introduced an isotropic form of the Dyson equation with a SE that is diagonal in the normal state KS orbitals. To improve upon the SC KS DOS, we keep the SE used in the functional construction of Chapter 6 but then use it to solve the Dyson equation. This is the SC analog of the well known G0W0 approximation to improve semi-conductor gaps. Thus, the SE is given solely by SpinSCDFT data and the DOS from the resulting GF can be computed without a self-consistent iteration. In a final step we kept the dependence of the SE on the interacting GF. When we approximate the SE to be independent of the underlying KS states (assume it to be energy independent in the isotropic formulation) we arrived at the Eliashberg equations similar to their usual form for the spin degenerate system. The self-consistent solution to these equations constitutes a reference for the phononic coupling for comparison to our SpinSCDFT results.



# 8. Application to an Exchange-Splitted Free Electron Gas Model

In Chapters 6 and 7 we have derived several new methods that allow us to compute SC properties of real materials. These generalize earlier works in the sense that we can handle magnetic fields while computing  $T_c$ . Furthermore, we can compute excitation spectra of the KS or the Many-Body system (in the G0W0 like approximation).

In addition, as part of this work, the following equations were implemented in a code:

1. The isotropic Sham-Schlüter Eq. (6.97) in the linear approximation.
2. The isotropic version of the non-linear gap equation Eq. (6.74) as derived from Eq. (6.97).
3. The KS excitation spectrum according to Eq. (G.23).
4. The one-cycle Many-Body (G0W0) DOS and LDOS with the KS SE that lead to Eq. (7.48).
5. The isotropic Eliashberg Eqs. (7.82) to (7.85).
6. Tools to average the coupling matrix elements on equal center of energy and splitting surfaces as well as routines to compute the (local) double DOS  $\varrho(\epsilon)$  ( $\varrho_\sigma(\mathbf{e}\mathbf{r})$ ).

In this Section we test the machinery on the easiest system possible: The free electron gas with an exchange splitting parameter. We give details of the model in Section 8.1 where essentially only the temperature and a homogeneous splitting of electronic states are left as parameters. In Section 8.2 we discuss  $T_c(J)$  curves from the linearized SSE (Eq. (6.91)) in several approximations discussed in the previous Part. In addition, we present the shape of individual contributions to  $\check{S}_\beta$ . In Section 8.3 we solve the SSE in the form of the gap equation (Eq. (6.74)) via a fixed point iteration. While the right eigenfunction to a singular eigenvalue of  $\check{S}_\beta$  is only defined up to the norm, the fully non-linear gap equation allows to compute  $\Delta_s^s$  with a defined magnitude also at temperatures different from  $T_c$ . We use the resulting  $\Delta_s^s$  to compute the SC DOS of the G0W0 interacting system. In Section 8.4 we briefly discuss the results if a static Coulomb interacting is included before, in the Section 8.5, we solve the Eliashberg equations derived in Section 7.3 for comparison.

## 8.1. Details of the Model

We want to study the basic features of SpinSCDFT in the most simple model possible to avoid further, material specific, complications. For this purpose we briefly introduce the free electron gas model in this Section and add a phononic coupling to make it SC. Then, as an additional step, we add a homogeneous external magnetic field that splits electronic states with different spin in energy. While the dependence of  $T_c$  on the phononic coupling is well understood and not the main topic of this thesis - we fix it to loosely resemble the coupling of MgB<sub>2</sub> - we are concerned with the effect of splitting of the underlying electronic structure on SC properties in SpinSCDFT. The implementation in a computer code uses Hartree atomic units throughout. As we have seen earlier in Sec. 3.6.2, the phase of the gap function is not fixed in the equation and we choose to make the gap real and positive at the Fermi level.

### 8.1.1. The Double DOS Function $\varrho(\epsilon)$ of the Splitted Electron Gas

The dispersion relation of the free electron gas, subject to a homogenous field  $B_0$  is

$$\epsilon_{\mathbf{k}\sigma} = \frac{\hbar^2}{2m_e} \mathbf{k}^2 - E_f + \text{sign}(\sigma)\mu_B B_0. \quad (8.1)$$

Thus  $\frac{\epsilon_{\mathbf{k}\uparrow} - \epsilon_{-\mathbf{k}\downarrow}}{2} = \mu_B B_0$  and  $\frac{\epsilon_{\mathbf{k}\uparrow} + \epsilon_{-\mathbf{k}\downarrow}}{2} = \frac{\hbar^2 \mathbf{k}^2}{2m_e} - E_f$  and it immediately follows from the definition of the double DOS Eq. (6.92), that

$$\varrho^{\text{EG}}(\epsilon) = \sum_{\mathbf{k}} \delta\left(\frac{\hbar^2 \mathbf{k}^2}{2m_e} - E_f - \epsilon\right) \delta(\mu_B B_0 - J) = \delta(\mu_B B_0 - J) \rho^{\text{EG}}(\epsilon). \quad (8.2)$$

Here,  $\rho^{\text{EG}}(\epsilon)$  is evaluated in energy space, not frequency space, to comply with the computer code. The difference is a factor of  $2\pi/\hbar$  that multiplies function in frequency, but not in energy space. The factor in turn ensures that the DOS integrates to  $n_e$  electrons per unit cell up to  $E_f$ , where the  $2\pi$  cancels the Fourier normalization in frequency space. We use the relation of the DOS for the spin degenerate free electron gas (per spin channels. See [63, p. 44]):

$$\rho^{\text{EG}}(E) = \frac{\Omega_{\text{UC}}}{\sqrt{2\pi^2}} \left(\frac{m_e}{\hbar^2}\right)^{\frac{3}{2}} \sqrt{E + E_f} \quad (8.3)$$

$$= \frac{3}{4E_f} \frac{n_e}{\Omega_{\text{UC}}} \sqrt{\frac{E + E_f}{E_f}}. \quad (8.4)$$

Again, we have to be careful that  $\frac{\epsilon_{\mathbf{k}\uparrow} + \epsilon_{-\mathbf{k}\downarrow}}{2}$  has the weight of a single spin channel, equivalent to  $\epsilon_{\mathbf{k}\sigma}$ . This is why we have to take the single spin channel DOS of the free electron gas. We are going to treat  $J$  as a parameter to investigate the dependence of the SpinSCDFT kernels on an external magnetic field.

The scale of  $J$  in experiment could be interpreted as the range of magnetic fields before vortices appear. Experimentally, in the example of  $\text{MgB}_2$  (a Type II SC) the lower critical field  $B_0$  is in the range of  $\mathcal{O}(10^{-2}\text{T})$  to  $\mathcal{O}(10^{-1}\text{T})$  [64].  $J = 0.1\text{mHa}$  corresponds to an external field of

$$B_0(J = 0.1\text{mHa}) \approx 4.7\text{T}. \quad (8.5)$$

Thus, in reality  $J \geq \mathcal{O}(0.01\text{mHa})$  must be considered unrealistic for  $\text{MgB}_2$  because we cannot describe the vortex state and we should limit the discussion to Type I SC. Since we intend to study the behavior of the SpinSCDFT functionals this is of no concern to us at this point. We postpone the comparison with experiment to the next Part II.

The Fermi energy is defined by integrating the DOS Eq. (8.3) up to  $E_f$  to have  $n_e$  electrons in the system. This defining equation can be inverted to give  $E_f$  as a function of the volume of the unit cell and the number of electrons. In zeroth order in  $\frac{\mu_B B_0}{E_f} \approx 0$  we obtain the normal relation for the free electron gas  $E_f^0 = (3\pi^2 \frac{n_e}{\Omega_{\text{UC}}})^{\frac{2}{3}} \frac{\hbar^2}{2m_e}$  which has to be regarded as almost exact for our small splitting energies. As parameters we set  $\frac{n_e}{\Omega_{\text{UC}}} = 1 a_0^{-3}$  ( $a_0$  is the Bohr radius, the length measure in Hartree units) which leads to a relatively large Fermi Energy of 4.78 Ha.

### 8.1.2. The Model for the Phononic Coupling $\alpha^2 F$

We use an electron-phonon coupling in a three parameter model

$$\alpha^2 F(\omega, \mathbf{e}, \mathbf{e}') \equiv \alpha^2 F(\omega) = \lambda \frac{\omega}{2} \frac{1}{\omega_w \sqrt{\pi}} e^{-\frac{1}{2}(\frac{\omega - \omega_0}{\omega_w})^2} \quad (8.6)$$

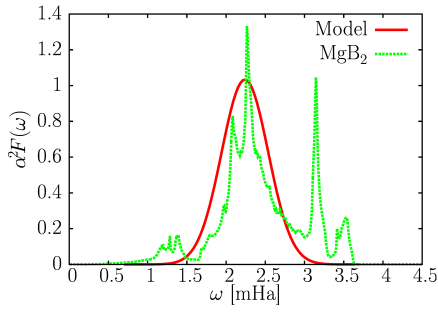


Figure 8.1.:  $\alpha^2 F(\omega)$  of the model and  $\text{MgB}_2$  for comparison.

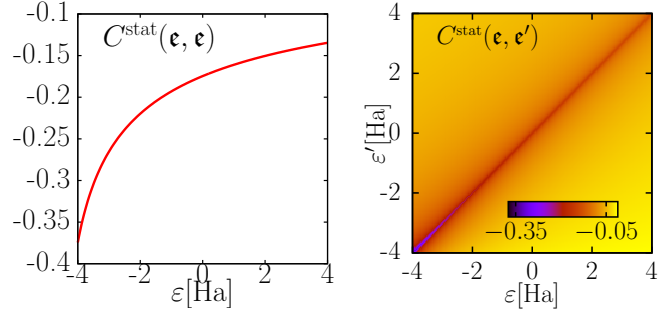


Figure 8.2.: Model  $C^{\text{stat}}(\boldsymbol{\epsilon}, \boldsymbol{\epsilon}')$  according to Eq. (8.7). Parameters are  $E_f = 4.78$  Ha and  $k_{\text{TF}}^2 = (0.005)^2$  Ha.

with the electron-phonon coupling constant  $\lambda$ . To model the frequency dependence we employ a Gaussian, centered about the Einstein frequency  $\omega_0$  with a width  $\omega_w$ . We use the parameters  $\hbar\omega_0 = 2.2\text{mHa}$ ,  $\hbar\omega_w = 0.5\text{mHa}$  and  $\lambda = 0.7$  throughout the Chapter. With these parameters the resulting coupling loosely resembles the main peak in  $\alpha^2 F(\omega)$  of  $\text{MgB}_2$ . The resulting curve is given in Fig. 8.1 with the computed one for  $\text{MgB}_2$  for comparison.

### 8.1.3. The Model for the Coulomb Coupling $C^{\text{stat}}(\boldsymbol{\epsilon}, \boldsymbol{\epsilon}')$

For simplicity we neglect the Coulomb interaction in most parts of this Chapter. If we consider it, we use a simple model that is based on the Thomas-Fermi screening theory, valid for slowly varying electronic potentials. From Ref. [62] and Ref. [21] we take the formula

$$C^{\text{stat}}(\boldsymbol{\epsilon}, \boldsymbol{\epsilon}') \approx -\frac{\pi \ln\left(\frac{\epsilon + \epsilon' + 2E_f + 2\sqrt{(\epsilon + E_f)(\epsilon' + E_f) + \frac{1}{2}k_{\text{TF}}^2}}{\epsilon + \epsilon' + 2E_f - 2\sqrt{(\epsilon + E_f)(\epsilon' + E_f) + \frac{1}{2}k_{\text{TF}}^2}}\right)}{2\sqrt{(\epsilon + E_f)(\epsilon' + E_f)}} \rho^{\text{EG}}(\boldsymbol{\epsilon}'). \quad (8.7)$$

To arrive at the above equation one has to assume a slowly varying density in real space and consider the free electron gas KS wavefunctions and average on energy isosurfaces. For details see Ref. [62], [21] and references therein. The Thomas Fermi vector is taken here as an additional parameter while in principle its value is determined by the free electron gas model to be  $k_{\text{TF}}^2 = 4\pi\rho^{\text{EG}}(0)$ . In real space, the Thomas Fermi interaction is [21]

$$v(\mathbf{r}, \mathbf{r}') = \frac{e^{-k_{\text{TF}}|\mathbf{r} - \mathbf{r}'|}}{|\mathbf{r} - \mathbf{r}'|} \quad (8.8)$$

and thus  $k_{\text{TF}}^{-1}$  has the interpretation of a screening length. With our high density  $\frac{n_e}{\Omega_{\text{uc}}} = 1 a_0^{-3}$  the screening would be extremely effective ( $k_{\text{TF}}^2 \approx 1.4\text{Ha}$ ) and the Coulomb repulsion has an extremely short range. We employ a greatly reduced  $k_{\text{TF}}^2 = (0.005)^2\text{Ha}$  to increase the range which allows us to see the effect of the Coulomb renormalization (discussed later in Sec. 9.3) in a more pronounced way. The shape of the modeled  $C^{\text{stat}}(\boldsymbol{\epsilon}, \boldsymbol{\epsilon}')$  is shown in Fig. 8.2 (right) with the diagonal to the left.

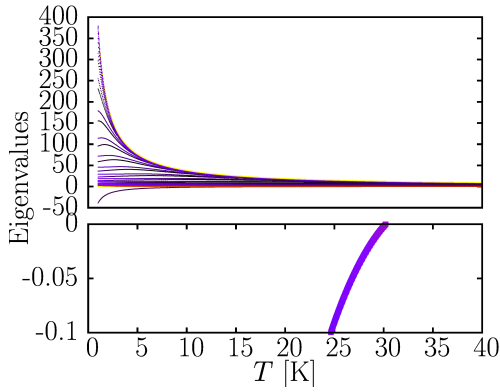


Figure 8.3.: Spectrum of  $\check{S}_\beta(J = 0.0\text{mHa})$  as a function of  $T$ . We find only one singular point.

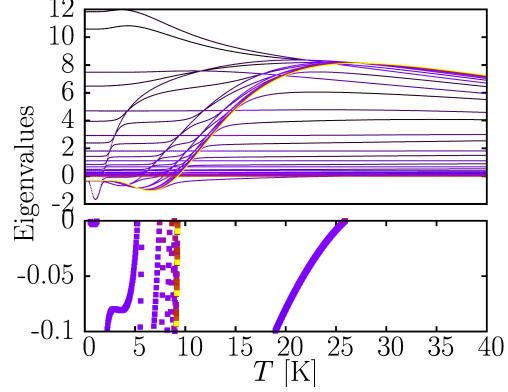


Figure 8.4.: Spectrum  $\check{S}_\beta(J = 0.1\text{mHa})$  as a function of  $T$ . We use  $\check{S}_\beta^{\text{TPHS}}$  together with  $\check{S}_{\text{ph}\beta}^{\text{e}}$  and find many singular points.

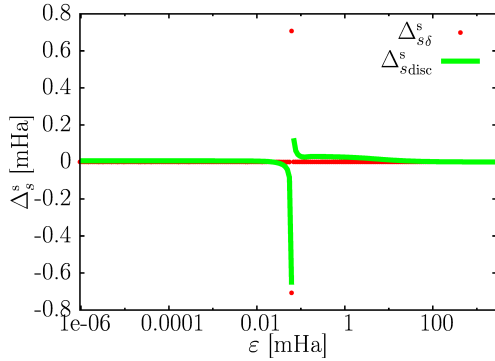


Figure 8.5.: Eigenfunctions to a singular eigenvalue at  $T \approx T_{\text{cross}}$ . All eigenfunctions investigated except one are of either type.

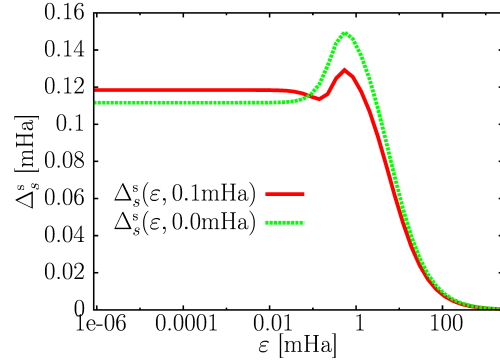


Figure 8.6.: Eigenfunctions at  $T_c$  for  $J = 0.0\text{mHa}, 0.1\text{mHa}$ .

## 8.2. Behavior of SpinSCDFT Kernels and $T_c(J)$ in the second order regime

In this Section we study the linearized SSE (Eq. 6.126). In the Subsection 8.2.1 we perform an eigenvalue decomposition of the matrix  $\check{S}_\beta$  as a function of temperature. We discuss the general shape of the contributions  $\check{S}_\beta^{\text{M}}(\mathbf{e})$ ,  $\check{S}_\beta^{\text{D}}(\mathbf{e})$  (both diagonal) and  $\check{S}_\beta^{\text{e}}(\mathbf{e}, \mathbf{e}')$  in Subsection 8.2.2. Based on the analysis of  $\check{S}_\beta(\mathbf{e}, \mathbf{e}')$ , in Subsection 8.2.3, we compute and discuss  $T_c(J)$ . If the splitting passes the point where the arbitrarily small solutions cease to exist (compare the BCS solution Chapter 2 and Fig. 2.1), the initial assumption of the linearization, namely the existence of a small  $\Delta_s^s$ , is not met. Then, the linearization cannot give sensible results. Still, to compare with earlier spin-degenerate results and because in a fairly large regime we expect a second order phase transition, the linear SSE is important. All eigenfunctions we show are normalized to a common value.

### 8.2.1. Critical Temperatures and the Shape of $\Delta_s^s$

The linear SSE has a solution,  $\Delta_s^s$ , if we can find a zero eigenvalue. In Fig. 8.3 we show the

spectrum for the spin-degenerate case  $J = 0\text{mHa}$  using 100 points on an exponential grid in  $\varepsilon$ . As a general feature we see that the eigenvalues smoothly decrease in size with temperature. At low temperatures we have precisely one negative eigenvalue that crosses zero at a certain temperature ( $\approx 30\text{K}$  in this example) and the matrix  $\check{S}_\beta$  becomes positive definite. In Fig. 8.3 and 8.4, we have highlighted the region closely below 0.0 to see the crossing in a more pronounced way. For  $J = 0\text{mHa}$  we find only one singular eigenvalue.

In Fig 8.4, we investigate the spectrum of the Sham-Schlüter matrix using  $\check{S}_{\text{ph}\beta}^e$  and  $\check{S}_\beta^{\text{TPHS}}$  at a fixed exchange-splitting of  $J = 0.1\text{mHa}$ . Note that using only singlet contributions  $\check{S}_{\text{ph}\beta}^{se}$  and/or replacing  $\check{S}_\beta^{\text{TPHS}}$  with  $\check{S}_\beta^{\text{PHS}}$  has essentially no effect on the spectrum (we do not show the results). As compared to the  $J = 0\text{mHa}$  case the spectrum is fundamentally different. For small  $T$  we have many negative eigenvalues. As the most striking result we find many solutions  $\det(\check{S}_\beta) = 0$  at low temperatures. There is a certain small temperature range, here  $T_{\text{cross}} \approx 10\text{K}$ , in which most negative eigenvalues cross zero and become positive but some also before. Beyond  $T_{\text{cross}}$  only one remaining eigenvalue is negative, is crossing later at  $T \approx 25\text{K}$  and thereby making the matrix positive definite. Smoothly reducing  $J$ , this specific eigenvalue/eigenfunction pair can be traced to the original solution to the SSE in the spin-degenerate limit. Although we do not show this here, it is found that  $T_{\text{cross}}$  goes to zero with  $J$  and there is only one negative eigenvalue below  $T_c$  (compare Fig. 8.3). With several formal solutions, we need to define what the **critical** temperature should be, because we can find zero eigenvalues at multiple temperatures.

We study the shape of the eigenfunctions to the singular eigenvalues and find that they all appear numerically unbound except one. In this example, the bound, continuous solution to the linear SSE appears at  $T \approx 25\text{K}$  for  $J = 0.1\text{mHa}$ . With decreasing  $J$  it is continuously going to the solution of the spin-degenerate system. Examples for the other eigenfunctions are given in Fig. 8.5. In fact, we find only two distinct types of numerically unbound eigenfunctions to singular eigenvalues<sup>1</sup>. While type one has a pole, the second kind has a delta peak like structure, i.e. the value at one sampling point (the one at the discontinuity of the first kind) is large while the rest is extremely small. Increasing the sampling points increased the value at the discontinuity so this lead to the conclusion that we are numerically sampling an unbound function.

It has to be understood that an unbound solution to a linearized equation is not similar the originally non-linear fixed-point equation because a the singularity the function cannot be made small. Since the solution is not small, the linearization was not justified. Thus, we conclude that the solutions in Fig. 8.4 are artifacts of the non-existence of a small pairing and that in the non-linear equation these type of solutions will be suppressed. Thus we **define** the critical temperature to be the temperature at which the **numerically bound** solution passes zero. We show two eigenfunctions at  $T_c$  with a splitting of  $J = 0.1\text{mHa}$  or without in Fig. 8.6. Equipped with this definition we compute  $T_c$  as a function of the splitting parameter  $J$ . Before, however, we discuss the contributions to the Sham-Schlüter operator in detail. We keep the high resolution of 400 points for the rest of the Section to show smoother plots. Note that this increased sampling also slightly reduces  $T_c$  for example from 30.5K to 29.0K for  $J = 0\text{mHa}$ . For our purpose to study the general behavior of the theory we consider 100 points as converged. When we study the non-linear equation we use 100 sampling points for a better performance.

<sup>1</sup>The number of sampling points was increased to 400 to make the jump better visible.

### 8.2.2. Temperature Dependence of $\check{S}_\beta$

In this Subsection we present the individual contributions  $\check{S}_\beta^M$ ,  $\check{S}_\beta^D$  and  $\check{S}_\beta^e$  as a function of  $T$  for  $J = 0.1\text{mHa}$  and  $J = 0.0\text{mHa}$ . For the diagonal matrices  $\check{S}_\beta^M$  and  $\check{S}_\beta^D$  we use a color scale to indicate the temperature while for the matrices we choose the 5 temperatures 1K, 5K, 10K, 15K and 30K. Note the logarithmic scale in all plots discussed in this Section. In the first row of Fig. 8.7 we show the temperature dependence of diagonal  $\check{S}_\beta^D$ . The difference between the total  $\check{S}_\beta^{\text{TPHS}}$  (middle) and the partially particle-hole symmetrized  $\check{S}_\beta^{\text{PHS}}$  (right) is negligible. The shape of  $\check{S}_\beta^{\text{PHS}}$  at  $J = 0.1\text{mHa}$  distinguishes from the non-splitted limit (left) mainly in the range  $\varepsilon \leq J$  in being negative and going to zero for small temperatures. At  $T$  a bit larger than  $T_{\text{cross}}$ , both  $\check{S}_\beta^{\text{PHS}}$  and  $\check{S}_\beta^{\text{TPHS}}$  cross zero at the Fermi level and assume the sign of the non-splitted limit. In the second row, the diagonal of the term  $\check{S}_\beta^M$  is given for the non-splitted limit (left) and for  $J = 0.1\text{mHa}$  (middle). We see that also this term goes to zero for  $\varepsilon < J$  at low temperatures. We observe that approximately at  $T_{\text{cross}}$  for finite splitting  $\check{S}_\beta^M + \check{S}_\beta^D \approx 0$  at the Fermi level.

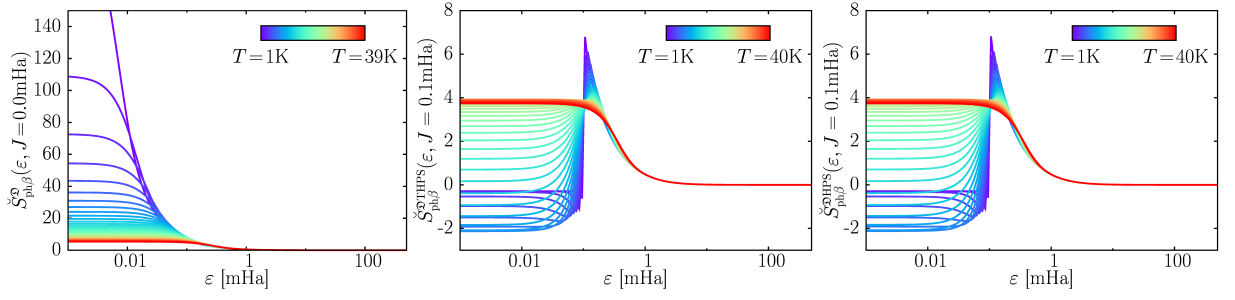
The remainder of the plots in Fig. 8.7 show the non-diagonal  $\check{S}_\beta^e(\mathbf{e}, \mathbf{e}')$  term for the spin-degenerate limit (third row), the purely singlet (fourth row) and the full term including intermediate triplet contributions (fifth row). The color scale for negative values of blue to white to green is chosen with the maximum of  $\check{S}_\beta^M$  (white) as a reference point, indicated on the right of every plot. This is because  $\check{S}_\beta^M$  serves as a scale that other kernel contributions have to be compared to. For positive values, we use red to yellow to white. Zero contours are indicated by a purple curve. For  $J = 0\text{mHa}$  we note that the size of  $\check{S}_\beta^e(\mathbf{e}, \mathbf{e}')$  decays faster with temperature than those of the diagonal  $\check{S}_\beta^M(\mathbf{e})$  and  $\check{S}_\beta^D(\mathbf{e})$  (compare the position of the white point in the color scale). Being both positive,  $\check{S}_\beta^M(\mathbf{e})$  and  $\check{S}_\beta^D(\mathbf{e})$  alone would result in a positive definite Sham-Schlüter matrix. Thus, technically, the phase transition from the SC to the NS is induced by this relative reduction of  $\check{S}_\beta^e(\mathbf{e}, \mathbf{e}')$ .

As a side note, we observe that  $\check{S}_\beta^e(\varepsilon, 0, \varepsilon', 0)$  changes shape from a triangular to a more rectangular structure. This means for low temperatures its decay is dominated by  $\varepsilon + \varepsilon'$  while for higher temperatures this changes to  $\max(\varepsilon, \varepsilon')$ .

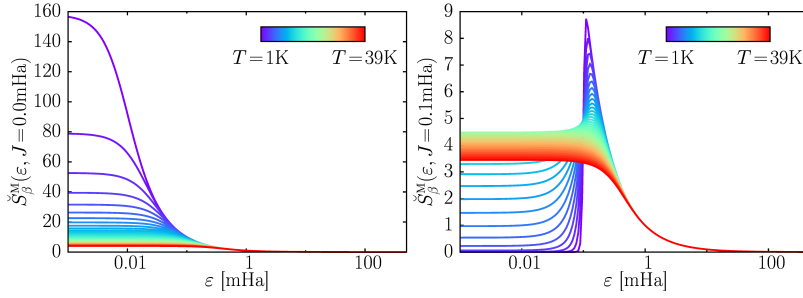
The relative scale reduction is also found for the splitted kernels. At the Fermi level, however, we stay much below the scale of  $\check{S}_\beta^M(\mathbf{e})$  and exceed it only for higher temperatures. Moreover,  $\check{S}_\beta^D(\mathbf{e})$  features a sign change effectively reducing the diagonal repulsion.

The zero contour shows that for very low  $T$ , both  $\check{S}_\beta^e(\mathbf{e}, \mathbf{e}')$  and  $\check{S}_\beta^{se}(\mathbf{e}, \mathbf{e}')$  are positive for approximately the plain where  $(|\varepsilon| - J)(|\varepsilon'| - J) < 0$  and have a sharp negative spike at  $\varepsilon = \varepsilon' \approx J$ . For increasing temperatures the positive parts of  $\check{S}_\beta^{se}(\mathbf{e}, \mathbf{e}')$  shrink to the region where the center of energy  $\varepsilon$  has the size of the splitting. Approximately at  $T_{\text{cross}}$  both  $\check{S}_\beta^e(\mathbf{e}, \mathbf{e}')$  and  $\check{S}_\beta^{se}(\mathbf{e}, \mathbf{e}')$  become totally negative and, for even increasing temperatures, approach the shape and size of the spin degenerate limit.

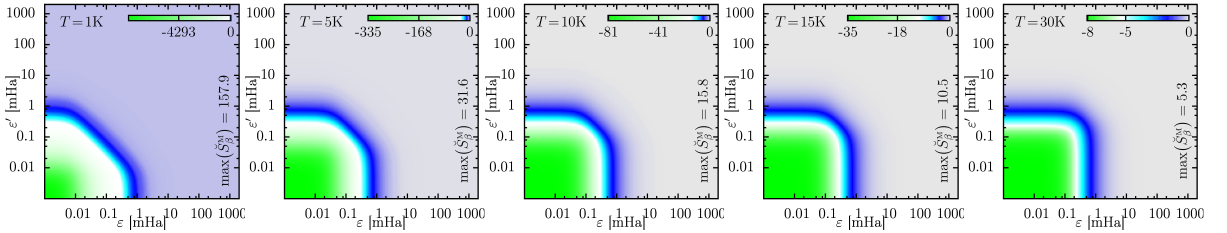
In summary we can say that we see dramatic changes in the spin splitted SSE for the low temperature limits in the region  $|\varepsilon| < |J|$  as compared to the spin degenerate case. Then, at larger temperatures, the splitting becomes less important. From the form of the Bogoliubov eigenvalues  $E_\sigma^\alpha = \text{sign}(\sigma)J + \text{sign}(\alpha)\sqrt{\varepsilon^2 + |\Delta_s^\alpha|^2}$  we guess that if  $\Delta_s^\alpha$  is larger than  $J$  in this  $|\varepsilon| < |J|$  region we would see less dramatic changes from  $J = 0$  to  $J \neq 0$ . The reason is that then only the  $\alpha = +$  branch has positive excitation energies  $E_\sigma^+ \geq 0$  and means the ground state does not correspond to some of the excitations  $\hat{\gamma}_k$  being occupied (see the discussion in Subsection 3.5.2).



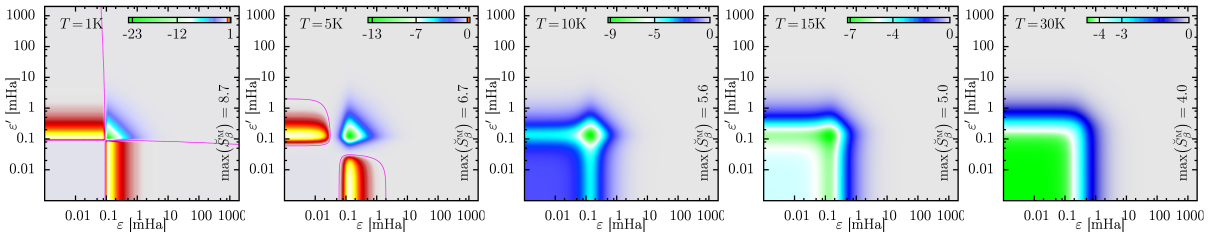
$\check{S}_\beta^{\text{TPHS}}(\mathbf{e})$  (middle) and  $\check{S}_\beta^{\text{PHS}}(\mathbf{e})$  (right) for  $J=0.1\text{mHa}$ . For  $J=0\text{mHa}$  (left) both approximation agree.



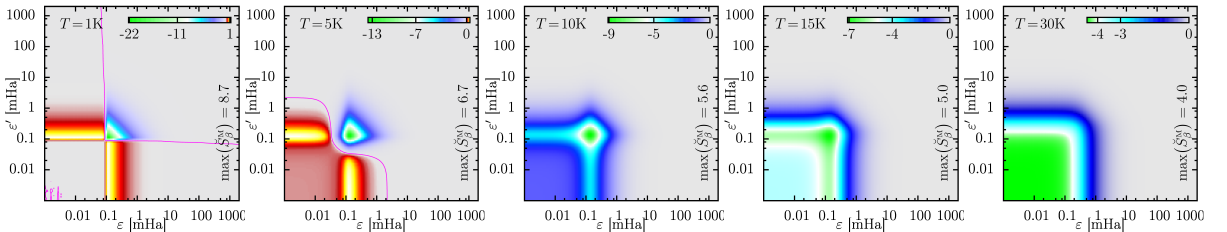
$\check{S}_\beta^{\text{M}}(\mathbf{e})$  for  $J = 0.0\text{mHa}$  (left) and  $J = 0.1\text{mHa}$  (middle)



$\check{S}_\beta^{\text{e}}(\mathbf{e}, \mathbf{e}')$  for  $J = 0.0\text{mHa}$  the temperatures (l. to r.)  $T = 1\text{K}, 5\text{K}, 10\text{K}, 15\text{K}$  and  $30\text{K}$



$\check{S}_\beta^{\text{e}}(\mathbf{e}, \mathbf{e}')$  for  $J = 0.1\text{mHa}$  at the temperatures (l. to r.)  $T = 1\text{K}, 5\text{K}, 10\text{K}, 15\text{K}$  and  $30\text{K}$



$\check{S}_\beta^{\text{se}}(\mathbf{e}, \mathbf{e}')$  for  $J = 0.1\text{mHa}$  at the temperatures (l. to r.)  $T = 1\text{K}, 5\text{K}, 10\text{K}, 15\text{K}$  and  $30\text{K}$

Figure 8.7.: Behavior of the contributions to the linear SSE.

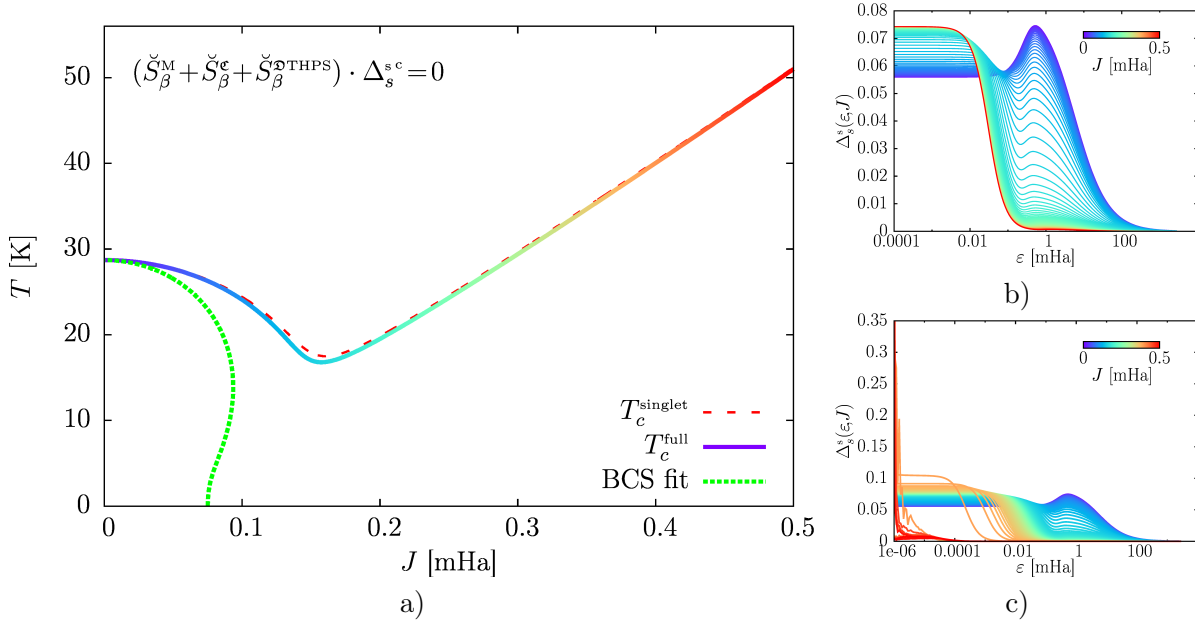


Figure 8.8.: a)  $T_c(J)$  and the linear BCS curve with the same  $T_c(0)$ . Both SpinSCDFT  $T_c(J)$  curves start to increase at  $J \approx 0.15$  mHa. The normalized  $\Delta_s^{\text{sc}}$  are shown for  $\check{S}_\beta^{\text{sc}}$  b) and  $\check{S}_\beta^e$  c). For  $\check{S}_\beta^e$ , the solutions become numerically unstable at large  $J$ .

### 8.2.3. Splitting Dependence of $T_c$

In Fig. 8.8 a) we show the  $T_c(J)$  curves obtained with  $\check{S}_\beta^M, \check{S}_\beta^{\text{TPHS}}$  and  $\check{S}_\beta^e$  or  $\check{S}_\beta^{\text{sc}}$ . For comparison we include the linear BCS curve that is normalized to the same  $T_c(J = 0)$  mHa) in the plot. We observe that the SC phase is predicted to be more stable against a splitting in SpinSCDFT in the low  $J$  regime where a linearization is valid. We will see later that the Eliashberg theory agrees with SpinSCDFT in this fact. Moreover, in the regime where we expect a first order transition, we obtain an almost linear increase starting at  $J \approx 0.15$  mHa. Upon this unexpected behavior, the eigenfunctions shown in b) become extremely limited to the Fermi level  $\epsilon \approx 0$  region with increasing splitting and increasingly numerically noisy in the case of  $\check{S}_\beta^e$  c).

In order to make the strong coupling SpinSCDFT theory more similar to the weak coupling BCS approach we disregard the electronic mass renormalization contained in  $\check{S}_\beta^{\text{sc}}$  in Fig. 8.9. In this case we are only considering the effectively attractive coupling among electrons via phonons, similar to Fröhlich [65] and BCS. The effective Fröhlich interaction requires the coupling to be small and, moreover, we neglect the phonon influence on the normal state (Nambu diagonal) part of the SE entirely. Thus, this approximation is called the weak coupling limit. As expected, the resulting  $T_c^{\text{SpinSCDFT}}(J)/T_c^{\text{SpinSCDFT}}(0)$  and  $T_c^{\text{BCS}}(J)/T_c^{\text{BCS}}(0)$  behave very similarly. Here the  $T_c(J)$  curves shown in Fig. 8.9 a) also feature the linear increase for high splitting. Moreover we observe a discontinuous jump of the  $T_c(J)$  at a certain splitting  $J_c$  which is accompanied by the eigenfunctions in b) and c) changing shape. After the jump, the solution does not have a common sign convention but shows positive and negative parts.

This points out that the  $\check{S}_\beta^{\text{sc}}$  term does not simply scale  $T_c(J)$  down in a self-similar transformation. Instead,  $\check{S}_\beta^{\text{sc}}$  leads to a larger  $T_c(J)$  reduction at small  $J$ . Thus we conclude that strong coupling systems are less affected by an exchange splitting.

**Conclusion** We find that the linearized functional from a spin-splitted generalization of the SSE properly describes the regime of the second order phase transition. The linearized BCS curve  $T_c^{\text{BCS}}(J)$  decays faster with  $J$  in the second order regime but this could be explained by



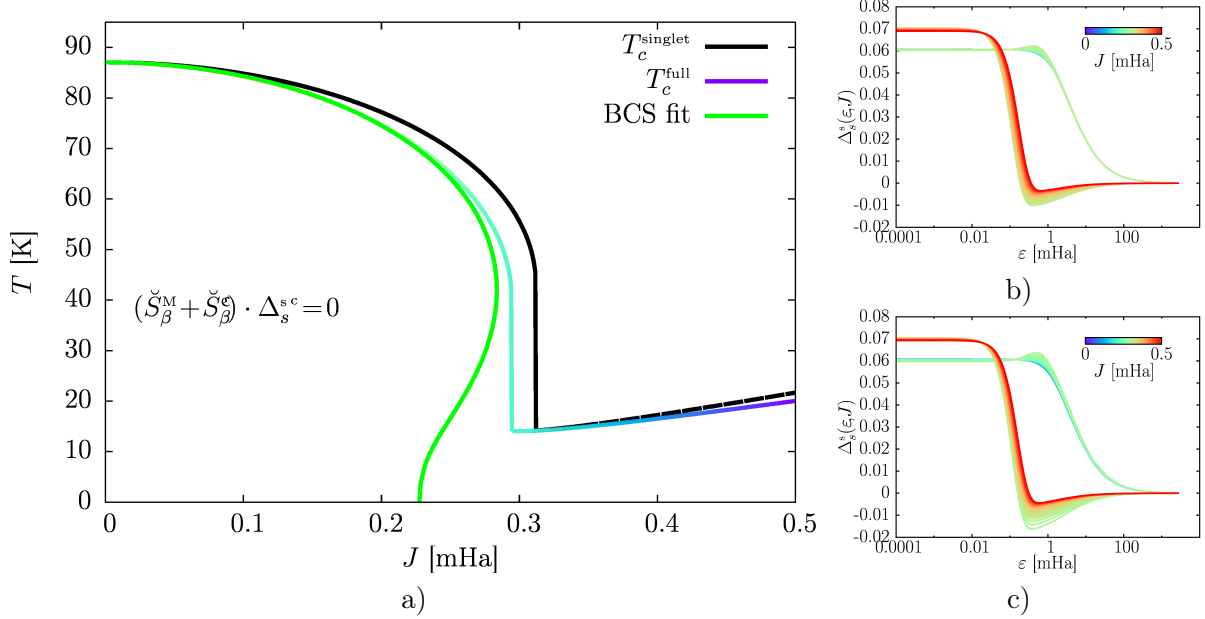


Figure 8.9.: a)  $T_c(J)$  without  $\check{S}_\beta^D$  and the linear BCS curve (left). The shape of the BCS and  $(\check{S}_\beta - \check{S}_\beta^D)$  curves are very similar, however, after a jump of  $T_c(J)$  we still find the linear increase. The normalized  $\Delta_s^s$  for  $\check{S}_\beta^{se}$  b) and  $\check{S}_\beta^e$  c) discontinuously change shape at the jump.

the form of the effective interaction. In the first order regime of the phase diagram, where the linearization cannot give sensible results, SpinSCDFT behaves differently as compared to BCS. While the linear BCS curve bends inwards the SpinSCDFT curve bends outwards and starts a curious linear increase in a large magnetic field.

With increasing splitting, the region  $\varepsilon < J$  becomes more pronounced in the solutions. From the discussion in Sec. 6.5 we can speculate that there are problems with the dependence of  $\chi(\mathbf{r}, \mathbf{r}')$  on  $\Delta_s^s$  (Fig. 6.1) in the theory. SpinSCDFT reproduces  $\chi$  of the Many-Body system but at least in the SDA  $\chi$  is only weakly dependent on  $\Delta_s^s$  in this  $\varepsilon \ll J$  region for small temperatures. At least the many discontinuous solutions, are expected to be suppressed in a non-linear treatment.

Concerning the technical reason why the increase happens, we note that in the region  $\varepsilon \leq J$  the contributions  $\check{S}_\beta^D(\mathbf{e})$  and  $\check{S}_\beta^M(\mathbf{e})$  are very small (compare Fig. 8.7 first and second row, second plot). This prevents the penalty one usually finds on the diagonal of the matrix in the spin-degenerate case leaving  $\check{S}_\beta^e$  alone to allow for a solutions that are typically very limited to the problematic region around the Fermi level. Even if  $\check{S}_\beta^D$  is removed the problem remains because of a sign change of  $\check{S}_{\text{ph}\beta}^e$ . The origin of the unusual behavior of  $\check{S}_{\text{ph}\beta}^e$  and  $\check{S}_\beta^D$  lies in the combination of Matsubara sums  $L$  of Eq. D.7 which in turn is a consequence of the energy/frequency structure of the SC KS GF. In the non-linear equation it will turn out that the SC KS system is not gapped at  $T \rightarrow 0$  while the interacting system is. Thus we suspect that for  $\varepsilon$  smaller than  $J$  the SC KS GF is not sufficient to replace the full  $\tilde{G}$  in the SE in the way we had derived the functionals. We will come back to this point later after we have studied the non-linear equation.

It is a surprising fact that adding the intermediate triplet contributions lowers the critical temperature. In neglecting the possibility to condense into a triplet state one would expect to underestimate the critical temperature. In any case, the difference to removing the intermediate triplet SE parts are minor. Thus, in the following we will not remove any triplet SE contributions although this formal inconsistency certainly deserves further investigation. This, however is beyond the scope of this thesis.

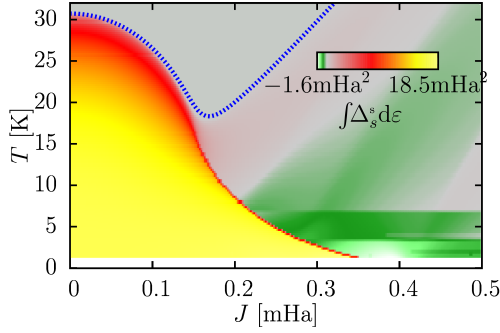


Figure 8.10.: Phase diagram of the non-linear SSE. We include  $T_c^{\text{full}}(J)$  (dashed blue) from the linearized SSE (Fig. 8.8).

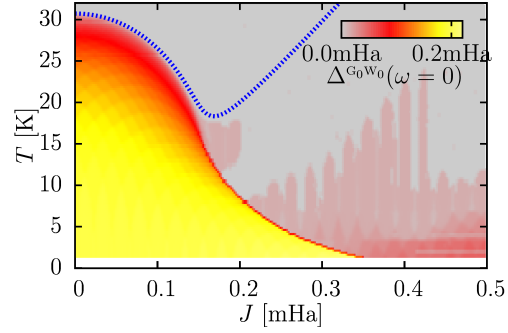


Figure 8.11.: Phase diagram of the gap in the SC G0W0 DOS. The dashed blue line is the linear  $T_c^{\text{full}}(J)$  of Fig. 8.8.

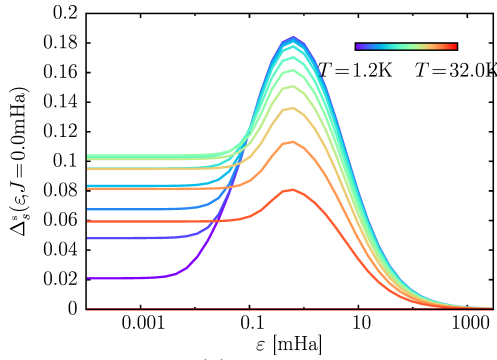


Figure 8.12.:  $\Delta_s^s(\epsilon)$  for  $J = 0.0 \text{ mHa}$  and several  $T$ . We find that  $\Delta_s^s$  goes to zero at  $\epsilon \approx 0$  for low  $T$ .

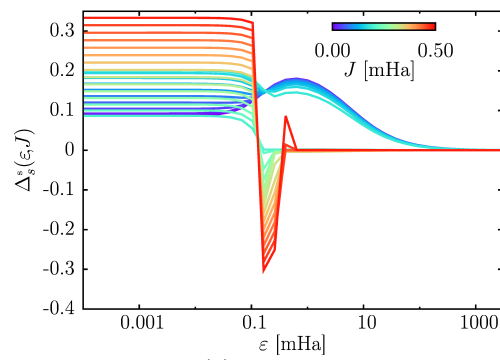


Figure 8.13.:  $\Delta_s^s(\epsilon)$  for  $T = 10 \text{ K}$  for several  $J$ . At  $J \approx 0.2 \text{ mHa}$  the  $\Delta_s^s(\epsilon)$  suddenly change shape.

### 8.3. The Non-Linear Gap Equation

We solve the non-linear SSE Eq. (6.97) with the splitting matrix  $B = S_\beta^M(\epsilon, 0.0 \text{ mHa})$ . In Fig. 8.12 we show results for several  $T$  along the iso-splitting line  $J = 0.0 \text{ mHa}$ . The non-linear equation has not been investigated in this form, not even in the spin-degenerate limit. A. Sanna implemented a version that uses a numerical Matsubara summation. We find features similar to what he obtained in the sense that we also obtain a  $\Delta_s^s(\epsilon)$  that goes to zero at the Fermi level  $\epsilon \approx 0$  for low  $T$  (purple  $\Delta_s^s(\epsilon)$  in Fig. 8.12). This means the SC KS system is not gaped (still maintaining  $\chi \neq 0$ ) and we cannot directly interpret the SC KS excitations as quasi particles.

To complete the discussion of the  $J$  and  $T$  dependence of SpinSCDFT, we need a characteristic number of a given  $\Delta_s^s(\epsilon)$  solution.  $\Delta_s^s(\epsilon = 0, J)$  is not a sensible choice because it neither corresponds to an excitation gap nor is it a measure for the size of the potential  $\Delta_s^s(\epsilon)$ . Instead, we chose  $\int \Delta_s^s(\epsilon) d\epsilon$  and the resulting SpinSCDFT phase diagram of Fig. 8.10 shows a transition at a point where, from the shape of the non-linear BCS diagram (Fig. 2.1 a) the first order phase transition is to be expected. However, following this discontinuous transition, the solutions  $\Delta_s^s(\epsilon)$  do not vanish but have a different shape. In Fig. 8.13, we show the  $\Delta_s^s(\epsilon)$  with increasing  $J$  at  $T = 10 \text{ K}$  and the transition is clearly seen. In general, while before a critical splitting  $J_c(T)$  the potential is little affected by the splitting, past  $J_c(T)$  the solutions  $\Delta_s^s(\epsilon)$  localize at the Fermi level and show positive as well as negative regions. This behavior is similar to the normalized  $\Delta_s^s(\epsilon)$  from the linearized  $\check{S}_\beta$  as given in Fig. 8.8. We include  $T_c(J)$  from the linear SSE in Fig. 8.10 and see that, past the range in  $J$  of the second order phase transition, it marks the border of the appearance of the curious solutions in the non-linear equation.

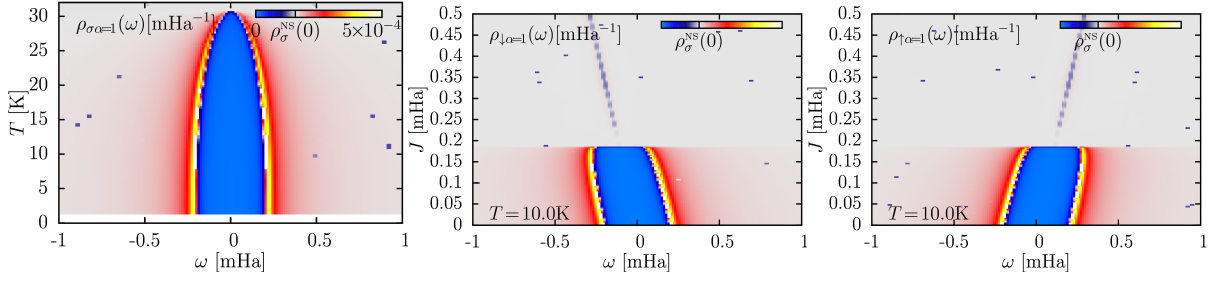


Figure 8.14.: SC G0W0 DOS for  $J = 0$  mHa (left) with  $\Delta_s^s$  of Fig. 8.12. The system is gaped at  $T \rightarrow 0$ . We present the DOS (middle:  $\sigma = \downarrow$ , right:  $\sigma = \uparrow$ ) using  $\Delta_s^s$  of Fig. 8.13 at  $T = 10$  K. The first order transition can be clearly identified.

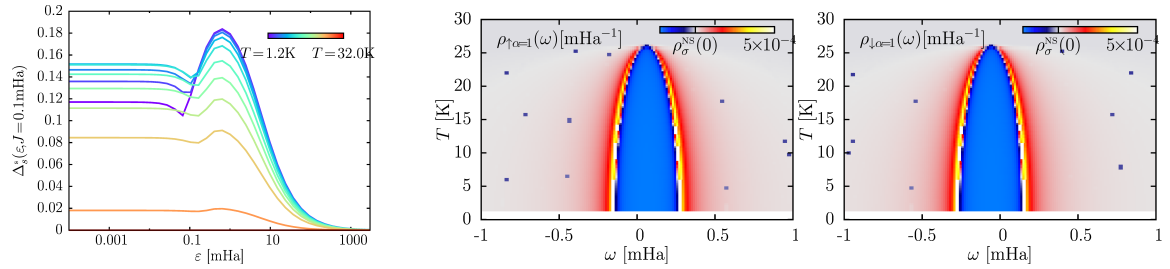


Figure 8.15.:  $\Delta_s^s(\epsilon)$  at  $J = 0.1$  mHa for several  $T$ .

Figure 8.16.: SC G0W0 DOS at  $J = 0.1$  mHa with  $\sigma = \uparrow$  ( $\sigma = \downarrow$ ) on the left (right).

In Fig. 8.11 we compute the G0W0 DOS at every point in  $J$  and  $T$  and extract the SC gap. We find that the curious solutions past the transition  $J_c(T)$  lead to almost no excitation gap. The reason is that for the SE in the calculation of the SC DOS in Section 7.2  $\Delta_s^s(\epsilon)$  is integrated in  $\epsilon$ . If  $\Delta_s^s(\epsilon)$  in the high  $\epsilon$  region is extremely small, as in the KS potential past the  $J_c(T)$ , the effect on the excitation gap is negligible.

Comparing the SpinSCDFT G0W0 gap of Fig. 8.11<sup>2</sup> with BCS (Fig. 2.1) we conclude that the point of the phase transition can be clearly identified and has a similar shape. Moreover this one-cycle correction sheds light onto the appearance of the Fermi-level localized solutions past the critical field  $J_c(T)$ . We have seen that for small  $T$  and  $J = 0$  the non-linear  $\Delta_s^s(\epsilon)$  go to zero at the Fermi level (compare Fig. 8.12) while the analogous property of the G0W0 GF, the excitation gap of Fig. 8.11, takes its largest value at  $T = 0$  and shows the expected monotonous decay with temperature to  $T_c$ . This implies a significant difference in the quasi particle states if a splitting occurs with such a  $\Delta_s^s(\epsilon)$ . While the KS particle with the dispersion  $E_\sigma^\alpha = \text{sign}(\sigma)J + \alpha(\epsilon^2 + \Delta_s^s(\epsilon)^2)^{1/2}$  is strongly altered by the splitting because the Bogoliubov branches change their order (compare the discussion in Section 3.5.2) this is not the case in the true quasi particle structure. In fact, from Fig. 8.15, we see that the SC solutions  $\Delta_s^s(\epsilon)$  if  $J > 0$  do not go to zero and, instead, rise with  $J$  to prevent this situation. On the other hand, after the discontinuous transition we find  $\Delta_s^s(0, J) < J$  in Fig. 8.13.

In the functional construction, the replacement  $\bar{G} \rightarrow \bar{G}^{\text{KS}}$  is thus a strong suspect for the occurrence of this curious solutions past the SC transition. This is because  $\bar{G}$  and  $\bar{G}^{\text{KS}}$  deviate in that the latter can be non-gaped while still corresponding to a SC solution. We conclude that the SpinSCDFT functional derived in Chapter 6 can be improved using a fitting technique as introduced for the spin degenerate SCDFT functional to improve its  $T_c$  prediction (see the discussion at the end of Subsection 6.3.1). Such an approach would use the Eliashberg results of the Section 8.5 as a starting point.

<sup>2</sup>The few blue dots are points where the adaptive integration routine fails to find the pole in the integrand of Eq. (7.48). This can be avoided with a higher integral precision.

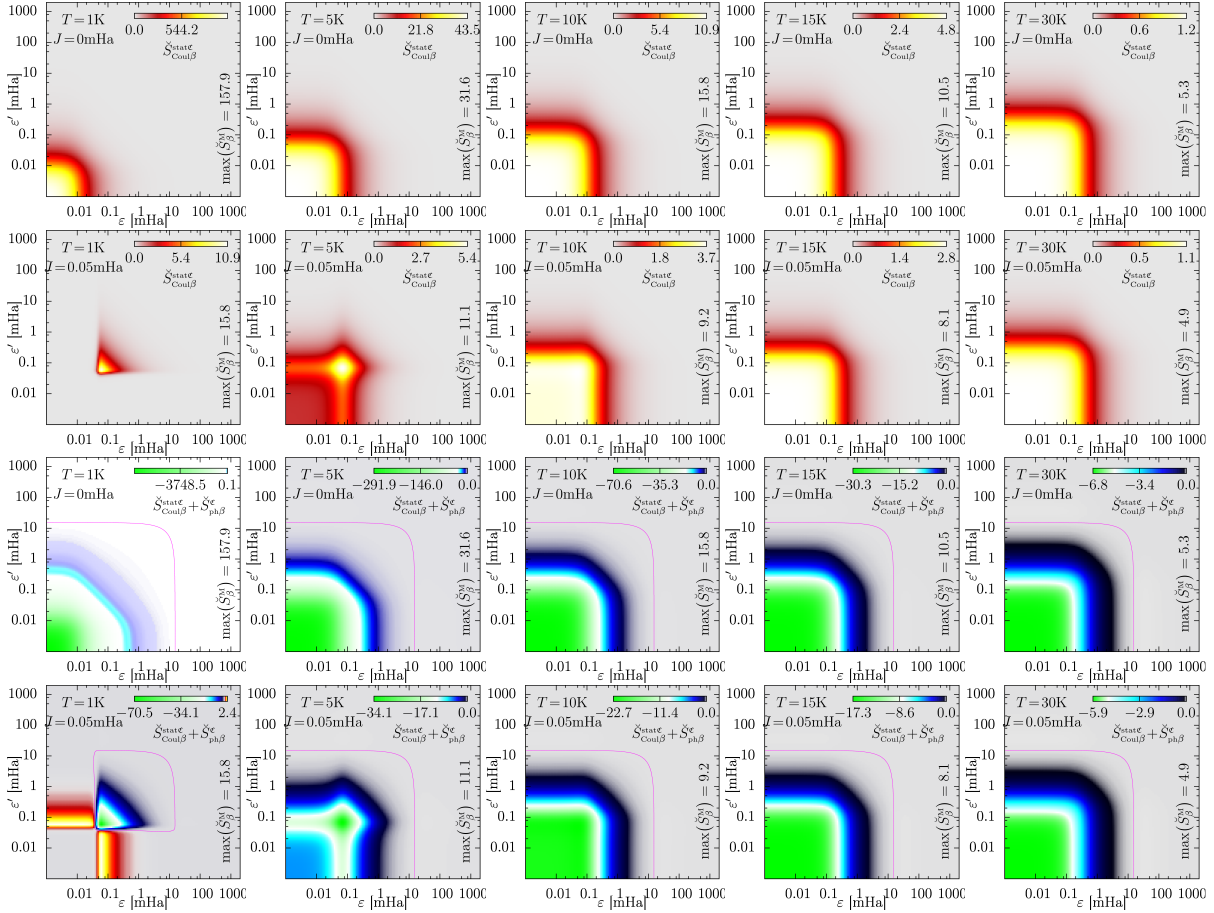


Figure 8.17.:  $\check{S}_{\text{Coul}\beta}^{\text{stat}e}$  (1. and 2. row) and  $\check{S}_{\text{Coul}\beta}^{\text{stat}e} + \check{S}_{\text{ph}\beta}^e$  (3. and 4. row).  $J$  is 0.0mHa (1. and 3. row) or 0.05mHa (2. and 4. row).

## 8.4. The Effect of the Static Coulomb Interaction

In order to complete our analysis, we investigate the effect of a static Coulomb potential in a simplified form of Eq. (8.7). We show the shape of the Coulomb part  $\check{S}_{\text{Coul}\beta}^{\text{stat}e}$  in Fig. 8.17 in the first ( $J = 0\text{mHa}$ ) and second row ( $J = 0.05\text{mHa}$ ) and for comparison  $\check{S}_{\text{Coul}\beta}^{\text{stat}e} + \check{S}_{\text{ph}\beta}^e$  in the third ( $J = 0\text{mHa}$ ) and fourth ( $J = 0.05\text{mHa}$ ) row. The purple line in Fig. 8.8 indicates that  $\check{S}_{\beta}^e = \check{S}_{\text{Coul}\beta}^{\text{stat}e} + \check{S}_{\text{ph}\beta}^e$  features a sign change at higher energies. The FL is strongly attractive and the HE region is, while much larger (note the logarithmic scale), weakly repulsive. The pair potential  $\Delta_s^s$  utilizes the negative high energy region by changing sign with the matrix elements to, once more, add positively to the Fermi level  $\Delta_s^s$  during the self-consistent iterations. This effect is how the well known Coulomb renormalization [66] appears in SpinSCDFT.

In Fig. (8.10) we had chosen the integrated  $\Delta_s^s(\epsilon)$  to plot the phase diagram because the purely phononic  $\Delta_s^s(\epsilon)$  is positive for the physical solutions before the transition. In the present case, due to the Coulomb renormalization, we will find a negative HE part in the  $\Delta_s^s(\epsilon)$ . Thus, we show the number of condensed electrons in the system according to Eq. (3.134) as a function of  $T$  and  $J$  in Fig. 8.18. Since it is based on the SC order parameter, this physical property is exactly reproduced by the SC KS system. We observe that apart from the usual reduction of the critical temperature  $T_c(J = 0)$ , the shape of the SC region in the  $J - T$  diagram remains very similar to the purely phononic coupling case of Section 8.2. In addition, as seen in Fig. 8.19, the eigenfunctions change sign a little away from the Fermi level as the result of the Coulomb

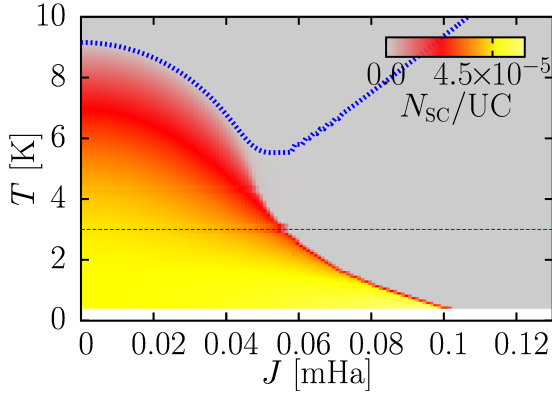


Figure 8.18.:  $N_{sc}(T, J)$  and the linear  $T_c(J)$  (dashed blue) including the Coulomb repulsion. The  $\Delta_s^\epsilon(\epsilon)$  after the transition lead to almost no condensed electrons.

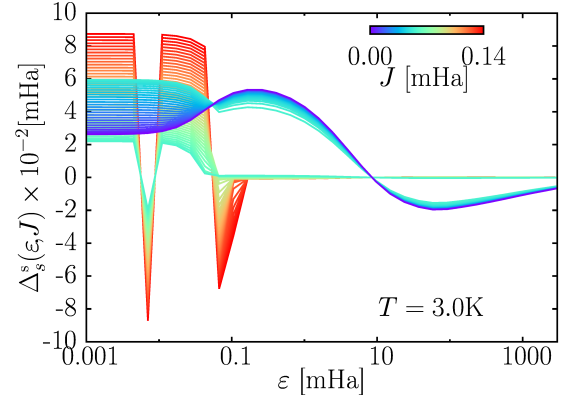


Figure 8.19.:  $\Delta_s^\epsilon(\epsilon)$  at  $T = 3\text{K}$  for several  $J$  along the dashed green line in Fig. (8.18). The  $\Delta_s^\epsilon(\epsilon)$  past the transition have similar features as without the Coulomb repulsion.

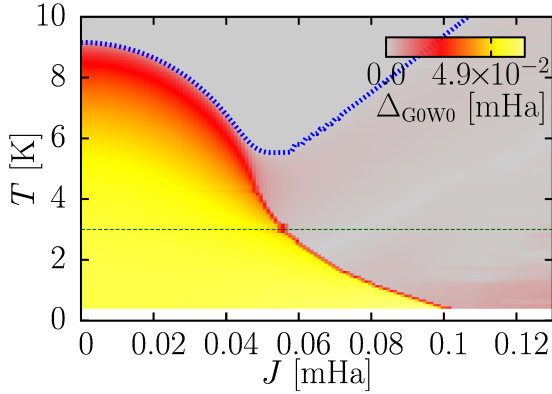


Figure 8.20.: G0W0 gap according to Eq. (7.49) using  $\omega_0^{\sigma\gamma}(\epsilon = 0)$ .

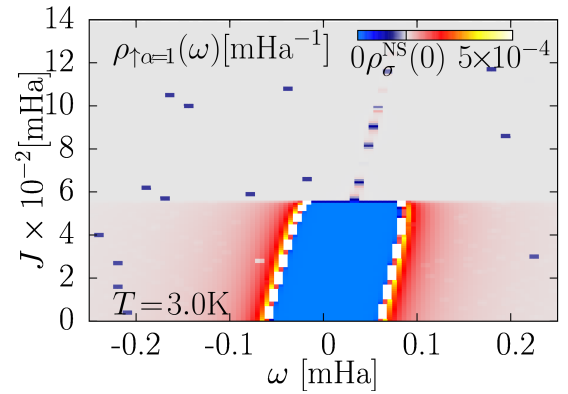


Figure 8.21.: Upspin channel of the G0W0 DOS along the dashed green line in Fig. (8.20) at  $T = 3\text{K}$ . Past the transition, we see small features from the unphysical solutions.

renormalization. The solutions past the transition lead to almost no condensed electrons while the linear  $T_c(J)$  still features the increase for  $J$  above the second order regime.

We compute the G0W0 gap according to Eq. (7.49). There we assume that the smallest excitation is the quasi particle at the original FS without SC, namely  $\epsilon = 0$ . We then solve Eq. (7.49) at  $\epsilon = 0$  for given  $\sigma$  at both  $\gamma = \pm 1$  and compute the minimal distance above and below the  $\omega = 0$ . This distance is twice the gap. The corresponding phase diagram is given in Fig. 8.20. Clearly, it follows the shape of  $N_{sc}(T, J)$  in Fig. 8.18. This procedure is significantly more efficient as compared to the extraction of the gap from the G0W0 DOS in Fig. 8.11 while it leads to largely similar results. In Fig. (8.21), we show the upspin channel of the G0W0 DOS at  $T = 3\text{K}$ .

In summary we can say that the Coulomb interaction does not affect the consequences of the replacement  $\bar{G} \rightarrow \bar{G}^{\text{KS}}$ .

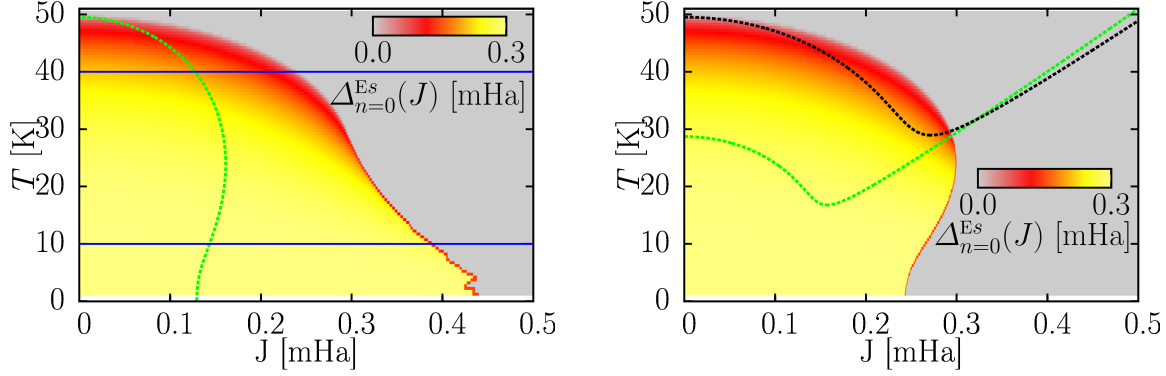


Figure 8.22.:  $T - J$ -diagram of the excitation gap ( $\Delta_{n=0}^{Es}$ ) of the Eliashberg equations. We follow  $\Delta_n^{Es}(J) \neq 0$  (left) or  $\Delta_n^{Es}(J) = 0$  (right). There is a region where both are (meta) stable. In Fig. 8.23, we plot  $\Delta_n^{Es}(J)$  along the blue lines. The green (black) dotted line on the left (right) is the linear BCS (SpinSCDFT) curve, fitted to the same  $T_c(0)$ . The green dotted line on the right is  $T_c^{\text{full}}(J)$  of Fig. 8.8.

## 8.5. Solutions to the Eliashberg Equations

We solve the Eliashberg Eqs. (7.82) to (7.85). To arrive at these equations we assume a phononic coupling that does not depend on  $\varepsilon$ . Further we are not considering the Coulomb interaction that in the static approximation would correspond to the  $\mu^*$  pseudo-potential (compare Chapter 7). The best overview is obtained by plotting a characteristic SC property vs  $T$  and  $J$ . Here, we choose  $\Delta_n^{Es}(J)$  at  $n = 0$  as it corresponds to the single particle excitation gap.

In this non-linear equation we may have several stable solutions and, in fact, we find that results depend on the starting value  $\Delta_0$  in some ranges of the parameters  $T$  and  $J$ . In this work we always start with constant, finite  $\Delta_n^{Es} = \Delta_0$  or an already converged solution of some different point in  $T$  and  $J$ . At  $J = 0$  this is not the case and below  $T_c$  we always reach a non-zero SC solutions if our starting value is non-zero. We call this finite  $\Delta_n^{Es}$  solution the SC fixed point. After some critical splitting  $J_c$  we arrive at the normal state  $\Delta_n^{Es}(J) = 0$  even if we start with a small symmetry breaking field  $\Delta_0$ . With a large starting value  $\Delta_0$ , however, we arrive at a converged finite solution  $\Delta_n^{Es}(J) \neq 0$ . To investigate this systematically, we follow the SC fixed point in the left panel of Fig. 8.22. “Follow” means we take a converged solution  $\Delta_n^{Es}(J)$  from the last calculation as input for the next set of parameters  $J$  and  $T$ . Following the SC fixed point means to compute the data for the plot “from left to right” while we follow the normal state fixed point in the right panel which means we generate the data “from right to left”. Comparing left and right panel of Fig. 8.22 we see that there is a region at  $J \approx 0.3$  mHa where the system supports a SC solution while the normal state is meta stable within a finite basin of attraction. This means that small SC perturbations converge to the respective fixed point via a self-consistency iteration.

We show the linear BCS results of Fig. 2.1, fitted to the same  $T_c(J = 0)$  as Eliashberg theory, in the plots of Fig. 8.22 as a dotted green line. The shape of the linear BCS curve is very similar to the border between stability and instability of the normal state fixed point. However, Eliashberg predicts a higher critical field as compared to BCS theory in agreement with SpinSCDFT. The linear SpinSCDFT curve is shown as a green dotted line on the right panel and, scaled to the same  $T_c(0)$ , once more as a black dotted line. First we see explicitly that Eliashberg theory predicts a higher  $T_c(0)$ . This is known [21, 22] and due to the violation of Migdal’s theorem. Apart from this, in the region of the second order phase transition we see deviations from the black, scaled SpinSCDFT curve.

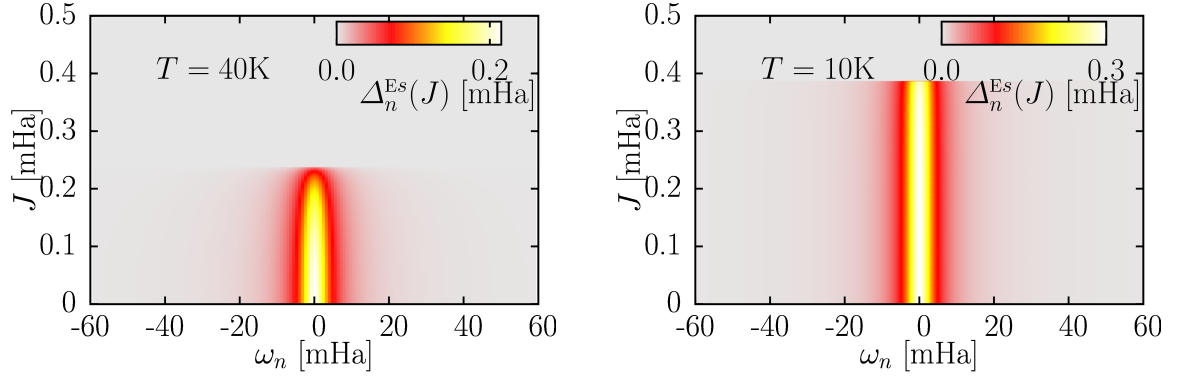


Figure 8.23.:  $\Delta_n^{Es}(J)$  for  $T = 40\text{K}$  (left) and  $T = 10\text{K}$  (right) along the blue lines of the left panel of Fig. 8.22.

We show the shape of the solutions  $\Delta_n^{Es}(J)$  for  $T = 10\text{K}$  (right) and  $40\text{K}$  (left) as a function of  $J$  in Fig. 8.23. The only effect of the splitting is to scale down the gapfunction up until the point where it suddenly vanishes. For low temperatures the down-scaling is much less pronounced and it is safe to say that the pairing is almost unaffected by the presence of a splitting up until the point where SC is lost. This behavior is much different from the energy dependent pair potential in SpinSCDFT in the heuristic partial linearization but more similar to the non-linear solutions.

Comparing  $T_c(J = 0)$  we see that the prediction of the Eliashberg equations is much higher than the one of SCDFT where  $T_c^{\text{SCDFT}}(J = 0) \approx 29.0\text{K}$  while  $T_c^{\text{Eliash}}(J = 0) \approx 50\text{K}$ . This problem is the result of the violation of Migdal's theorem due to our replacement  $\bar{\Sigma}[\bar{G}] \rightarrow \bar{\Sigma}[\bar{G}^{\text{KS}}]$  and, as mentioned before, was solved by A. Sanna with a fitting procedure.

# Summary and Outlook

We have derived ab-initio methods for a SC in a magnetic field. Our analysis disregards orbital currents and is solely based on the destructive effect of the separation of single electronic states due to a magnetic field via the Zeemann term. The focus is on the extension DFT for SC. There, we employ a SC KS system to reproduce the densities of the interacting system. Using Many-Body perturbation theory and the Sham-Schlüter connection we have derived  $xc$  functionals. In this first approach we rely on the replacement of the interacting with the KS GF in the SSE. In a specialization, we neglect triplet SC and assume that SC does not hybridize KS states other than to a given particle, the corresponding time reversed hole state. We refer to this as the SDA. Because our SC KS system reproduces the interacting densities, but not the excitation spectrum we have derived equations for a G0W0 like GF. From this interacting GF we have constructed equations for the DOS. We have further derived Eliashberg equations that do not rely on the replacement of the GF but are otherwise based on very similar approximations: We assume the SE to be diagonal in the space of KS orbitals and do not consider triplet SC.

During this work we have developed a code from scratch that solves these equations numerically to test the quality of the functionals derived. We have tested the new methods on the free electron gas with a homogeneous magnetic field (as a parameter) and phononic and Thomas-Fermi screened Coulomb coupling.

In agreement with earlier work on spin-degenerate SCDFE [54, 57], we recover the  $T_c$  underestimation as compared to the Eliashberg solution. Both, Eliashberg and SpinSCDFE, however, predict that the SC state is more stable against a splitting field than a similar BCS model with the same  $T_c$ . We could trace this to the strong coupling Nambu-diagonal SE contributions that are not considered in BCS. In the regime where the SC transition is of second order, the linearized SSE of SpinSCDFE properly describes the  $T_c(J)$  curve. In the non-linear SSE we can clearly identify the transition by a sudden change of shape in the solution, however the  $\Delta_s^s$  do not vanish past this point. Computing the G0W0 DOS shows that the curious solutions correspond to almost no gap in the excitation spectrum.

From this encouraging result we believe that a similar fit of the SE as used by A. Sanna to improve  $T_c(J = 0)$  will remove the high  $J$  solutions. While we believe it to be a promising approach it can become a time-consuming task: 1) One has to choose a set of fitting parameters and 2) match numerical conditions from Eliashberg theory with a SpinSCDFE calculation for each individual value. Moreover, we believe that the  $J - T$  spectra from the present functional have already the qualitatively correct shape. We thus leave the functional improvement to a future project and apply SpinSCDFE to a realistic material in the next Part II.



Part II.

# Superconductivity of Surfaces: Lead Monolayer on Silicon

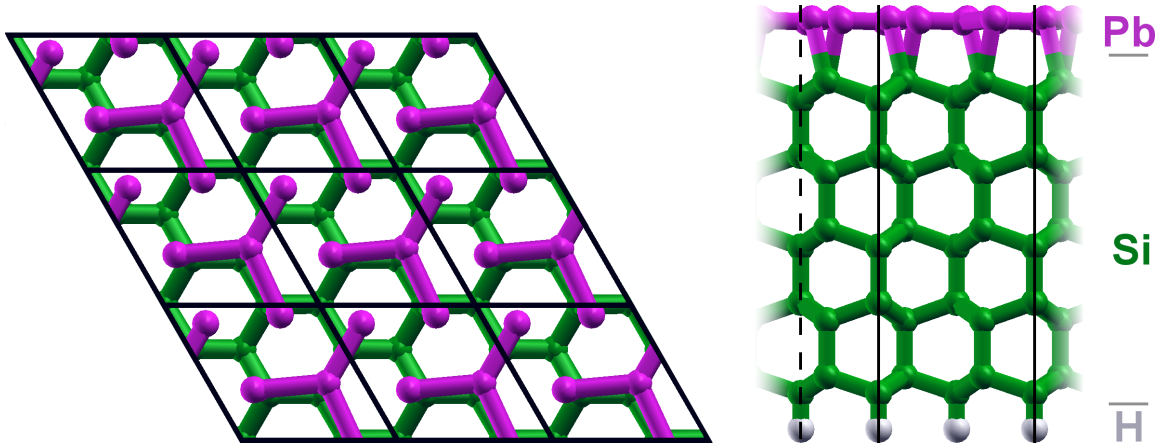


Figure 8.24.: Striped incommensurate phase configuration of Pb on the Si (111) substrate. On the left we present the top view, and on the right the side view. Black lines mark the simulated unit cell.

## Introduction

Part I dealt with the theoretical methods and their implementation. If we want to compare the results of Part I with experiment, a realistic system has to be considered where SpinSCDFT is applicable in its present implementation. At the moment there is no implementation of a feedback mechanism of the SC condensation to the magnetization of the substance. In a realistic situation the Meißner effect will prevent the system from being homogeneously magnetized as we had supposed in our free electron gas toy model. There is however great interest in the study of SC of thin surface layers[24], where in general the thickness is much less than the penetration depth of the magnetic field. Here we suppose that SC is directly altered by the presence of a nearly homogenous external magnetic field without the necessity to consider the Meißner effect.

The exponential growth in computing power over the last decades allows for the numerical ab-initio simulation of large systems, even for surfaces where the broken translational symmetry requires large unit cells with enormous numbers of electrons. Improvements in experimental techniques on the other hand have enormously reduced the effective size, i.e. the number of atomic layers, of the surfaces under study, which allows the direct comparison between numerical simulations and experimental results.

In this work we simulate a single layer of Pb in the striped incommensurate phase configuration on a Si(111) substrate with  $T_c = 1.86\text{K}$  in experiment [24]. In Fig. 8.24 we show the simulated unit cell of this system.

Before we can study the SC phase of a thin surface on a computer, several challenges have to be faced. We describe the calculation of the normal state ingredients to a (Spin-) SCDFT calculation in Chapter 9. In Chapter 10 we discuss the SC of the system without an external magnetic field which allows for a very interesting discussion by itself before we turn to the effects of a magnetic field in Chapter 11. We do not have an improved functional that accounts for the inaccuracy of the replacement  $\bar{\Sigma}[\bar{G}] \rightarrow \bar{\Sigma}[\bar{G}^{\text{KS}}]$  in the magnetic case. However, the accurate  $T_c$  prediction turns out to be crucial for the theoretical study of the Pb on Si(111) surface and we use a mixed approach. We discuss some of the features of the SC of the system such as the  $T_c$  and gap at  $T = 0$  using the improved functional, but then compute properties like the DOS, the LDOS and the effect of a magnetic field using the functional derived in this work.

# 9. Electronic and Phononic Properties of Pb on Si(111)

In this Chapter, we discuss the results of first principle calculations of a single layer of lead on a silicon substrate including a full treatment of phononic and RPA screened Coulomb interactions. We constructed the Si-Pb system as shown in Fig. 8.24. Lead arranges in this system in the so-called striped incommensurate phase configuration. We model the Si substrate by a (111) oriented slab, which we passivate on the opposite side of the lead surface using hydrogen. We converge the number of silicon layers with respect to the purely phononic  $T_c$  of the SCDFT calculation to ensure that the electron phonon coupling is accurately accounted for. A relatively large width of five Si-bilayers reduces the effects of the limited size of the substrate on the Pb layer. To resemble more closely to the experimental setup we constrain the hexagonal (xy) Si unit cell to its bulk size. Since we work with periodic boundary conditions, a vacuum of  $\sim 8 \text{ \AA}$  separates the periodic replica of the system. Within these constraints, we performed a full relaxation. A similar system has been studied before by Noffsinger and Cohen [67]. We work in a different approximation in using a larger Si bulk and, we explicitly include silicon phonon modes in our calculations. Most importantly we allow different pairings for bulk and surface and discuss the influence of the Coulomb interaction. The SC of this system is the topic of the next Chapter 10. We have calculated relaxations, electronic structure, phonons and electron-phonon interactions within KS DFT. All normal state calculations employ the LDA for the  $xc$  functional [68] using norm conserving pseudo-potentials to account for core electronic states. We use a cutoff of 80 Ry in the plane wave expansion of the KS states and the Brillouin zone has been sampled with a mesh of  $12 \times 12 \times 1$  k-points. Phonons and electron phonon coupling have been calculated within linear response DFT [35] using the ESPRESSO package [52]. We discuss the electronic bands in Section 9.1 and the vibrational structure in Section 9.2. In Section 9.4 we discuss the connection of the surface and the substrate with respect to electronic couplings.

## 9.1. Electronic Structure

One property of the undoped electronic band structure (Fig. 9.1 , black dotted lines) is the presence of both Pb and substrate bands at the fermi level. This means that the Pb deposition acts as a dopand to the Si substrate, which develops a surface metallic region. This metallic region fades within a few layers. The presence of this additional metallic band is relevant for two reasons. First it may be providing a contribution to the electron-phonon coupling and, second, it may stabilize fluctuations of the order parameter of the SC phase by effectively enhancing the three-dimensionality of the condensate. These Si metallic bands can be removed by using a n-doped substrate. We explicitly consider this case by substituting one Si atom (in the deep bulk) with a virtual mixture of P and Si, corresponding to a doping of 1 part per 240 Si. Doping has a small effect on the filling level of the Pb bands, but completely saturates the Si- hole pockets (see Fig. 9.1, thick colored lines). This doped system is experimentally realized [24] and allows for direct comparison with results of the calculation.

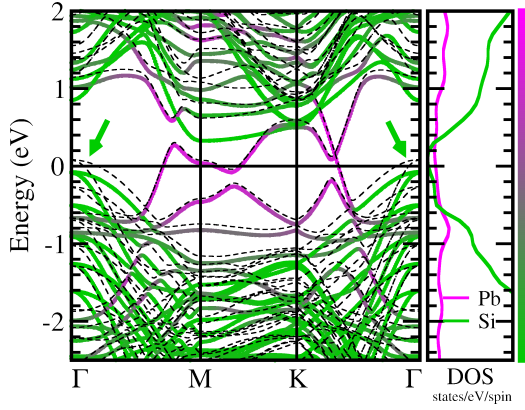


Figure 9.1.: Band Structure and DOS. Thick (thin dashed) lines correspond to a P doped (undoped) system. The doping has little effect on the purple Pb bands while it fills the green silicon hole pockets (green arrows).

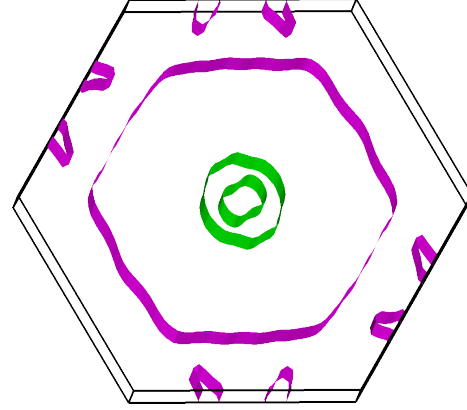


Figure 9.2.: FS of Pb on undoped Si(111). The 2D nature of the system leads to no dispersion along  $k_z$ . The doping removes the green Si states from the FS (compare Fig. 9.1).

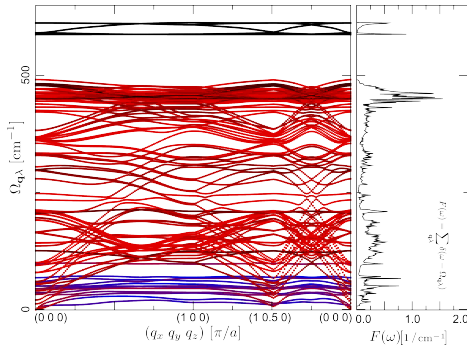


Figure 9.3.: Phonon dispersion and DOS of Pb on Si(111). Blue (red) corresponds to a motion of Pb (Si) and black to H atoms. Optical modes of H appear up to  $2000\text{cm}^{-1}$ .

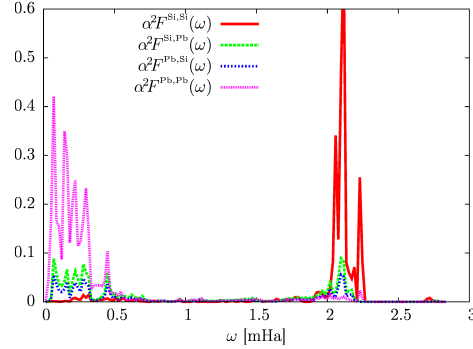


Figure 9.4.:  $\alpha^2 F^{i,j}(\omega)$  for states at the FS of the undoped system. We resolve the Si and Pb FS sheets.

## 9.2. Phononic Structure

We show the results of the phonon calculation in Fig. 9.3 . We choose the color according to the normalized motion of the type of atom due to a given phonon mode  $\Omega_{\mathbf{q}\lambda}$ : Blue corresponds to the Pb surface motion, red corresponds to the Si substrate and black to the H atoms we used for saturation of the Si bonds. We point out that we find many modes that involve only the motion of a certain type of atom, so similar to the electronic states at the Fermi level also the phonon mode structure is decoupled. We expect that the blue lead phonon modes in the spectrum will be unchanged if we alter the silicon configuration far from the surface. However we cannot hope that the silicon modes remain unchanged if we add more layers.

Following the discussion in Sec. 4.1, we note that the electron phonon coupling is due to the local potential variation induced by a phonon mode. The coupling matrix elements are the overlap among electronic states that is created by this local potential. In the calculation of SC, the coupling of states directly at the FS is the most relevant. Thus, the electron phonon

|         | $\lambda^{\text{Pb,Pb}}$ | $\lambda^{\text{Pb,Si}}$ | $\lambda^{\text{Si,Si}}$ | $\lambda_{\text{av}}$ | $\max[\lambda_i]$ | $\rho_{\text{Pb}}(0\text{mHa})$ | $\rho_{\text{Si}}(0\text{mHa})$ |
|---------|--------------------------|--------------------------|--------------------------|-----------------------|-------------------|---------------------------------|---------------------------------|
| undoped | 0.95                     | 0.13                     | 0.06                     | 0.78                  | 0.98              | $0.0265(\text{mHa})^{-1}$       | $0.0162(\text{mHa})^{-1}$       |
| doped   | 1.03                     | 0.00                     | 0.00                     | 1.03                  | 1.03              | $0.0291(\text{mHa})^{-1}$       | $0.0000(\text{mHa})^{-1}$       |

Table 9.1.:  $\lambda^{i,j}$  is the FS sheet resolved coupling matrix.  $\lambda_{\text{av}} = \frac{1}{\rho(0)} \sum_{i,j} \lambda^{i,j} \rho_i(0)$  is the average electron phonon coupling where  $\rho_i(0)$  are the FS sheet resolved DOSs and  $\rho(0)$  is total DOS.  $\max[\lambda_i]$  is the maximal eigenvalue of  $\lambda^{i,j}$  that in BCS determines  $T_c$ [69].

coupling is as localized in real space as are the states at the FS. From the little hybridization of the phonon modes in Figure 9.3 we conclude that at least the lead electron phonon coupling will be largely independent on additional layers. Here, the calculated full electron phonon coupling strength for the undoped system results is  $\lambda = 0.78$  (see Table 9.1). We can well separate Fermi surface sheets into Pb and Si like states (Fig. 9.2). We compute the coupling constant matrix  $\lambda^{i,j}$  among fermi surfaces sheets, i.e. states in the Pb and Si (first) and from one to the other ( $i, j = \text{Pb, Si}$ ) (second) and show them in Table 9.1. The internal coupling of lead alone is larger than the averaged one and points out that we have to consider the possibility that this system is a multiband SC. Note that because the coupling is weighted by the DOS, we have to use the formula  $\lambda_{\text{av}} = \frac{1}{\rho(0\text{mHa})} \sum_{i,j} \lambda^{i,j} \rho_i(0\text{mHa})$  to average isotropic band resolved coupling constants. If a hole dopand is present we calculate an even slightly increased Pb, Pb coupling as compared to the undoped case.

### 9.3. Coulomb Coupling

We compute the static screened Coulomb coupling matrix elements Eq. (4.14) with dielectric screening in the RPA using the YAMBO code<sup>1</sup>. Due to the size of the system we have to remove 3 double layers of Si from the ab-initio calculation. Then we average the anisotropic matrix elements on equal-energy surfaces. The results resemble closely to 3 times the electron gas model analogous to Eq. (8.7) with different paramters each: First a hole gas for the Si hole pocket (green arrow in Fig. 9.1). Second, an electron gas for the rest of the Si bulk and third an electron gas for Pb surface layer. The averaging process and the final fitting results in  $C_{nn'}^{\text{stat}}(\mathbf{e}, \mathbf{e}')$  which we show in Fig. 9.5 . The Thomas-Fermi screened Coulomb coupling our model of the last Part in Fig. 8.2 has a slightly different shape as compared to Fig. 9.5. This is due to the unrealistically small screening of  $k_{\text{TF}}$  we had chosen in our toy model. The hole band of silicone leads to a pronounced peak because of the matrix elements approaching the low  $\mathbf{q}$  limit of the Coulomb interacting on the top of the hole pocket.

<sup>1</sup><http://www.yambo-code.org/>

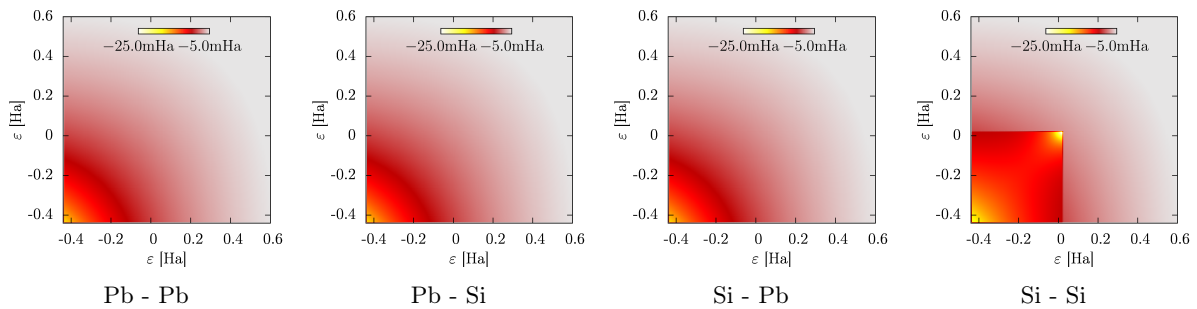


Figure 9.5.: The statically screened Coulomb coupling  $C_{ij}^{\text{stat}}(\mathbf{e}, \mathbf{e}')$  divided by  $\rho_i(\mathbf{e}')$ .

## 9.4. Interaction of Surface and Substrate

In this Section we combine the analysis of the Sections 9.1, 9.2 and 9.3 to investigate how the NS KS particles (taken as quasi particles) behave in this system. We can distinguish three main effects that describe how the KS electrons of the Pb surface and the substrate are coupled: chemical hybridization, electron phonon coupling and the Coulomb interaction.

The *chemical hybridization* between surface and substrate states can be made visible by projecting the KS states on the Pb atomic orbitals. This type of projection determines the color scale we used in Fig. 9.1 and shows that the KS states near the Fermi energy are either located in the lead surface or inside the silicon bulk, with essentially no overlap.

The *electron-phonon coupling* is computed for the KS system via linear response. Phonons may provide pairing between bulk and surface states. In Section 9.2 Table 9.1 we give the Fermi surface sheet resolved electron phonon coupling. While in the undoped case the phonons do couple the electron states of the surface and substrate, the doping fills the hole pockets and removes all substrate states from the range of the phonon energies.

Moreover the electrons are subject to a *screened Coulomb* scattering which we treat within the RPA [70]. This kind of interaction in bulk materials is often overlooked, since, acting both as a repulsive (directly) and attractive interaction (via Coulomb renormalization mechanism [66, 71, 27]) its effect on the SC pairing appears very often to be largely material independent. Compare also Section 8.4 on how this effect is incorporated in the purely energy (electronic state) dependent SCDFt. The material independence is the reason for the usually lax way the Coulomb interaction is treated in Eliashberg based methods [44, 72] where the well-known rule of thumb is to take  $\mu^* \sim 0.13$  [73].

To understand why the behavior of the Coulomb potential is different in the context of surfaces, we want to emphasize the DOS in Fig. 9.1. The purple, almost constant, DOS is due to states in the lead surface layer. The green one is due to states in the silicon and goes to zero at the Fermi level, leaving the lead alone to give a metallic region. The Coulomb matrix elements connect all states in a broad energy region about the Fermi level. Moreover, the variation on the narrow energy scale of SC at the Fermi level is small and for the following discussion we can view the potential as constant. Then, the size of the coupling matrix elements  $C_{ij}^{\text{stat}}(\mathbf{e}, \mathbf{e}')$  is determined by the number of states at given energy that are connected with the states at another given energy. Thus, for almost constant coupling matrix elements this would be proportional to the DOS at the first, times the DOS at the second energy. Because we had to normalize the average coupling in Eq. (6.114) by the first DOS the result is essentially proportional to the second DOS alone. There are very few states of lead as compared to silicon due to the reduced dimensionality of the surface layer as compared to the large bulk. This means the Fermi level Pb to Pb Coulomb repulsion is small while the rest of the energy spectrum is not. In the Section 8.4 we understood that this high to low energy coupling is what causes the Coulomb renormalization in SCDFt. We conclude that this interaction is much less destructive in the present system as in a usual bulk geometry: The effectively repulsive Fermi level to Fermi level Coulomb interaction is small and the effectively attractive high energy to Fermi level coupling is large.

This insight is not specific to lead on silicon. It will always arise when we have a metallic layer on an insulating substrate and, then, we cannot simply use the usual, averaged  $\mu^* \sim 0.13$ .

# 10. The SC Si–Pb Surface without Magnetic Field

A simple approach to computing the  $T_c$  of a material is the McMillan formula [72]. With a standard value for the effective Coulomb coupling parameter  $\mu^* = 0.10$  we obtain an estimation for  $T_c = 1.98\text{K}$ . This is in perfect agreement with the experimental  $T_c$  of  $1.86\text{K}$ [24]. This is in spite of the Mermin-Wagner theorem [74] claiming the absence of SC ordering in 2D due to the onset of fluctuations in the order parameter. While this system is not truly 2D, we expect a high susceptibility with respect fluctuations and a dynamical reduction of  $T_c$ . According to the agreement of the McMillan formula with experiment at first it seems that SC in this 2D limit can be understood from the electronic coupling alone and no fluctuations are necessary to explain the physics of this system. Considering a fully averaged coupling  $\lambda_{\text{av}}$  and ignoring the energy dependence of DOS and screened Coulomb interactions (by approximating them with the value at the Fermi energy), SCDF<sup>1</sup> results are equivalent to McMillan. Within these assumptions, we obtain  $T_c = 2.01\text{K}$  in SCDF for Pb on the undoped substrate and  $T_c$  even rises to  $2.74\text{K}$  for the doped Si substrate. The difference in  $T_c$  between the doped and undoped system is caused by the fact that the undoped material has an average coupling which is much weaker than the coupling among the lead states alone (compare Table 9.1). This implies that the full isotropic approximation is unjustified and we have to allow the substrate and the lead monolayer to develop different pair amplitudes. Forcing both parts of the system to have the same pairing leads to an underestimation of  $T_c$ . Thus, multiband-SC (compare Section 9.2) has to be considered as in  $\text{MgB}_2$  [59].

Using a two isotropic band approach, SCDF predicts for the undoped(doped) system  $T_c = 3.42(3.54)\text{K}$  (compare Tab. 10.1). The computed  $T_c$  turns out to be much higher than the experimental value of  $1.86\text{K}$ . As discussed in Subsection 6.6.1 the isotropization relies on the assumption that in a fully anisotropic calculation the pairing depends on the Bloch vector only via the single particle energy. The McMillan formula relies on the fully isotropic assumption and its good agreement has to be the result of error compensation. Because we cannot reproduce experiment we have to determine which effects have been left out in our approximations and what their effect would be if included. We believe that the only reasonable explanation for the experimental  $T_c$  suppression is the onset of fluctuations of the SC order parameter. To justify this conclusion we have to be able to exclude other mechanisms that possibly suppress  $T_c$ .

I) We have assumed the RPA for the Coulomb interaction. This is reliable in the high-density limit when screening is good. We estimate the effective density of Pb using the density of Pb states at the FS and then using the density of a free electron gas with the same DOS at  $E_f$ . This procedure leads to an effective sphere volume for an electron with radius  $r_s \approx 0.7a_0$ . Therefore the Pb layer is expected to be well described in the RPA. An equivalent procedure for the Si hole pocket (effective  $E_f \approx 20\text{mHa}$ ) leads to a very low density with an average  $r_s \approx 33a_0$  and cannot be expected to be well described by the RPA. However, the strong Coulomb repulsion will

<sup>1</sup>We are using A. Sanna’s improved functional unless not otherwise specified.

|         | $T_c$ [K] | $\Delta^{\text{Pb}}(0)$ [mHa] | $\Delta^{\text{Si}}(0)$ [mHa] | $T_c^{\text{av}}$ [K] |
|---------|-----------|-------------------------------|-------------------------------|-----------------------|
| undoped | 3.42      | 0.026                         | 0.012                         | 2.01                  |
| doped   | 3.54      | 0.027                         | —                             | 2.74                  |

Table 10.1.:  $T_c$  and the SC gaps in the Pb- and Si FS,  $\Delta^{\text{Pb}}(0)$  and  $\Delta^{\text{Si}}(0)$ , respectively via multi-band SCDF.  $T_c^{\text{av}}$  uses an average coupling on both FS, ignoring the energy dependence of DOS and Coulomb interactions (corresponding to a  $\mu^*$  like approximation).

prevent a significant contribution to SC, therefore this inaccuracy cannot affect the estimated  $T_c$  significantly. In the doped system these bands are even beyond the range of SC.

II) Due to Migdal's theorem [48], vertex corrections to the electron phonon coupling are ignored. Due to its shape, the theorem does not apply to the Si hole pocket. However, this cannot have a significant influence since, as discussed before, this band effectively does not take part in the condensation.

III) We consider only a statically screened Coulomb interaction. The result of dynamic (plasmonic) effects could lead to important modifications of the dielectric screening in the case of low energy surface plasmons. However this effect is known to give a positive contribution to SC (enhancement of coulomb renormalization by the plasmonic peak). Therefore, if relevant, it would lead to a higher  $T_c$  prediction.

IV) We use the LDA in the low dimensional limit. This issue has been investigated in detail by Pollack and Perdew [75] showing that LDA performs well as soon as the ratio between the layer thickness and the  $r_s$  coefficient of the gas is  $\gtrsim 2$ . In our case this ratio is  $\approx 5$  and we expect the LDA to perform as reliably as usual.

V) Due to the poor metal-substrate hybridization, the calculated single particle excitation spectrum of Si has a fundamental gap that is about one half of the observed gap in bulk silicon. This may lead to an overestimation in the Coulomb renormalization, and then in an overestimation of  $T_c$ . We have therefore accounted for this effect in our calculations by including a scissor correction on the Si bands and the resulting effect on  $T_c$  correction is  $< 0.1\text{K}$ .

We believe that we have considered all relevant electronic pairing effects. In the bulk limit the critical temperature in SCDFT in the same approximations used for the slab is 6.3K that compares well with the experimental value of 7.2K.

We have not accounted for fluctuations in the order parameter in the present functionals, while this could be in principle captured in SCDFT. According to model calculations, these are strongly suspected to suppress SC. The Mermin-Wagner theorem[74, 23] states that these fluctuations completely forbid SC in two dimensions. In 3D systems of constrained geometry (as surfaces) model calculations for Bose gases and spin systems show that these fluctuations may still be relevant in the limit in which the thickness is on the atomic scale and the in-plane dimension of the system is macroscopic[76, 77]. Due to the strong confinement of the SC phase to the lead layer one would expect to be in a regime where these fluctuation effects are relevant. The disagreement between the calculated and experimental critical temperature then strongly suggests that  $T_c$  is experimentally limited by fluctuations. The SC phase rapidly approaches a value similar to the bulk with an increasing number of Pb layers [78, 79] (see Fig. 10.1), strengthening this conclusion.

While especially in this system  $T_c$  is the most interesting, we compute additional physical properties of this SC system. As mentioned, we perform the following calculations using the functional of Part I, not the spin-degenerate, improved version that yields the accurate results of this Section. We study the undoped system which allows us to see the behavior of a multi-band SC. We show the solutions to the non-linear SSE for the undoped system in Fig. 10.2 . The  $\epsilon$  dependence of the Coulomb coupling makes the gap asymmetric. A two gap structure is clearly visible: The green Si pairing is much less pronounced than the purple Pb. From the linearized

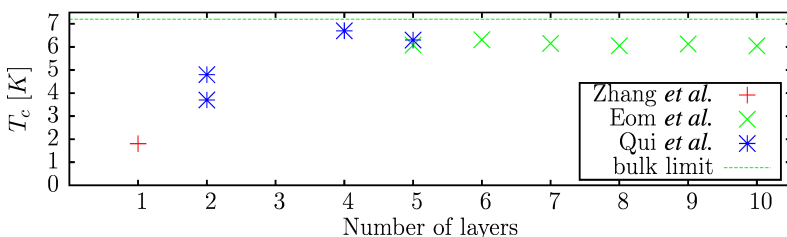


Figure 10.1.:  $T_c$  as a function of the number of layers. Experimental data is from the Refs. [24, 78, 79].



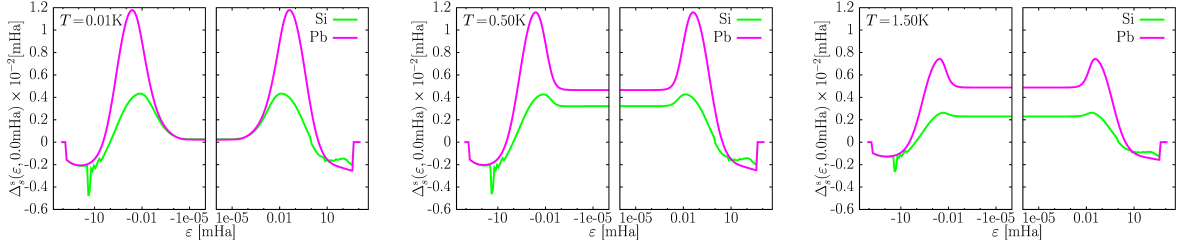


Figure 10.2.:  $\Delta_s^s(\epsilon)$  of the undoped system at  $T = 0.01\text{K}, 0.5\text{K}$  and  $1.5\text{K}$  (l. to r.).

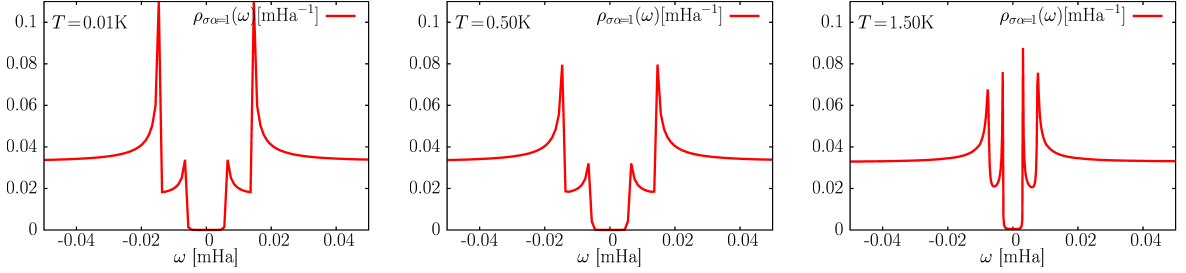


Figure 10.3.: G0W0 DOS for the undoped system at  $T = 0.01\text{K}, 0.5\text{K}$  and  $1.5\text{K}$  (l. to r.).

equation we obtain a critical temperature with the functional of Part I of  $T_c = 1.806\text{K}$  which is much reduced as compared to the functional we have used before in this Section to arrive at the results of Table 10.1. We compute the G0W0 DOS and show the results in Fig. 10.3 . The double gap structure leads to two overlaid dips in the excitation spectrum, one smaller for Si and one larger for Pb. This behaviour is also visible in the local DOS of the SC surface in Fig. 10.4. In the doped case, the Si disappears from the Fermi level. We take  $T = 0.5\text{K}$  and show several frequency steps in the range of SC of this system. The lead states are first enhanced before we enter the Pb gap and they vanish from the plots where only the Si remains. Then the Si states are enhanced before the DOS vanishes in the SC gap.

We conclude this Chapter plotting the real space structure of the order parameter of Fig. 10.5, that has the interpretation of the wavefunction of electrons in the condensed phase. The shape allows us to immediately identify the regions in the unit cell that take part in the SC condensation. We see that the effect of the Coulomb renormalization is to extend the phase into the substrate (dark blue) while the strongest magnitudes are reached in the Pb layer. Being positive, the Pb layer with its high attractive coupling is responsible for SC in this system while proximity effect also makes the Si substrate a SC, due to the Coulomb interacting even in the doped case.

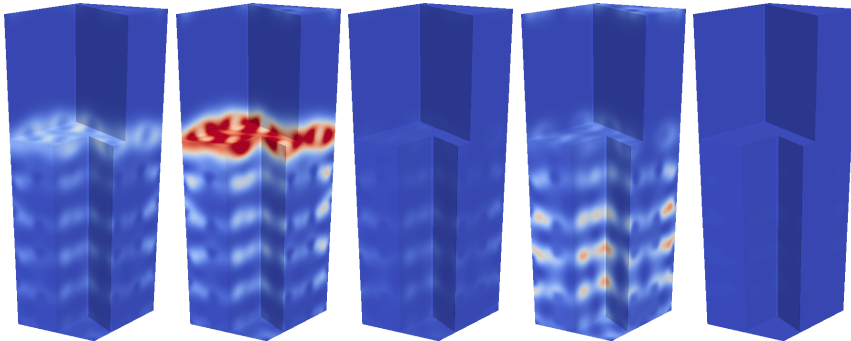


Figure 10.4.: LDOS of SC lead on Si(111) at  $T = 0.5\text{K}$  without external magnetic field. We show (l. to r.) the LDOS 1) before the SC range close to the Fermi level, 2) the larger gap Pb peak, 3) the range after the Pb peak, 4) the Si peak and 5) the excitation gap.

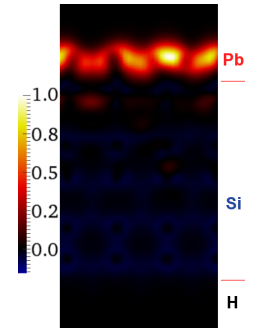


Figure 10.5.: Real-space structure of  $\chi(\mathbf{R}, \mathbf{0})$  normalized to its maximal value of 0.0002765.

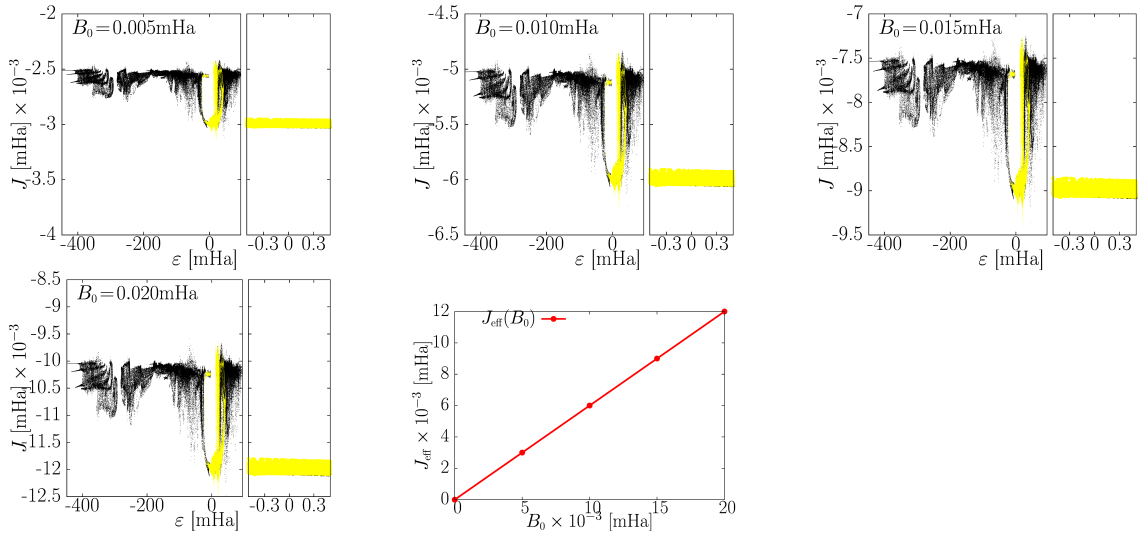


Figure 11.1.:  $J(k)$  vs  $\varepsilon(k)$  for  $B_0 = 0.005, 0.01, 0.015$  and  $0.02$  mHa. Each yellow (black) dot is a  $k = \mathbf{k}, n$  associate with Pb (Si). We highlight the low  $\varepsilon$  region on the left of each plot. We see  $J(k) \approx J_{\text{eff}}$  in the FL region and  $J_{\text{eff}}/B_0 \approx 0.6$ .

## 11. The Si–Pb Surface in a Magnetic Field

In this Section we investigate the SC phase as a function of a small, constant, homogenous magnetic field and of temperature. First, we have to address the question, whether or not we can neglect the current in our calculations. We point out that experimentally, vortices are found [24] that we cannot describe in SpinSCDFT. However, for computing the critical field we expect that the comparison of energies will be the most important, where the Zeemann term dominates the current term. We expect that in our calculation, SC is not fully suppressed by the magnetic field. As before, we attribute this to the replacement  $\bar{\Sigma}[\bar{G}] \rightarrow \bar{\Sigma}[\bar{G}^{\text{KS}}]$ . In addition the replacement will lower the overall predicted  $T_c$  while we expect qualitative agreement.

From the analysis of Part I we expect the critical field for SC of this system in the order of  $10^{-3}$  mHa. Thus, we assume that the coupling matrix elements and thereby the isotropic couplings  $\alpha^2 F_n(\omega)$  and  $C_{nn'}^{\text{stat}}(\mathbf{e}, \mathbf{e}')$  do not change significantly. In Section 11.1 we discuss the isotropization of the system, i.e. to what extent the homogenous field results in an effective splitting parameter  $J_{\text{eff}}$ . Then, in Section 11.2, we compute SC of the system as a function of temperature and field strength  $B_0$ .

### 11.1. Isotropization of the Si – Pb Surface in a Magnetic Field

Screening effects may result in an anisotropic magnetic field, even if the applied external field is homogenous. We sample the KS single particle energy distribution  $\varepsilon_{k\sigma}$  on a random grid in first Brillouin zone with a higher acceptance probability close to  $E_f$ . For the external fields  $B_0 = 0.005$  mHa,  $0.01$  mHa,  $0.015$  mHa and  $0.02$  mHa, for each such point  $k = (\mathbf{k}, n)$  we compute  $\varepsilon(k) = (\varepsilon_{k\uparrow} + \varepsilon_{-k\downarrow})/2$  and  $J(k) = (\varepsilon_{k\uparrow} - \varepsilon_{-k\downarrow})/2$  and plot a dot in Fig. 11.1. We see that the screening of the magnetic field is anisotrop and  $\varepsilon$  dependent. Note, however, that we always compare  $J$  with  $\varepsilon$  in the equations of Part I and thus the only relevant splitting parameter is the value at the Fermi level. We highlight a smaller range about  $\varepsilon \approx 0$  on the right of every plot in Fig. 11.1. In this range we clearly see that to a good approximation  $J(k) \approx J_{\text{eff}}$ . For our four values of the fields we extract the effective splitting parameters  $J_{\text{eff}} \approx 0.003, 0.006, 0.009$  and  $0.012$  mHa which results in  $J_{\text{eff}} \approx 0.6 B_0$ . This allows us to compute the critical magnetic field taking some of the (non SC) screening of the magnetic field into account.

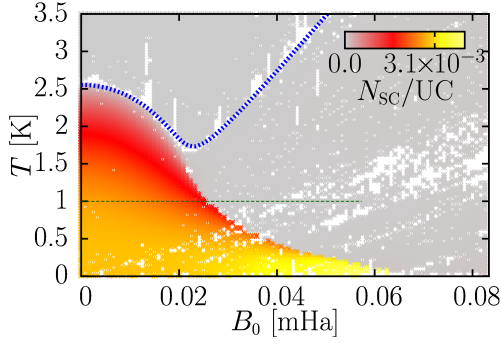


Figure 11.2.:  $N_{sc}(T, B_0)$  for Pb on doped Si(111) and the linear  $T_c(B_0)$  curve.

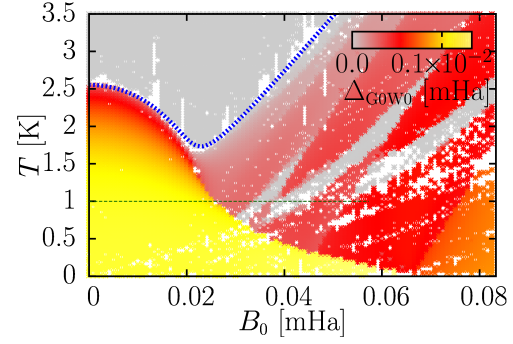


Figure 11.3.: The SC G0W0 gap of Pb on doped Si(111) as a function of  $T$  and  $B_0$ .

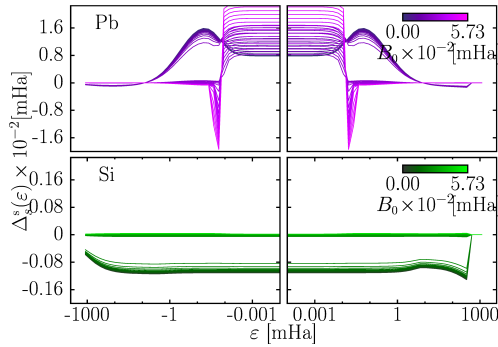


Figure 11.4.:  $\Delta_s^s(\epsilon)$  along the dashed green line in Fig. 11.2

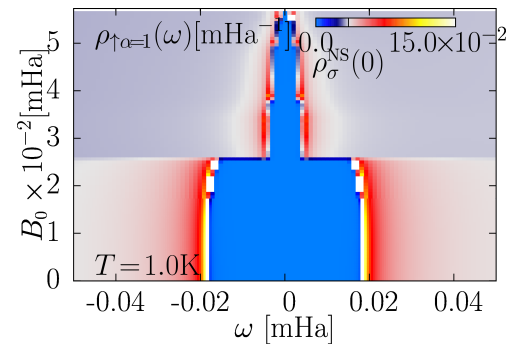


Figure 11.5.: The SC G0W0 gap of Pb on doped Si(111) at  $T = 1.0\text{K}$  along the dashed green line in Fig. 11.3.

## 11.2. Suppression of SC via a Magnetic Field

From the last Section 11.1 we conclude that to a good approximation the external  $B_0$  results in an effective splitting parameter of  $J_{\text{eff}} = 0.6B_0$ . Thus, we may use the tools of the last part to compute the phase diagram. For the analysis of this Section we use the doped system since it is realized in experiment [24]. While we can thus compute SC physical properties of a real material in a magnetic field such as excitation spectra and the critical field from first principles, the results have to be taken with care. The inclusion of fluctuation corrections is beyond the scope of this thesis as is the fitting procedure to account for the replacement of  $\bar{\Sigma} \rightarrow \bar{\Sigma}^{\text{KS}}$ . The earlier discussions suggests that these effects have to be considered. Similar to the  $T_c$  via the McMillan method, we do expect some error compensation. The experimental upper critical field (perpendicular to the surface as in our calculation) is estimated in Ref. [24] to be  $B_0^{\text{II}} = 0.145\text{T}$ . We cannot describe the vortex state, still, since in this geometry the field penetrates the SC, we expect that  $B_0^{\text{II}}$  is similar to a homogenous field that suppresses the SC phase. When we compare our results of Fig. 11.2<sup>1</sup> to experiment we have to take into account that the high field SC tail is not the minimum of the free energy similar to BCS in Fig. 2.1 b). Assuming that the corrected phase diagram has a similar shape as BCS in Fig. 2.1 b), we extract the critical field  $B_c \approx 0.03\text{mHa} = 1.4\text{T}$  from Fig. 11.2 at  $T = 0\text{K}$ . We note that this is one order of magnitude above  $B_0^{\text{II}}$ .  $B_0^{\text{II}}$  is the point where the vortices get too dense so that the super currents that allow the flux through the core become too localized, instead  $B_c$  is computed neglecting current contributions. Clearly, parts of the mismatch have to be attributed to the  $T_c$  overestimation. Also, impurity effects have been neglected that may significantly influence the result.

<sup>1</sup>The data of Fig. 11.2 and 11.3 was computed starting always from a constant initial guess while the data of Fig. 11.4 and 11.5 was obtained from low to high  $B_0$  in the sense of Sec. 8.5.

# Summary and Outlook

In this second Part we simulate the SC phase of the realistic system: A lead monolayer on a silicon (111) surface. We model the semi-infinite substrate with a 10 monolayer slab that is saturated with hydrogen. The SC of this system turns out to be interesting even without the magnetic field. Carefully revisiting common approximations in the context of SC we conclude that the agreement of the experimental  $T_c$  with the McMillan formula is due to error compensation. Allowing the surface and the substrate to develop different pair amplitudes we overestimate  $T_c$  by a factor of two. We attribute this overestimation to the fact that we do not include fluctuations in the order parameter which according to model calculations is a very important mechanism in constrained geometries.

Then, as a next step, we apply a perpendicular magnetic field  $B_0$  to the system and compute the number of condensed electrons per unit cell as a function of  $T$  and  $B_0$ . We estimate the critical field at  $T = 0\text{K}$  to be  $B_c \approx 1.4\text{T}$  which is one order of magnitude higher than the upper critical field  $B_0^{\text{H}}$  in experiment. We might conclude that in lead on silicone the critical field is limited by currents which are not part of the present description or the effect of impurities. Clearly a systematic investigation is in order.

Several questions have been left out to future investigations. For the most important question, we could argue that a fitting procedure similar to A. Sanna to rise the  $T_c(J = 0)$  to the experimental value is likely to remove the unphysical solutions past the first order phase transition. As a further interesting aspect we found that the functional construction generates triplet components in the order parameter. The effects of such contributions in the functional seem to be small, but the inclusion of triplet pairing clearly deserves further attention. As a further intriguing project we would like to include the effects of fluctuations in the order parameter into an ab-initio theory. Intuitively we expect that this will require the susceptibility of the SC state with respect to variations in the order parameter. A formal derivation of an effective interaction that involves the SC fluctuations appears desirable.

# Appendix

# A. Derivation of the Continuity Equation

The goal of this section is to compute the divergence of the current operator which will lead to the continuity equation for superconductors on an operator level. As the governing Hamiltonian, we consider the full SC Pauli equation, i. e. we take  $\hat{H}$  of Eq. (3.1) but we replace in the part  $\hat{H}_e$  of Eq. (3.2)

$$\hat{T}^e \rightarrow \hat{T}_A^e = \int d\mathbf{r} \hat{\psi}^\dagger(\mathbf{r}) \cdot \frac{1}{2m_e} \sigma_0 (-i\hbar\nabla + \frac{e}{c}\mathbf{A}(\mathbf{r}))^2 \cdot \hat{\psi}(\mathbf{r}). \quad (\text{A.1})$$

with the paramagnetic current operator

$$\hat{\mathbf{j}}_p(\mathbf{r}) = \frac{\hbar}{2m_e i} \sum_{\sigma} \{ \hat{\psi}^\dagger(\mathbf{r}\sigma) (\nabla \hat{\psi}(\mathbf{r}\sigma)) - (\nabla \hat{\psi}^\dagger(\mathbf{r}\sigma)) \hat{\psi}(\mathbf{r}\sigma) \}. \quad (\text{A.2})$$

We may write  $\hat{T}_A^e$  also as

$$\begin{aligned} \hat{T}_A^e = & - \sum_{\sigma} \int d\mathbf{r} \hat{\psi}^\dagger(\mathbf{r}\sigma) \frac{\hbar^2}{2m_e} \nabla^2 \hat{\psi}(\mathbf{r}\sigma) + \\ & + \frac{e^2}{2c^2} \int d\mathbf{r} \hat{n}(\mathbf{r}) \mathbf{A}^2(\mathbf{r}) + \int d\mathbf{r} \hat{\mathbf{j}}_p(\mathbf{r}) \frac{e}{c} \mathbf{A}(\mathbf{r}), \end{aligned} \quad (\text{A.3})$$

if we assume

$$\int \nabla (\mathbf{A}(\mathbf{r}) \hat{n}(\mathbf{r})) d\mathbf{r} \equiv 0 \quad (\text{A.4})$$

This can be viewed a reasonable assumption because the flow through the surface at infinity is zero. In the theoretical model of crystals with periodic boundary conditions the validity of this assumption is not so easily argued. We introduce the current operator that is connected with the paramagnetic current Eq. (A.2) via

$$\hat{\mathbf{j}}(\mathbf{r}) = \hat{\mathbf{j}}_p(\mathbf{r}) + \frac{e^2}{2c^2} \hat{n}(\mathbf{r}) \mathbf{A}_{\text{ext}}(\mathbf{r}) \quad (\text{A.5})$$

For the present purpose we neglect the vector potential acting on the nuclear kinetic operator Eq. (3.11). We thus evaluate

$$(\nabla \cdot \hat{\mathbf{j}}) = \left( \nabla \cdot \left( \hat{\mathbf{j}}_p + \frac{e}{2c} \hat{n}(\mathbf{r}) \mathbf{A}(\mathbf{r}) \right) \right). \quad (\text{A.6})$$

We consider the paramagnetic part first, is which readily seen to equal

$$(\nabla \cdot \hat{\mathbf{j}}_p) = \frac{\hbar}{2m_e i} \sum_{\sigma} \left\{ \hat{\psi}^\dagger(\mathbf{r}\sigma) (\nabla^2 \hat{\psi}(\mathbf{r}\sigma)) - (\nabla^2 \hat{\psi}^\dagger(\mathbf{r}\sigma)) \hat{\psi}(\mathbf{r}\sigma) \right\} \quad (\text{A.7})$$

because the terms  $(\nabla \hat{\psi}^\dagger(\mathbf{r}\sigma)) \cdot (\nabla \hat{\psi}(\mathbf{r}\sigma))$  cancel. Further, let us compute

$$\left[ \int \hat{\psi}^\dagger(\mathbf{r}) \nabla^2 \hat{\psi}(\mathbf{r}) d\mathbf{r}, \hat{\psi}^\dagger(\mathbf{x}\sigma') \hat{\psi}(\mathbf{x}\sigma') \right] \quad (\text{A.8})$$

Due to the peculiar behavior of the derivative operator we prefer to perform the calculation for matrix elements in a plane wave basis

$$\begin{aligned} & [\int \hat{\psi}^\dagger(\mathbf{r}\sigma) \nabla^2 \hat{\psi}(\mathbf{r}\sigma) d\mathbf{r}, \hat{\psi}^\dagger(\mathbf{x}\sigma') \hat{\psi}(\mathbf{x}\sigma')] = \\ & = - \sum_{kll'} [\hat{c}_{k\sigma}^\dagger \mathbf{k}^2 \hat{c}_{k\sigma}, \hat{c}_{l'\sigma'}^\dagger \hat{c}_{l\sigma'}] e^{-i\mathbf{x}\cdot\mathbf{l}'} e^{i\mathbf{x}\cdot\mathbf{l}} \end{aligned} \quad (\text{A.9})$$

with

$$[\hat{c}_{k\sigma}^\dagger \mathbf{k}^2 \hat{c}_{k\sigma}, \hat{c}_{l'\sigma'}^\dagger \hat{c}_{l\sigma'}] = \delta_{kl'} \delta_{\sigma\sigma'} \mathbf{k}^2 \hat{c}_{k\sigma}^\dagger \hat{c}_{l\sigma'} - \delta_{kl} \delta_{\sigma\sigma'} \hat{c}_{l'\sigma'}^\dagger \mathbf{k}^2 \hat{c}_{k\sigma} \quad (\text{A.10})$$

so that

$$\begin{aligned} & [\sum_{\sigma\sigma'} \int \hat{\psi}^\dagger(\mathbf{r}\sigma) \nabla^2 \hat{\psi}(\mathbf{r}\sigma) d\mathbf{r}, \hat{\psi}^\dagger(\mathbf{x}\sigma') \hat{\psi}(\mathbf{x}\sigma')] = \\ & = \sum_{\sigma l l'} (\hat{c}_{l'\sigma'}^\dagger \mathbf{l}^2 \hat{c}_{l\sigma} - \mathbf{l}'^2 \hat{c}_{l'\sigma'}^\dagger \hat{c}_{l\sigma'}) e^{-i\mathbf{x}\cdot\mathbf{l}'} e^{i\mathbf{x}\cdot\mathbf{l}} \end{aligned} \quad (\text{A.11})$$

$$= - \sum_{\sigma} \left\{ \hat{\psi}^\dagger(\mathbf{x}\sigma) (\nabla^2 \hat{\psi}(\mathbf{x}\sigma)) - (\nabla^2 \hat{\psi}^\dagger(\mathbf{x}\sigma)) \hat{\psi}(\mathbf{x}\sigma) \right\} \quad (\text{A.12})$$

$$= \frac{2m_e}{i\hbar} (\nabla \cdot \hat{\mathbf{j}}_p(\mathbf{x})) \quad (\text{A.13})$$

Similarly, in a plane wave expansion, we compute

$$[\int \hat{\mathbf{j}}_p(\mathbf{r}) \mathbf{A}_{\text{ext}}(\mathbf{r}) d\mathbf{r}, \hat{n}(\mathbf{x})] = \frac{\hbar}{im_e} \nabla (\hat{n}(\mathbf{r}) \mathbf{A}(\mathbf{r})). \quad (\text{A.14})$$

Finally for the diamagnetic, second part of Eq. (A.6), with

$$[\int \hat{n}(\mathbf{r}) \mathbf{A}_{\text{ext}}^2(\mathbf{r}) d\mathbf{r}, \hat{n}(\mathbf{r})] = 0, \quad (\text{A.15})$$

we arrive at the divergence of the physical current operator

$$(\nabla \cdot \hat{\mathbf{j}}(\mathbf{r})) = \frac{1}{i\hbar} [\hat{T}_A^e, \hat{n}(\mathbf{r})]. \quad (\text{A.16})$$

All the interaction potentials usually commute with the density operator, e.g. the Coulomb interaction and the electron phonon Coupling. This expresses the fact that those potentials conserve the particle number. Thus, in general,

$$[\hat{W}^{ee}, \hat{n}(\mathbf{r})] = [\hat{V}^e, \hat{n}(\mathbf{r})] = [\hat{U}^{en}, \hat{n}(\mathbf{r})] = [\hat{V}_s, \hat{n}(\mathbf{r})] = 0. \quad (\text{A.17})$$

It is straight forward to verify

$$[\hat{H}_B, \hat{n}(\mathbf{r})] = 0. \quad (\text{A.18})$$

However, using the total antisymmetry of  $\Delta_{\sigma\sigma'}(\mathbf{r}, \mathbf{r}')$

$$[\hat{H}_\Delta, \hat{n}(\mathbf{r}')] = \sum_{\sigma\sigma'} \int d\mathbf{r} (\Delta_{\sigma\sigma'}(\mathbf{r}, \mathbf{r}') \hat{\psi}(\mathbf{r}\sigma) \hat{\psi}(\mathbf{r}'\sigma') - \text{h.c.}) \neq 0. \quad (\text{A.19})$$

Thus, we find

$$(\nabla \cdot \hat{\mathbf{j}}(\mathbf{r})) = \frac{1}{i\hbar} [\hat{H}, \hat{n}(\mathbf{r})] - \frac{1}{i\hbar} [\hat{H}_\Delta, \hat{n}(\mathbf{r})], \quad (\text{A.20})$$

and represent the above equation in the Heisenberg picture. Recognizing the Heisenberg equation of motion

$$\frac{i}{\hbar}[\hat{H}, \hat{n}(\mathbf{r})]_H(t) = \partial_t \hat{n}_H(\mathbf{r}t) \quad (\text{A.21})$$

we obtain the continuity equation in the Heisenberg picture for a superconductor

$$(\nabla \cdot \hat{\mathbf{j}}(\mathbf{r}))_H(t) + \partial_t \hat{n}_H(\mathbf{r}t) + \frac{i}{\hbar}[\hat{H}_\Delta, \hat{n}(\mathbf{r})]_H(t) = 0 \quad (\text{A.22})$$

This procedure applies to every, interacting or non-interacting, Hamiltonian  $\hat{H}$ . Even a true time dependence is possible, although not considered here.

**A comment on the current as a density** If we attempt to add the paramagnetic current as an additional density to the KS system the continuity equations connects it with the pair potential. Since in a static system

$$\langle [\hat{H}, \hat{n}(\mathbf{r})] \rangle = 0, \quad (\text{A.23})$$

the continuity equation becomes equivalent to

$$\nabla \cdot \mathbf{j}(\mathbf{r}) = -\frac{i}{\hbar} \int d\mathbf{r}' \Im(\Delta(\mathbf{r}, \mathbf{r}') \cdot \chi(\mathbf{r}, \mathbf{r}')), \quad (\text{A.24})$$

so the imaginary part of the pair term acts as a source for the current. If we tried to choose  $\mathbf{j}(\mathbf{r})$  as a density we could equate Eq. (A.24) for the KS and the exact system and obtain a severe condition for the KS potential of the form  $\int d\mathbf{r}' \Im(\Delta_{\text{ext}}(\mathbf{r}, \mathbf{r}') \cdot \chi(\mathbf{r}, \mathbf{r}')) = \int d\mathbf{r}' \Im(\Delta_s(\mathbf{r}, \mathbf{r}') \cdot \chi(\mathbf{r}, \mathbf{r}'))$ . If just the paramagnetic current density is reproduced by the KS system we obtain similarly

$$\frac{e}{2c} \nabla \cdot (n(\mathbf{r})(\mathbf{A}_{\text{ext}}(\mathbf{r}) - \mathbf{A}_s(\mathbf{r}))) = -\frac{i}{\hbar} \int d\mathbf{r}' \Im((\Delta_{\text{ext}}(\mathbf{r}, \mathbf{r}') - \Delta_s(\mathbf{r}, \mathbf{r}')) \cdot \chi(\mathbf{r}, \mathbf{r}')) \quad (\text{A.25})$$

We may integrate this equation and drop the surface terms on the left to obtain condition for the pair potential

$$\int d\mathbf{r} \int d\mathbf{r}' \Im((\Delta_{\text{ext}}(\mathbf{r}, \mathbf{r}') - \Delta_s(\mathbf{r}, \mathbf{r}')) \cdot \chi(\mathbf{r}, \mathbf{r}')) = 0 \quad (\text{A.26})$$

with the physical interpretation that the total current source over all space due to the pair potential is equal in the KS as compared to the exact system.



## B. Relations for expansion coefficients in the Spin Decoupling Approximation

In this Appendix we want to introduce several relations among the  $u_{k\mu}^{k\alpha}, v_{k-\mu}^{-k\alpha}$  and  $E_{k\mu}^\alpha$ ,  $\alpha = \pm$  which are essential to follow the calculations done during the functional construction. Due to space limitations and because proving the those relations involves only a bit of algebra, we do not explicitly demonstrate the equations.

The first part uses mainly the Eqs. (3.158) to (3.161). We find

1.

$$|\Delta_{sk}^s|^2 = (E_{k\mu}^\alpha - \varepsilon_{k\mu})(\varepsilon_{-k-\mu} + E_{k\mu}^\alpha) \quad (\geq 0) \quad (\text{B.1})$$

2.

$$E_{k\mu}^\alpha - \varepsilon_{k\mu} = -\varepsilon_{-k-\mu} - E_{k\mu}^{-\alpha} = E_{-k-\mu}^\alpha - \varepsilon_{-k-\mu} \quad (\text{B.2})$$

$$E_{k\mu}^\alpha + \varepsilon_{-k-\mu} = \varepsilon_{k\mu} - E_{k\mu}^{-\alpha} = \varepsilon_{k\mu} + E_{-k-\mu}^\alpha \quad (\text{B.3})$$

3.

$$\text{sign}(\alpha) = \text{sign}(E_{k\mu}^\alpha - \varepsilon_{k\mu}) = \text{sign}(E_{k\mu}^\alpha + E_{-k-\mu}^\alpha) = \text{sign}(\varepsilon_{-k-\mu} + E_{k\mu}^\alpha) \quad (\text{B.4})$$

4.

$$(E_{k\mu}^\alpha - \varepsilon_{k\mu})(\varepsilon_{-k-\mu} + E_{k\mu}^\alpha) = \text{sign}(\alpha)^2 |E_{k\mu}^\alpha - \varepsilon_{k\mu}| |\varepsilon_{-k-\mu} + E_{k\mu}^\alpha| \quad (\text{B.5})$$

$$= |E_{k\mu}^\alpha - \varepsilon_{k\mu}| |\varepsilon_{-k-\mu} + E_{k\mu}^\alpha| (= |\Delta_{sk}^s|^2) \quad (\text{B.6})$$

Using the above relations we compute  $u_{k\mu}^{k\alpha}, v_{k-\mu}^{-k\alpha}$ . This involves first to normalize the eigenvector  $\tilde{g}_{k\mu}^\alpha$  of Eq. (3.157). Its norm is

$$|\tilde{g}_{k\mu}^\alpha| = \sqrt{\frac{|E_{k\mu}^\alpha + E_{-k-\mu}^\alpha|}{|E_{k\mu}^\alpha - \varepsilon_{k\mu}|}}. \quad (\text{B.7})$$

With Eq. B.4 it is clear that Eq. (B.1) also implies

$$\frac{\varepsilon_{-k-\mu} + E_{k\mu}^\alpha}{\text{sign}(\mu) \Delta_{sk}^{s*}} \sqrt{\frac{|E_{k\mu}^\alpha - \varepsilon_{k\mu}|}{|E_{k\mu}^\alpha + E_{-k-\mu}^\alpha|}} = \frac{\text{sign}(\alpha) |\Delta_{sk}^s|}{\text{sign}(\mu) \Delta_{sk}^{s*}} \sqrt{\frac{|\varepsilon_{-k-\mu} + E_{k\mu}^\alpha|}{|E_{k\mu}^\alpha + E_{-k-\mu}^\alpha|}} \quad (\text{B.8})$$

so

$$g_{k\mu}^\alpha = \frac{\tilde{g}_{k\mu}^\alpha}{|\tilde{g}_{k\mu}^\alpha|} = \left( \begin{array}{c} \frac{\text{sign}(\alpha) |\Delta_{sk}^s|}{\text{sign}(\mu) \Delta_{sk}^{s*}} \sqrt{\frac{|E_{k\mu}^\alpha + \varepsilon_{-k-\mu}|}{|E_{k\mu}^\alpha + E_{-k-\mu}^\alpha|}} \\ \sqrt{\frac{|E_{k\mu}^\alpha - \varepsilon_{k\mu}|}{|E_{k\mu}^\alpha + E_{-k-\mu}^\alpha|}} \end{array} \right) \quad (\text{B.9})$$

Here we see

$$v_{k-\mu}^{-k\alpha} = \sqrt{\frac{|E_{k\mu}^\alpha - \varepsilon_{k\mu}|}{|E_{k\mu}^+ + E_{-k-\mu}^+|}} \quad (\text{B.10})$$

$$u_{k\mu}^{k\alpha} = \text{sign}(\alpha)\text{sign}(\mu) \frac{|\Delta_{sk}^s|}{\Delta_{sk}^{s*}} \sqrt{\frac{|\varepsilon_{-k-\mu} + E_{k\mu}^\alpha|}{|E_{k\mu}^\alpha + E_{-k-\mu}^\alpha|}} \quad (\text{B.11})$$

Many further useful relations can be shown:

1.

$$E_{k\mu}^{\alpha 2} = \varepsilon_{-k-\mu}^2 + (\varepsilon_{k\mu} - \varepsilon_{-k-\mu})(\varepsilon_{-k-\mu} + E_{k\mu}^\alpha) + |\Delta_{sk}^s|^2 \quad (\text{B.12})$$

2.

$$|u_{k\mu}^{k\alpha}|^2 |u_{-k-\mu}^{-k\alpha}|^2 + |v_{k-\mu}^{-k\alpha}|^2 |v_{-k\mu}^{k\alpha}|^2 = \frac{(\varepsilon_{k\mu} + \varepsilon_{-k-\mu})^2 + 2|\Delta_{sk}^s|^2}{|E_{k\mu}^\alpha + E_{-k-\mu}^\alpha|^2} \quad (\text{B.13})$$

3.

$$|u_{k\mu}^{k\alpha}|^2 |v_{k-\mu}^{-k\alpha'}|^2 = \frac{|\Delta_{sk}^s|^2 \delta_{\alpha\alpha'} + (\varepsilon_{-k-\mu} + E_{k\mu}^\alpha)^2 \delta_{\alpha, -\alpha'}}{(E_{k\mu}^\alpha + E_{-k-\mu}^\alpha)^2} \quad (\text{B.14})$$

4.

$$|u_{k\mu}^{k\alpha}|^2 |u_{-k-\mu}^{-k\alpha}|^2 = \frac{(\varepsilon_{-k-\mu} + E_{k\mu}^\alpha)^2}{(E_{k\mu}^\alpha - E_{k\mu}^{-\alpha})^2} \quad (\text{B.15})$$

5.

$$u_{k\mu}^{k\gamma} v_{k-\mu}^{-k\gamma*} (= u_{-k-\mu}^{-k-\gamma} v_{-k\mu}^{k-\gamma*}) = \text{sign}(\mu)\text{sign}(\gamma) \frac{\Delta_{sk}^s}{|E_{k\mu}^+ - E_{k\mu}^-|} \quad (\text{B.16})$$

6.

$$u_{k\mu}^{k\gamma*} v_{k-\mu}^{-k\gamma} = (u_{k\mu}^{k\gamma} v_{k-\mu}^{-k\gamma*})^* = \text{sign}(\mu)\text{sign}(\gamma) \frac{\Delta_{sk}^{s*}}{|E_{k\mu}^+ - E_{k\mu}^-|} \quad (\text{B.17})$$

7.

$$|u_{k\mu}^{k\alpha}|^2 = |u_{-k-\mu}^{-k\alpha}|^2 = |v_{-k\mu}^{k-\alpha}|^2 = |v_{k-\mu}^{-k-\alpha}|^2 \quad (\text{B.18})$$

8.

$$(\varepsilon_{-k-\mu} + E_{k\mu}^+)^2 + (\varepsilon_{-k-\mu} + E_{k\mu}^-)^2 = (\varepsilon_{-k-\mu} + \varepsilon_{k\mu})^2 + 2|\Delta_{sk}^s|^2 \quad (\text{B.19})$$

# C. The Coulomb Potential in Fourier Space and Integral Representations of $\chi^{pol}$ and $\epsilon^{-1}$ .

## C.1. The Coulomb Potential in Fourier Space

Let us consider a potential with the property of being independent on the absolute position in the lattice

$$V(\mathbf{r} + \mathbf{T}_j, \mathbf{r}' + \mathbf{T}_j) = V(\mathbf{r}, \mathbf{r}') \quad (\text{C.1})$$

where  $\mathbf{T}_j$  is a lattice translation. Disregarding the surface of a real material one expects such a symmetry in almost every physical system. The general Fourier transform of a function  $V$  with this property<sup>1</sup> is

$$V(\bar{\mathbf{q}}, \bar{\mathbf{q}}') = \sum_{\mathbf{T}_i, \mathbf{T}_j} \iint_{\text{UC}} d\bar{\mathbf{r}} d\bar{\mathbf{r}}' V(\bar{\mathbf{r}} + \mathbf{T}_i, \bar{\mathbf{r}}' + \mathbf{T}_j) e^{-i\bar{\mathbf{q}} \cdot (\bar{\mathbf{r}} + \mathbf{T}_i)} e^{i\bar{\mathbf{q}}' \cdot (\bar{\mathbf{r}}' + \mathbf{T}_j)} \quad (\text{C.2})$$

If we also separate  $\bar{\mathbf{q}} = (\mathbf{q} \in \text{BZ}) + \mathbf{G}$ , we obtain

$$V(\mathbf{q} + \mathbf{G}, \mathbf{q}' + \mathbf{G}') = \sum_{\mathbf{T}_{ij}} \iint_{\text{UC}} d\bar{\mathbf{r}} d\bar{\mathbf{r}}' V(\bar{\mathbf{r}} + \mathbf{T}_{ij}, \bar{\mathbf{r}}') e^{-i\mathbf{q} \cdot \mathbf{T}_{ij}} e^{-i(\mathbf{q} + \mathbf{G}) \cdot \bar{\mathbf{r}}} e^{i(\mathbf{q}' + \mathbf{G}') \cdot \bar{\mathbf{r}}'} \underbrace{\sum_{\mathbf{T}_j} e^{i(\mathbf{q}' - \mathbf{q}) \cdot \mathbf{T}_j}}_{N_q \delta_{\mathbf{q}', \mathbf{q}}} \quad (\text{C.3})$$

Thus we may put this as

$$V(\mathbf{q} + \mathbf{G}, \mathbf{q}' + \mathbf{G}') = N_q V(\mathbf{q}, \mathbf{G}, \mathbf{G}') \delta_{\mathbf{q}', \mathbf{q}} \quad (\text{C.4})$$

with

$$V(\mathbf{q}, \mathbf{G}, \mathbf{G}') = \sum_{\mathbf{T}_i} \iint_{\text{UC}} d\bar{\mathbf{x}} d\bar{\mathbf{x}}' V(\bar{\mathbf{x}} + \mathbf{T}_i, \bar{\mathbf{x}}') e^{-i(\mathbf{q} + \mathbf{G}) \cdot \bar{\mathbf{x}}} e^{i(\mathbf{q} + \mathbf{G}') \cdot \bar{\mathbf{x}}'} e^{-i\mathbf{q} \cdot \mathbf{T}_i} \quad (\text{C.5})$$

For such a function we see that  $\mathbf{q}'$  needs to be  $\mathbf{q}$  up to an arbitrary vector of the reciprocal lattice  $\mathbf{G}_q$ . It is found that for two opposite vectors  $\mathbf{q}' = -\mathbf{q}$ ,  $\mathbf{G}_q = \mathbf{0}$ .

Application of the above to the Coulomb potential

$$V^{\text{Coul}}(\mathbf{r}, \mathbf{r}') = \frac{1}{4\pi\epsilon_0} \frac{e^2}{|\mathbf{r} - \mathbf{r}'|} \quad (\text{C.6})$$

results in the Fourier transform

$$V^{\text{Coul}}(\mathbf{q}, \mathbf{G}, \mathbf{G}') = \frac{e^2}{4\pi\epsilon_0} \sum_{\mathbf{T}_i} \iint_{\text{UC}} d\bar{\mathbf{r}} d\bar{\mathbf{r}}' \frac{e^{-i(\mathbf{q} + \mathbf{G}) \cdot \bar{\mathbf{r}}} e^{i(\mathbf{q} + \mathbf{G}') \cdot \bar{\mathbf{r}}'} e^{-i\mathbf{q} \cdot \mathbf{T}_i}}{|\bar{\mathbf{r}} - \bar{\mathbf{r}}' + \mathbf{T}_i|} \quad (\text{C.7})$$

---

<sup>1</sup>We distinguish: Vectors in real space with a bar  $\bar{\mathbf{r}}$  are defined in the first uni cell and  $\mathbf{r}$  gives the total position. Instead vectors in reciprocal space  $\mathbf{q}$  **without** a bar are defined in the first BZ and  $\bar{\mathbf{q}}$  is given in the full reciprocal lattice.

Since the straight forward evaluation of the integral is ill-defined we take the Yukawa form of the coupling and the limit of “zero mass” after the transformation

$$V^{Coul}(\mathbf{q}, \mathbf{G}, \mathbf{G}') = \frac{e^2}{4\pi\epsilon_0} \lim_{\eta \rightarrow 0^+} \sum_{\mathbf{T}_i} \iint_{UC} d\bar{\mathbf{r}} d\bar{\mathbf{r}}' \frac{e^{-\eta|\bar{\mathbf{r}}-\bar{\mathbf{r}}'+\mathbf{T}_i|}}{|\bar{\mathbf{r}}-\bar{\mathbf{r}}'+\mathbf{T}_i|} e^{-i\mathbf{G}\cdot\bar{\mathbf{r}}} e^{i\mathbf{G}'\cdot\bar{\mathbf{r}}'} e^{-i\mathbf{q}\cdot(\bar{\mathbf{r}}-\bar{\mathbf{r}}'+\mathbf{T}_i)} \quad (C.8)$$

Reintroducing  $\mathbf{r} = \bar{\mathbf{r}} + \mathbf{T}_i$  and  $\mathbf{x} = \mathbf{r} - \bar{\mathbf{r}}'$  the above becomes

$$V^{Coul}(\mathbf{q}, \mathbf{G}, \mathbf{G}') = \frac{e^2}{4\pi\epsilon_0} \lim_{\eta \rightarrow 0^+} \int_{vol} d\mathbf{x} \int_{UC} d\bar{\mathbf{r}}' \frac{e^{-\eta|\mathbf{x}|}}{|\mathbf{x}|} e^{-i\mathbf{G}\cdot\mathbf{x}} e^{i\mathbf{G}\cdot(\mathbf{T}_i-\bar{\mathbf{r}}')} e^{i\mathbf{G}'\cdot\bar{\mathbf{r}}'} e^{-i\mathbf{q}\cdot\mathbf{x}} \quad (C.9)$$

$$= \frac{e^2}{4\pi\epsilon_0} \lim_{\eta \rightarrow 0^+} \int_{UC} d\bar{\mathbf{r}}' e^{i(\mathbf{G}'-\mathbf{G})\cdot\bar{\mathbf{r}}'} \int_0^\infty dx \int_{-1}^1 d\cos(\theta) \int_0^{2\pi} d\varphi x^2 \frac{e^{-\eta x}}{x} e^{i|\mathbf{G}+\mathbf{q}|x \cos(\theta)} \quad (C.10)$$

$$= \int_{UC} d\bar{\mathbf{r}}' e^{i(\mathbf{G}'-\mathbf{G})\cdot\bar{\mathbf{r}}'} 2\pi \lim_{\eta \rightarrow 0^+} \left( \frac{1}{i|\mathbf{G}+\mathbf{q}|(|\mathbf{G}+\mathbf{q}|-\eta)} + \frac{1}{i|\mathbf{G}+\mathbf{q}|(|\mathbf{G}+\mathbf{q}|+\eta)} \right) \quad (C.11)$$

where the limit  $\eta \rightarrow 0^+$  is safely taken. Using  $\int_{UC} d\bar{\mathbf{r}}' e^{i(\mathbf{G}'-\mathbf{G})\cdot\bar{\mathbf{r}}'} = \Omega_{UC} \delta_{\mathbf{G}', \mathbf{G}}$  we obtain

$$V^{Coul}(\mathbf{q}, \mathbf{G}, \mathbf{G}') = -\frac{e^2 \Omega_{UC}}{\epsilon_0 |\mathbf{q} + \mathbf{G}|^2} \delta_{\mathbf{G}', \mathbf{G}} \quad (C.12)$$

$$V^{Coul}(\bar{\mathbf{r}}, \bar{\mathbf{r}}', \mathbf{T}_i) = -\frac{e^2}{N_{\mathbf{q}} \Omega_{UC} \epsilon_0} \sum_{\mathbf{G}} \frac{1}{|\mathbf{q} + \mathbf{G}|^2} e^{i(\mathbf{q}+\mathbf{G})\cdot(\bar{\mathbf{r}}-\bar{\mathbf{r}}'+\mathbf{T}_i)} \quad (C.13)$$

in terms of the original interaction

$$V^{Coul}(\mathbf{r}, \mathbf{r}') = -\frac{\epsilon_0^{-1} e^2}{N_{\mathbf{q}} \Omega_{UC}} \sum_{\mathbf{q}, \mathbf{G}} \frac{1}{|\mathbf{q} + \mathbf{G}|^2} e^{i(\mathbf{q}+\mathbf{G})\cdot(\mathbf{r}-\mathbf{r}')} \quad (C.14)$$

$$V^{Coul}(\mathbf{q} + \mathbf{G}, \mathbf{q}' + \mathbf{G}') = N_{\mathbf{q}} V^{Coul}(\mathbf{q}, \mathbf{G}, \mathbf{G}') \delta_{\mathbf{q}', \mathbf{q}} = -\frac{e^2 N_{\mathbf{q}} \Omega_{UC}}{\epsilon_0 |\mathbf{q} + \mathbf{G}|^2} \delta_{\mathbf{G}', \mathbf{G}} \delta_{\mathbf{q}', \mathbf{q}} \quad (C.15)$$

## C.2. Integral Representation of $\chi^{pol}$ and $\epsilon^{-1}$

The thermal average in Eq. (4.6) in terms of Many-Body states  $|E_i\rangle$  reads

$$\chi^{pol}(\mathbf{r}, \mathbf{r}', \nu_n) = -\sum_{i,j} \frac{e^{-\beta E_i}}{Z} \int_0^{\hbar\beta} d\tau \langle E_i | \hat{\Delta}n(\mathbf{r}) | E_j \rangle \langle E_j | \hat{\Delta}n(\mathbf{r}') | E_i \rangle e^{\frac{1}{\hbar}\tau(E_i-E_j)} e^{i\nu_n \tau}. \quad (C.16)$$

We introduce the spectral density

$$S(\mathbf{r}, \mathbf{r}', \omega) = 2\pi \sum_{i,j} (1 - e^{\beta(E_i-E_j)}) \langle E_i | \hat{\Delta}n(\mathbf{r}) | E_j \rangle \langle E_j | \hat{\Delta}n(\mathbf{r}') | E_i \rangle \frac{e^{-\beta E_i}}{Z} \delta\left(\omega - \frac{1}{\hbar}(E_j - E_i)\right) \quad (C.17)$$

and obtain the Lehmann representation of the polarization propagator

$$\chi^{pol}(\mathbf{r}, \mathbf{r}', \nu_n) = \int_{-\infty}^{\infty} \frac{d\omega}{2\pi} \frac{S(\mathbf{r}, \mathbf{r}', \omega)}{i\nu_n - \omega} \quad (C.18)$$

The spectral density satisfies

$$S(\mathbf{r}, \mathbf{r}', \omega) = S(\mathbf{r}', \mathbf{r}, \omega)^* \quad (C.19)$$

$$S(\mathbf{r}, \mathbf{r}', -\omega) = -S(\mathbf{r}, \mathbf{r}', \omega)^* \quad (C.20)$$

which is readily verified. Note that the first relation implies that  $S(\mathbf{r}, \mathbf{r}', \omega)$  is hermitian. We may use the second relation to obtain the hermitian part of  $\chi^{pol}(\mathbf{r}, \mathbf{r}', \nu_n)^2$

$$\Re \chi^{pol}(\mathbf{r}, \mathbf{r}', \nu_n) = - \int_0^\infty \frac{d\omega}{2\pi} \frac{2\omega S(\mathbf{r}, \mathbf{r}', \omega)}{\omega^2 + \nu_n^2} \quad (\text{C.21})$$

Similarly we compute the antihermitian part and see that it vanishes

$$\Im \chi^{pol}(\mathbf{r}, \mathbf{r}', \nu_n) = 0 \quad (\text{C.22})$$

While this form is sufficient to compute the appearing Matsubara sum analytically, we want to end this subsection by pointing out the connection with physical linear density response of the system. This has the advantage of being implemented in several existing codes. For the following we consider the retarded density fluctuation GF

$$\chi^{ret}(\mathbf{r}, \mathbf{r}', t - t') = -i\theta(t - t') \langle [\hat{\Delta}n(\mathbf{r}, t), \hat{\Delta}n(\mathbf{r}', t')]_- \rangle. \quad (\text{C.23})$$

Using

$$\theta(t) = - \lim_{\eta \rightarrow 0} \frac{1}{2\pi i} \int_{-\infty}^{\infty} d\omega \frac{1}{\omega + i\eta} e^{-it\omega} \quad (\text{C.24})$$

$$\delta(\omega - \omega') = \int_{-\infty}^{\infty} \frac{dt}{2\pi} e^{-it(\omega' - \omega)} \quad (\text{C.25})$$

we obtain the integral representation

$$\chi^{ret}(\mathbf{r}, \mathbf{r}', t) = \frac{1}{2\pi} \int_{-\infty}^{\infty} d\omega \sum_{ij} \frac{e^{-\beta(E_j - E_i)} - 1}{\omega + \frac{1}{\hbar}(E_i - E_j) + i\eta} \langle E_i | \hat{\Delta}n(\mathbf{r}) | E_j \rangle \langle E_j | \hat{\Delta}n(\mathbf{r}') | E_i \rangle \frac{e^{-\beta E_i}}{Z} e^{-it\omega}. \quad (\text{C.26})$$

Identifying the delta distribution and the spectral density Eq. (C.18) we obtain the Fourier transform

$$\chi^{ret}(\mathbf{r}, \mathbf{r}', \omega) = \int_{-\infty}^{\infty} \frac{d\tilde{\omega}}{2\pi} \frac{S(\mathbf{r}, \mathbf{r}', \tilde{\omega})}{\omega + i\eta - \tilde{\omega}} \quad (\text{C.27})$$

With

$$\lim_{\eta \rightarrow 0} \frac{1}{\pi} \frac{\eta}{(\omega - \tilde{\omega})^2 + \eta^2} = \delta(\omega - \tilde{\omega}) \quad (\text{C.28})$$

we see that the antihermitian part becomes simply

$$\Im \chi^{ret}(\mathbf{r}, \mathbf{r}', \omega) = -\frac{1}{2} S(\mathbf{r}, \mathbf{r}', \omega). \quad (\text{C.29})$$

Together with Eq. (4.8) we find

$$\chi^{pol}(\mathbf{r}, \mathbf{r}', \nu_n) = \int_0^\infty \frac{d\omega}{\pi} \frac{2\omega \Im \chi^{ret}(\mathbf{r}, \mathbf{r}', \omega)}{\omega^2 + \nu_n^2}. \quad (\text{C.30})$$

It immediately follows for the Fourier coefficients that

$$\chi^{pol}(\mathbf{q}, \mathbf{G}, \mathbf{G}', \nu_n) = \int_0^\infty \frac{d\omega}{\pi} \frac{2\omega \Im \chi^{ret}(\mathbf{q}, \mathbf{G}, \mathbf{G}', \omega)}{\omega^2 + \nu_n^2}. \quad (\text{C.31})$$

---

<sup>2</sup>The symbol  $\Re$  means to take the hermitian part of a matrix  $\Re A \equiv \frac{1}{2}(A + A^\dagger)$ . Similarly  $\Im$  times the imaginary unit is the antihermitian part:  $\Im A = \frac{1}{2i}(A - A^\dagger)$ . Only for symmetric matrices this is equivalent to taking the real  $\Re$  and imaginary part  $\Im$  of each component.

Note that, of course,  $\chi^{pol}(\mathbf{q}, \mathbf{G}, \mathbf{G}', \nu_n)$  is still hermitian, i.e.

$$\chi^{pol}(\mathbf{q}, \mathbf{G}, \mathbf{G}', \nu_n) = \chi^{pol}(\mathbf{q}, \mathbf{G}', \mathbf{G}, \nu_n)^* . \quad (\text{C.32})$$

Using Eq. (4.8) we can establish the analogous equation for the dielectric function. The physical dielectric screening satisfies on the real axis  $\omega \in \mathbb{R}$

$$\epsilon^{-1}(\mathbf{q}, \mathbf{G}, \mathbf{G}', \omega) = \delta_{\mathbf{G}\mathbf{G}'} + \frac{e^2}{\hbar\epsilon_0} \frac{\chi^{ret}(\mathbf{q}, \mathbf{G}, \mathbf{G}', \omega)}{\Omega_{UC}|\mathbf{q} + \mathbf{G}'|^2} \quad (\text{C.33})$$

because  $\chi^{ret}(\mathbf{q}, \mathbf{G}, \mathbf{G}', \omega)$  is the true linear response of a density perturbation on the ground state. Inserting Eq. (4.8) and the antihermitian part of the above equation into Eq. (C.31) we obtain finally

$$\epsilon^{-1}(\mathbf{q}, \mathbf{G}, \mathbf{G}', \nu_n) = \delta_{\mathbf{G}\mathbf{G}'} + \int_0^\infty \frac{d\omega}{\pi} \frac{2\omega \Im \epsilon^{-1}(\mathbf{q}, \mathbf{G}, \mathbf{G}', \omega)}{\omega^2 + \nu_n^2} . \quad (\text{C.34})$$

## D. Analytic Matsubara Summations

The replacement of the interacting GF with the KS one in Section 6.3 allows us to compute the appearing Matsubara summations explicitly. For this we use the contour integration technique (see [45] page 80ff) where we view the Matsubara frequency as a continuous variable and need to sum the residues of the Matsubara integrand

$$\frac{1}{\beta} \sum_n F(i\hbar\omega_n) = - \int_{\circlearrowleft} \frac{dz}{2\pi i} F(z) f_{\beta}(z) = \sum_i \text{Res}\{F(z) f_{\beta}(z), z_i\}. \quad (\text{D.1})$$

Here  $F(i\hbar\omega_n)$  stands for some arbitrary function of Matsubara frequencies. Analytically continued as  $F(z)$  it needs to die off faster than  $z^{-1}$  and we use the Fermi function  $f_{\beta}(z)$  evaluated on the full complex plain. The sum includes all poles  $z_i$  of  $F(z)$  but not the ones of  $f_{\beta}(z)$ .

**Susceptibility-like diagrams** In the potential terms, the Matsubara summation

$$P_s(E, E') = \frac{1}{\beta} \sum_n \frac{1}{(i\omega_n - \frac{1}{\hbar}E)(i\omega_n - \frac{1}{\hbar}E')} \quad (\text{D.2})$$

appears. Eq. D.2 is evaluated using partial fraction and Eq. D.1 with the result

$$P_s(E, E') = \frac{f_{\beta}(E) - f_{\beta}(E')}{E - E'} \quad \lim_{E' \rightarrow E} P_s(E, E') = -\beta f_{\beta}(E) f_{\beta}(-E) \quad (\text{D.3})$$

where the following symmetries are found

$$P_s(E, E') = P_s(-E, -E') \quad (\text{D.4})$$

$$P_s(E, E') = P_s(E', E). \quad (\text{D.5})$$

**Single-interaction-line diagrams** The Matsubara frequency summation of the objects

$$I(\Omega, E_1, E_2, E_3) = \frac{1}{\beta^2} \sum_{nn'} \frac{1}{i\omega_n - \frac{1}{\hbar}E_1} \frac{1}{i(\omega_n - \omega_{n'}) - \Omega} \frac{1}{i\omega_{n'} - \frac{1}{\hbar}E_2} \frac{1}{i\omega_n - \frac{1}{\hbar}E_3} \quad (\text{D.6})$$

$$L(\Omega, E_1, E_2, E_3) = I(-\Omega, E_1, E_2, E_3) - I(\Omega, E_1, E_2, E_3) \quad (\text{D.7})$$

is in principle straight forward. The resulting formulas, are large and computer algebra becomes essential for the evaluation of the residues and limiting cases, necessary for an implementation in a code. Using `Mathematica`, we evaluate the sum Eq. D.6 to

$$\begin{aligned} I(\Omega, E_1, E_2, E_3) &= \\ &= \hbar^4 (1 + n_{\beta}(\hbar\Omega)) \left( \frac{f_{\beta}(E_1)}{(E_1 - E_3)(E_2 - E_1 + \hbar\Omega)} \right. \\ &\quad \left. + \frac{f_{\beta}(E_3)}{(E_3 - E_1)(E_2 - E_3 + \hbar\Omega)} \right) - \frac{f_{\beta}(E_2) f_{\beta}(E_1)}{(E_1 - E_3)(E_2 - E_1 + \hbar\Omega)} \\ &\quad - \frac{f_{\beta}(E_2) f_{\beta}(E_3)}{(E_3 - E_1)(E_2 - E_3 + \hbar\Omega)} - \frac{n_{\beta}(\hbar\Omega) f_{\beta}(E_2)}{(E_2 - E_1 + \hbar\Omega)(E_2 - E_3 + \hbar\Omega)} \end{aligned} \quad (\text{D.8})$$

And related, with some simplification

$$\begin{aligned}
L(\Omega, E_1, E_2, E_3) &= \\
&= \hbar^4 \left( \frac{f_\beta(E_2)n_\beta(\hbar\Omega)}{(E_2 - E_1 + \hbar\Omega)(E_2 - E_3 + \hbar\Omega)} + \frac{f_\beta(E_2)(1 + n_\beta(\hbar\Omega))}{(E_1 - E_2 + \hbar\Omega)(E_3 - E_2 + \hbar\Omega)} + \right. \\
&\quad + \frac{f_\beta(E_1)(1 - f_\beta(E_2) + n_\beta(\hbar\Omega))}{(E_1 - E_3)(E_1 - E_2 - \hbar\Omega)} + \frac{f_\beta(E_3)(1 - f_\beta(E_2) + n_\beta(\hbar\Omega))}{(E_1 - E_3)(E_2 - E_3 + \hbar\Omega)} + \\
&\quad \left. + \frac{f_\beta(E_1)(f_\beta(E_2) + n_\beta(\hbar\Omega))}{(E_1 - E_3)(E_1 - E_2 + \hbar\Omega)} + \frac{f_\beta(E_3)(f_\beta(E_2) + n_\beta(\hbar\Omega))}{(E_3 - E_1)(E_3 - E_2 + \hbar\Omega)} \right). \tag{D.9}
\end{aligned}$$

Note that in terms of the SE Matsubara sum, Eq. 6.25

$$L(\Omega, E_1, E_2, E_3) = \frac{1}{\beta} \sum_n \frac{I_s(\hbar\Omega, E_2, \omega_n)}{(i\omega_n - \frac{1}{\hbar}E_1)(i\omega_n - \frac{1}{\hbar}E_3)} \tag{D.10}$$

From the initial definition we expect (and find) the symmetry

$$L(\Omega, E_1, E_2, E_3) = L(\Omega, E_3, E_2, E_1) \tag{D.11}$$

$$L(-\Omega, E_1, E_2, E_3) = -L(\Omega, E_3, E_2, E_1) \tag{D.12}$$

$$\begin{aligned}
(L(\Omega, E_1, E_2, E_3))^* &= L(-\Omega, -E_3, -E_2, -E_1) = -L(\Omega, -E_3, -E_2, -E_1) \\
&\equiv -L(\Omega, -E_1, -E_2, -E_3) \tag{D.13}
\end{aligned}$$

Clearly some points, e.g.  $E_1 = E_3$  are numerically problematic, so whenever  $E_1 \approx E_3$  we may have to evaluate the limiting formula instead. In general, the various limits where the denominators are zero, all exist and can be computed explicitly, again using **Mathematica**. The results are

$$\begin{aligned}
\lim_{E_1 \rightarrow E_3} L(\Omega, E_1, E_2, E_3) &= \\
&= f_\beta(E_2) \left( \frac{n_\beta(\hbar\Omega)}{(E_2 - E_3 + \hbar\Omega)^2} + \frac{1 + n_\beta(\hbar\Omega)}{(E_2 - E_3 - \hbar\Omega)^2} \right) \\
&\quad - f_\beta(E_3) \left( \frac{f_\beta(-E_2) + n_\beta(\hbar\Omega)}{(E_2 - E_3 + \hbar\Omega)^2} + \frac{f_\beta(E_2) + n_\beta(\hbar\Omega)}{(E_2 - E_3 - \hbar\Omega)^2} \right) \\
&\quad - \frac{\beta f_\beta(-E_3)}{(E_2 - E_3)^2 - (\hbar\Omega)^2} \left( (f_\beta(E_2) - f_\beta(-E_2))\hbar\Omega + (2n_\beta(\hbar\Omega) + 1)(E_2 - E_3) \right) \tag{D.14}
\end{aligned}$$

and further

$$\begin{aligned}
\lim_{\Omega \rightarrow E_3 - E_2} \lim_{E_1 \rightarrow E_3} L(\Omega, E_1, E_2, E_3) &= \\
&= \frac{f_\beta(E_2) + f_\beta(E_3)(f_\beta(-E_2) - f_\beta(E_2))}{4(E_2 - E_3)^2} \\
&\quad + \beta \frac{(1 + f_\beta(E_2) + n_\beta(E_3 - E_2))f_\beta(-E_3)f_\beta(E_3)}{2(E_2 - E_3)} \\
&\quad + \beta^2 f_\beta(-E_2) \left( 1 + \frac{1}{2}n_\beta(E_3 - E_2) \right) f_\beta(E_3) (1 - 2f_\beta(E_3)). \tag{D.15}
\end{aligned}$$

Moreover



$$\begin{aligned}
& \lim_{\Omega \rightarrow E_1 - E_2} L(\Omega, E_1, E_2, E_3) = \\
& = \frac{f_\beta(E_1)(f_\beta(E_2) + n_\beta(E_1 - E_2))}{2(E_1 - E_2)(E_1 - E_3)} + \frac{f_\beta(E_2)(1 + n_\beta(E_1 - E_2))}{2(E_1 - E_2)(E_1 - 2E_2 + E_3)} \\
& + \frac{f_\beta(E_3)(n_\beta(E_1 - E_2) + f_\beta(-E_2)) - f_\beta(E_2)n_\beta(E_1 - E_2)}{(E_1 - E_3)^2} \\
& + \frac{f_\beta(E_3)(f_\beta(E_2) + n_\beta(E_1 - E_2))}{2(E_3 - E_1)(E_1 - 2E_2 + E_3)} + \beta \frac{f_\beta(-E_1)f_\beta(E_2)n_\beta(E_1 - E_2)}{E_3 - E_1} \quad (D.16)
\end{aligned}$$

and further

$$\begin{aligned}
& \lim_{E_1 \rightarrow 2E_2 - E_3} \lim_{\Omega \rightarrow E_1 - E_2} L(\Omega, E_1, E_2, E_3) = \\
& = \frac{f_\beta(E_2)(1 + n_\beta(E_2 - E_3))}{2(E_2 - E_3)} \left( \beta f_\beta(-E_3) - \frac{1}{2(E_2 - E_3)} \right). \quad (D.18)
\end{aligned}$$

That said we note that the Limit  $\Omega_{(\mathbf{q} \rightarrow 0)\lambda} \rightarrow 0$  does not exist but is also unimportant as the  $g_{ij}^{\lambda\mathbf{q}}$  go to zero in the limit  $\mathbf{q} \rightarrow 0$  even faster than  $L$  diverges. As a side note the test of an analytic zero temperature limit  $\beta \rightarrow \infty$  did not converge so it remains unknown at this point if or under what conditions it exists. For the Coulomb parts we further need for static part

$$L_W(E_1, E_2, E_3) = \frac{1}{\beta} \sum_{n'} \frac{1}{i\omega_{n'} - \frac{1}{\hbar}E_2} \frac{1}{\beta} \sum_n \frac{1}{i\omega_n - \frac{1}{\hbar}E_1} \frac{1}{i\omega_n - \frac{1}{\hbar}E_3} \quad (D.19)$$

$$= \frac{1}{\hbar} f_\beta(E_2) P_s(E_1, E_3) \quad (D.20)$$

and for the dynamic part

$$L_M(\hbar\omega, E_1, E_2, E_3) = L(\hbar\omega, E_1, E_2, E_3) - \frac{2}{\omega} L_W(E_1, E_2, E_3). \quad (D.21)$$

## E. Inverse Spin-Decoupled KS Greensfunction

For solving the Dyson equation starting from a KS system within the SDA via inversion we need the inverse matrix  $(\bar{G}^{\text{KS}})^{-1}$ . This can be calculated explicitly which is the content of this Appendix.

Within the Decoupling Approximation we have the explicit form of the KS GF of Eq. 5.43. Using the form

$$\bar{G}_{ij}^{\text{KS}} = \begin{pmatrix} \delta_{ij}G_{11,i\uparrow}^{\text{KS}} & 0 & 0 & \delta_{i,-j}G_{12,i\uparrow}^{\text{KS}} \\ 0 & \delta_{ij}G_{11,-i\downarrow}^{\text{KS}} & \delta_{i,-j}G_{12,i\downarrow}^{\text{KS}} & 0 \\ 0 & \delta_{i,-j}G_{21,i\uparrow}^{\text{KS}} & \delta_{ij}G_{22,i\uparrow}^{\text{KS}} & 0 \\ \delta_{i,-j}G_{21,-i\downarrow}^{\text{KS}} & 0 & 0 & \delta_{ij}G_{22,-i\downarrow}^{\text{KS}} \end{pmatrix} \quad (\text{E.1})$$

we compute the inverse of the full matrix  $\sum_j \bar{G}_{ij}^{\text{KS}} \cdot \bar{G}_{jl}^{\text{KS}-1} = \delta_{il}\tau_0\sigma_0$ . Note that with (invertible!) pivoting matrices we need to invert the  $2 \times 2$  sub-matrices on the diagonal

$$G_{i\sigma} = \begin{pmatrix} G_{11,i\sigma}^{\text{KS}} & G_{12,i\sigma}^{\text{KS}} \\ G_{21,-i-\sigma}^{\text{KS}} & G_{22,-i-\sigma}^{\text{KS}} \end{pmatrix} \quad (\text{E.2})$$

which is done with the determinant

$$D_{i\sigma} = G_{11,i\sigma}^{\text{KS}}G_{22,-i-\sigma}^{\text{KS}} - G_{12,i\sigma}^{\text{KS}}G_{21,-i-\sigma}^{\text{KS}} \quad (\text{E.3})$$

and the formula

$$G_{i\sigma}^{-1} = \frac{1}{D_{i\sigma}} \begin{pmatrix} G_{22,-i-\sigma}^{\text{KS}} & -G_{12,i\sigma}^{\text{KS}} \\ -G_{21,-i-\sigma}^{\text{KS}} & G_{11,i\sigma}^{\text{KS}} \end{pmatrix} \quad (\text{E.4})$$

We first compute  $D_{i\sigma}$ . We obtain the surprisingly simple result

$$G_{11,i\sigma}^{\text{KS}}G_{22,-i-\sigma}^{\text{KS}} - G_{12,i\sigma}^{\text{KS}}G_{21,-i-\sigma}^{\text{KS}} = \frac{1}{(i\omega_n - \frac{1}{\hbar}E_{i\sigma}^+)(i\omega_n - \frac{1}{\hbar}E_{i\sigma}^-)}. \quad (\text{E.5})$$

Inserting this into Eq. (E.4) while replacing the  $u$  and  $v$  with the help of the Eqs. (B.16), (3.164) and (3.165) we obtain

$$G_{i\sigma}^{-1} = \frac{1}{D_{i\sigma}} \sum_{\alpha} \frac{1}{|E_{i\sigma}^+ - E_{i\sigma}^-|} \begin{pmatrix} \frac{|\varepsilon_{i\sigma} - E_{i\sigma}^{\alpha}|}{i\omega_n - \frac{1}{\hbar}E_{i\sigma}^{\alpha}} & -\frac{\text{sign}(\sigma)\text{sign}(\alpha)\Delta_{si}}{i\omega_n - \frac{1}{\hbar}E_{i\sigma}^{\alpha}} \\ \frac{\text{sign}(\sigma)\text{sign}(\alpha)\Delta_{si}^*}{i\omega_n + \frac{1}{\hbar}E_{-i-\sigma}^{\alpha}} & \frac{|\varepsilon_{-i-\sigma} + E_{i\sigma}^{\alpha}|}{i\omega_n - \frac{1}{\hbar}E_{i\sigma}^{\alpha}} \end{pmatrix}. \quad (\text{E.6})$$

Now

$$\begin{aligned} & \sum_{\alpha} \frac{1}{|E_{i\sigma}^+ - E_{i\sigma}^-|} \frac{|\varepsilon_{i\sigma} - E_{i\sigma}^{\alpha}|}{i\omega_n - \frac{1}{\hbar}E_{i\sigma}^{\alpha}} (i\omega_n - \frac{1}{\hbar}E_{i\sigma}^+)(i\omega_n - \frac{1}{\hbar}E_{i\sigma}^-) = \\ & = i\omega_n - |v_{i\sigma}^{i+}|^2 \frac{1}{\hbar}E_{i\sigma}^- - |u_{i\sigma}^{i+}|^2 \frac{1}{\hbar}E_{i\sigma}^+ \end{aligned} \quad (\text{E.7})$$

and with the abbreviation  $F_{i\sigma} = \sqrt{\left(\frac{\varepsilon_{i\sigma} + \varepsilon_{-i-\sigma}}{2}\right)^2 + |\Delta_{si}^s|^2} \equiv \frac{1}{2}|E_{i\sigma}^+ - E_{i\sigma}^-|$

$$\begin{aligned} & \frac{(E_{i\sigma}^+ - \varepsilon_{i\sigma})}{|E_{i\sigma}^+ - E_{i\sigma}^-|} E_{i\sigma}^- + \frac{(E_{i\sigma}^+ + \varepsilon_{-i-\sigma})}{|E_{i\sigma}^+ - E_{i\sigma}^-|} E_{i\sigma}^+ \\ &= \frac{\varepsilon_{i\sigma} - \varepsilon_{-i-\sigma}}{2} + \frac{\varepsilon_{i\sigma} + \varepsilon_{-i-\sigma}}{2} = \varepsilon_{i\sigma}. \end{aligned} \quad (\text{E.8})$$

Similarly

$$\begin{aligned} & \sum_{\alpha} \frac{1}{|E_{i\sigma}^+ - E_{i\sigma}^-|} \frac{|\varepsilon_{-i-\sigma} + E_{i\sigma}^{\alpha}|}{i\omega_n - \frac{1}{\hbar} E_{i\sigma}^{\alpha}} (i\omega_n - \frac{1}{\hbar} E_{i\sigma}^+) (i\omega_n - \frac{1}{\hbar} E_{i\sigma}^-) = \\ &= i\omega_n - |u_{i\sigma}^{i+}|^2 \frac{1}{\hbar} E_{i\sigma}^- - |v_{i\sigma}^{i+}|^2 \frac{1}{\hbar} E_{i\sigma}^+ \end{aligned} \quad (\text{E.9})$$

and

$$\begin{aligned} & \frac{(E_{i\sigma}^+ - \varepsilon_{i\sigma})}{|E_{i\sigma}^+ - E_{i\sigma}^-|} E_{i\sigma}^+ + \frac{(E_{i\sigma}^+ + \varepsilon_{-i-\sigma})}{|E_{i\sigma}^+ - E_{i\sigma}^-|} E_{i\sigma}^- \\ &= \frac{\varepsilon_{i\sigma} - \varepsilon_{-i-\sigma}}{2} - \frac{\varepsilon_{i\sigma} + \varepsilon_{-i-\sigma}}{2} = -\varepsilon_{-i-\sigma}. \end{aligned} \quad (\text{E.10})$$

Further

$$\sum_{\alpha} \frac{-\text{sign}(\sigma)\text{sign}(\alpha)\Delta_{si}^s}{|E_{i\sigma}^+ - E_{i\sigma}^-| (i\omega_n - \frac{1}{\hbar} E_{i\sigma}^{\alpha})} (i\omega_n - \frac{1}{\hbar} E_{i\sigma}^+) (i\omega_n - \frac{1}{\hbar} E_{i\sigma}^-) = -\text{sign}(\sigma) \frac{1}{\hbar} \Delta_{si}^s \quad (\text{E.11})$$

and

$$\sum_{\alpha} \frac{\text{sign}(\sigma)\text{sign}(\alpha)\Delta_{si}^{s*}}{|E_{i\sigma}^+ - E_{i\sigma}^-| (i\omega_n + \frac{1}{\hbar} E_{-i-\sigma}^{\alpha})} (i\omega_n - \frac{1}{\hbar} E_{i\sigma}^+) (i\omega_n - \frac{1}{\hbar} E_{i\sigma}^-) = -\text{sign}(\sigma) \frac{1}{\hbar} \Delta_{si}^{s*}. \quad (\text{E.12})$$

Where we arrive at the inverse of the block diagonal

$$G_{i\sigma}^{-1} = \begin{pmatrix} i\omega_n - \frac{1}{\hbar} \varepsilon_{i\sigma} & -\text{sign}(\sigma) \Delta_{si}^s \\ -\text{sign}(\sigma) \Delta_{si}^{s*} & i\omega_n + \frac{1}{\hbar} \varepsilon_{-i-\sigma} \end{pmatrix} \quad (\text{E.13})$$

so back-pivoting to the original notation

$$(\bar{G}^{\text{KS}})^{-1}_{ij} = \frac{1}{\hbar} \begin{pmatrix} (i\hbar\omega_n - \varepsilon_{i\uparrow})\delta_{ij} & 0 & 0 & -\Delta_{si}^s \delta_{i,-j} \\ 0 & (i\hbar\omega_n - \varepsilon_{-i\downarrow})\delta_{ij} & \Delta_{si}^s \delta_{i,-j} & 0 \\ 0 & \Delta_{si}^{s*} \delta_{i,-j} & (i\hbar\omega_n + \varepsilon_{i\uparrow})\delta_{ij} & 0 \\ -\Delta_{si}^{s*} \delta_{i,-j} & 0 & 0 & (i\hbar\omega_n + \varepsilon_{-i\downarrow})\delta_{ij} \end{pmatrix}. \quad (\text{E.14})$$

In terms of basis vectors

$$\begin{aligned} (\bar{G}^{\text{KS}})^{-1}_{ij}(\omega_n) &= \delta_{ij} (i\hbar\omega_n \tau_0 \sigma_0 - \left(\frac{\varepsilon_{i\uparrow} + \varepsilon_{-i\downarrow}}{2}\right) \tau_z \sigma_0 - \left(\frac{\varepsilon_{i\uparrow} - \varepsilon_{-i\downarrow}}{2}\right) \tau_z \sigma_z) \\ &+ \delta_{i,-j} ((i\tau_y)(i\sigma_y) \Re \Delta_{si}^s + \tau_x (i\sigma_y) i \Im \Delta_{si}^s). \end{aligned} \quad (\text{E.15})$$

## F. Wick Theorem for Superconductors

In this Appendix we show that for any set of Nambu fields

$$\begin{aligned} & \sum_{1\dots} \dots w(1, 2, 3, 4) \dots \langle T \{ \hat{\Psi}_I(\mathbf{r}\tau\alpha) \hat{\Psi}_I(1) \dots \hat{\Psi}_I^\dagger(\mathbf{r}'\tau'\alpha') \} \rangle_0 \\ &= \sum_{1\dots} \dots w(1, 2, 3, 4) \dots \left\{ \text{Sum of all possible contractions} \right\} \end{aligned} \quad (\text{F.1})$$

where a contraction is defined as  $\langle T \{ \hat{\Psi}_I(\mathbf{r}\tau\alpha) \hat{\Psi}_I^\dagger(\mathbf{r}'\tau'\alpha') \} \rangle_0$ . We follow the usual proof given in for example in the book [45] together with a peculiarity in the prefactors that we were made aware of in the book [19]. To show the theorem, let us go to the single particle basis where the single particle Hamiltonian  $\hat{H}_0$  is diagonal. We want to be general and allow  $\hat{H}_0$  to contain pair potential contributions. Thus we have to rotate with Bogoliubov transformations similar to Eq. (3.102) in order to achieve a diagonal form. We could take  $\hat{H}_0$  to be the Hartree electronic Hamiltonian Eq. 5.17 in which case we would obtain a series for  $\bar{\Sigma}$  directly. Being a single particle operator,  $\hat{H}_0$  can be written as

$$\hat{H}_0 = \int d\mathbf{r} \int d\mathbf{r}' \hat{\Psi}^\dagger(\mathbf{r}) \cdot \frac{1}{2} \hat{H}_0(\mathbf{r}, \mathbf{r}') \cdot \hat{\Psi}(\mathbf{r}') \equiv \sum_k E_k \hat{\Phi}_k^\dagger \cdot \frac{1}{2} \tau_z \cdot \hat{\Phi}_k \quad (\text{F.2})$$

With the Nambu spinor  $\hat{\Phi}_k$  that diagonalizes  $\hat{H}_0$

$$\hat{\Phi}_{k\alpha} = \begin{pmatrix} \hat{\gamma}_k \delta_{\alpha,1} \\ \hat{\gamma}_k^\dagger \delta_{\alpha,-1} \end{pmatrix} \quad \hat{\Psi}^\dagger(\mathbf{r}) = \sum_k \begin{pmatrix} \vec{u}_k(\mathbf{r}) & \vec{v}_k^*(\mathbf{r}) \\ \vec{v}_k(\mathbf{r}) & \vec{u}_k^*(\mathbf{r}) \end{pmatrix} \cdot \hat{\Phi}_k^\dagger \quad (\text{F.3})$$

where

$$\int d\mathbf{r} \int d\mathbf{r}' \begin{pmatrix} \vec{u}_k(\mathbf{r}) & \vec{v}_k^*(\mathbf{r}) \\ \vec{v}_k(\mathbf{r}) & \vec{u}_k^*(\mathbf{r}) \end{pmatrix}^\dagger \cdot \hat{H}_0(\mathbf{r}, \mathbf{r}') \cdot \begin{pmatrix} \vec{u}_{k'}(\mathbf{r}') & \vec{v}_{k'}^*(\mathbf{r}') \\ \vec{v}_{k'}(\mathbf{r}') & \vec{u}_{k'}^*(\mathbf{r}') \end{pmatrix} = \delta_{kk'} \begin{pmatrix} \tilde{E}_k & 0 \\ 0 & -\tilde{E}_k \end{pmatrix}. \quad (\text{F.4})$$

Note that in computing the time ordered product, we have to apply this transformation to each field operator

$$\begin{aligned} & \langle T \{ \hat{\Psi}_I(\mathbf{r}\tau\alpha) \dots \hat{\Psi}_I^\dagger(\mathbf{r}'\tau'\alpha') \} \rangle_0 = \\ & \sum_{k\dots k'} \sum_{\alpha_1 \dots \alpha'_1} \begin{pmatrix} \vec{u}_k(\mathbf{r}) & \vec{v}_k^*(\mathbf{r}) \\ \vec{v}_k(\mathbf{r}) & \vec{u}_k^*(\mathbf{r}) \end{pmatrix}_{\alpha\alpha_1} \dots \begin{pmatrix} \vec{u}_{k'}(\mathbf{r}') & \vec{v}_{k'}^*(\mathbf{r}') \\ \vec{v}_{k'}(\mathbf{r}') & \vec{u}_{k'}^*(\mathbf{r}') \end{pmatrix}_{\alpha'_1\alpha'_1} \cdot \langle T \{ \hat{\Phi}_{kI}(\tau\alpha_1) \dots \hat{\Phi}_{k'I}^\dagger(\tau'\alpha'_1) \} \rangle_0 \end{aligned} \quad (\text{F.5})$$

Considering  $\langle T \{ \hat{\Phi}_{kI}(\tau\alpha_1) \dots \hat{\Phi}_{k'I}^\dagger(\tau'\alpha'_1) \} \rangle_0$  this may be computed explicitly from the fact that the commutator with the propagating Hamiltonian  $\hat{H}_0$  is known. It reads

$$[\hat{H}_0, \hat{\Phi}_{k'}(\alpha)]_- = \left[ \sum_k \hat{\Phi}_k^\dagger \cdot \frac{1}{2} \begin{pmatrix} \tilde{E}_k & 0 \\ 0 & -\tilde{E}_k \end{pmatrix} \cdot \hat{\Phi}_k, \hat{\Phi}_{k'}(\alpha) \right] = -\tilde{E}_{k'} \text{sign}(\alpha) \hat{\Phi}_{k'}(\alpha). \quad (\text{F.6})$$

Thus we see that

$$e^{\pm\beta\hat{H}_0}\hat{\Phi}_{k'}(\alpha) = \hat{\Phi}_{k'}(\alpha)e^{\mp\beta\text{sign}(\alpha)\tilde{E}_{k'}}e^{\pm\beta\hat{H}_0} \quad (\text{F.7})$$

and similarly

$$e^{\pm\beta\hat{H}_0}\hat{\Phi}_{k'}^\dagger(\alpha) = \hat{\Phi}_{k'}^\dagger(\alpha)e^{\pm\beta\text{sign}(\alpha)\tilde{E}_{k'}}e^{\pm\beta\hat{H}_0}. \quad (\text{F.8})$$

We want to introduce a symbol that helps to distinguish the many cases, let

$$a = \dagger, (\text{no dagger}) \quad (\text{F.9})$$

$$\text{sign}(a) \equiv \begin{cases} +1 & a = \dagger \\ -1 & a = (\text{no dagger}) \end{cases}. \quad (\text{F.10})$$

Then in short we may write

$$e^{\pm\beta\hat{H}_0}\hat{\Phi}_{k'}^a(\alpha) = \hat{\Phi}_{k'}^a(\alpha)e^{\pm\beta\text{sign}(a)\text{sign}(\alpha)\tilde{E}_{k'}}e^{\pm\beta\hat{H}_0}. \quad (\text{F.11})$$

Most importantly the result allows us to pull the imaginary time ordering out of the thermodynamic average because

$$e^{\tau\hat{H}_0}\hat{\Phi}_k^a(\alpha)e^{-\tau\hat{H}_0} = \hat{\Phi}_k^a e^{\tau\text{sign}(a)\text{sign}(\alpha)\tilde{E}_k} \quad (\text{F.12})$$

so the time ordered thermal average becomes

$$\begin{aligned} & \langle \hat{\Phi}_{k_1 I}^a(\tau_1\alpha_1)\hat{\Phi}_{k_2 I}^b(\tau_2\alpha_2)\dots\hat{\Phi}_{k_N I}^c(\tau_N\alpha_N) \rangle_0 \\ &= \text{Tr}\left\{\hat{\rho}_0\hat{\Phi}_{k_1}^a(\alpha_1)\hat{\Phi}_{k_2}^b(\alpha_2)\dots\hat{\Phi}_{k_N}^c(\alpha_N)\right\}e^{\tau_1\text{sign}(a_1)\text{sign}(\alpha_1)\tilde{E}_{k_1}}\dots e^{\tau_N\text{sign}(a_N)\text{sign}(\alpha_N)\tilde{E}_{k_N}}. \end{aligned} \quad (\text{F.13})$$

Now consider an even number of operators that are being evaluated where with

$$\begin{aligned} & \text{Tr}\left\{\hat{\rho}_0\hat{\Phi}_{k_1}^a(\alpha_1)\hat{\Phi}_{k_2}^b(\alpha_2)\dots\hat{\Phi}_{k_N}^c(\alpha_N)\right\} \\ &= \text{Tr}\left\{\hat{\rho}_0[\hat{\Phi}_{k_1}^a(\alpha_1),\hat{\Phi}_{k_2}^b(\alpha_2)]_+\dots\hat{\Phi}_{k_N}^c(\alpha_N)\right\} - \text{Tr}\left\{\hat{\rho}_0\hat{\Phi}_{k_2}^b(\alpha_2)[\hat{\Phi}_{k_1}^a(\alpha_1),\dots]_+\dots\hat{\Phi}_{k_N}^c(\alpha_N)\right\} \\ & \quad \pm\dots - \text{Tr}\left\{\hat{\rho}_0\hat{\Phi}_{k_2}^b(\alpha_2)\dots\hat{\Phi}_{k_N}^c(\alpha_N)\hat{\Phi}_{k_1}^a(\alpha_1)\right\} \end{aligned} \quad (\text{F.14})$$

but because of the cyclic invariance of the trace for the last term may be written as

$$\text{Tr}\left\{\hat{\Phi}_{k_1}^a(\alpha_1)\hat{\rho}_0\hat{\Phi}_{k_2}^b(\alpha_2)\dots\hat{\Phi}_{k_N}^c(\alpha_N)\right\} = \text{Tr}\left\{\hat{\rho}_0e^{-\beta\text{sign}(a_1)\text{sign}(\alpha_1)\tilde{E}_{k_1}}\hat{\Gamma}_{k_1}^a(\alpha)\hat{\Gamma}_{k_1}^b(\alpha_1)\dots\hat{\Gamma}_{k_N}^c(\alpha')\right\}. \quad (\text{F.15})$$

Thus Eq. (F.14) becomes

$$\begin{aligned} & \text{Tr}\left\{\hat{\rho}_0\hat{\Phi}_{k_1}^a(\alpha_1)\hat{\Phi}_{k_2}^b(\alpha_2)\dots\hat{\Phi}_{k_N}^c(\alpha_N)\right\} \\ &= \frac{[\hat{\Phi}_{k_1}^a(\alpha_1),\hat{\Phi}_{k_2}^b(\alpha_2)]_+}{1+e^{-\beta\text{sign}(a_1)\text{sign}(\alpha_1)\tilde{E}_{k_1}}}\text{Tr}\left\{\hat{\rho}_0\dots\hat{\Phi}_{k_N}^c(\alpha_N)\right\} \\ & \quad - \frac{[\hat{\Phi}_{k_1}^a(\alpha_1),\dots]_+}{1+e^{-\beta\text{sign}(a_1)\text{sign}(\alpha_1)\tilde{E}_{k_1}}}\text{Tr}\left\{\hat{\rho}_0\hat{\Phi}_{k_2}^b(\alpha_2)\dots\hat{\Phi}_{k_N}^c(\alpha_N)\right\} \\ & \quad \pm\dots \end{aligned} \quad (\text{F.16})$$

The single particle propagator, we define here to be a contraction, is easily evaluated

$$\langle T\left\{\hat{\Phi}_{k_1}^a(\alpha_1\tau_1)\hat{\Phi}_{k_2}^b(\alpha_2\tau_2)\right\} \rangle_0 = \frac{[\hat{\Phi}_{k_1}^a(\alpha_1),\hat{\Phi}_{k_2}^b(\alpha_2)]_+}{1+e^{-\beta\text{sign}(a_1)\text{sign}(\alpha_1)\tilde{E}_{k_1}}}\text{Tr}\left\{\hat{\rho}_0\hat{\Phi}_{k_1}^a(\alpha_1)\hat{\Phi}_{k_2}^b(\alpha_2)\dots\hat{\Phi}_{k_N}^c(\alpha_N)\right\}e^{\tau_1\text{sign}(a_1)\text{sign}(\alpha_1)\tilde{E}_{k_1}}e^{\tau_2\text{sign}(a_2)\text{sign}(\alpha_2)\tilde{E}_{k_2}} \quad (\text{F.17})$$

This relation shows that the time ordered product of  $N$  operators is related to  $N - 1$  times the single particle propagator times the  $N - 1$  reordered product. We conclude

$$\langle \hat{\Phi}_{k_1 I}^a(\tau_1 \alpha_1) \hat{\Phi}_{k_2 I}^b(\tau_2 \alpha_2) \dots \hat{\Phi}_{k_N I}^c(\tau_N \alpha_N) \rangle_0 = \left\{ \text{Sum of all possible contractions} \right\} \quad (\text{F.18})$$

Moreover

$$\langle T \hat{\Psi}_I(\mathbf{r} \tau \alpha) \hat{\Psi}_I^\dagger(\mathbf{r}' \tau' \alpha') \rangle_0 = \sum_{kk'} \sum_{\alpha_1 \alpha'_1} \begin{pmatrix} \vec{u}_k(\mathbf{r}) & \vec{v}_k^*(\mathbf{r}) \\ \vec{v}_k(\mathbf{r}) & \vec{u}_k^*(\mathbf{r}) \end{pmatrix}_{\alpha_1} \begin{pmatrix} \vec{u}_{k'}(\mathbf{r}') & \vec{v}_{k'}^*(\mathbf{r}') \\ \vec{v}_{k'}(\mathbf{r}') & \vec{u}_{k'}^*(\mathbf{r}') \end{pmatrix}_{\alpha'_1}^\dagger \langle T \hat{\Phi}_k(\alpha_1 \tau) \hat{\Phi}_{k'}^\dagger(\alpha'_1 \tau') \rangle_0 \quad (\text{F.19})$$

where we identify, using the notation  $1 = (\alpha_1 \mathbf{r}_1 \sigma_1)$

$$\begin{aligned} \langle T \hat{\Psi}_I^a(1\tau_1) \hat{\Psi}_I^b(2\tau_2) \hat{\Psi}_I^c(3\tau_3) \dots \hat{\Psi}_I^d(4\tau_4) \rangle_0 &= \langle T \hat{\Psi}_I^a(1\tau_1) \hat{\Psi}_I^b(2\tau_2) \rangle_0 \times \\ &\times \langle T \hat{\Psi}_I^c(3\tau_3) \dots \hat{\Psi}_I^d(4\tau_4) \rangle_0 - \langle T \hat{\Psi}_I^a(1\tau_1) \hat{\Psi}_I^c(3\tau_3) \rangle_0 \langle T \hat{\Psi}_I^b(2\tau_2) \dots \hat{\Psi}_I^d(4\tau_4) \rangle_0 \pm \dots \end{aligned} \quad (\text{F.20})$$

which almost proves Wicks theorem Eq. (5.60) since at this point we may insert the left side for the remaining uncontracted terms on the right hand side. Note a problem here, that we encounter the GF  $\langle T \hat{\Psi}_I(\mathbf{r} \tau) \otimes \hat{\Psi}_I^\dagger(\mathbf{r}' \tau') \rangle_0$  but also the GF  $\langle T \hat{\Psi}_I(\mathbf{r} \tau) \otimes \hat{\Psi}_I(\mathbf{r}' \tau') \rangle_0$ . We follow Vonsovsky and show that in a perturbative expansion this part cancels the puzzling factors of  $\frac{1}{2^n}$  in the  $n$  particle interaction. For definiteness consider a two particle interaction in time ordering

$$\hat{H}^I = \frac{1}{4} \sum_{1,2,3,4} \hat{\Psi}^\dagger(1) \hat{\Psi}(2) W(1234) \hat{\Psi}^\dagger(3) \hat{\Psi}(4). \quad (\text{F.21})$$

Then in the contractions there will appear the term according to

$$\begin{aligned} &\sum_{1,2,\dots} \langle T \dots \hat{\Psi}_I^\dagger(1\tau_1) W(1256) \hat{\Psi}_I(2\tau_2) \dots \hat{\Psi}_I^a(3\tau_3) \dots \hat{\Psi}_I^b(4\tau_4) \rangle_0 \\ &= \sum_{1,2,\dots} W(1256) \langle T \hat{\Psi}_I^\dagger(1\tau_1) \hat{\Psi}_I^b(4\tau_4) \rangle_0 \langle T \hat{\Psi}_I(2\tau_2) \hat{\Psi}_I^a(3\tau_3) \rangle_0 \langle \dots \rangle_0 + \\ &\quad - \sum_{1,2,\dots} W(1256) \langle T \hat{\Psi}_I(2\tau_2) \hat{\Psi}_I^b(4\tau_4) \rangle_0 \langle T \hat{\Psi}_I^\dagger(1\tau_1) \hat{\Psi}_I^a(3\tau_3) \rangle_0 \langle \dots \rangle_0. \end{aligned} \quad (\text{F.22})$$

Let us rename in the sum in second term  $1 \leftrightarrow 2$

$$\begin{aligned} &\sum_{1,2,\dots} \langle T \dots \hat{\Psi}_I^\dagger(1\tau_1) W(1256) \hat{\Psi}_I(2\tau_2) \dots \hat{\Psi}_I^a(3\tau_3) \dots \hat{\Psi}_I^b(4\tau_4) \rangle_0 \\ &= \sum_{1,2,\dots} W(1256) \langle T \hat{\Psi}_I^\dagger(1\tau_1) \hat{\Psi}_I^b(4\tau_4) \rangle_0 \langle T \hat{\Psi}_I(2\tau_2) \hat{\Psi}_I^a(3\tau_3) \rangle_0 \langle \dots \rangle_0 + \\ &\quad - \sum_{1,2,\dots} W(2156) \langle T \hat{\Psi}_I(1\tau_1) \hat{\Psi}_I^b(4\tau_4) \rangle_0 \langle T \hat{\Psi}_I^\dagger(2\tau_2) \hat{\Psi}_I^a(3\tau_3) \rangle_0 \langle \dots \rangle_0. \end{aligned} \quad (\text{F.23})$$

Together with and

$$\hat{\Psi}_I(\mathbf{r}_1 \tau_1 \alpha_1 \sigma_1) = \hat{\Psi}_I^\dagger(\mathbf{r}_1 \tau_1, -\alpha_1, \sigma_1) \quad (\text{F.24})$$

we may sum  $-1, -2$  instead and use the symmetry Eq. (5.57) that essentially represents the condition that the interaction can be written without the Nambu formalism. Then we obtain

$$\begin{aligned} & \sum_{1,2,\dots} \langle T \dots \hat{\Psi}_I^\dagger(1\tau_1) W(1256) \hat{\Psi}_I(2\tau_2) \dots \hat{\Psi}_I^a(3\tau_3) \dots \hat{\Psi}_I^b(4\tau_4) \rangle_0 = \\ & = 2 \sum_{1,2,\dots} W(1256) \langle T \hat{\Psi}_I^\dagger(1\tau_1) \hat{\Psi}_I^b(4\tau_4) \rangle_0 \langle T \hat{\Psi}_I(2\tau_2) \hat{\Psi}_I^a(3\tau_3) \rangle_0 \langle \dots \rangle_0 \end{aligned} \quad (\text{F.25})$$

$$= -2 \sum_{1,2,\dots} W(1256) \langle T \hat{\Psi}_I(1\tau_1) \hat{\Psi}_I^b(4\tau_4) \rangle_0 \langle T \hat{\Psi}_I^\dagger(2\tau_2) \hat{\Psi}_I^a(3\tau_3) \rangle_0 \langle \dots \rangle_0 \quad (\text{F.26})$$

because there is always just as many creation as annihilation operators and all but two are integrated over with matrix elements that have the assumed symmetry we see that is is sufficient to consider only

$$\bar{G}_0(\mathbf{r}\tau, \mathbf{r}'\tau') = \langle \bar{T} \hat{\Psi}_I(\mathbf{r}\tau) \otimes \hat{\Psi}_I^\dagger(\mathbf{r}'\tau') \rangle_0 \quad (\text{F.27})$$

and at the same time get rid of the factors  $\frac{1}{2^{n+m}}$  that appear for an  $n$  particle interaction in  $m$ th order perturbation theory. This very convenient fact shows that we obtain formally the same diagrammatic expansion as for a normal system, except that the GF is here the  $4 \times 4$  matrix  $\langle T \hat{\Psi}_I(\mathbf{r}\tau) \otimes \hat{\Psi}_I^\dagger(\mathbf{r}'\tau') \rangle_0$  and the reordered interactions  $\hat{H}_I^\dagger(\tau)$  have to be translated into the Nambu formalism which will lead to different vertices that in the case of a local interaction the bare vertex will be proportional to

$$\Gamma \propto \sigma_0 \tau_z \quad (\text{F.28})$$

Note that these interactions must not break the symmetry of Eq. (5.57). With this understanding the results from the normal diagrammatic perturbation theory may be transferred.

## G. The KS Excitation Spectrum

One of the key advantages of DFT in e.g. the LDA approximation for the  $xc$  potential[80], is that the single particle states of the KS system are often comparable to the true quasi particle spectrum. This is in some sense accidental because the KS system only yields the exact densities. There are also cases known where the KS band structure is not a good approximation to the true single particle excitation spectrum. Two of the most prominent examples in the context of SC being the High- $T_c$  cuprates [81, Section 7.1, Page 378] and the iron based SC [82]. To improve upon the KS DFT excitation spectrum, for example with the spectrum of the G0W0 GF, can be numerically demanding. In the full non-linear SSE, we obtain a potential that is not gaped at low temperatures. However, there exists a so-called partial linearization [21, 22] that multiplies the BCS non-linear factor to the linearized gap equation. There, the gap shows the usual behaviour and compares well with experiment. This procedure is ill defined in the range of a first order phase transition, since we cannot linearize the equation, still it justifies the effort to calculate the KS excitation spectrum for the use in the spin degenerate limit.

We employ the Lehmann representation of the KS GF Eq. (5.20) with the spectral function of Eq. (5.31) and (5.27)

$$\bar{A}^{\text{KS}}(\mathbf{r}, \mathbf{r}', \omega) = -2\mathfrak{Im}(\bar{\mathcal{G}}^{\text{KS}}(\mathbf{r}, \mathbf{r}', \omega)) \quad (\text{G.1})$$

$$\bar{G}^{\text{KS}}(\mathbf{r}, \mathbf{r}', \omega_n) = \int_{-\infty}^{\infty} \frac{d\omega}{2\pi} \frac{\bar{A}^{\text{KS}}(\mathbf{r}, \mathbf{r}', \omega)}{i\omega_n - \omega} \quad (\text{G.2})$$

According to Eq. (5.36) with the explicit expression for  $\bar{G}^{\text{KS}}(\mathbf{r}, \mathbf{r}', \omega_n)$ ,  $\bar{A}^{\text{KS}}$  is given by

$$\begin{aligned} \bar{A}^{\text{KS}}(\mathbf{r}, \mathbf{r}', \omega) &= 2\pi \sum_k \begin{pmatrix} \vec{u}_k(\mathbf{r}) \otimes \vec{u}_k^*(\mathbf{r}') & \vec{u}_k(\mathbf{r}) \otimes \vec{v}_k^*(\mathbf{r}') \\ \vec{v}_k(\mathbf{r}) \otimes \vec{u}_k^*(\mathbf{r}') & \vec{v}_k(\mathbf{r}) \otimes \vec{v}_k^*(\mathbf{r}') \end{pmatrix} \delta(\omega - \frac{1}{\hbar}E_k) + \\ &+ 2\pi \sum_k \begin{pmatrix} \vec{v}_k^*(\mathbf{r}) \otimes \vec{v}_k(\mathbf{r}') & \vec{v}_k^*(\mathbf{r}) \otimes \vec{u}_k(\mathbf{r}') \\ \vec{u}_k^*(\mathbf{r}) \otimes \vec{v}_k(\mathbf{r}') & \vec{u}_k^*(\mathbf{r}) \otimes \vec{u}_k(\mathbf{r}') \end{pmatrix} \delta(\omega + \frac{1}{\hbar}E_k) \end{aligned} \quad (\text{G.3})$$

The LDOS is obtained from the diagonal of  $\bar{A}^{\text{KS}}(\mathbf{r}, \mathbf{r}', \omega)$ . Aside from this technicality it is interesting to find the wavefunction of a SC KS particle in real space  $\Psi_{k\alpha}^{\text{B}}(\mathbf{r})$  (the B is for Bogolon), i.e. the state that is created by one of the  $\hat{\Phi}_{k\alpha}^{\dagger}$  operators of Eq. (5.36). In principle, the  $\hat{\Phi}_{k\alpha}^{\dagger}$  are no different from usual electron operators and we should be able to transfer results for non-interacting properties. First, because they are the single particle KS states of the SC KS system the  $\Psi_i^{\text{B}}(\mathbf{r})$  should add up to the KS LDOS in the form  $\sum_i |\Psi_i^{\text{B}}(\mathbf{r})|^2 \delta(E_i - \hbar\omega)$ . Second, we should also find the KS GF as

$$\bar{G}^{\text{KS}}(\mathbf{r}, \mathbf{r}', \omega_n) = \sum_i \frac{\Psi_i^{\text{B}}(\mathbf{r}) \otimes \Psi_i^{\text{B}*}(\mathbf{r}')}{i\omega_n - \frac{1}{\hbar}\tilde{E}_i} \quad (\text{G.4})$$

where from the dimensionality of the KSBdG equations (3.108) we conclude that  $i$  is twice the set of the normal state KS quantum numbers. The KS system's diagonal KS GF  $\bar{\mathfrak{G}}_{kk'}(\omega_n)$  is given in Eq. (5.35) or in real space as  $\bar{G}^{\text{KS}}(\mathbf{r}, \mathbf{r}', \omega_n)$  in Eq. (5.36). From the form Eq. (5.35) we identify

$$\tilde{E}_{i=k,\alpha} = \text{sign}(\alpha)E_k, \quad (\text{G.5})$$



and from the KS GF in terms of Valatin transformations Eq. (5.40) we find

$$\Psi_{k\alpha}^{\text{B}}(\mathbf{r}) = \begin{pmatrix} \vec{u}_k(\mathbf{r}) \\ \vec{v}_k(\mathbf{r}) \end{pmatrix} \delta_{\alpha,1} + \begin{pmatrix} \vec{v}_k^*(\mathbf{r}) \\ \vec{u}_k^*(\mathbf{r}) \end{pmatrix} \delta_{\alpha,-1} \quad (\text{G.6})$$

Here  $\alpha$  labels the branch (+ or -) of the eigenvalues  $E_{k\alpha}$ .  $\Psi_{k\alpha}^{\text{B}}$  is not a pure Nambu spinor as is clearly seen from the above equation. It is not surprising that the spectral function Eq. (G.3) may be also written with the Bogolon state of Eq. (G.6) as

$$\bar{A}^{\text{KS}}(\mathbf{r}, \mathbf{r}', \omega) = 2\pi \sum_{k\alpha} \Psi_{k\alpha}^{\text{B}}(\mathbf{r}) \otimes \Psi_{k\alpha}^{\text{B}*}(\mathbf{r}') \delta(\omega - \frac{1}{\hbar} \tilde{E}_{k\alpha}) \quad (\text{G.7})$$

which is consistent with  $\bar{G}^{\text{KS}}$  in Eq. (G.2). With the definition of the  $u, v$  coefficients of Eq. (3.111) and Eq. (3.112), further

$$\Psi_{k\alpha}^{\text{B}}(\mathbf{r}) = \sum_{k'\sigma} \begin{pmatrix} (u_k^{k'\sigma} \delta_{\alpha,1} + (v_k^{k'\sigma})^* \delta_{\alpha,-1}) \vec{\varphi}_{k'\sigma}(\mathbf{r}) \\ (v_k^{k'\sigma} \delta_{\alpha,1} + (u_k^{k'\sigma})^* \delta_{\alpha,-1}) \vec{\varphi}_{k'\sigma}^*(\mathbf{r}) \end{pmatrix}. \quad (\text{G.8})$$

Note here that  $\Psi_{k\alpha}^{\text{B}}(\mathbf{r})$  is in general neither a pure state in Nambu nor in spin space so that the particle is neither an electron nor a hole but a mixture of both. This transformation allows one to study the Bogolon also in the SDA where spin becomes a good quantum number

$$\Psi_{k\alpha\sigma}^{\text{B}}(\mathbf{r}) = \sum_{\alpha'} \begin{pmatrix} u_{k\sigma}^{k\alpha'} \theta(E_{k\sigma}^{\alpha'}) \delta_{\alpha,1} \vec{\varphi}_{k\sigma}(\mathbf{r}) + (v_{k,-\sigma}^{-k\alpha'})^* \theta(E_{k\sigma}^{\alpha'}) \delta_{\alpha,-1} \vec{\varphi}_{-k,-\sigma}(\mathbf{r}) \\ v_{k,-\sigma}^{-k\alpha'} \theta(E_{k\sigma}^{\alpha'}) \delta_{\alpha,1} \vec{\varphi}_{-k,-\sigma}^*(\mathbf{r}) + (u_{k\sigma}^{k\alpha'})^* \theta(E_{k\sigma}^{\alpha'}) \delta_{\alpha,-1} \vec{\varphi}_{k\sigma}^*(\mathbf{r}) \end{pmatrix} \quad (\text{G.9})$$

The KS LDOS is defined as  $\rho_{\sigma\alpha}^{\text{KS}}(\mathbf{r}, \omega) = \bar{A}_{\alpha\alpha}^{\text{KS}\sigma\sigma}(\mathbf{r}, \mathbf{r}, \omega)$  which results in

$$\begin{aligned} \rho_{\sigma\alpha}^{\text{KS}}(\mathbf{r}, \omega) &= \frac{2\pi}{\hbar} \sum_{ijk} \left( u_k^{i\sigma} (u_k^{j\sigma})^* \delta(\hbar\omega - \text{sign}(\alpha) E_k) \right. \\ &\quad \left. + (v_k^{i\sigma})^* v_k^{j\sigma} \delta(\hbar\omega + \text{sign}(\alpha) E_k) \right) \varphi_i(\mathbf{r}\sigma) \varphi_j^*(\mathbf{r}\sigma). \end{aligned} \quad (\text{G.10})$$

Integrating the local DOS over the unit cell we obtain the total DOS. The orthonormality of the pure spin basis leads to

$$\rho_{\sigma\alpha}^{\text{KS}}(\omega) = \frac{2\pi}{\hbar} \sum_{ik} \left( |u_k^{i\sigma}|^2 \delta(\hbar\omega - \text{sign}(\alpha) E_k) + |v_k^{i\sigma}|^2 \delta(\hbar\omega + \text{sign}(\alpha) E_k) \right). \quad (\text{G.11})$$

For a singlet superconductor (compare Subsection 3.5.1) the equations simplify to

$$\begin{aligned} \rho_{\sigma\alpha}^{\text{KS}}(\mathbf{r}, \omega) &= \frac{2\pi}{\hbar} \sum_{ijk} \left( u_{k\sigma}^i (u_{k\sigma}^j)^* \delta(\hbar\omega - \text{sign}(\alpha) E_{k\sigma}) + \right. \\ &\quad \left. + (v_{k,-\sigma}^i)^* v_{k,-\sigma}^j \delta(\hbar\omega + \text{sign}(\alpha) E_{k,-\sigma}) \right) \varphi_i(\mathbf{r}\sigma) \varphi_j^*(\mathbf{r}\sigma) \end{aligned} \quad (\text{G.12})$$

$$\rho_{\sigma\alpha}^{\text{KS}}(\omega) = \frac{2\pi}{\hbar} \sum_{ik} \left( |u_{k\sigma}^k|^2 \delta(\hbar\omega - \text{sign}(\alpha) E_{k\sigma}) + |v_{k,-\sigma}^k|^2 \delta(\hbar\omega + \text{sign}(\alpha) E_{k,-\sigma}) \right). \quad (\text{G.13})$$

Further, within the SDA (compare Subsection 3.5.2) we find

$$\rho_{\sigma\alpha}^{\text{KS}}(\mathbf{r}, \omega) = \frac{2\pi}{\hbar} \sum_{k\alpha'} |u_{k\sigma}^{k\alpha'}|^2 \delta(\hbar\omega - \text{sign}(\alpha) E_{k\sigma}^{\alpha'}) |\varphi_k(\mathbf{r}\sigma)|^2 \quad (\text{G.14})$$

$$\rho_{\sigma\alpha}^{\text{KS}}(\omega) = \frac{2\pi}{\hbar} \sum_{k\alpha'} |u_{k\sigma}^{k\alpha'}|^2 \delta(\hbar\omega - \text{sign}(\alpha) E_{k\sigma}^{\alpha'}). \quad (\text{G.15})$$

With the definition of the isotropization procedure of Eq. (6.93) and the local double DOS

$$\varrho_\sigma(\mathbf{e}, \mathbf{r}) \equiv \sum_k \delta\left(\frac{\varepsilon_{k\uparrow} + \varepsilon_{-k\downarrow}}{2} - \varepsilon\right) \delta\left(\frac{\varepsilon_{k\uparrow} - \varepsilon_{-k\downarrow}}{2} - J\right) |\varphi_k(\mathbf{r}\sigma)|^2 \quad (\text{G.16})$$

we arrive at the isotropic version

$$\rho_{\sigma\alpha}^{\text{KS}}(\mathbf{r}, \omega) = \frac{2\pi}{\hbar} \sum_{\alpha'} \int d\mathbf{e} (u^2 \delta_{\alpha',1} + v^2 \delta_{\alpha',-1}) \delta(\hbar\omega - \text{sign}(\alpha) E_\sigma^{\alpha'}) \varrho_\sigma(\mathbf{e}, \mathbf{r}) \quad (\text{G.17})$$

$$\rho_{\sigma\alpha}^{\text{KS}}(\omega) = \frac{2\pi}{\hbar} \sum_{\alpha'} \int d\mathbf{e} (u^2 \delta_{\alpha',1} + v^2 \delta_{\alpha',-1}) \delta(\hbar\omega - \text{sign}(\alpha) E_\sigma^{\alpha'}) \varrho(\mathbf{e}). \quad (\text{G.18})$$

Because the expressions are similar (replace  $\varrho(\mathbf{e})$  with  $\varrho_\sigma(\mathbf{e}, \mathbf{r})$ ) we limit the discussion to the total DOS. Now with  $u^2 = \frac{F+\varepsilon}{2F}$  and  $v^2 = \frac{F-\varepsilon}{2F}$

$$\rho_{\sigma\alpha}^{\text{KS}}(\omega) = \frac{\pi}{\hbar} \sum_{\alpha'} \int d\mathbf{e} \frac{F + \text{sign}(\alpha')\varepsilon}{F} \delta\left(\hbar\omega - \text{sign}(\alpha)(\text{sign}(\sigma)J + \text{sign}(\alpha')F)\right) \varrho(\mathbf{e}). \quad (\text{G.19})$$

The property of the Dirac delta distribution

$$\int d\varepsilon f(\varepsilon) \delta(g(\varepsilon)) = \sum_{\{\varepsilon_0 | g(\varepsilon_0)=0\}} \frac{f(\varepsilon_0)}{|g'(\varepsilon_0)|} \quad (\text{G.20})$$

can be used to eliminate the energy integral. Instead of the energy integral, we have to sum the roots of the function in the delta distribution and divide by its derivative. Here the derivative becomes

$$\left| \left( \frac{d}{d\varepsilon} \left( \hbar\omega - \text{sign}(\alpha)(\text{sign}(\mu)J + \text{sign}(\alpha')\sqrt{\varepsilon^2 + |\Delta_s^s(\mathbf{e})|^2}) \right) \right)^{-1} \right| = \frac{\sqrt{\varepsilon^2 + |\Delta_s^s(\mathbf{e})|^2}}{|\varepsilon + \Re(\Delta_s^s(\mathbf{e})\partial_\varepsilon \Delta_s^s(\mathbf{e}))|} \quad (\text{G.21})$$

When we define  $\varepsilon_{0\alpha\alpha'}^\sigma(J, \omega)$  as the set of  $\varepsilon$  that solves

$$\hbar\omega - \text{sign}(\alpha) \left( \text{sign}(\sigma)J + \text{sign}(\alpha')\sqrt{\varepsilon_0^2 + |\Delta_s^s(\varepsilon_0, J)|^2} \right) = 0 \quad (\text{G.22})$$

for given  $J$  and  $\omega$  we write the KS DOS as

$$\rho_{\sigma\alpha}^{\text{KS}}(\omega) = \frac{\pi}{\hbar} \int dJ \sum_{\alpha'} \sum_{\varepsilon_{0\alpha\alpha'}^\sigma} \frac{\text{sign}(\alpha')\varepsilon_{0\alpha\alpha'}^\sigma + \sqrt{\varepsilon_{0\alpha\alpha'}^\sigma{}^2 + |\Delta_s^s(\varepsilon_{0\alpha\alpha'}^\sigma, J)|^2}}{|\varepsilon_{0\alpha\alpha'}^\sigma + \Re(\Delta_s^s(\varepsilon_{0\alpha\alpha'}^\sigma, J)\partial_\varepsilon \Delta_s^s(\varepsilon_{0\alpha\alpha'}^\sigma, J))|} \varrho(\varepsilon_{0\alpha\alpha'}^\sigma, J) \quad (\text{G.23})$$

We check the non-superconducting limit of  $\rho_{\sigma\alpha}^{\text{KS}}(\omega)$  for consistency. We see with

$$\rho_\sigma^{\text{NS}}(\omega) = \frac{2\pi}{\hbar} \sum_k \delta(\varepsilon_{k\sigma} - \hbar\omega) \quad (\text{G.24})$$

that

$$\lim_{\Delta \rightarrow 0} \rho_{\sigma\alpha}^{\text{KS}}(\omega) = \rho_\sigma^{\text{NS}}(\text{sign}(\alpha)\omega) \quad (\text{G.25})$$

and we recover the normal state DOS or the DOS with hole excitations if  $\alpha$  is  $-$ .

## H. Limiting cases of the Eliashberg Equations

In this Appendix we want provide high and low temperature limits to the Eliashberg equations Eqs. (7.82) to (7.85). Let us first consider the high temperature limit and derive the behavior of the equations. From  $\omega_n = \frac{\pi}{\beta}(2n+1)$  we see  $n$  and  $n+1$  are always  $2\pi k_B T$  apart. If  $2\pi k_B T$  is much larger than the scale of the coupling  $\alpha^2 F$  we note  $\mathfrak{K}_{n,n'}^\sigma$  and  $\mathfrak{L}_{n,n'}$  behave as Kronecker deltas

$$\lim_{T \rightarrow \infty} \mathfrak{K}_{n,n'}^\sigma(0, J, 0, J') = \delta_{nn'} \int d\omega \frac{2\alpha^2 F_\sigma^D(0, J, 0, J', \omega)}{\omega} = \delta_{nn'} \lambda_\sigma^D(J, J') \quad (\text{H.1})$$

$$\lim_{T \rightarrow \infty} \mathfrak{L}_{n,n'}(0, J, 0, J') = \delta_{nn'} \int d\omega \frac{2\alpha^2 F(0, J, 0, J', \omega)}{\omega} = \delta_{nn'} \lambda(J, J') \quad (\text{H.2})$$

where  $\lambda_\sigma^D(J, J')$  and  $\lambda(J, J')$  are the analog of the electron-phonon coupling parameter  $\lambda = \int d\omega \frac{2\alpha^2 F(\omega)}{\omega}$  for this spin splitted system. Then follows

$$\lim_{T \rightarrow \infty} Z_n^E(J) = 1 + \frac{i}{4\hbar\pi(2n+1)} \int dJ' \sum_\sigma \lambda_\sigma^D(J, J') \mathfrak{M}_{n\sigma}(J') \quad (\text{H.3})$$

$$\lim_{T \rightarrow \infty} \tilde{A}_n^{E\omega z}(J) = \frac{k_B T}{4Z_n^E(J)} \int dJ' \sum_\sigma \text{sign}(\sigma) \lambda_\sigma^D(J, J') \mathfrak{M}_{n\sigma}(J') \quad (\text{H.4})$$

$$\lim_{T \rightarrow \infty} \Delta_n^E(J) = -\frac{k_B T}{2Z_n^E(J)} \int dJ' \lambda(J, J') Z_n^E(J') \Delta_n^E(J') \mathfrak{N}_n(J'). \quad (\text{H.5})$$

This is because<sup>1</sup>

$$\lim_{T \rightarrow \infty} \mathfrak{S}_{n,\sigma}^E = \sqrt{(i\hbar\omega_n Z_n^E)^2} = -i\hbar k_B \pi(2n+1) Z_n^E T \quad (\text{H.6})$$

$$\Rightarrow \lim_{T \rightarrow \infty} \mathfrak{M}_{n\sigma} = \pi i(-1-1) + \pi i(-1+1) = -2\pi i \quad (\text{H.7})$$

$$\Rightarrow \lim_{T \rightarrow \infty} \mathfrak{N}_n = -\frac{2}{\hbar k_B(2n+1) Z_n^E T}, \quad (\text{H.8})$$

where we assume  $Z_n^E$ ,  $\Delta_n^E$  and  $\tilde{A}_n^{E\omega z}$  to be bounded<sup>2</sup>. Inserting this into the Eq. (H.4) we see that our assumption that  $\tilde{A}_n^{E\omega z}$  is bounded is violated (instead we find  $\tilde{A}_n^{E\omega z} = \mathcal{O}(T)$ ) and we have to assume the coupling to be spin channel independent  $\lambda_\sigma^D = \lambda_{-\sigma}^D \equiv \lambda^D$  in which case  $\tilde{A}_n^{E\omega z} = 0$  and the previous analysis is correct. This does not mean  $\tilde{A}_n^{E\omega z}$  diverges if the coupling depends on the spin channel because the energy integrals Eq. (H.7) and (H.8) are not so easily evaluated if  $\tilde{A}_n^{E\omega z} Z_n^E$  cannot be dropped against  $\mathfrak{S}_{n,\sigma}^E$ . Taking  $\tilde{A}_n^{E\omega z} = 0$  for now we obtain

$$\lim_{T \rightarrow \infty} Z_n^E(J) = 1 + \frac{1}{\hbar(2n+1)} \int dJ' \lambda^D(J, J') \quad (\text{H.9})$$

$$\lim_{T \rightarrow \infty} \Delta_n^E(J) = -\frac{1}{\hbar Z_n^E(J)} \int dJ' \lambda(J, J') \Delta_n^E(J') \quad (\text{H.10})$$

<sup>1</sup>Note that the minus sign in  $\mathfrak{S}_{n,\sigma}^E$  is due to the principle branch of the square root.

<sup>2</sup>Of course we also assume  $J$  to be bounded, so it can be dropped when compared to  $T$ .

If we are dealing with a spin independent system, i.e.  $J = 0$  and all properties dependent on  $J$  as a delta function, clearly  $\Delta_n^E = -\text{scalar} \times \Delta_n^E$  and  $\Delta_n^E = 0$  is the only solution.

In the low temperature limit the  $\omega_n$  are infinitely dense, with an interval length of  $2\pi k_B T$  and we transform the summation into an integral. Again we shall assume  $\lambda_\sigma^D = \lambda_{-\sigma}^D \equiv \lambda^D$ , i.e.  $\tilde{A}^{E\omega z} = 0$ . The equations remain rather complicated and we impose the simplification of zero splitting. Here we may replace  $\frac{\pi}{\beta}(2n' + 1)$  with  $\frac{2\pi}{\beta}n'$  because  $\frac{2\pi}{\beta}n'$  and  $\frac{2\pi}{\beta}(n' + 1)$  are infinitesimally apart and integrate  $\tilde{n}' = \frac{2\pi\hbar}{\beta}n'$ . Then we have to solve

$$Z^E(\tilde{n}) = 1 + \frac{1}{\tilde{n}} \int d\omega \int d\tilde{n}' \frac{\omega \alpha^2 F(\omega)}{(\tilde{n} - \tilde{n}')^2 + \omega^2} \frac{\tilde{n}'}{\sqrt{\Delta^E(\tilde{n}')^2 + (\tilde{n}')^2}} \quad (\text{H.11})$$

$$\Delta^E(\tilde{n}) = \frac{1}{Z^E(\tilde{n})} \int d\omega \int d\tilde{n}' \frac{\omega \alpha^2 F(\omega)}{(\tilde{n} - \tilde{n}')^2 + \omega^2} \frac{\Delta^E(\tilde{n}')}{\sqrt{\Delta^E(\tilde{n}')^2 + (\tilde{n}')^2}} \quad (\text{H.12})$$

Neglecting  $\Delta^E(\tilde{n}')^2$  we may compute how  $Z^E(\tilde{n})$  behaves in the normal state. Thus we compute

$$Z^E(\tilde{n}) = 1 + \frac{1}{\tilde{n}} \int d\omega \int d\tilde{n}' \frac{\omega \alpha^2 F(\omega)}{(\tilde{n} - \tilde{n}')^2 + \omega^2} \text{sign}(\tilde{n}') \quad (\text{H.13})$$

$$= 1 + \frac{2}{\tilde{n}} \int d\omega \arctan\left(\frac{\tilde{n}}{\omega}\right) \alpha^2 F(\omega) \quad (\text{H.14})$$

as an interesting fact we note

$$\lim_{\tilde{n} \rightarrow 0} \lim_{\Delta^s \rightarrow 0} Z^E(\tilde{n}) = 1 + \int d\omega \frac{2\alpha^2 F(\omega)}{\omega} = 1 + \lambda \quad (\text{H.15})$$

$$\lim_{\tilde{n} \rightarrow \infty} \lim_{\Delta^s \rightarrow 0} Z^E(\tilde{n}) = 1 \quad (\text{H.16})$$

These analytic results provide aid in the implementation.

# Bibliography

- [1] H. K. Onnes, Leiden Comm (1911).
- [2] R. O. Walther Meissner, Naturwissenschaften **21**, 787 (1933).
- [3] J. Bardeen, L. N. Cooper, and J. R. Schrieffer, Phys. Rev. **108**, 1175 (1957).
- [4] S. Weinberg, CERN Courier (2008).
- [5] P. W. Anderson, Phys. Rev. **130**, 439 (1963).
- [6] J. Schrieffer and J. Brooks, *Handbook of High -Temperature Superconductivity: Theory and Experiment* (Springer, 2007).
- [7] P. J. Hirschfeld, M. M. Korshunov, and I. I. Mazin, Reports on Progress in Physics **74**, 124508 (2011).
- [8] G. R. Stewart, Rev. Mod. Phys. **83**, 1589 (2011).
- [9] D. A. Dikin, M. Mehta, C. W. Bark, C. M. Folkman, C. B. Eom, and V. Chandrasekhar, Phys. Rev. Lett. **107**, 056802 (2011).
- [10] B. J. Powell, J. F. Annett, and B. L. Györfy, Journal of Physics A: Mathematical and General **36**, 9289 (2003).
- [11] P. Fulde and R. A. Ferrell, Phys. Rev. **135**, A550 (1964).
- [12] O. Y. Larkin, A.I., Sov. Phys. JETP .
- [13] A. Bianchi, R. Movshovich, C. Capan, P. G. Pagliuso, and J. L. Sarrao, Phys. Rev. Lett. **91**, 187004 (2003).
- [14] H. A. Radovan, N. A. Fortune, T. P. Murphy, S. T. Hannahs, E. C. Palm, S. W. Tozer, and D. Hall, Nature **425**, 51 (2003).
- [15] R. Lortz, Y. Wang, A. Demuer, P. H. M. Böttger, B. Bergk, G. Zwicknagl, Y. Nakazawa, and J. Wosnitza, Phys. Rev. Lett. **99**, 187002 (2007).
- [16] A. Yazdani, B. A. Jones, C. P. Lutz, M. F. Crommie, and D. M. Eigler, Science **275**, 1767 (1997), <http://www.sciencemag.org/content/275/5307/1767.full.pdf> .
- [17] K. J. Franke, G. Schulze, and J. I. Pascual, Science **332**, 940 (2011), <http://www.sciencemag.org/content/332/6032/940.full.pdf> .
- [18] M. Schossmann and E. Schachinger, Phys. Rev. B **33**, 6123 (1986).
- [19] S. Vonsovsky, Y. Izyumov, E. Kurmaev, E. Brandt, and A. Zavarnitsyn, *Superconductivity of Transition Metals: Their Alloys and Compounds*, Springer Series in Solid-State Sciences Series (Springer London, Limited, 1982).
- [20] L. N. Oliveira, E. K. U. Gross, and W. Kohn, Phys. Rev. Lett. **60**, 2430 (1988).

- 
- [21] M. Lüders, M. A. L. Marques, N. N. Lathiotakis, A. Floris, G. Profeta, L. Fast, A. Continenza, S. Massidda, and E. K. U. Gross, *Phys. Rev. B* **72**, 024545 (2005).
- [22] M. A. L. Marques, M. Lüders, N. N. Lathiotakis, G. Profeta, A. Floris, L. Fast, A. Continenza, E. K. U. Gross, and S. Massidda, *Phys. Rev. B* **72**, 024546 (2005).
- [23] P. C. Hohenberg, *Phys. Rev.* **158**, 383 (1967).
- [24] T. Zhang, P. Cheng, W.-J. Li, Y.-J. Sun, G. Wang, X.-G. Zhu, K. He, L. Wang, X. Ma, X. Chen, Y. Wang, Y. Liu, H.-Q. Lin, J.-F. Jia, and Q.-K. Xue, *Nat. Phys.* **6**, 104 (2010).
- [25] A. Linscheid, *Real-Space Structure of the Superconducting Order Parameter*, Master's thesis, FU Berlin (2010).
- [26] K. Capelle and E. Gross, *Physics Letters A* **198**, 261 (1995).
- [27] J. Schrieffer, *Theory of Superconductivity*, Advanced Book Program Series (Advanced Book Program, Perseus Books, 1999).
- [28] Y. Nambu, *Phys. Rev.* **117**, 648 (1960).
- [29] G. Sarma, *Journal of Physics and Chemistry of Solids* .
- [30] B. S. Chandrasekhar, *Applied Physics Letters* **1**, 7 (1962).
- [31] A. M. Clogston, *Phys. Rev. Lett.* **9**, 266 (1962).
- [32] M. Levy, *Proceedings of the National Academy of Sciences* **76**, 6062 (1979), <http://www.pnas.org/content/76/12/6062.full.pdf+html> .
- [33] N. D. Mermin, *Phys. Rev.* **137**, A1441 (1965).
- [34] E. Gross, E. Runge, and O. Heinonen, *Many-Particle Theory*, (Adam Hilger, 1991).
- [35] S. Baroni, S. de Gironcoli, A. Dal Corso, and P. Giannozzi, *Rev. Mod. Phys.* **73**, 515 (2001).
- [36] P. deGennes, *Superconductivity of Metals and Alloys* (Perseus Books, 1994).
- [37] P. W. Anderson, *Phys. Rev.* **112**, 1900 (1958).
- [38] J. Valatin, *Nuovo Cimento* **7**, 843 (1958).
- [39] N. Bogolubov, *Sov. Phys. JETP* **34**, 51 (1958).
- [40] A. J. Coleman, *Journal of Low Temperature Physics* **74**, 1 (1989).
- [41] M. Tinkham, *Introduction to Superconductivity*, Dover books on physics and chemistry (Dover Publications, 2004).
- [42] A. P. Mackenzie and Y. Maeno, *Rev. Mod. Phys.* **75**, 657 (2003).
- [43] P. Anderson, *Journal of Physics and Chemistry of Solids* **11**, 26 (1959).
- [44] G. M. Eliashberg, *Sov. Phys. JETP* **11** (1960).
- [45] A. Fetter and J. Walecka, *Quantum Theory of Many-particle Systems*, Dover Books on Physics Series (Dover Publications, Incorporated, 1971).

- [46] F. Essenberg, *Density Functional Theory for Superconductors: Extension to Pairing Mediated by Spin Excitations*, Ph.D. thesis (2013).
- [47] W. Nolting, *Grundkurs Theoretische Physik 7: Viel-Teilchen Theorie*, Grundkurs Theoretische Physik (Springer, 2005).
- [48] A. B. Migdal, *Sov. Phys. JETP* **34** (1958).
- [49] A. Linscheid and F. Essenberg, To be published .
- [50] L. J. Sham, *Phys. Rev. B* **32**, 3876 (1985).
- [51] L. J. Sham and M. Schlüter, *Phys. Rev. Lett.* **51**, 1888 (1983).
- [52] P. Giannozzi, S. Baroni, N. Bonini, M. Calandra, R. Car, C. Cavazzoni, D. Ceresoli, G. L. Chiarotti, M. Cococcioni, I. Dabo, A. Dal Corso, S. de Gironcoli, S. Fabris, G. Fratesi, R. Gebauer, U. Gerstmann, C. Gougoussis, A. Kokalj, M. Lazzeri, L. Martin-Samos, N. Marzari, F. Mauri, R. Mazzarello, S. Paolini, A. Pasquarello, L. Paulatto, C. Sbraccia, S. Scandolo, G. Sclauzero, A. P. Seitsonen, A. Smogunov, P. Umari, and R. M. Wentzcovitch, *Journal of Physics: Condensed Matter* **21**, 395502 (19pp) (2009).
- [53] J. D. et al, <http://elk.sourceforge.net/> .
- [54] M. Marques, *Density Functional Theory for Superconductors: Exchange and Correlation Potentials for Inhomogeneous Systems*, Ph.D. thesis (2000).
- [55] S. Kurth, *Exchange-Correlation Functionals for Inhomogeneous Superconductors*, Ph.D. thesis (1995).
- [56] A. Marini, G. Onida, and R. Del Sole, *Phys. Rev. Lett.* **88**, 016403 (2001).
- [57] M. Lueders, *Density Functional Theory for Superconductors: A first principles approach to the superconducting phase*, Ph.D. thesis (1998).
- [58] V. Istratescu, *Fixed Point Theory: An Introduction*, Mathematics and Its Applications (Springer, 2001).
- [59] A. Floris, G. Profeta, N. N. Lathiotakis, M. Lüders, M. A. L. Marques, C. Franchini, E. K. U. Gross, A. Continenza, and S. Massidda, *Phys. Rev. Lett.* **94**, 037004 (2005).
- [60] M. S. Hybertsen and S. G. Louie, *Phys. Rev. Lett.* **55**, 1418 (1985).
- [61] G. Onida, L. Reining, and A. Rubio, *Rev. Mod. Phys.* **74**, 601 (2002).
- [62] A. Sanna, *Applications of Density Functional Theory for Superconductors to real materials*, Ph.D. thesis (2007).
- [63] N. W. Ashcroft and D. N. Mermin, *Solid state physics*, 1st ed. (Thomson Learning, Toronto, 1976).
- [64] M. Eisterer, *Superconductor Science and Technology* **20**, R47 (2007).
- [65] H. Fröhlich, *Proc. R. Soc. Lond. A* **215**, 291 (1952).
- [66] P. Morel and P. W. Anderson, *Phys. Rev.* **125**, 1263 (1962).
- [67] J. Noffsinger and M. L. Cohen, *Solid State Communications* **151**, 421 (2011).

- 
- [68] J. P. Perdew and A. Zunger, Phys. Rev. B **23**, 5048 (1981).
- [69] H. Suhl, B. T. Matthias, and L. R. Walker, Phys. Rev. Lett. **3**, 552 (1959).
- [70] S. Massidda, F. Bernardini, C. Bersier, A. Continenza, P. Cudazzo, A. Floris, H. Glawe, M. Monni, S. Pittalis, G. Profeta, A. Sanna, S. Sharma, and E. K. U. Gross, Superconductor Science and Technology **22**, 034006.
- [71] D. J. Scalapino, J. R. Schrieffer, and J. W. Wilkins, Phys. Rev. **148**, 263 (1966).
- [72] W. L. McMillan, Phys. Rev. **167**, 331 (1968).
- [73] J. P. Carbotte, Rev. Mod. Phys. **62**, 1027 (1990).
- [74] N. D. Mermin and H. Wagner, Phys. Rev. Lett. **17**, 1133 (1966).
- [75] L. Pollack and J. P. Perdew, Journal of Physics: Condensed Matter **12**, 1239 (2000).
- [76] D. Jasnow and M. E. Fisher, Phys. Rev. B **3**, 895 (1971).
- [77] M. E. Fisher and D. Jasnow, Phys. Rev. B **3**, 907 (1971).
- [78] D. Eom, S. Qin, M.-Y. Chou, and C. K. Shih, Phys. Rev. Lett. **96**, 027005 (2006).
- [79] S. Qin, J. Kim, Q. Niu, and C.-K. Shih, Science **324**, 1314 (2009), <http://www.sciencemag.org/content/324/5932/1314.full.pdf> .
- [80] E. K. U. G. R. M. Dreizler, *Density Functional Theory. An approach to the quantum many-body-problem.* (Springer-Verlag, 1990).
- [81] N. Plakida, *High-Temperature Cuprate Superconductors: Experiment, Theory, and Applications*, Springer series in solid-state sciences (Springer, 2010).
- [82] I. I. Mazin, M. D. Johannes, L. Boeri, K. Koepernik, and D. J. Singh, Phys. Rev. B **78**, 085104 (2008).



# Publications

- *Ab initio calculation of a Pb single layer on a Si substrate: two-dimensionality and superconductivity.*  
A. Linscheid, A. Sanna and E. K. U. Gross – Submitted to Phys. Rev. Lett.
- *Real space properties of a superconductor from ab-initio calculations.*  
A. Linscheid, A. Sanna, A. Floris and E. K. U. Gross – Submitted to Phys. Rev. Lett.
- *Superconducting pairing mediated by spin-fluctuations from first principles.*  
F. Essenberger, A. Sanna, A. Linscheid, F. Tandetzky and E. K. U. Gross  
– <http://arxiv.org/abs/1409.7968> (Submitted to Phys. Rev. B.)
- *Hedin-Equations for Superconductors.*  
A. Linscheid, F. Essenberger – To be submitted to Phys. Rev. B.
- *Ab Initio Theory of Superconductivity in a Magnetic Field I. : Spin Density Functional Theory For Superconductors and Eliashberg Equations.*  
A. Linscheid, A. Sanna, F. Essenberger and E. K. U. Gross – To be submitted to Phys. Rev. B.
- *Ab Initio Theory of Superconductivity in a Magnetic Field II. : Numerical solution.*  
A. Linscheid, A. Sanna and E. K. U. Gross – To be submitted to Phys. Rev. B.
- *Thin Superconducting Layer on a Substrate: Ab-initio Description and Application to Pb and TiS<sub>2</sub>.*  
A. Linscheid, A. Sanna, A. Davydov, S. Gliga and E. K. U. Gross – In preparation
- *Superconductivity of hole doped graphene.*  
A. Sanna, A. Linscheid and E. K. U. Gross – In preparation

# Acknowledgments

As the last step in the course of this thesis I wish to thank several people who contributed in many different ways to the outcome of this work.

First and foremost I would like to thank my adviser, Hardy Gross, for the freedom and his encouragement to find and pursue independent projects. As such, I could invest the time to study very interesting topics which are not directly related to superconductivity. I have profited enormously from the group seminars that were held in a very relaxed and friendly atmosphere on very diverse research topics.

The entire work was carried out in very close collaboration with Antonio Sanna. His expertise in superconductivity and material science and his hands-on approach to the most difficult problems provided both a guidance and practical help in numerous cases. I have profited enormously from many stimulating discussions. For all this, his general support and, in addition, the proof reading of this thesis I wish to express my deep gratitude.

Frank Essenberger has been my office mate and in addition we shared an apartment in Halle. Probably we spend more time together during these years, than with our girlfriends. It is not overstated to say that being in Halle was as enjoyable because of him and I wish to thank him for this harmonic time. With our PhD projects being related scientifically, I enjoyed our numerous fruitful discussions. In addition, I want to thank him for the proof reading of all the chapters of the thesis and his valuable suggestions.

Furthermore, Klaus Pototzky and Falk Tandetzky deserve many thanks for their proof reading of many chapters of the thesis and many discussions about scientific topics and unrelated matters.

I wish to thank the entire group for creating a very relaxing and friendly atmosphere and the good discussions. In particular, I want to mention Kevin Krieger, who shared the apartment for some time with Frank and me, Kay Dewhurst and Sangeeta Sharma, Federica Agostini and Florian Eich.

Last but not least, I want to thank my family for their love and support during this stage of my life.

I want to conclude, mentioning our group of fellow students from Berlin: Frank Essenberger, Kai Schmitz, Max Hoffmann and Chris Bronner. I hope that we keep in contact even now, that we are scattered over the world.

# Deutsche Kurzfassung

Bei der ab-initio Beschreibung von Phänomenen, welche die Wechselwirkung von Magnetismus und Supraleitung beinhalten, stoßen herkömmliche Verfahren bislang weitgehend an ihre Grenzen. In dieser Arbeit wird die Dichtefunktionaltheorie für Supraleiter für den Fall verallgemeinert, in welchem neben der elektronischen Dichte, der Dichte der Kerne und der Dichte von kondensierten Elektronenpaaren auch die magnetische Dichte Berücksichtigung findet. Hierbei erfolgt die approximative Lösung des wechselwirkenden Systems indem die exakten Dichten in einem einfacheren, nicht wechselwirkenden, Kohn-Sham System reproduziert werden. Für die Funktionentwicklung des Austauschkorrelationseinteilchenpotentials des Kohn-Sham Systems, was integraler Bestandteil jeder Dichtefunktionaltheorie ist, wird in dieser Arbeit die Sham-Schlüter Gleichung verwendet. Zu deren Herleitung verwendet man die teile der beiden Greensfunktionen im Kohn-Sham- und wechselwirkenden System, welche zu den Dichten korrespondieren, per Konstruktion identisch sind. Wendet man diese Überlegungen auf die Störentwicklung vom Kohn-Sham zum wechselwirkenden System an, ergibt sich eine Approximation des Austauschkorrelationpotentials in Abhängigkeit der Selbstenergie.

Im einfachsten Fall, welcher die Situation in vielen physikalisch relevanten System akkurat beschreibt, reduziert sich die Paarung von Elektronen auf solche, welche miteinander über Zeitinverteilung in Verbindung stehen. Für diesen Fall lösen wir die meisten hergeleiteten Gleichungen dieser Arbeit numerisch.

Um die erreichten Resultate besser vergleichen zu können wird in der Arbeit das Bardeen-Cooper-Schrieffer System als Funktion eines homogenen Magnetfeldes und der Temperatur gelöst. Hier zeigt sich das erste mal das der Phasenübergang zum ferromagnetischen System erster Ordnung sein muss. Um die Selbstenergie besser zu verstehen wird des weiteren in der selben Notation eine Verallgemeinerung der Eliashberg Gleichungen für den Magnetischen Fall vorgenommen. Es zeigt sich das obwohl das System supraleitend bleibt, das Kohn-Sham System bei  $T = 0$  keine supraleitende Anregungslücke aufweist, was in Einklang mit dessen Konstruktion ist da eine Reproduktion des Einteilchenspektrums nicht unbedingt erwartet werden kann. Um auch ein adäquates Einteilchenspektrum vorhersagen zu können führen wir eine zur G0W0 Approximation verwandten Prozedur durch, in welcher die Dyson-Gleichung einmal mit der Selbstenergie aus der Funktionalonstruktion gelöst wird. Zum Abschluss der theoretischen Herleitungen testen wir die Gleichungen an einem freien Elektronengas mit justierbarem Magnetfeld.

Anschließend wird der Formalismus auf eine simulierte Oberfläche von einem Monolayer Blei auf einem Silizium (111) Substrat angewendet welche experimentell untersucht ist. Hier zeigen sich auch ohne Magnetfeld schon interessante Effekte. Zum Beispiel ist die vorhergesagte kritische Temperatur sehr viel größer als der normale Fehler einer derartigen Rechnung erwarten lässt. In 2D ist Aufgrund von langwelligen Fluktuationen keine supraleitende Ordnung zu erwarten. Dennoch ist experimentell Supraleitung in dem untersuchten System nachgewiesen. In dem Zusammenhang ergibt sich somit die Möglichkeit den Begriff der "Nähe" zu einem 2D System weiter zu quantifizieren. In dieser Arbeit wird ein solcher Versuch unternommen indem vernachlässigte Effekte auf ihren Einfluss auf die Sprungtemperatur untersucht werden. Es muss geschlossen werden das die viel zu hohe vorhergesagte Sprungtemperatur der Vernachlässigung von langwelligen Fluktuationen geschuldet ist.

Im letzten Schritt legen wir ein homogenes, externes Magnetfeld an das System an und untersuchen seinen Einfluss.

# Angaben zur Person und wissenschaftlichem Werdegang

|   |   |
|---|---|
| Vorname, Familienname:  | Andreas Linscheid                               |
| Geburtsdatum, Ort:  | 13.01.1985 in Herdecke                          |
| Staatsangehörigkeit:  | deutsch   |
| Geschlecht:   | männlich  |
| Meldeadresse:   | Lipaer Str. 12a 12203 Berlin                    |
| Email:  | alinsch@mpi-halle.mpg.de                        |
| Akademischer Grad:  | Diplom Physiker                                 |
| <br>  |   |
| Fachgebiet der Promotion:                                     | Theoretische Festkörperphysik                   |
| <br>  |   |
| Beschäftigung am Max-Planck Institut für Mikrostrukturphysik: |   |
| 02/2014 – heute   | Postdoc Stipendium der Max-Planck-Gesellschaft  |
| 04/2010 – 01/2014   | Promotionstipendium der Max-Planck-Gesellschaft |
| <br>  |   |
| Studium:  |   |
| 10/2005 – 03/2010   | Diplomstudium Physik – Freie Universität Berlin |
| <br>  |   |
| Schulische Ausbildung:  |   |
| 1999 – 2004   | Paulsen Oberschule (Gymnasium) Berlin           |
| 1995 – 1999   | Ruhrtal Gymnasium Schwerte                      |

## Eidesstattliche Erklärung

Hiermit erkläre ich, dass keine Vorstrafen gegen mich vorliegen und keine Ermittlungsverfahren eingeleitet worden sind.

Hiermit erkläre ich, gemäß §5 Abs. 4 der Promotionsordnung der Naturwissenschaftlichen Fakultät II – Chemie, Physik und Mathematik der Martin-Luther Universität Halle-Wittenberg vom August 2012, dass ich die vorliegende Arbeit selbständig und ohne fremde Hilfe verfasst habe. Es wurden keine, außer die angegebenen Quellen und Hilfsmittel benutzt und die den benutzten Werken wörtlich oder inhaltlich entnommenen Stellen wurden als solche kenntlich gemacht. Desweiteren erkläre ich gemäß §5 Abs. 5 der Promotionsordnung, dass ich bisher keine vergeblichen Promotionsversuche an dieser oder einer anderen Fakultät unternommen habe.

Halle (Saale), den 9. Oktober 2014

Andreas Linscheid